

THE UNIVERSITY OF MICHIGAN
INDUSTRY PROGRAM OF THE COLLEGE OF ENGINEERING

SOLUTE INTERACTIONS WITH ZINC
IN DILUTE SOLUTION WITH MOLTEN BISMUTH



A dissertation submitted in partial fulfillment
of the requirements for the degree of
Doctor of Philosophy in the
University of Michigan
Department of Chemical and Metallurgical Engineering
1965

May, 1965

IP-707

ACKNOWLEDGEMENTS

The author would like to acknowledge with gratitude all those who directly or indirectly aided in the conduct of the research and the preparation of this thesis. Special thanks are offered to the following:

The Doctoral Committee:

Professor R. D. Pehlke, Chairman and Director of the sponsoring research project, for offering the opportunity to perform this research, for helpful suggestions, and for critical discussions during the investigation.

Professor E. E. Hucke for his tutelage and valuable discussions of thermodynamics in metallurgy.

Professors R. E. Balzhiser, M. J. Sinnott, and E. F. Westrum for their advice, cooperation, and service on the committee.

Dr. D. V. Ragoné for encouragement of these graduate studies.

Mr. P. D. Goodell for many valuable discussions and for invaluable assistance during the hectic moments at the start of each experimental run.

Mr. Weldon Daines and Mr. Robert Moore for spectrographic analyses.

Dr. C. W. Phillips of the Ford Motor Co. for arranging donation of gold.

Mr. W. M. Boorstein for basic construction of the experimental apparatus.

My fellow graduate students for helpful and interesting discussions.

The Atomic Energy Commission for financial support under
Contract AT(11-1)1352.

The Industry Program of the College of Engineering, University
of Michigan, for reproducing this thesis.

My wife and children for patience and encouragement throughout
the graduate studies and experimental program.

TABLE OF CONTENTS

	<u>Page</u>
ACKNOWLEDGEMENTS.....	ii
LIST OF TABLES.....	vi
LIST OF FIGURES.....	vii
NOMENCLATURE.....	xii
ABSTRACT.....	ix
I. INTRODUCTION.....	1
II. REVIEW OF THE LITERATURE.....	4
A. Concept and Experimental Development of the Interaction Parameter.....	4
B. Theoretical Studies of Solute Interactions.....	9
C. Experimental Methods.....	12
D. Previous Studies of Binary and Ternary Systems Involving Zinc and Bismuth.....	13
III. EXPERIMENTAL PROGRAM.....	16
A. Experimental Design.....	16
B. Experimental Procedures.....	49
IV. EXPERIMENTAL RESULTS.....	75
A. Zinc-Bismuth Binary System.....	75
B. Zinc-Bismuth-j Ternary Systems.....	90
C. Prediction of Zinc Activity in Multi-Component Solu- tions.....	134
D. Confirmation of Basic Assumptions.....	151
V. DISCUSSION.....	166
A. Rationale for Observed Interactions in Ternary Alloys....	166
B. Prediction of Ternary Interactions from Simple Solution Models.....	217
C. Validity of Wagner's Prediction Model for Multi-Component Solutions.....	239
D. Limitations of Experimental Results.....	246
E. Suggested Further Research.....	247

TABLE OF CONTENTS (CONT'D)

	<u>Page</u>
VI. SUMMARY AND CONCLUSIONS.....	250
APPENDIX A - Experimental Data for Multi-Component Alloy Studies.....	255
APPENDIX B - Alternate Derivations of the Temperature Dependence of Interaction Parameters.....	257
APPENDIX C - Interaction Parameter Determination by Linear Regres- sion Technique.....	263
REFERENCES.....	271

LIST OF TABLES

<u>Table</u>	<u>Page</u>
I. Sources of Error in Galvanic Cell Determination of Activity.....	30
II. Standard Free Energy of Formation for Various Metal Chlorides.....	40
III. Minimum Values of ΔG_I° or ΔG_{II}° for One Per Cent Displacement Error in Measured Electrode Potentials.....	43
IV. Section of Periodic Table Incorporating Suitable Solutes and Solvents for Galvanic Cell Studies of Activity at 450 to 650°C.....	45
V. Experimental Materials.....	60
VI. Experimental Data for Binary Bismuth-Zinc Alloys.....	77
VII. Summary of Binary Electrode Potentials and Activity Coefficients for Bismuth-Zinc Alloys.....	88
VIII. Experimental Data for Bismuth-Zinc-j Ternary Alloys.....	92
IX. Summary of Interactions with Zinc in Dilute Solution with Molten Bismuth.....	96
X. Temperature Dependence Constants for Interactions with Zinc in Dilute Solution with Molten Bismuth in the Range 450 to 650°C.....	127
XI. Results of Multi-Component Solution Studies of Additivity Hypothesis.....	143
XII. Results of Chemical Analyses of Alloy Electrodes.....	162
XIII. Electronegativity Values for Elements Interacting with Zinc in Bismuth.....	182
XIV. Factors for Thermodynamic Evaluation of Zinc-j Binary Systems.....	197
XV. Comparison of Observed and Predicted Ternary Interaction Parameters Using Simple Solution Models.....	224
XVI. Quantitative Comparisons of Multi-Component Interaction Prediction Models.....	242

LIST OF FIGURES

<u>Figure</u>	<u>Page</u>
1. Methods of Evaluating Interaction Parameters.....	17
2. Binary Phase Diagrams of the Bismuth-Zinc and Lead-Zinc Systems in the Zinc-Dilute Region.....	46
3. Galvanic Cell Apparatus.....	50
4. Schematic Diagram of Multi-Electrode Galvanic Cell.....	52
5. Schematic Diagram of Temperature Control and Potential Measurement Circuits.....	55
6. Schematic Diagram of Atmosphere System.....	57
7. Activity of Zinc versus Mole Fraction of Zinc in Bismuth at 550°C.....	79
8. Activity of Zinc versus Mole Fraction of Zinc in Bismuth at 600°C.....	80
9. Slope of EMF-Temperature Curves versus Mole Fraction of Zinc in Bismuth.....	81
10. Determination of Zinc Self-Interaction in Dilute Solution with Molten Bismuth.....	84
11. Natural Logarithm of Zinc Activity Coefficient versus Mole Fraction Copper - for Indicated Constant Mole Fractions of Zinc.....	106
12. Determination of Cu-Zn Interactions in Molten Bismuth.....	107
13. Temperature Dependence of First-Order Cu-Zn Interaction Parameter.....	107
14. Natural Logarithm of Zinc Activity Coefficient versus Mole Fraction Gallium - for Indicated Constant Mole Fractions of Zinc.....	108
15. Determination of Ga-Zn Interactions in Molten Bismuth.....	109
16. Temperature Dependence of First-Order Ga-Zn Interaction Parameter.....	109

LIST OF FIGURES (CONT'D)

<u>Figure</u>	<u>Page</u>
17. Natural Logarithm of Zinc Activity Coefficient versus Mole Fraction Silver - for Indicated Constant Mole Fractions of Zinc.....	110
18. Determination of Ag-Zn Interactions in Molten Bismuth.....	111
19. Temperature Dependence of First-Order Ag-Zn Interaction Parameter.....	111
20. Natural Logarithm of Zinc Activity Coefficient versus Mole Fraction Cadmium - for Indicated Constant Mole Fractions of Zinc.....	112
21. Determination of Cd-Zn Interactions in Molten Bismuth.....	113
22. Temperature Dependence of First-Order Cd-Zn Interaction Parameter.....	113
23. Natural Logarithm of Zinc Activity Coefficient versus Mole Fraction Indium - for Indicated Constant Mole Fraction of Zinc.....	114
24. Determination of In-Zn Interactions in Molten Bismuth.....	115
25. Temperature Dependence of First-Order In-Zn Interaction Parameter.....	115
26. Natural Logarithm of Zinc Activity Coefficient versus Mole Fraction Tin - for Indicated Constant Mole Fractions of Zinc.....	116
27. Determination of Sn-Zn Interactions in Molten Bismuth.....	117
28. Temperature Dependence of First-Order Sn-Zn Interaction Parameter.....	117
29. Natural Logarithm of Zinc Activity Coefficient versus Mole Fraction Antimony - for Indicated Constant Mole Fractions of Zinc.....	118
30. Determination of Sb-Zn Interactions in Molten Bismuth.....	119
31. Temperature Dependence of First-Order Sb-Zn Interaction Parameter.....	119

LIST OF FIGURES (CONT'D)

<u>Figure</u>	<u>Page</u>
32. Natural Logarithm of Zinc Activity Coefficient versus Mole Fraction Gold - for Indicated Constant Mole Fraction of Zinc.....	120
33. Determination of Au-Zn Interactions in Molten Bismuth.....	121
34. Temperature Dependence of First-Order Au-Zn Interaction Parameter.....	121
35. Natural Logarithm of Zinc Activity Coefficient versus Mole Fraction Mercury - for Indicated Constant Mole Fractions of Zinc.....	122
36. Natural Logarithm of Zinc Activity Coefficient versus Mole Fraction Lead - for Indicated Constant Mole Fractions of Zinc.....	123
37. Determination of Pb-Zn Interactions in Molten Bismuth.....	124
38. Temperature Dependence of First-Order Pb-Zn Interaction Parameter.....	124
39. Summary Plot of Temperature Dependence of Interaction Parameters.....	126
40. Electrode Potentials versus Temperature for Bi-Zn-Au Alloys..	130
41. Isotherms for Bi-Zn-Au System Showing Liquidus Boundaries in the Bismuth Corner.....	131
42. Electrode Potentials versus Temperature for Bi-Zn-Cu Alloys..	132
43. Isotherms for Bi-Zn-Cu System Showing Liquidus Boundaries in the Bismuth Corner.....	133
44. Logarithm of Zinc Activity Coefficient versus Total Mole Fraction of Added Solutes for Quaternary Alloys of Bi-Zn-Ag-Sb - Comparison of Observed and Predicted Values.....	144
45. Logarithm of Zinc Activity Coefficient versus Total Mole Fraction of Added Solutes for Quaternary Alloys of Bi-Zn-In-Sb and Bi-Zn-Ag-Pb - Comparison of Observed and Predicted Values.....	145

LIST OF FIGURES (CONT'D)

<u>Figure</u>	<u>Page</u>
46. Logarithm of Zinc Activity Coefficient versus Total Mole Fraction of Added Solutes for Quinary Alloys Based on Bi-Zn - Comparison of Observed and Predicted Values.....	148
47. Schematic Diagram of Electrode Potential Behavior During the Faraday Yield Experiment.....	156
48. First-Order Zinc-j Interaction Parameters versus Atomic Number of j - Correlation by Period.....	168
49. First-Order Zinc-j Interaction Parameters versus Atomic Number of j - Correlation by Sub-Group.....	169
50. Second-Order Zinc-j Interaction Parameters versus Atomic Number of j - Correlation by Period.....	170
51. First-Order Zinc-j Interaction Parameters versus Second-Order Zinc-j Interaction Parameters.....	171
52. First-Order Interaction Parameters for Zinc-j versus Electronegativities of the Added Solute j.....	183
53. First-Order Zinc-j Interaction Parameters versus Atomic Volume of Added Solute j.....	187
54. First-Order Zinc-j Interaction Parameters versus Atomic Radius of Added Solute j.....	188
55. First-Order Zinc-j Interaction Parameters versus Ionic Radius of Added Solute j.....	189
56. Darken-Gurry Plot of Atomic Radius and Electronegativity for Zinc, Bismuth, and Added Solutes.....	190
57. Electronegativity-Size Factor Correlation Attempts for First-Order Zinc-j Interaction Parameters.....	192
58. First-Order Zinc-j Interaction Parameters versus Solubility Parameter of Added Solute j.....	195
59. First-Order Zinc-j Interaction Parameters versus Excess Partial Molal Free Energy of Mixing of Zinc for Equimolar Mixture of Zinc and j.....	200

LIST OF FIGURES (CONT'D)

<u>Figure</u>		<u>Page</u>
60.	First-Order Zinc-j Interaction Parameters versus Partial Molal Heat of Mixing of Zinc in Equimolar Mixture of Zinc and j.....	201
61.	First-Order Zinc-j Interaction Parameters versus First and Second Ionization Potentials of Bismuth, Zinc, and Added Solutes j.....	204
62.	First-Order Zinc-j Interaction Parameters versus Work Function for Bismuth, Zinc, and Added Solutes j.....	206
63.	First-Order Zinc-j Interaction Parameters versus Standard Free Energy of Formation of Chlorides at 550°C.....	207

NOMENCLATURE

- A, A' Intercept in slope-intercept equations
 B, B' Slope in slope-intercept equations
 C_p Heat capacity at constant pressure
 E Observed electrode potential difference between alloy and standard electrodes
 F Faraday's constant, 23,060 calories per volt
 G Gibbs free energy $\equiv H - TS$
 G^e Molar excess free energy of mixing
 \bar{G}_i^{xs} Excess partial molar free energy of mixing of $i \equiv \bar{G}_i - G_i^\circ$
 $\bar{G}_{i(j)}^{ex}$ "Extra" excess partial molal free energy of mixing of i due to addition of j
 \bar{G}_i Partial molal free energy of i
 $\bar{G}_{i\infty}$ Partial molal free energy of i at high dilution of i
 G_i° Molal free energy of pure liquid i
 ΔG_f° Standard free energy of formation
 $\Delta G_{\pm}^\circ, \Pi$ Minimum difference in standard free energy of formation to limit displacement error to one per cent of measured potential
 H, \bar{H}_i, etc Enthalpy and related enthalpy quantities defined similar to those for G
 K Activity coefficient factor appearing in Equation (68)
 R Gas constant, 1.987 cal/mole/°K
 S, \bar{S}_i, etc Entropy and related entropy quantities defined similar to those for G
 T Temperature, °K
 V_i Molar volume of i

- V^M Average molar volume of mixture
 W_{ij} Interchange energy between i and j
 \bar{X} Electronegativity
 Z Coordination number in solution
 a_i Thermodynamic activity of component i
 e Electron
 f_i Activity coefficient of component $i \equiv \frac{a_i}{(\%i)}$ (weight)
 i (as subscript) Primary dilute solute
 j (as subscript) Added dilute solute
 k (as subscript) Solvent
 \ln Natural logarithm
 \log Common logarithm
 m (as running index) Number of additional solutes besides primary
 n Number of electrochemical equivalents, also valence
 n (as subscript) Additional solutes
 \bar{n} Number of bonds between two components in solution
 X_i, X_j Mole fraction
 z Valence electrons
 \sup Exponent, e
 $i^j, i(j)$ Binary solution of i and j ; i in j
 $i(jk), i(j+k)$ Ternary solution; i dilute in j and k
 Δ Difference
 γ^1 Activity coefficient $\equiv \frac{a_i}{x_i}$
 γ_i^0 Activity coefficient at infinite dilution, the Henry's Law Constant

- δ Solubility parameter
 $\bar{\delta}$ Volume-weighted solubility parameter in ternary solution
 ϵ_i^i Self or binary interaction parameter $\equiv \left(\frac{\partial \ln \gamma_i^i}{\partial x_i} \right)_{x_i=0}$
 ϵ_i^j Ternary interaction parameter (first order) $\equiv \left(\frac{\partial \ln \gamma_i^i}{\partial x_j} \right)_{x_i=x_j=0}$
 ϵ_i^j Ternary interaction parameter (second order) $\equiv \left(\frac{\partial^2 \ln \gamma_i^i}{\partial x_j \partial x_i} \right)_{x_i=x_j=0}$
 η "Extra" excess partial molar enthalpy of i
 σ "Extra" excess partial molar entropy of i
 η_1 First-order contribution to η
 σ_1 First-order contribution to σ
 η_2^* Second-order contribution to η
 σ_2^* Second-order contribution to σ
 ϕ Volume fraction
 M_e Chemical potential of electrons
 M_{ion} Chemical potential of ions
 $I, 1$ (as subscript) First order effect
 $II, 2$ (as subscript) Second order effect

ABSTRACT

An investigation was made of the effect of small amounts of added solutes on the thermodynamic activity of zinc in dilute solution with molten bismuth in the temperature range 450 to 650°C. The investigation was designed to test two hypotheses: that interaction effects in ternary systems are periodic with the atomic number of the added solute; and that ternary effects may be used to predict the activity in higher-order solutions. The experimental measurements of activity were made in a multi-electrode galvanic cell apparatus using a fused LiCl-KCl electrolyte.

The initial measurements defined the activity of zinc in binary solution with bismuth. Thermodynamic interactions with zinc were determined for ten Group-B elements from the 4th, 5th, and 6th periods of the Periodic Table. The activity of zinc was then measured in higher-order solutions through septenary, made by alloying various combinations of these solute elements to the basic solution of zinc in bismuth. The prediction of the ternary effects was considered on the basis of periodicity, alloying criteria, thermodynamic factors, and the application of solution theories.

The activity of zinc in the binary solution obeyed Henry's Law to at least .050 mole fraction. The addition of lead, gallium, or indium increased the activity of zinc. Cadmium or tin additions slightly

decreased zinc activity. Copper, mercury, silver, or antimony caused moderate decreases while gold strongly decreased the zinc activity. The interaction effects for copper, gold, silver, and antimony had a linear dependence on reciprocal absolute temperature, while the effects caused by the other elements were essentially independent of temperature. The temperature dependence is related to additional contributions to zinc entropy and enthalpy caused by the solute addition.

The ternary effects were periodic except for tin and antimony. Consequently, the hypothesis of purely periodic behavior was rejected. A semi-quantitative explanation of the effects was possible with a free-electron model where relative electronegativities are used to express changes in the electron/atom ratio caused by the solute additions. The thermodynamic behavior of the binary solution between zinc and the added solute also accounted for much of the ternary effect.

The regular solution model correctly predicted half of the ternary interactions while random solution and quasi-chemical models correctly predicted almost all cases to which they could be applied. The prediction of zinc activity in quaternary and higher-order solutions was found to be excellent using a phenomenological model based on the ternary effects. The linearity of the results for the ternaries permitted these predictions to be carried to relatively concentrated solutions with fair success.

The position of the liquidus phase boundaries was determined in a portion of the bismuth corner of the systems Bi-Zn-Cu and Bi-Zn-Au.

I. INTRODUCTION

The formulation of quantitative thermodynamic relations for metallurgical processes such as alloying, refining, electrolysis, or diffusion, or for experimental situations where a solid or liquid metal alloy is affected by its environment, rests on defining the free energy change. This may be in explicit terms, such as a reaction constant or a chemical potential, or implicitly, such as a solubility. The general procedure is to formulate an expression in terms of the standard free energies plus a means to "correct" or account for the fact that the reacting species may be present in some condition other than their standard state. The corrections are made using the thermodynamic activities of the products and reactants so defined that the activity in the standard state is unity.

However, it was observed experimentally that constituents not directly concerned in a reaction may also affect its equilibrium or kinetics. For example, to take two cases from ferrous metallurgy, manganese affects the deoxidizing power of silicon in molten iron or chromium may affect the carbon-oxygen reaction. Recognition of such effects helped give impetus to an intensive study by a number of experimenters of means of representing the thermodynamic properties of multi-component systems and, in particular, the interactions between elements present at dilute concentrations. A great amount of experimental data has been obtained for ferrous systems.

The practical uses of such formulations in ferrous and non-ferrous metallurgical practice are manifest: the physical chemistry of steelmaking, the refining of ores, corrosion involving liquid metal coolants, multi-component diffusion, etc; however, such information is also necessary for quantitative understanding of alloy phase diagrams and the physical structure or constitution of metallic phases and solid or liquid solutions.

The approaches to obtaining such information may be phenomenological, i.e., "what mathematical function adequately describes observed behavior and permits extrapolation to new situations?", or theoretical, such as an explicit model for solution behavior. Ideally, both approaches should eventually converge.

The most accepted and useful means for organizing interaction behavior in dilute solutions is Wagner's concept of the interaction parameter. From the development of this concept a phenomenological model has arisen in the literature with two major hypotheses that have not as yet been fully and systematically investigated. To summarize them briefly: (1) The activity of a given solute in a multi-component system may be obtained by summing effects of interactions with each of the additional solute elements taken as individuals. This arose from Wagner's proposal that a Taylor series be used to represent $\ln \gamma_i$, where γ_i is the activity coefficient defined as $\frac{a_i}{x_i}$. The interaction parameters are the coefficients of the series. (2) For interactions occurring with a solute i in a given solvent k , the direction and magnitude of the interactions caused by an additional solute j may be a periodic function of the atomic number of j .

The first hypothesis can be termed "additivity" and the second termed "periodicity".

The purpose of this investigation was to test these hypotheses in a non-ferrous system where all the dilute solutes were metallic. The experimental alloys are not particularly useful in a practical sense but were chosen for experimental convenience and the requirement that periodic variations of the added solute element must be possible. The quantity measured was the activity of zinc in dilute solution with molten bismuth in the temperature range 450-650°C. A multi-electrode galvanic cell apparatus was used. The hypothesis of periodicity was investigated by studies of ternary additions of 10 Group-B elements from the 4th, 5th, and 6th periods in the Periodic Table. Following the determination of the ternary interactions, the activity of zinc was measured in higher-order solutions through septenary, made by alloying various combinations of the previously studied solute elements added to the basic solution of zinc plus bismuth. The hypothesis of additivity was investigated by comparing the observed activity coefficients with those calculated by summing the effects of the individual solute elements. The experimental results from ternary alloys were studied in terms of the periodicity, thermodynamic factors, and alloying considerations as related to Wagner's electron model for solution interactions. The applicability of several simple solution theories and models of interaction behavior was tested. In particular, attention was given to the methods of Alcock and Richardson (17,27) and Wada and Saito.(15)

II. REVIEW OF THE LITERATURE

The literature is reviewed in terms of the historical development of the interaction parameter concept and the available experimental studies. The theoretical background of solution thermodynamics and experimental methods is reviewed. A summary is given of previous thermodynamic studies of the alloy systems studied in this investigation.

A. Concept and Experimental Development of the Interaction Parameter

The question of solute interactions in ternary liquid metallic solutions has been a matter of specific experimental and practical concern for approximately 25 years. Richardson⁽¹⁾ attributed the first experimental studies (carbon and oxygen in liquid iron) to Marshall and Chipman's 1942 studies,⁽²⁾ although he noted that Sievert's 1910 measurements on gas solubilities were made in ternary solutions but no attempt was made to express the results in dilute alloys in terms of the interactions between solutes.

Chipman and co-workers continued experimental and other studies of ternary interactions. In 1949, Chipman and Elliott⁽³⁾ showed that Körber's work on reactions of molten iron-manganese alloys with silicate slags could be interpreted to show the effects of various alloying elements on the activity of silicon. By 1951, Chipman and a series of co-workers had accumulated enough of their own data, supplemented by the results of others, to present relations for the effects of several elements on the activity coefficient of sulfur or oxygen in liquid iron.⁽⁴⁾

The method used was to plot $\log \frac{f_i}{f'_i}$ versus $\%j$, where f_i is the activity coefficient of i in the ternary with j and f'_i the activity coefficient in the corresponding binary alloy of the same content of i .

The accepted present-day concepts of accounting for solute interactions stem from Wagner's suggestion in 1952, (5) that a Taylor series could be used to express the partial molar free energy of a solute or else the logarithm of the activity coefficient of the solute. If the series for the logarithm is expanded about the point $x_i = 0$, the following expression is obtained:

$$\ln \gamma'_i = \ln \gamma_i^0 + x_i \left(\frac{\partial \ln \gamma'_i}{\partial x_i} \right) + x_j \left(\frac{\partial \ln \gamma'_i}{\partial x_j} \right) + \frac{1}{2} x_i^2 \left(\frac{\partial^2 \ln \gamma'_i}{\partial x_i^2} \right) + \frac{1}{2} x_j^2 \left(\frac{\partial^2 \ln \gamma'_i}{\partial x_j^2} \right) + x_i x_j \left(\frac{\partial^2 \ln \gamma'_i}{\partial x_i \partial x_j} \right) + \dots + \dots \quad (1)$$

(all derivatives at infinite dilution with respect to solutes)

The partial differential coefficients of the series thereby explicitly express the effects of the various additional solute elements on the activity coefficient of the primary solute. If, as the expression is usually formulated, the second-order and higher terms are neglected, the equation becomes a linear function of the mole fraction of the various solutes:

$$\ln \gamma'_i = \ln \gamma_i^0 + x_i \left(\frac{\partial \ln \gamma'_i}{\partial x_i} \right) + x_{j_1} \left(\frac{\partial \ln \gamma'_i}{\partial x_{j_1}} \right) + x_{j_2} \left(\frac{\partial \ln \gamma'_i}{\partial x_{j_2}} \right) + \dots + x_{j_n} \left(\frac{\partial \ln \gamma'_i}{\partial x_{j_n}} \right) \quad (2)$$

This expression summarizes the hypothesis of additivity.

The partial differential coefficients of the truncated series are termed the interaction parameters and are defined as:

$$\epsilon_i^i = \text{self interaction parameter} = \left(\frac{\partial \ln \gamma_i^i}{\partial X_i} \right)_{X_i=0} \quad (2a)$$

$$\epsilon_i^j = \text{ternary interaction parameter} = \left(\frac{\partial \ln \gamma_i^j}{\partial X_j} \right)_{X_i=0, X_j=0} \quad (2b)$$

Since the excess free energy of mixing of component i is given by the thermodynamic relation $\Delta \bar{G}_i^{\text{XS}} = RT \ln \gamma_i$, (76) the interaction parameters can directly show the change in excess free energy occasioned by the addition of the various solutes. In the region where Henry's Law applies and the activity is directly proportional to concentration, $\ln \gamma_i = \ln \gamma_i^0 = \text{constant}$ and hence $\epsilon_i^i = 0$.

Wagner further showed from the definition of the partial molar free energy, $\bar{G}_i = \left(\frac{\partial G}{\partial n_i} \right)_{n_j, \dots}$, that the Maxwell relations of thermodynamics could be used to show in infinitely dilute solution that

$$\epsilon_i^j = \epsilon_j^i \quad (3)$$

This expression has been termed the reciprocity relation and has the advantage that the effects of i on j and j on i are determined from the same set of data.

In 1955 Chipman⁽⁶⁾ showed that his earlier concepts were equivalent to Wagner's approach and presented an extensive determination and compilation of interaction parameters between various metals and carbon, oxygen, nitrogen, silicon, and sulfur in liquid iron. As more data became available for these and other elements, this compilation for a liquid iron solvent has been revised and up-dated. The latest form was presented by Elliott, Gleiser, and Ramakrishna⁽⁷⁾ in 1963.

A considerable amount of experimental effort has been expended towards defining interaction effects in molten iron. Although this listing is by no means all-inclusive, some of the more important investigators have been Chipman, Elliott, and co-workers in the United States, Turkdogan and co-workers in Great Britain in the 1950's, Schenck, Neumann, et al in Germany, and a number of researchers in Japan. Additional summaries and theoretical interpretations of experimental results in liquid iron have been made by Ohtani and Gokcen⁽⁸⁾ in 1960 and Wada⁽⁹⁾ in 1964.

Evidence for periodic variation of the interaction effects in liquid iron with the atomic number of the added solute was cited by Turkdogan,⁽¹⁰⁾ Wada,⁽⁹⁾ Fuwa and Chipman,⁽¹¹⁾ Neumann, Schenck and Patterson,⁽¹²⁾ and Ohtani and Gokcen⁽⁸⁾ among others.

Schenck, Frohberg, and Steinmetz⁽¹³⁾ and Daines and Phelke⁽¹⁴⁾ noted a comparable effect for ternary metallic additions on carbon dissolved in molten cobalt. However, all these authors were concerned with cases where the primary solute was carbon, sulfur, nitrogen, oxygen, or hydrogen - all gases or small-sized non-metallic elements. Wada and Saito⁽¹⁵⁾

and Wada⁽⁹⁾ collected the limited data for cases where two metal solutes were dissolved in liquid iron, but the data were too sparse to indicate if consistently periodic behavior existed.

Whereas a considerable amount of data are available for ferrous systems, the available information for non-ferrous systems is more limited. This is not to say that the thermodynamic properties of non-ferrous systems have not been investigated; there are a great many such studies reported in the literature. Compilations and critical evaluation of binary data and a limited amount of ternary data have been made by Kubaschewski and Catterall,⁽⁵³⁾ Kubaschewski and Evans⁽⁴⁰⁾ and Hultgren et al.⁽⁵⁴⁾ However, in most cases the data are unsuitable for the calculation of interaction parameters since the dilute solution region was not adequately covered. Dealy and Pehlke⁽¹⁶⁾ presented in 1963 a compilation of non-ferrous interaction parameters for those cases where data in the literature were complete enough to justify extrapolation to infinite dilution. Only experimental data were used that included solutions at least as dilute as 10 mole per cent and it was commented, "This is far from an ideal situation, and indeed, the results represent only the authors' best estimate from available sources." Values for only about 25 ternary systems were given together with a much greater number of values for self-interaction parameters.

Experimental studies specifically aimed at determining ternary interactions in non-ferrous systems at elevated temperatures have been quite limited. Wagner⁽²³⁾ studied interactions in mercury amalgams, but these were conducted at low temperatures. At higher temperatures,

Alcock and Richardson⁽¹⁷⁾ studied interactions with sulfur in several non-ferrous binary systems. Balzhiser⁽¹⁸⁾ investigated third-component interactions with the uranium-bismuth system. Obenchain⁽¹⁹⁾ studied third element interactions with bismuth-aluminum and lead-aluminum alloys. Wilder and Elliott⁽²⁰⁾ reported interactions in the aluminum-bismuth-lead system. Pehlke and co-workers^(21,63) have recently conducted studies of interactions in ternary non-ferrous systems. A limited test of the additivity hypothesis was recently made by Okajima and Pehlke⁽⁷³⁾ for multi-component additions to a solution of cadmium in lead. The ternary interaction parameters used to predict the multi-component effects were taken from the compilation of Dealy and Pehlke⁽¹⁶⁾ and it was stated that a quantitative evaluation of the additivity hypothesis in a non-ferrous system could not be made because of the limited accuracy of the available ternary interaction parameters. It was mentioned that a few tests were reported in the literature for ferrous systems involving sulfur, carbon, or nitrogen as the primary solute.

B. Theoretical Studies of Solute Interactions

Paralleling the phenomenological and experimental studies of solute interactions has been an extensive theoretical effort aimed at understanding the nature of the interactions and developing means for their prediction. Much of this has necessarily rested on the general development of thermodynamic theories of solution behavior.

Although other parameters have been proposed, the most commonly accepted ones are Wagner's which derive from the truncated Taylor series

for the natural logarithm of the activity coefficient. Schenck, Froberg and Steinmetz⁽¹³⁾ proposed an "efficiency" parameter and Turkdogan proposed a solubility difference function,⁽¹⁰⁾ both of which find use where the interaction is measured as a solubility effect. Ohtani and Gokcen⁽⁸⁾ proposed parameters which are not limited to the case where all solutes are dilute. The various parameters can be shown to be related by appropriate correction terms^(11,13) and most reduce to Wagner's parameters in the case where all solutes are dilute. The temperature dependence of interaction parameters has recently been discussed by Dealy and Pehlke⁽¹⁶⁾ and by Chipman and Corrigan.⁽²²⁾

The basis for theoretical study of the interaction parameters is the fact that excess free energy is given by the equation $\Delta\bar{G}_i^{XS} = RT \ln \gamma_i$. Hence, any thermodynamic formulation to explain partial solution behavior of component i should be differentiable with respect to the mole fraction of j to obtain the interaction parameter. Conversely, the adequacy of any solution theory can be tested by comparing observed interaction effects with the predicted effects.

The theoretical approaches to the interaction effects may thus be divided into cases where the interaction is considered directly or where it follows as a consequence of some solution model.

Specific discussion of interaction theory on a physical basis has been made by Wagner^(5,23) and Himmler⁽²⁴⁾ in terms of free electrons. The activity coefficient of a solute is expected to be increased by an additional solute if both of them change the electron/atom ratio in

solution in the same direction. If the electron/atom ratio is changed in opposite directions, the interaction is expected to be negative. Periodicity of interaction behavior was discussed by Schenck, Froberg, and Steinmetz⁽¹³⁾ in terms of valency electrons and the competition between the solutes and solvent for electrons to fill their unfilled inner shells. Other recent discussions of solution behavior in terms of electronic constitution and physical parameters have been made by Kleppa⁽²⁵⁾ and by Laurie and Pratt.⁽²⁶⁾ Many of these concepts follow the lead of Wagner^(5,23) from his series of papers and his classic book, "Thermodynamics of Alloys."

Somewhat more consideration has been given to the interaction consequences of solution models. Alcock and Richardson^(17,27) and Wada and Saito⁽¹⁵⁾ have derived specific expressions for the calculation of interaction parameters from statistical or chemical approaches to pair-interactions in solutions. Bonnier and co-workers^(29,30) have considered similar models for solution interactions. The general applicability of some simple models to metallurgical solutions was recently discussed by Oriani⁽³⁰⁾ and Oriani and Alcock.⁽³¹⁾ Additional general comments on common solution theories have been made by Richardson.^(1,32) Although the general question of solution thermodynamics and exact solution models continues to be a question occupying metallurgists, physicists and physical chemists (as evidenced by theoretical discussions in such journals as Journal of Chemical Physics, Acta Metallurgica, Journal of Physical Chemistry, etc.), the application to the metallurgical field continues to be in terms of the less sophisticated (and more practically useful)

solution models. These consist of the regular solution discussed by Hildebrand and Scott,^(33,34) the sub-regular solution model of Hardy⁽³⁵⁾ which has been applied to ternary systems by Yokokawa, Doi, and Niwa,⁽³⁶⁾ and the quasi-chemical model of Guggenheim.⁽³⁷⁾ This latter formed the basis for Wada and Saito's and Alcock and Richardson's approaches. Lumsden⁽³⁸⁾ also examined the thermodynamics of metallic alloys in terms of their experimental behavior and the statistical mechanics of liquid solutions.

The status and prospects for solution thermodynamics has been discussed periodically in conferences and symposia. In particular, the 1948 Discussion of the Faraday Society, the 1949 Seminar on Thermodynamics in Physical Metallurgy of the American Society for Metals, the 1958 Symposium on The Physical Chemistry of Metallic Solutions and Intermetallic Compounds of the National Physical Laboratory (Great Britain), the 1961 International Symposium on the Physical Chemistry of Process Metallurgy (Pittsburgh), and the 1964 Conference on Applications of Fundamental Thermodynamic Principles to Metallurgical Processes (University of Pittsburgh), have yielded valuable information on the uses and limitations of solution theories and their application to dilute solute interactions.

C. Experimental Methods

The determination of interaction effects necessarily requires that activity measurements be made in dilute solutions. General summaries and critical discussions of the available experimental methods have

been made by Chipman and Elliott,⁽³⁾ Chipman, Elliott, and Averbach,⁽³⁹⁾ Kubaschewski and Evans,⁽⁴⁰⁾ Wagner,⁽⁵⁾ and Lumsden.⁽³⁸⁾

The most important experimental methods are those involving equilibrium distribution of the solutes, static or dynamic vapor pressure measurements, or galvanic cell measurements.⁽³⁾

The galvanic cell method, which was used in this investigation, has been utilized by a number of workers. Wagner⁽⁵⁾ mentions a number of the experimental studies. Elliott and Chipman⁽⁴¹⁾ attribute the first elevated temperature galvanic cell studies to Taylor⁽⁴²⁾ in 1923. A comprehensive bibliography of galvanic cell studies was given by Elliott and Chipman in 1949,⁽⁵⁾ while additional studies since that time are too numerous to summarize here. The general limitations of the galvanic cell method for thermodynamics studies have been considered by Chipman, Elliott, and Averbach⁽³⁹⁾ and Wagner⁽⁵⁾ and Wagner and Werner.⁽⁴³⁾ Dealy and Pehlke⁽⁴⁴⁾ recently discussed the specific limitations of the galvanic cell method in the determination of interaction parameters.

D. Previous Studies of Binary and Ternary Systems Involving Zinc and Bismuth

The basic system on which the interaction measurements were made was the dilute solution of zinc in bismuth. Although previous studies have been conducted on this binary system and several of the ternary systems used on the present investigation, no systematic activity data are available in the literature that cover the dilute solution range below .052 mole fraction zinc.

Galvanic cell studies of the binary system zinc-bismuth were made at 600°C by Kleppa⁽⁴⁴⁾ and by Kleppa and Thalmayer.⁽⁴⁶⁾ Lantratov and Tsarenko⁽⁴⁷⁾ also used galvanic cell measurements to cover approximately the same composition range at temperatures between 420 and 800°C. Yokokawa, Doi, and Niwa⁽³⁶⁾ used a dynamic vapor pressure method to determine the activity of zinc at 352°C at three compositions between .052 and .151 mole fraction zinc. Wittig, Muller, and Schilling⁽⁴⁸⁾ calorimetrically studied the heats of mixing in the bismuth-zinc system at 470°C. An activity investigation of the zinc-bismuth system was also reported by Oleari, Fiorani, and Valenti⁽⁴⁹⁾ but the reference was unavailable. Critical evaluations of binary data for the zinc-bismuth system (primarily based on Kleppa's results) were made by Kubaschewski and Catterall⁽⁵³⁾ and Hultgren et al.⁽⁵⁴⁾

Activity measurements of zinc in ternary systems involving bismuth were made by Valenti, Oleari, and Fiorani⁽⁵⁰⁾ for Zn-Bi-Pb at 440 and 520°C, by Fiorani and Oleari⁽⁵¹⁾ for Au-Cd-Bi at 450 to 550°C, and by Oleari and Fiorani⁽⁵²⁾ on Zn-Sn-Bi at 450 to 550°C, all by the galvanic cell method. Dynamic vapor pressure measurements were used by Yokokawa et al.⁽³⁶⁾ to determine zinc activities in the Sn-Zn-Bi and In-Zn-Bi ternaries at 352°C. All of these investigations were conducted at constant mole ratios of bismuth to the secondary solute and none of the composition ranges approached the region where the solution was dilute with respect to both solutes. Iso-activity plots presented by Oleari and co-workers gave qualitative indication of the expected direction of the dilute solution interaction as did the data of Yokokawa et al.

The indications were that cadmium would have a very slight effect on the activity of zinc but the direction was uncertain. Indium and lead apparently increased the zinc activity, while tin decreased it.

Phase diagrams were available for several of the experimental systems. The zinc-bismuth binary system is discussed in Hansen's compilation of binary diagrams.⁽⁵⁵⁾ A ternary diagram for the Bi-Zn-Cu system was presented by Henglein and Köster,⁽⁵⁶⁾ while Geurtler et al.⁽⁵⁷⁾ summarized the available ternary information for the Bi-Zn-Ag, Bi-Zn-Sn, Bi-Zn-Sb, and Bi-Zn-Pb systems. Oleari and co-workers⁽⁵⁰⁻⁵²⁾ presented information on the liquidus surface boundaries for the Bi-Zn-Cd, Bi-Zn-Sn, and Bi-Zn-Pb systems.

III. EXPERIMENTAL PROGRAM

The experimental program was planned so that a simultaneous study could be made of the hypotheses of periodicity and additivity of interaction effects in a system where all the components were non-ferrous metals. The interaction parameters were determined for a series of third-element additions to a given solute-solvent system, zinc in bismuth. The choice of the third elements allowed the test of the periodicity hypothesis. Once the ternary systems were studied, the added solutes were combined to form higher-order solutions for the test of the additivity hypothesis.

In the sections which follow, the experimental design for interaction parameter determination is considered. The advantages and limitations of the various experimental methods are discussed and the basis for the selection of the zinc-bismuth system is reviewed. Finally, the experimental equipment, procedures, and treatment of the data are discussed.

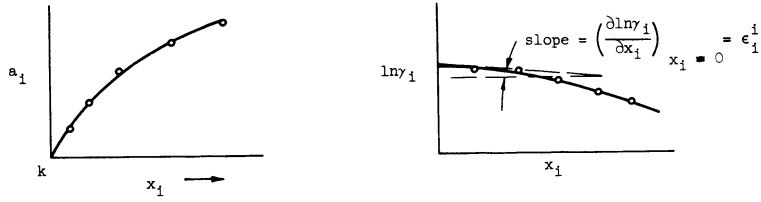
A. EXPERIMENTAL DESIGN

1. Methods of Evaluating Interaction Parameters

Before discussing the choice of the experimental method, the experimental design for the determination of interaction parameters should be considered.

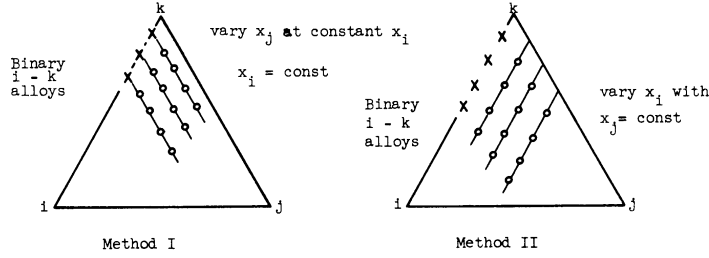
The binary or self-interaction parameter, $\epsilon_i^i = \left(\frac{\partial \ln y_i}{\partial x_i} \right)_{x_i=0}$,

is evaluated as the limiting slope of a plot of $\ln y_i$ versus x_i and is obtained from activity measurements made on dilute binary alloys. (See Figure 1)

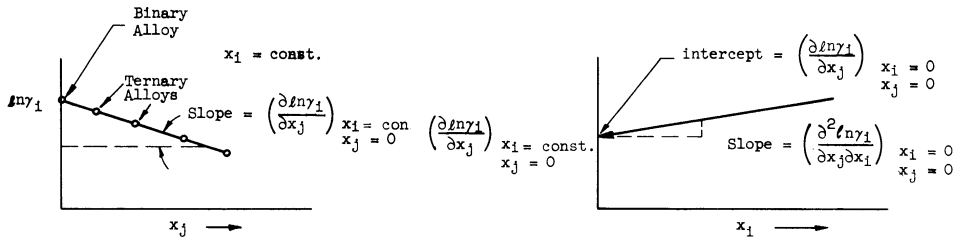


1. Determine a_i for values of x_i
2. Calculate $\gamma_i = \frac{a_i}{x_i}$
3. Plot $\ln \gamma_i$ versus x_i
4. Limiting slope is interaction parameter.

a) Determination of Self-Interaction Parameter.

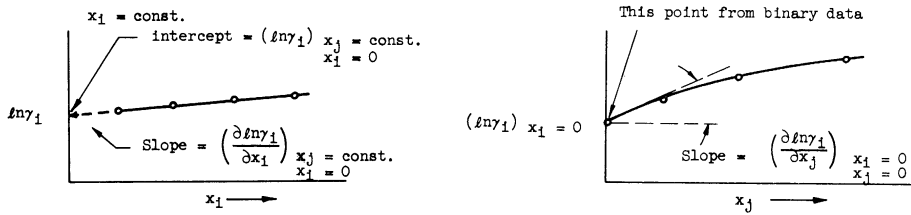


b) Experimental Compositions for Interaction Parameter Measurements Using Runs at Constant Mole Fraction of One Solute.

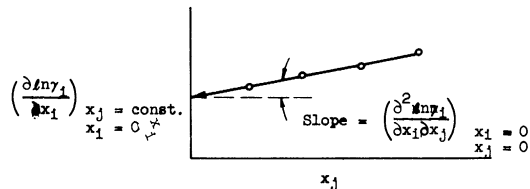


1. Plot data from each run, then determine slope.
2. Extrapolate slopes to $x_i = 0$; slope of this plot is 2nd-order parameter.

c) Method I. Runs at Constant x_i , Varying x_j



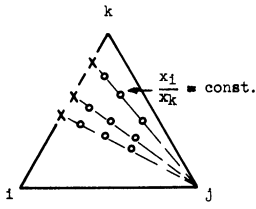
1. Plot data from each run, extrapolate to $x_i = 0$.
2. Plot extrapolated values versus x_j , limiting slope is ϵ_1^j .



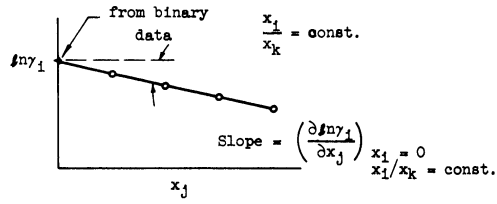
3. Determine 2nd-order parameter from separate plot of slopes of extrapolation lines used in Step 1.

d) Method II. Runs at Constant x_j , Varying x_i

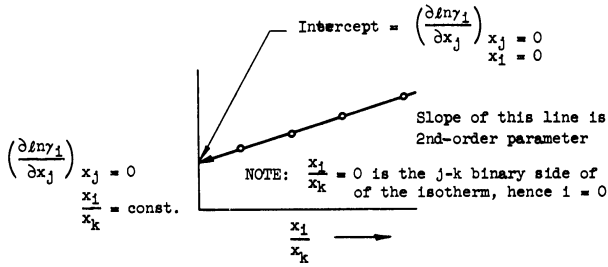
Figure 1. Methods of Evaluating Interaction Parameters.



1. Conduct runs along constant mole ratio lines.

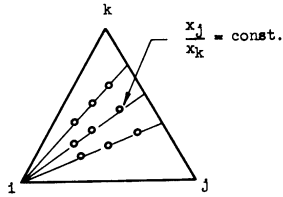


2. Plot data from each run, then determine slope.

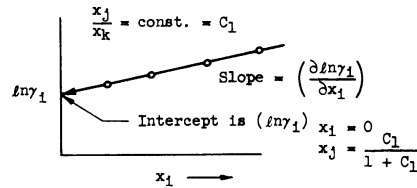


3. Plot slopes versus $\frac{x_1}{x_k}$, intercept is ϵ_1^j

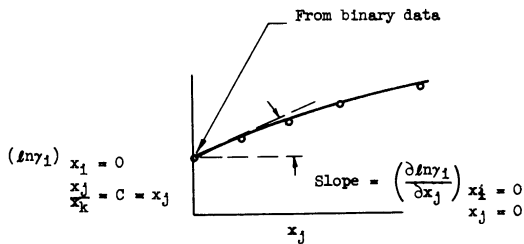
e) Method III. Runs at Constant $\frac{x_1}{x_k}$, Varying x_j .



1. Conduct runs along constant mole ratio lines.



2. For each constant $\frac{x_j}{x_k}$, extrapolate $\ln \gamma_1$ to $x_1 = 0$; Note that at $x_1 = 0$, $\frac{x_j}{x_k}$ reduces to binary case and $x_j = \frac{C_1}{1 + C_1}$.



3. Plot extrapolated values versus x_j , limiting slope is ϵ_1^j .

f) Alternate Method III. Runs at Constant $\frac{x_j}{x_k}$, Varying x_1 .

Figure 1 (Cont'd)

The definitive expression for the first-order ternary parameter, $\epsilon_i^j = \left(\frac{\partial \ln \gamma_i}{\partial x_j} \right)_{x_i=0, x_j=0}$, requires that the activity coefficient of constituent

i be determined to vanishingly small concentrations of both solute elements. Several methods by which this can be accomplished are indicated schematically in Figure 1. First, a systematic series of experimental runs could be made in which the concentration of the third element or added solute is varied while holding constant the concentration of primary solute. A second method would be one in which the third element concentration is held constant and the primary solute concentration is varied. Finally, it is possible to hold constant the ratio of either solute to the solvent while the concentration of the other solute is varied. By suitable manipulation of plots of $\ln \gamma_i$ versus concentration, the interaction parameter is found as the appropriate slope or intercept at zero concentration of the two solutes. The various methods will be discussed below in greater detail.

Method I, which was used in the present investigation, requires that the activity coefficient of constituent i be determined as a function of the third element content, x_j , at several constant values of x_i . The limiting slope of a plot of $\ln \gamma_i$ versus x_j is $\left(\frac{\partial \ln \gamma_i}{\partial x_j} \right)_{x_i=\text{const.}, x_j=0}$.

By plotting the slope values versus x_i and then extrapolating to $x_i = 0$, the intercept is $\left(\frac{\partial \ln \gamma_i}{\partial x_j} \right)_{x_i=0, x_j=0}$, the desired parameter. The limiting slope

of this plot is, in turn, $\left(\frac{\partial^2 \ln y_i}{\partial x_j \partial x_i} \right)_{\substack{x_i=0 \\ x_j=0}}$, a second-order interaction

parameter. It is desirable that as many data points as possible be available to allow a reasonable decision regarding the limiting slope. For this purpose Method I is of advantage since the end-point of the relation between $\ln y_i$ and x_j at $x_j = 0$ is known independently from binary data. Thus, if n data points are known from the ternary alloys, an $n + 1^{\text{th}}$ point is available to aid in constructing the intermediate plot.

Method II requires the same amount of experimental data as Method I, however, in this case the amount of the third element, x_j , is held constant and the amount of the primary solute, x_i , is varied systematically. The intercept at $x_i = 0$ of a plot of $\ln y_i$ versus x_i is the value $\left(\ln y_i \right)_{\substack{x_i=0 \\ x_j=\text{const.}}}$. The limiting slope of a plot of

$\left(\ln y_i \right)_{\substack{x_i=0 \\ x_j=\text{const.}}}$ versus x_j is the desired parameter, $\epsilon_i^j = \left(\frac{\partial \ln y_i}{\partial x_j} \right)_{\substack{x_i=0 \\ x_j=0}}$.

The second-order parameter $\left(\frac{\partial^2 \ln y_i}{\partial x_i \partial x_j} \right)_{\substack{x_i=0 \\ x_j=0}}$ is found as the limiting slope of a plot of $\left(\frac{\partial \ln y_i}{\partial x_i} \right)_{\substack{x_j=\text{const} \\ x_i=0}}$ versus x_j . The values of $\left(\frac{\partial \ln y_i}{\partial x_i} \right)_{\substack{x_j=\text{const} \\ x_i=0}}$

are previously determined as the limiting slopes of the plots of $\ln y_i$ versus x_i , but are subject to some error because the limiting portion of the plot is extrapolated. In using Method II, the binary data are of no help in constructing the intermediate plots for the determination

of ϵ_i^j , however, they do provide the value of $\ln \gamma_i$ which is the end-point of the final plot.

Method III requires that several runs be made where the ratio of one solute to the solvent is held constant while the amount of the other solute is varied. That is, either $\frac{x_i}{x_k} = \text{const.}$ and x_j is varied, or $\frac{x_j}{x_k} = \text{const.}$ and x_i is varied. Then, for example, the values of $\ln \gamma_i$ are plotted versus x_j . The limiting slopes of these plots

$\left(\frac{\partial \ln \gamma_i}{\partial x_j} \right)_{\frac{x_i}{x_k} = \text{const.}}$ are plotted versus the ratio at which they were obtained $\frac{x_i}{x_k}$. The intercept of this plot at $\frac{x_i}{x_k} = 0$ corresponds to the condition $x_i = 0, x_k = 1$ and is the desired parameter $\left(\frac{\partial \ln \gamma_i}{\partial x_j} \right)_{\substack{x_i=0 \\ x_j=0}}$.

The limiting slope of this plot is $\left(\frac{\partial^2 \ln \gamma_i}{\partial x_j \partial x_i} \right)_{\substack{x_i=0 \\ x_j=0}}$ and is the second-order parameter. (This will be discussed later in detail).

It is preferable that the data employed in each intermediate plot (where the mole fraction of one solute is held constant) be obtained under comparable experimental conditions. Consequently, the use of a multi-alloy experimental apparatus is highly desirable.

Of the various methods described, a sequence of experiments following Method I is preferable since this has the advantage of clearly showing the nature of the interaction as the data are being obtained. Thus, in each run at constant x_i , the effect of the additions, x_j , is directly evident.

Furthermore, as noted previously, data from binary alloys provide an independent end-point to the relation between $\ln \gamma_i$ and x_i , and finally another advantage of Method I is that the second-order parameter is easily obtained. By using the same sequence of compositions for both x_i and x_j , i.e., if a regular matrix of compositions is employed, a set of data can be analyzed by Method I and cross-checked by Method II. This was done in several cases and virtually identical results were obtained. Method I is slightly preferred since the final parameter is obtained by extrapolation of the slopes taken from the intermediate plots. Each of these slopes has the same mathematical form as the final interaction parameter and is an intermediate parameter describing the effect at some finite composition. Statistical studies on a representative set of data showed that closer confidence limits could be placed on the first-order interaction parameter if Method I were used rather than Method II. (Appendix C)

By proper selection of the compositions to be studied, Method III would also permit cross-checks between its two variations, however, the advantage would be lost of varying x_j at constant x_i and thus clearly showing the interaction independent of the value of x_i . The only advantage of Method III is that it would provide data at constant mole ratio which is required by some methods of ternary integration of the Gibbs-Duhem equation.^(3,60) However, if needed, these values could be obtained by interpolation of data obtained by Method I if a regular matrix of compositions were used. Since the principal purpose of this investigation

was to determine the interaction parameters, Method III was of no advantage.

2. Experimental Methods for Determining Activity

Although a number of experimental methods are available for the measurement of activities and activity coefficients it has been pointed out⁽³⁾ that fundamentally they reduce to two cases. First, a solution may be equilibrated with another phase in which the activity is known or may be calculated, or, second, a partial equilibrium may be established and then the potential determined to bring the system to complete equilibrium.

For liquid metallic solutions the available methods are those related to either static or dynamic vapor pressure measurements, the equilibrium distribution of a solute between immiscible solvents, the deduction of the activity from the equilibrium constant of a chemical reaction provided that the activities of the other constituents are known or can be fixed, or by means of electrode potential (galvanic cell) measurements.

Chipman and Elliott⁽³⁾ state that, where applicable, the electrode potential method is one of the most precise methods for determining activities. Kubaschewski and Evans⁽⁴⁰⁾ reported that the electrode potential method is considered slightly superior to other equilibrium methods.

In the present investigation it was necessary that a large number of alloys be investigated under reproducible conditions and, in order to make best use of Method I for the evaluation of interaction parameters, preferably in groups where the concentration of one solute could be held constant and that of the other varied systematically.

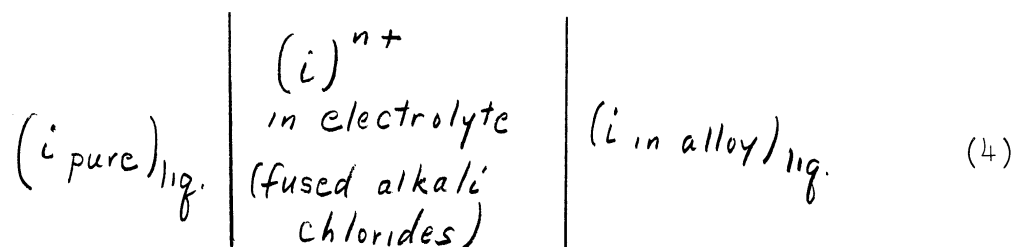
The use of the equilibrium distribution method would limit the investigation to systems where multiphase equilibrium is expected and would be dependent on the ability to deduce or fix the activity in at least one of the phases. The precision of the method depends on the ability to analyze chemically for small differences in concentration of the constituent of interest while in the presence of other alloying elements.

Vapor pressure measurements require that only the constituent of interest have an appreciable vapor pressure or that a multi-component effluent vapor must then be analyzed chemically or that a radioactive isotope of the constituent of interest be used. Norman, Winchell, and Staley⁽⁵⁸⁾ used a mass spectrometer to analyze the effluent vapor from liquid In-Sb-Zn alloys. The reported accuracy of such measurements is 90 per cent or less and has the disadvantage that the alloy is depleted of the volatile component in order to make a measurement. The available vapor pressure methods are in general not readily adaptable to multi-alloy experimental runs.

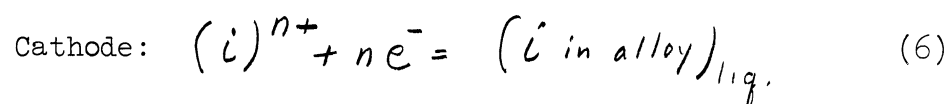
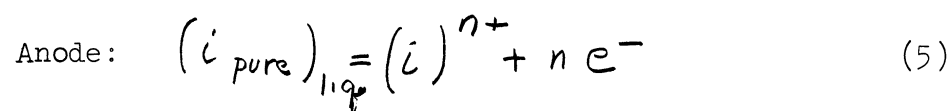
In the case of electrode potential or galvanic cell measurements, a direct measurement of the activity is possible through the free

energy relationships and thus the problems of deducing activity from chemical or other analyses can be avoided. Furthermore, the yield of data per experiment can be increased substantially by using a multi-electrode apparatus since a series of compositions can be investigated at one time, using a common reference electrode, without interference from each other. The galvanic cell is thus ideally suited for the application of Method I for the evaluation of the interaction parameter.

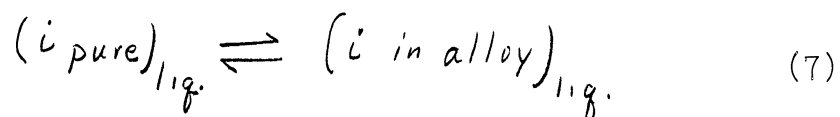
In order to use the electrode potential method at elevated temperatures, concentration cells of the following type are set up:⁽³⁾



The electrode reactions are written as:



The net reaction of the cell is:



The alloy might consist of merely metal *i* plus its solvent or might include the additional solutes. At elevated temperatures,

electrolytes of fused alkali chlorides have been successfully used by a number of investigators. (5, 20, 21, 39, etc.)

At constant temperature and pressure, the free energy change of the reaction (Equation (7)) is given (60, 76) by:

$$\Delta \bar{G}_i = \bar{G}_i - G_i^\circ = -nFE = RT \ln \frac{a_i \text{ (in alloy)}}{a_i \text{ (pure liquid)}} \quad (8)$$

If the standard state is taken as pure liquid i and the activity in the standard state is taken as one, then Equation (8) becomes:

$$-nFE = RT \ln a_i \text{ (in alloy)} \quad (9)$$

By definition, the activity coefficient is

$$\gamma_i = \frac{a_i}{X_i} \quad (10)$$

Thus, Equation (9) can be rewritten as:

$$\frac{-nFE}{RT} - \ln X_i = \ln \gamma_i \quad (11)$$

Or in equivalent form:

$$\gamma_i = \frac{1}{X_i} \exp -\frac{nFE}{RT} \quad (12)$$

(i dissolved in alloy)

The assumptions inherent in the use of the measured potentials in these equations are the following:

1. The cell is reversible.
2. The electrolyte exhibits only ionic conductance.
3. The net cell reaction is the only one that occurs to a significant extent.
4. The alloy compositions are as stated, are single-phase, or if multi-phase, their compositions are known.

The interaction parameters are then obtained by suitable manipulation of the logarithm of the activity coefficient as discussed in the preceding section.

When the experimental runs are conducted by Method I (constant x_i while varying x_j), the interaction parameters can be calculated directly from the electrode potentials by virtue of the following relationships.

Since, by definition,
$$E_i^j = \left(\frac{\partial \ln \gamma_i}{\partial X_j} \right)_{x_i=0, x_j=0} \quad (2a)$$

Equation (11) can be differentiated with respect to x_j , while holding P, T, and x_i constant.

$$\left. \frac{\partial}{\partial X_j} (\ln \gamma_i) \right|_{x_i, P, T} = - \frac{nF}{RT} \left(\frac{\partial E_i}{\partial X_j} \right)_{x_i, P, T} + \left. \frac{\partial}{\partial X_j} \ln x_i \right|_{x_i, P, T} \quad (13)$$

The limiting slope of a plot of E_i versus x_j (at constant $P, T,$ and x_i) is

$$\left(\frac{\partial E_i}{\partial x_j} \right)_{\substack{x_i = \text{const} \\ x_j = 0 \\ P, T}} = - \frac{RT}{nF} \left(\frac{\partial \ln a_i}{\partial x_j} \right)_{\substack{x_i = \text{const} \\ x_j = 0 \\ P, T}} \quad (14)$$

Then by Method I, cross-plotting $\left(\frac{\partial E_i}{\partial x_j} \right)_{\substack{x_i = \text{const} \\ x_j = 0}}$ versus x_i

and extrapolating to $x_i = 0$, the intercept is

$$\left(\frac{\partial E_i}{\partial x_j} \right)_{\substack{x_i = 0 \\ x_j = 0 \\ P, T}} = - \frac{RT}{nF} \left(\frac{\partial \ln a_i}{\partial x_j} \right)_{\substack{x_i = 0 \\ x_j = 0 \\ P, T}} \quad (15)$$

or

$$E_i^j = - \frac{nF}{RT} \left(\frac{\partial E_i}{\partial x_j} \right)_{\substack{x_i = 0 \\ x_j = 0 \\ P, T}} \quad (16)$$

3. Sources of Error in Galvanic Cell Measurements

The application of the galvanic cell method requires more than that alloys of proper composition be coupled with a fused alkali-chloride electrolyte, and a potential measured across a pair of leads extending into the alloys. The method depends on the realization in practice of the assumptions listed on p.27, and furthermore, as aptly stated by Chipman et al, (39) "because of very subtle conditions that may be present

in a given cell, the unwary experimentalist may be deluded into thinking that the results may have high accuracy and precision, whereas they may have only high precision."

It is essential that the various sources of error that might affect the measured potentials be recognized and their affects alleviated. The means available for this may rest in the design and construction of the experimental apparatus, the care and consistency in the experimental procedures, or in the choice of the alloy systems studied. In some cases where errors are unavoidable, their extent should be estimated and minimized, if possible, by means of the experimental design.

A summary of the various sources of error that might conceivably be encountered in an investigation such as the present one has been made in Table I.^(3,5,39) For convenience, the error sources have been classified in three major categories:

1. Deviations in electrode compositions from physical or chemical causes.
2. Effects occurring within the electrolyte.
3. Effects related to the cell operation.

The various errors are loosely classified as systematic or random. This distinction is intended to indicate that if such an error occurs it may affect the measured cell potential consistently in one direction or in either direction.

At first glance, Table I indicates that an imposing list of pitfalls may be encountered in galvanic cell studies, however, closer examination reveals that many of the sources of error can be alleviated

TABLE I
SOURCES OF ERROR IN GALVANIC CELL DETERMINATION OF ACTIVITY

<u>Classification</u>	<u>Possible Effect on Observed EMF</u>	<u>Remedy</u>
<u>Deviation in Electrode Compositions</u>		
<u>Physical Effects</u>		
Initial Composition	Random, but probably slight	Care in calculations and weighings; be certain alloy is single phase
Loss of Constituents From System		
a. Solubility on Electrolyte	Systematic; if active element, increases EMF; if third element, decreases inter-action	Use excess of metal chloride in electrolyte; maintain almost static atmosphere at increased pressure
b. Volatilization		
Change of Composition Within System (Material Transfer)		
a. Current Flow	Generally random; redistribution by diffusion can decrease observed EMF	Avoid lengthy closing of circuit and possible short circuiting; improve cell geometry; make running time short; use care in handling assembled cell
b. Diffusion		
c. Spillage or Mixing		
<u>Chemical Effects (Side Reactions)</u>		
Reactions With Cell Materials	Random	Use fresh, clean refractories; be sure lead materials do not dissolve
Reaction With Metal Chlorides in Electrolyte		
a. With Solvent	Systematic; decreases EMF since active element is displaced from electrolyte into alloy	Restrict systems studied to those meeting criteria for minimum difference standard free energy of chloride formation (see Tables II and III)
b. With Third Element		
<u>Effects Within the Electrolyte</u>		
Non-Ionic Conductivity	Systematic, increases EMF	Use alkali-chloride electrolyte with only a small amount of the active metal chloride
Multi-valency of Ions	Systematic, increases EMF due to oxidation and change of "n" in activity calculations	Keep concentration of active metal chloride small, confirm valence by Faraday's Law
Moisture or Oxides	Systematic, decreases EMF due to reduction of active metal chloride	Dry electrolyte materials and use care in handling; Maintain dry, inert atmosphere above cell
Liquid Junction Potentials	Random, opposes desired EMF by superimposition	Allow time for diffusion in electrolyte before starting readings; agitate electrode leads; refer measurements to a reference binary electrode replicated from cell to cell
Concentration Gradients	Random, enhances or opposes desired EMF by a superimposed concentration cell	"
<u>Effects Related to Cell Operation</u>		
Irreversibility	Systematic, reduces EMF by unwanted material transfer	Be certain cell is at equilibrium for readings; check by changes of electrode position
Thermal Equilibrium	Systematic, opposes or increases EMF	Allow time between temperature changes to insure thermal equilibrium
Polarization	Random, may affect EMF either direction depending on current flow	Close circuit for readings only momentarily; allow time for diffusion between readings; use liquid electrodes for faster diffusion
Temperature Measurement		
a. Thermocouple Calibration	Variable effect on EMF, not predictable	Check calibration of thermocouples and temperature distribution in cell
b. Thermocouple Placement		
Thermal Potentials		
a. Temperature Gradients	Variable effect on EMF, not predictable	Check temperature distribution; agitate electrolyte to minimize gradients; be sure leads are homogeneous or else measure thermocouple effect separately and compensate readings; use liquid electrodes
b. Thermocouple Effect From Dissimilar Leads		
c. Thermocouple Effect From Inhomogeneous Electrodes		

by careful experimental procedures, while others can be eliminated in the experimental design.

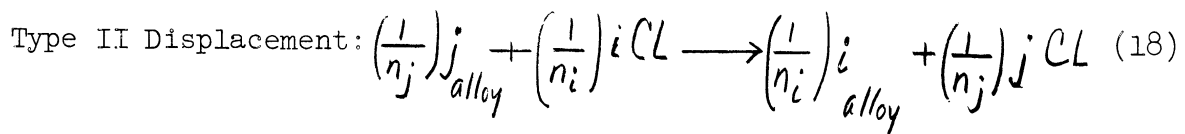
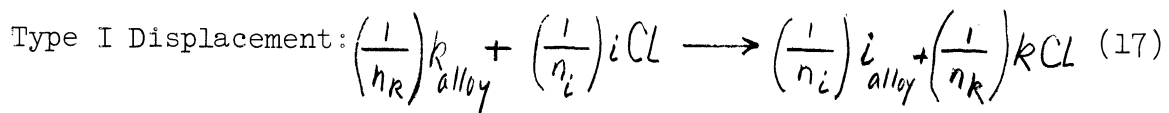
The principal source of errors whose effects are always in one direction are the possibilities of compositional changes - either gains or losses. The loss of an alloy constituent may occur by volatilization or by solution in the electrolyte, while an increase in the concentration of the primary solute may occur from side reactions taking place at the electrolyte/alloy interface.

The initial compositions also could be in error by virtue of purely mechanical errors in charge calculations or weighings. Furthermore, there are processes which could tend to redistribute the alloying elements within the cell. This could occur if the circuit is closed for an excessive time during the measurement of the potentials or at some other time by a short circuit across the leads. The redistribution might also take place by a diffusional process. If the cell is handled roughly or the electrodes agitated too severely, it is even possible to transfer material by spilling. Any process which causes a decrease in x_i will result in an increase in the measured potential, while any loss of the secondary solute j reduces the extent of the interaction in whatever direction it occurs. When the electrodes are solid, there is the possibility that compositional inhomogeneities or residual strains might give rise to extraneous potentials.

Purely chemical effects are termed "side"-reactions and are those reactions which can occur in addition to the net cell reaction.

These can be subdivided into reactions that might take place with the cell materials and those arising from the electrolyte. The first type can be controlled by using only fresh, clean materials in assembling the cell, using care to insure that no impurities are introduced and by being certain that the lead and containing materials are unattacked by the alloys or the electrolyte.

The side reactions which occur at the alloy/electrolyte interface are unavoidable but can be minimized by judicious choice of the systems to be investigated. These reactions are also termed displacement reactions since they can result in an unwanted reduction or displacement of the i-metal-chloride in the melt by either the solvent or the second solute.^(5, 43, 44) The two types of displacement reactions are written as:



where n_i , n_j , n_k are the valences in the electrolyte of the metal ions of the solutes i and j and the solvent k .

The result of either reaction is that the concentration of i increases in the alloy and concentration gradients also result in both the electrolyte and the alloy, thus causing overpotentials. The

estimation and control of these reactions has been discussed by Wagner and Werner⁽⁴³⁾ and by Dealy and Pehlke.⁽⁴⁴⁾ By assuming chemical equilibrium at the interface, and that $a_i = x_i \gamma_i^\circ$, $a_k \cong 1$, $\gamma_{kCl}^\circ \cong \gamma_{iCl}^\circ \cong 1$, a thermodynamic analysis can be made of the expected error in potential due to either reaction. For Type I reactions the expression for the error takes the form:

$$\text{relative error} \cong \frac{n_k}{n_i} \left[\exp \frac{-n_k \Delta G_I^\circ}{RT} \right] \left(\frac{x_{iCl}}{x_i \gamma_i^\circ} \right)^{\frac{n_k}{n_i}} \left(\frac{1}{x_{iCl}} + \frac{1}{x_{i_{alloy}}} \right) \quad (19)$$

where ΔG_I° is the standard free energy change for the reaction and is the difference in the standard free energies of formation for the appropriate metal chlorides. For Type II reactions, the expression has a slightly different form:

$$\text{relative error} \cong \frac{n_j}{n_i} \gamma_j x_j \left[\exp \frac{-n_j \Delta G_{II}^\circ}{RT} \right] \left(\frac{x_{iCl}}{x_i \gamma_i^\circ} \right)^{\frac{n_j}{n_i}} \left(\frac{1}{x_{iCl}} + \frac{1}{x_{i_{alloy}}} \right) \quad (20)$$

It can be seen that the error in measured potential increases as x_j is increased, increases as x_i is decreased, and increases as x_{iCl} is increased. It should also be noted that the chloride of the metal i whose activity is to be measured must have a free energy of formation more negative than those of the solvent or the other solutes.

If an acceptable level of error is fixed in advance and the minimum values of x_i and x_{iCl} and maximum value of x_j are also fixed, it is then possible to compute the minimum ΔG_I° or ΔG_{II}° which

meets these criteria. Thus, the feasibility of galvanic cell investigation of a proposed alloy system may be easily determined. The calculated values become less as the valence of the metals increase. Dealy and Pehlke⁽⁴⁴⁾ considered the case where the tolerable error was one per cent at 550°C and x_i , x_j and x_{iCl} were 0.01. A tabulation was made of the minimum ΔG° for both types of reaction as a function of n_i and n_j . The values of $\Delta G_{I,II}^\circ$ can be used in conjunction with the free energies of formation of various metal chlorides to aid in the selection of systems for study. It is also useful to convert the calculated minimum $\Delta G_{I,II}^\circ$ to corresponding potential differences which can be utilized for similar selection criteria with the electromotive force series determined by Laitinen and Liu⁽⁵⁹⁾ for the fused LiCl-KCl electrolyte. Thus, in the case of displacement reactions, the unavoidable error can be minimized in advance by means of the experimental design.

Errors arising from effects within the electrolyte are those due to the failure of the assumptions regarding the conductivity of the electrolyte or the valency of the i-ions, to the presence of impurities, or the existence of concentration gradients or junction potentials. It is generally held that the use of an electrolyte containing a small concentration of the i-metal chloride dissolved in an alkali-metal chloride, i.e., the LiCl-KCl eutectic, will minimize both the effects of non-ionicity of conduction and the possibility that the $(i)^{n+}$ ions may be present in more than one valency state.^(39,42) This is the major reason why the alkali-metal chlorides were developed in preference to merely

using the pure fused i-metal chloride as the electrolyte. If multivalent ions were present in significant amounts, current could flow by their oxidation to the more positive state at the cathode.

Displacement reactions similar to the types discussed previously may also be caused by the presence of oxidizing or reducing agents in the electrolyte. Hence, it is essential that the electrolyte be prepared as free as possible from moisture, that an inert atmosphere be maintained above it, and that the electrodes be kept as free as possible of oxidation during their preparation.

Further possibilities for error are that concentration gradients in the electrolyte might give rise to a liquid junction potential at the interface between regions of differing concentration or that a separate concentration cell may be superimposed on the desired cell.

The operation of the cell may also result in errors unless reasonable care is taken. The electrodes must have sufficient time for diffusion so that constitutional equilibrium is reached and a thermal equilibrium must also be established before meaningful readings can be made. In taking readings, the circuit must be closed only momentarily so that mass transfer and polarization are avoided. A null-balance potentiometer greatly alleviates this possibility since the current flow is slight and in random directions as the balance is attained. Polarization is minimized by allowing sufficient time for diffusion between readings.

Absolute errors in interpreting the data may also result from the temperature measurement practice. The thermocouples should be checked and their placement verified to confirm that the true cell temperature is being measured. It is also necessary to eliminate the possibility of thermal potentials due to temperature gradients. Another thermal effect is the imposition by a thermocouple effect of a potential on the leads if they happen to be dissimilar or non-homogeneous. If it is necessary to use dissimilar leads the effect can be compensated for by making a separate evaluation of the thermocouple formed by the leads and then using these results to correct the measured cell potentials.⁽⁷⁰⁾

4. Alleviation of Errors

Fundamentally there are only a few ways for dealing with the various sources of error that can occur in a galvanic cell investigation. The error source may be eliminated completely or made negligibly small by means of careful experimental technique and design, there may be reasonable grounds for assuming that it does not exist in a particular system, or a means can be introduced to compensate for the error.

The previous discussion of error sources included comments on the means of eliminating or reducing many of them. Primarily this consists of using care in the preparation and assembly of the cells, in the minimization of moisture and impurities in the electrolyte, and in confining measurements to systems where displacement reactions are negligible. In studying liquid cells at high temperatures, the diffusion rates are usually high enough to correct concentration gradients that may occur

from some transient effect such as current flow or a thermal gradient. The use of an electrolyte composed of only a few mole per cent of the i-metal chloride dissolved in eutectic LiCl-KCl has a number of advantages. Not only does this reduce the tendency for side reactions, but it inhibits the solution of the electrode metals in the electrolyte and minimizes the liquid junction potential.^(39,42) The reversibility of the cell may be inferred from the stability of the potentials and their reproducibility with time. The valency and the reversibility can also be confirmed by auxiliary experimental procedures in which known amounts of current are passed through the cell in both directions.

Nevertheless, despite taking all reasonable precautions in the experimental design and procedure, the large variety of possible error sources means that there still may be some random error possible from the cumulative effects of marginal sources. The utilization of a multi-electrode apparatus does provide a means for compensating these effects, and if Method I is used for the experimental design, it is possible to normalize the interaction parameter calculations to the same base point.

Method I requires that the mole fraction of the active element be held constant in each run while the concentration of the third element is varied in the other electrodes. By making one of the electrodes in each cell a binary alloy, it is then possible to directly evaluate the parameter from this base point since the parameter, a derivative, is a relative quantity. The experimental data from two such cells may be compared more accurately by normalizing the potentials from the ternary

alloys relative to the same value for the binary alloys. By this means, compensation can be made for effects operating on all the electrodes of a cell. Such effects might consist of the unavoidable residual impurities in the electrolyte or the standard or to a junction potential at the boundary between the standard and the electrolyte. By running a number of such binary alloys, and assuming that cumulative errors occur randomly, it is possible to make a statistical analysis of the inherent or "cell factor" errors systematically affecting the absolute value of the potential of each electrode and to establish standard values of potential for the binary alloys of each composition. By referring the interaction parameter calculations to such standard values or base points, the remaining scatter in the data can be inferred as primarily related to "third element" or ternary factors.

It is thus possible, through a combination of experimental technique and design, to realize in practice the assumptions on which rest the use of the equation for activity determination.

5. Choice of Alloy Systems

The choice of the alloy system to be studied was based on the desire to test hypotheses regarding the periodicity and the additivity of the interactions with added solutes. It was thus necessary to choose a binary system permitting dilute solute additions taken in distinct sequences in the Periodic Table and also that would be expected to form single-phase liquid solutions in both ternary and multi-component systems. However, a number of other requirements had to be met. In order to form

the galvanic cells the primary solute had to be substantially more active in the electromotive force series than many other metals. The single phase liquid solutions had to exist at temperatures within the range of the materials used for cell construction and the alloys should attack neither the containers nor the electrode leads. The necessity of minimizing side reactions also governed the choice of the solute and the solvent. Finally, potential health hazards had to be considered with the use of certain materials.

The starting point for the selection of the alloy systems was to consider the possible cells from the standpoint of experimental convenience and the likelihood of displacement reactions. A preferable upper temperature limit for the studies was 650-700°C. The basis for the preliminary selection was the standard free energy of formation of the metal chlorides and calculations which provided criteria for assessing the possibilities of displacement reactions. These were based on the minimum difference in free energy of chloride formation so as to result in only one per cent error in the measured potentials assuming the worst cases where the mole fractions of the active metal and its chloride in the electrolyte were both .01 and the mole fraction of the third element was large.

Table II presents the ΔG_f° per gram equivalent at 550°C for the formation of a number of metal chlorides. The values summarized in this table were taken from several sources: Dealy and Pehlke⁽⁴⁴⁾ who made their calculations from values given in Pitzer and Brewer;⁽⁶⁰⁾ Yamagishi and Kamemoto;⁽⁶¹⁾ and Kellogg.⁽⁶²⁾ The table also includes

TABLE II
STANDARD FREE ENERGY OF FORMATION FOR VARIOUS METAL CHLORIDES

Metal	Valence	<u>-ΔG_f for Chlorides at 550°C -kcal/g.atom</u>			<u>EMF of Metal Relative to Pt</u>
		<u>Dealy and Pehlke⁽⁴⁴⁾</u>	<u>Yamagishi and Kamemoto⁽⁶¹⁾</u>	<u>Kellogg⁽⁶²⁾</u>	<u>in LiCl-KCl at 450°C -volts</u>
					<u>Laitinen and Liu⁽⁵⁹⁾</u>
K	1	85.7	85.7	--	--
Na	1	80.0	--	80.0	--
Ca	2	76.5	--	--	--
Li	1	--	80.6	--	-3.41
Gd	3	--	67.7	--	--
Mg	2	61.0	60.8	61.0	-2.58
Mn	2	44.8	42.9	44.5	-1.85
Al	3	42.1	--	46.0	-1.80
Tl	3	37.0	--	--	-1.37
Zn	2	36.8	36.2	36.5	-1.57
Cr ⁺²	2	--	36.0	--	-1.42
Cd	2	31.4	33.0	31.5	-1.32
Cr ⁺³	3	29.0	29.3	--	-0.63
In	3	--	29.0	--	-0.84
Pb	2	28.8	--	29.0	-1.10
Fe ⁺²	2	25.1	28.8	28.5	-1.17
Sn ⁺²	2	26.6	24.0	27.0	-1.08
Ga	3	--	--	--	-0.88
Cu ⁺¹	1	22.8	23.2	--	-0.85
Sb	3	19.2	23.1	--	-0.67
Co	2	24.2	23.0	--	-0.99
Sn ⁺⁴	4	--	22.9	--	--
Ag	1	20.5	20.4	20.2	-0.64
Fe ⁺³	3	19.7	20.3	--	--
Bi	3	19.2	19.1	19.0	-0.59
As	3	--	18.4	--	--
Hg	2	17.8	--	15	-0.50
Cu ⁺²	2	--	12.7	--	+0.04
Te	2	--	8.5	--	--
Pt	2	--	0	--	0
Au	1	--	--	+0.5	+0.31

values taken from Laitinen and Liu's⁽⁵⁹⁾ electromotive force series for LiCl-KCl electrolyte at 450°C since the displacement criteria may be interpreted as ΔG_I° or ΔE_I° . Wagner and Werner⁽⁴³⁾ suggested as an approximation that ΔE_I° values taken from Laitinen and Liu's series could also be used at considerably higher temperatures.

Without yet making recourse to the actual minimum ΔG° values, Table II was used for the preliminary selections by the following line of reasoning:

In order to form feasible cells and to minimize Type I displacement, it was desirable to use a solvent whose ΔG_F° for the chloride was quite low on the scale with respect to the primary solute. That is, the solvent should be a relatively noble metal. Starting from the bottom of Table II the elements that might be useful as solvents included mercury, antimony, bismuth, silver, nickel, copper, tin, lead, chromium, or cadmium. Mercury was eliminated because of its high vapor pressure and health hazard. The melting points for antimony, silver, nickel, copper, or chromium were all relatively high (600°C or more). This left lead, cadmium, tin, or bismuth as possible solvents since they were relatively low-melting, easily obtainable materials.

Leaving the solvent for a moment, the choice of the active metal was considered. In order to form a large number of cells, the active element should fall high in Table II. Since an alkali-metal chloride would form the major part of the electrolyte, the active metal had to be below the alkali metals. Again it was necessary to consider

the melting points since it was highly desirable that the standard electrode be liquid at the cell operating temperatures. On this basis, the first feasible active metals were thallium, zinc, or cadmium. Thallium was eliminated from consideration by virtue of its toxicity and ready oxidation. Of the choice between zinc and cadmium, zinc was preferable since it might be possible to use cadmium as a third-element addition to a zinc solution. Cadmium also remained as a possible solvent.

Assuming that zinc was chosen as the active metal it was then possible to apply the quantitative criteria for displacement reaction possibilities. Table III (which was extended from the calculations of Dealy and Pehlke⁽⁴⁴⁾) gives minimum values of ΔG_I° and ΔG_{II}° for one per cent displacement error for $x_i = x_{iCl} = .01$ and several mole fractions of the added solute j . All solutions were assumed Raoultian. Assuming that zinc (valence 2) is the active metal, the ΔG° between zinc chloride and cadmium chloride was 5,400. Table III shows that cadmium (valence 2) could not be used as a solvent with zinc, but it would be a feasible third element addition up to approximately five mole per cent. All other metals lying below cadmium in Table II would also be feasible third element additions from the standpoint of avoiding Type II displacement.

The table also shows that lead would not be a feasible solvent if cadmium were the active metal whereas if zinc were the active metal, lead just meets the criterion for avoiding substantial displacement effects. All metals below lead were feasible solvents. The metals remaining for practical consideration as solvents were bismuth, lead, or tin.

TABLE III

MINIMUM VALUES OF ΔG_I° OR ΔG_{II}° FOR ONE PERCENT DISPLACEMENT
 ERROR IN MEASURED ELECTRODE POTENTIALS
 (Calculated From Equations (19 and 20))

Active Metal	Valence		$\Delta G_{I\min}^\circ$ for		$\Delta G_{II\min}^\circ$ for	
	Solvent or Added Solute		Displacement By Solvent*		Displacement By Added Solute*	
			$X_{iCl} = .01$			
n_i	n_j or n_k		$X_i = .01$	$X_j = .01$.05	.10
1	1		16,250	8,700	11,310	12,480
	2		8,640	4,920	6,230	6,810
	3		5,990	3,500	4,370	4,760
2	1		15,100	7,550	10,200	11,310
	2		8,110	4,350	5,650	6,230
	3		5,640	3,120	3,990	4,370
3	1		14,500	6,900	9,500	10,670
	2		7,710	4,000	5,330	5,900
	3		5,420	2,900	3,770	4,150

* ΔG_I° is difference of standard free energy of formation of chlorides
 taken from Table II, k-cal/g. atom concentrations in mole fraction.

Next considered was the position of the various elements in the Periodic Table, a pertinent section of which is shown in Table IV. By comparing the displacement reaction criteria with this table it was noted that if either bismuth or lead were used as the solvent an uninterrupted sequence of third-element additions might be made with the Group-B elements of the 5th Period. If tin were the solvent, this sequence would be broken. Similarly, in the 6th Period, by using bismuth as the solvent in preference to lead, another almost complete sequence would be developed, although it would be broken since thallium did not meet the displacement criteria. Another reason for preferring bismuth to lead was based on a comparison of the phase diagrams for binary and ternary systems based on these elements. When the binary diagrams for Bi-Zn and Pb-Zn⁽⁵⁵⁾ were superimposed (Figure 2) it was noted for the zinc-poor compositions that the single-phase liquid region for Zn-Pb was much more restricted than the one for Zn-Bi. It was expected, therefore, that there would be a greater likelihood of finding single-phase liquid regions over wider concentration ranges at lower temperatures in multi-component solutions based on Zn-Bi. Further evidence to support this conclusion was gained from comparisons of the isotherms given by Guertler et al⁽⁵⁷⁾ for the Zn-Ag-Pb and Zn-Ag-Bi systems and was later confirmed by Okajima's⁽⁶³⁾ observations in the Zn-Pb-Ag system. The information available for the other ternary systems based on zinc plus bismuth was that wide single-phase liquid regions would be found in the bismuth corner at temperatures above 300-400°C.^(50-52, 57)

TABLE IV
SECTION OF PERIODIC TABLE INCORPORATING SUITABLE SOLUTES AND SOLVENTS
FOR GALVANIC CELL STUDIES OF ACTIVITY AT 450 TO 650°C

Period	I		II		III		IV		V		VI		VII		VIII	
	A	B	A	B	A	B	A	B	A	B	A	B	A	B	A	B
4	(K)	(Ca)	Sc?	Ti?	V?	[(Cr)]	(Mn)	[Fe]	Co	Ni	?					
		Cu	Zn	[Ge]	?As	?	?	?	?	?	?	?	?	?	?	?
5	Rb?	Sr?	Y?	Zr?	Nb?	Mo?	Tc?	Ru	Rh	Pd	?	?	?	?	?	?
		Ag	Cd	[Sn]	Sb	?Te	I									
6	Cs?	Ba?	Rare Earths ?	Hf?	[Ta]	[W]	Re?	Os,	[Ir]	Pt	?					
		Au	Hg	[Pb]	[Bi]	Po	At									

() Not feasible as third element additions with Zn or Cd due to displacement possibilities
 [] Not feasible as third element additions due to lack of solubility in Bi
 ○ Feasible as active elements
 □ Feasible as solvents
 — Feasible as third element additions by displacement criteria
 ? Insufficient information to determine suitability as third element, or solubility questionable

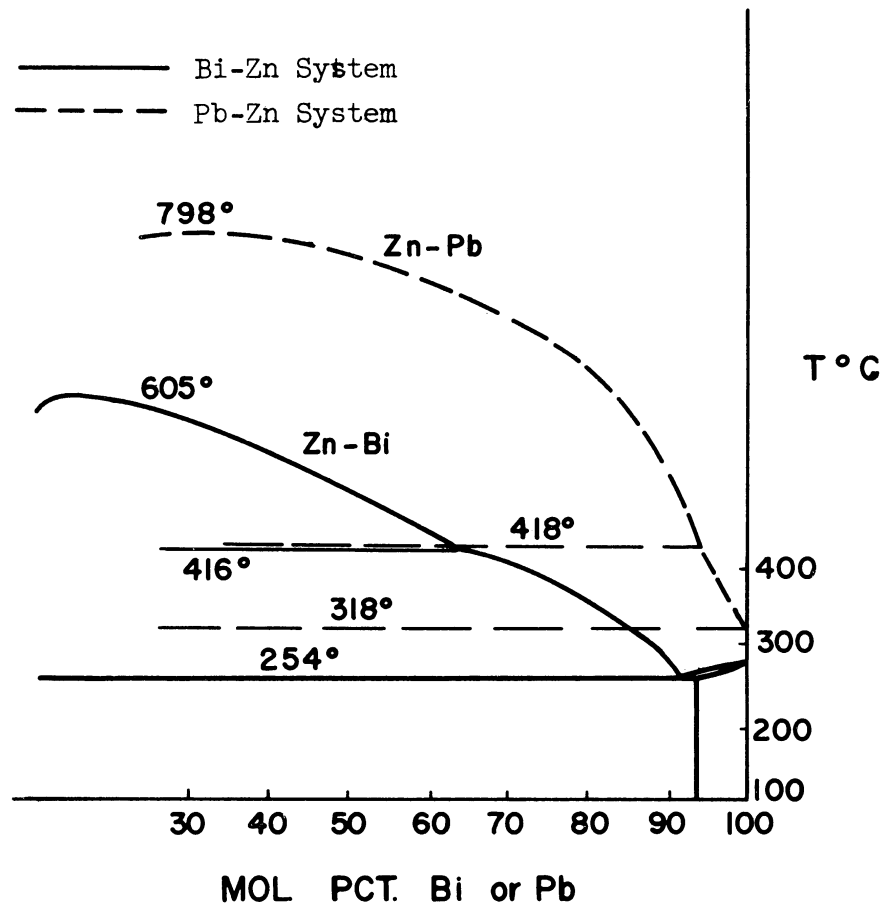


Figure 2. Binary Phase Diagrams of the Bismuth-Zinc and Lead-Zinc Systems in the Zinc-Dilute Region. (55)

Based on the above considerations, the following systems were chosen for study:

Active Element: Zn

Solvent : Bi

Added Solutes : Cu, Ga, Ag, Cd, In, Sn, Sb, Au, Hg, and Pb

The elements enclosed in parentheses in Table IV were deemed unsuitable as added solutes for the following reasons:

For Group-B elements: No information could be found to assess the displacement possibilities for actinium, germanium, or selenium. Arsenic presents a health hazard and its chloride is gaseous at the proposed operating temperatures. The chloride of tellurium is likewise gaseous. Thallium did not meet the displacement criteria. Bromine and iodine are not metallic and polonium is radioactive.

No suitable sequences of the Group-A elements were possible. Either the element lay above zinc in the electromotive force series or there was no information for assessing displacement possibilities. Furthermore, the binary phase diagrams of a number of the Group-A elements indicated negligible solubility in bismuth at the temperatures of investigation.

Beyond normal care in the handling of antimony, the only significant health problem was associated with mercury. The volatility of mercury made it both a health problem and a problem of retaining it in solution. It was decided to attempt only enough runs with mercury to establish the direction of its interaction with zinc, if any, and to estimate its extent. The runs would be made with extreme precautions to maintain the system closed to avoid mercury loss and the working area would be well ventilated.

In summary, the selection of the listed ternary additions to the basic system of zinc in dilute solution with molten bismuth was a logical process based on considerations of the hypotheses to be studied, the need for liquid, single-phase solutions at the temperatures of investigation, and the necessity of avoiding extraneous displacement reactions.

6. Choice of Composition Ranges

With the experimental scheme, method, and alloy system specified, the only remaining choice was the composition ranges to be studied.

The choice of compositions depended on two competing factors. First, it was desirable that the alloys be as dilute as possible with respect to the solutes, and yet a sufficient amount of the third element must be used to insure that its interaction was properly evaluated. On the other hand, the minimization of side reactions required that the concentration of the active element not be too low, nor that of the third element be too high. The available crucibles and containing tube materials for cell construction were of such sizes that a multi-electrode cell having five alloy electrodes and one pure zinc standard electrode was possible. One of these electrodes was used primarily as a reference binary, thus leaving space for four ternary alloys per run.

In order to allow some factor of safety with respect to displacement reactions, .015 mole fraction zinc was chosen as the lowest concentration to be studied. Similarly, .050 mole fraction was taken as

the upper limit of the third-element concentration. To allow the data to be evaluated by either Method I or Method II, (see pp. 19-21) a 4 x 4 matrix of the following levels of both solutes was adopted as the starting point for the studies: .015, .025, .0375, and .050 mole fraction. The binary alloys of zinc in bismuth consisted of the same mole fractions plus an additional alloy at .075 mole fraction so as to overlap the previous investigation of Kleppa⁽⁴⁵⁾ who had carried his studies down to .0639 mole fraction. It was expected that in some cases where the interaction might be strong, or that single-phase solubility was limited, the amount of third element addition could be reduced below .015, however, the attempts of other investigators⁽²¹⁾ to use active-metal concentrations of .010 mole fraction suggested that cell stability deteriorated rapidly if the concentration was too low.

The composition ranges for the multi-component solution studies were expected to be in the same general ranges. The zinc mole fraction would be .015 or .050, while the initial amounts of the third, fourth, fifth, etc. elements would also be .015 mole fraction each. Depending on the results of the initial studies, the total added solute concentration would then be increased in order to investigate the region of validity of the results.

B. Experimental Procedures

1. Equipment

The electrode potentials were determined in the multi-electrode galvanic cell apparatus which is shown in Figure 3. Apparatus of this

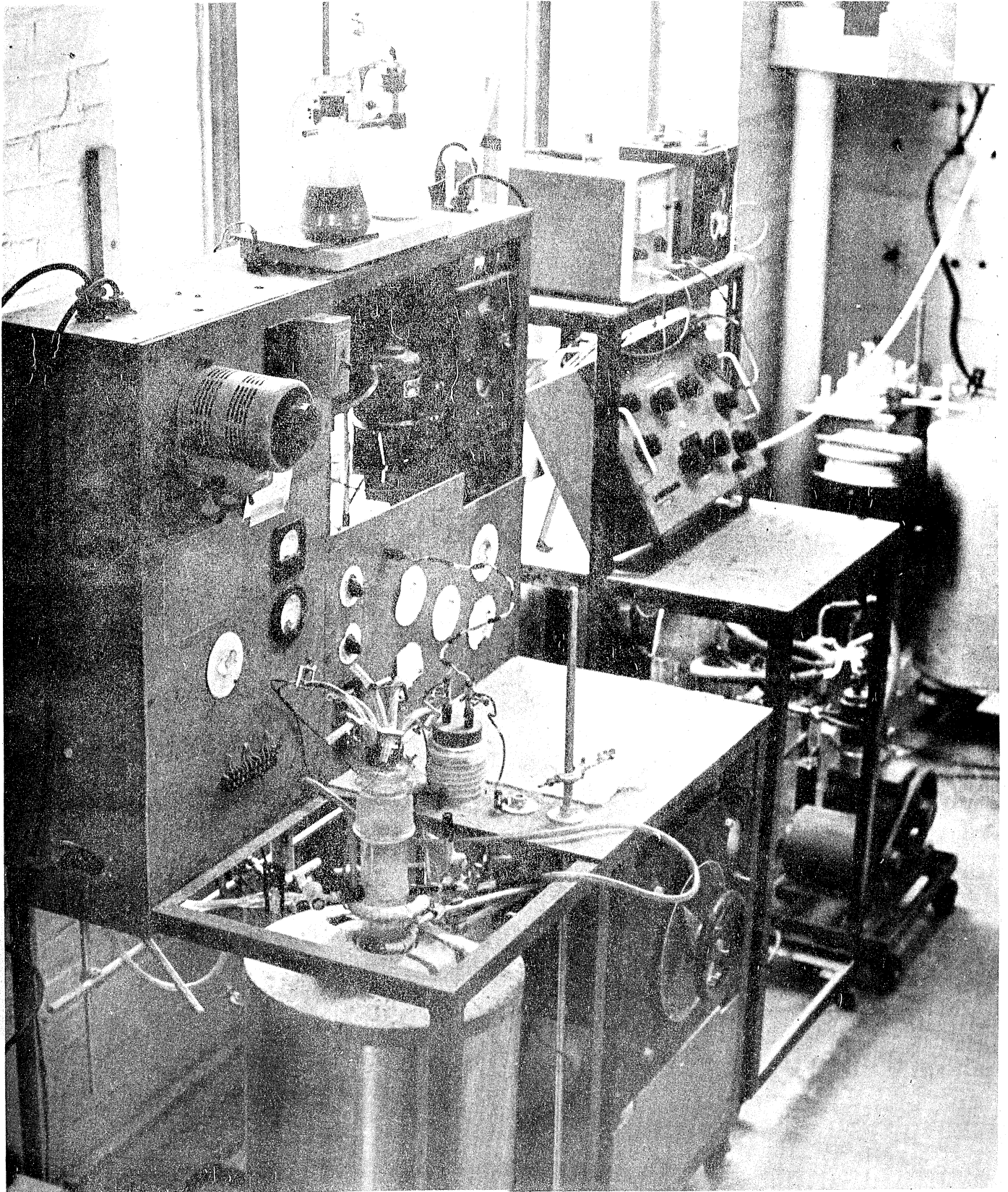


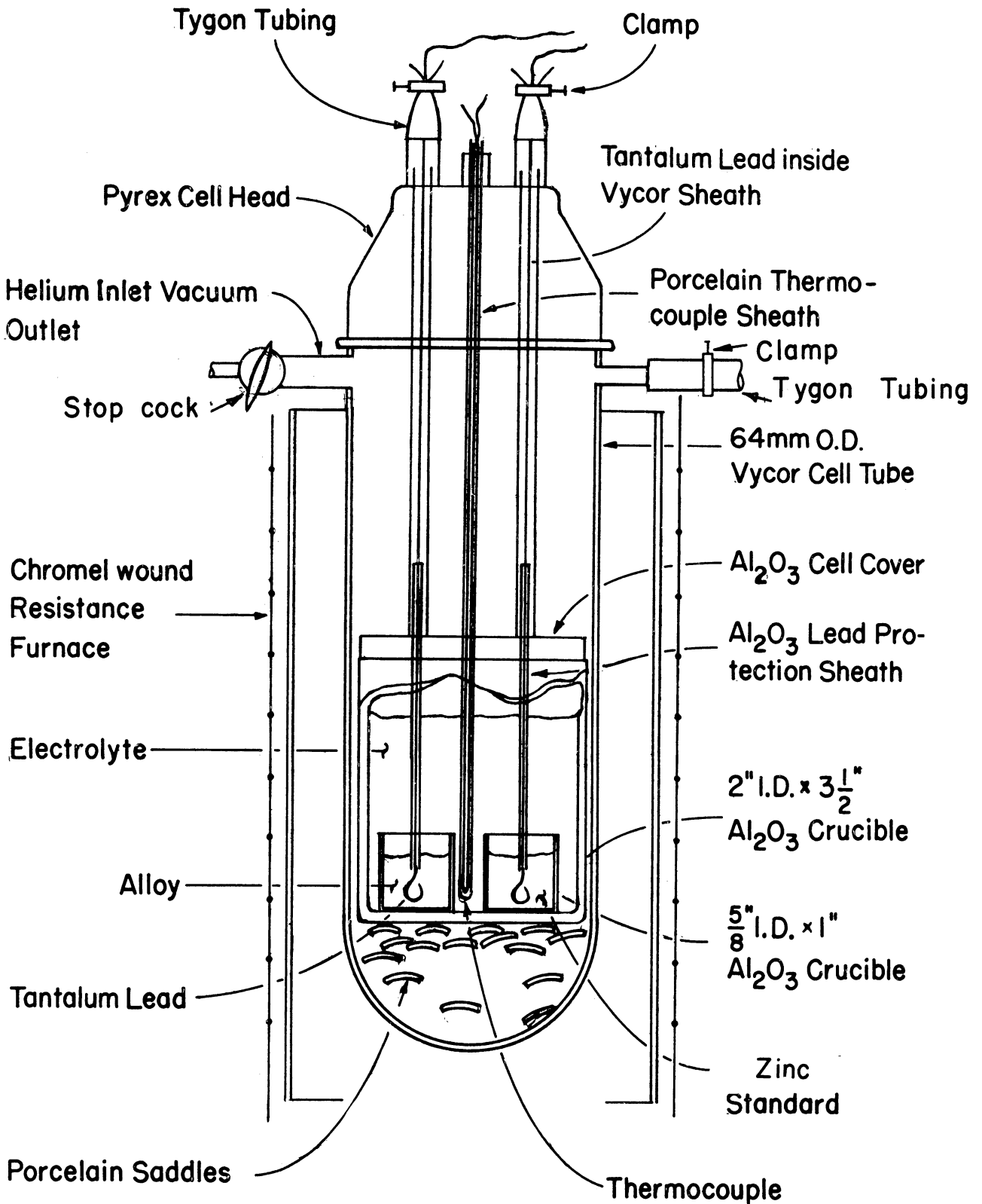
Figure 3. Galvanic Cell Apparatus.

type have been used previously by a number of investigators. The design of the present equipment, which was constructed by Boorstein⁽²¹⁾ and modified somewhat for this investigation, was adapted from those used by Wilder⁽⁶⁴⁾ and Weinstein.⁽⁶⁵⁾ The apparatus consisted of the cell itself, the furnace, the atmosphere system, the potential measuring circuits, and the auxiliary equipment for electrolyte preparation.

a. Galvanic Cell

The multi-electrode cell is illustrated schematically in Figure 4. The five individual alloy electrodes were contained in 15 mm diameter by 26 mm high recrystallized alumina crucibles arranged in a circle at the bottom of a 50 mm diameter by 90 mm high recrystallized alumina cell crucible. The reference standard of pure zinc was contained in a 10 mm diameter by 26 mm high recrystallized alumina crucible at the center of the circle of alloy electrodes. The entire set of electrodes was immersed in the molten salt electrolyte, which filled the large cell crucible to about one inch above the small crucibles. The large crucible rested on a bed of porcelain saddles at the bottom of the containing cell tube.

The electrode leads were 0.040 or 0.025-inch diameter tantalum wires approximately four feet long, protected from the molten salt at their lower ends by recrystallized alumina insulators extending into the alloy. The ends of the leads were bent into a circle in order to increase the area of contact with the liquid alloy.



(Only two of six leads and alloys shown)

FIGURE 4 MULTI-ELECTRODE GALVANIC CELL

Above the alumina insulators, the leads were enclosed in 6 mm diameter Vycor tubes, which protected their upper ends from salt fumes to some extent, acted as insulators, and guided them to the head of the cell tube. The shielded leads were held in position by an aluminum spacing disc that also served as the crucible cover.

The entire assembly was contained in a 64 mm ID Vycor cell tube about 25 inches long, extending into the furnace below the side arms about 19 inches. The top of the tube was closed by a tapered-joint connection to a Pyrex head, which provided six openings for the electrode leads and one for the thermocouple. The openings extended slightly above the surface of the head for the attachment of Tygon tubing, sealed to the head with Glyptal paint. The leads then passed through the Tygon tubing, which was closed by pinch clamps; this tubing was frequently renewed to avoid the possibility of leakage through cuts that could result from repeated clampings.

A 6 mm diameter Vycor tube, sealed at the bottom, served as the thermocouple well. The well extended to the bottom of the large cell crucible at the periphery of the circle of electrodes.

The side arms to the Vycor cell tube provided access to an atmosphere system for the evacuation of the system and the introduction and maintenance of a helium atmosphere. A stopcock was located in the inlet arm, while the outlet arm was permanently attached to a Tygon line which could be closed with a pinch clamp. A ball-joint was used to connect the inlet arm to the atmosphere system. Wire springs which stretched

from the side arms to ears on the Pyrex head were used to seal the system against positive internal pressure.

b. Furnace

The cell tube was clamped vertically and extended into a chromel wire-wound resistance furnace, shown schematically in Figure 4. The resistance coil was 18 gauge Chromel wire that had been coiled on a 1/4-inch mandrel and then wound about a 3-inch ID alumina inner furnace tube. The coil was sealed to the furnace tube with alundum cement and the space between the coil and shell insulated with vermiculite, with the coil spacing varied on the furnace tube so that a level temperature zone could be maintained. The total furnace resistance was 22 ohms. A chromel-alumel thermocouple in an alundum liner was butted to the furnace tube for use as the temperature control couple.

Temperature control was maintained by the "high-low" circuit shown schematically in Figure 5. The furnace power was obtained from a 230-volt Variac auto-transformer wired so that two unequal voltages could be tapped, and regardless of the voltage setting, the tapped voltages were 36 volts apart. Either high or low voltage was fed to the furnace coil by a relay connected to a Foxboro electro-mechanical temperature controller. To obtain a desired cell temperature, it was necessary to set both the controller and the Variac to predetermined levels. In order to maintain temperatures in the 450-650°C range, "high" voltages of 98-133 volts were required. Depending on the ambient temperature, it was normally possible to maintain the furnace temperature to about $\pm 1^\circ\text{C}$.

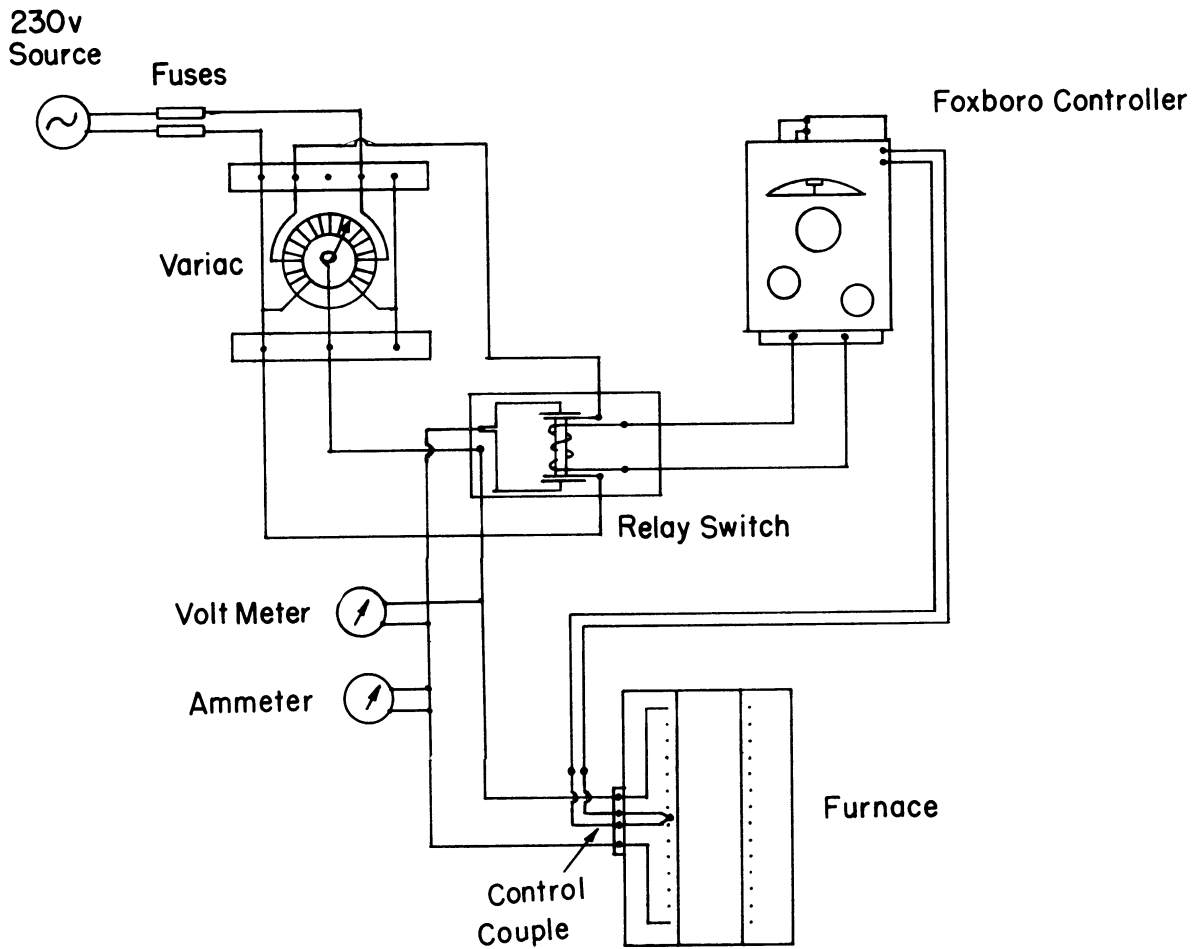
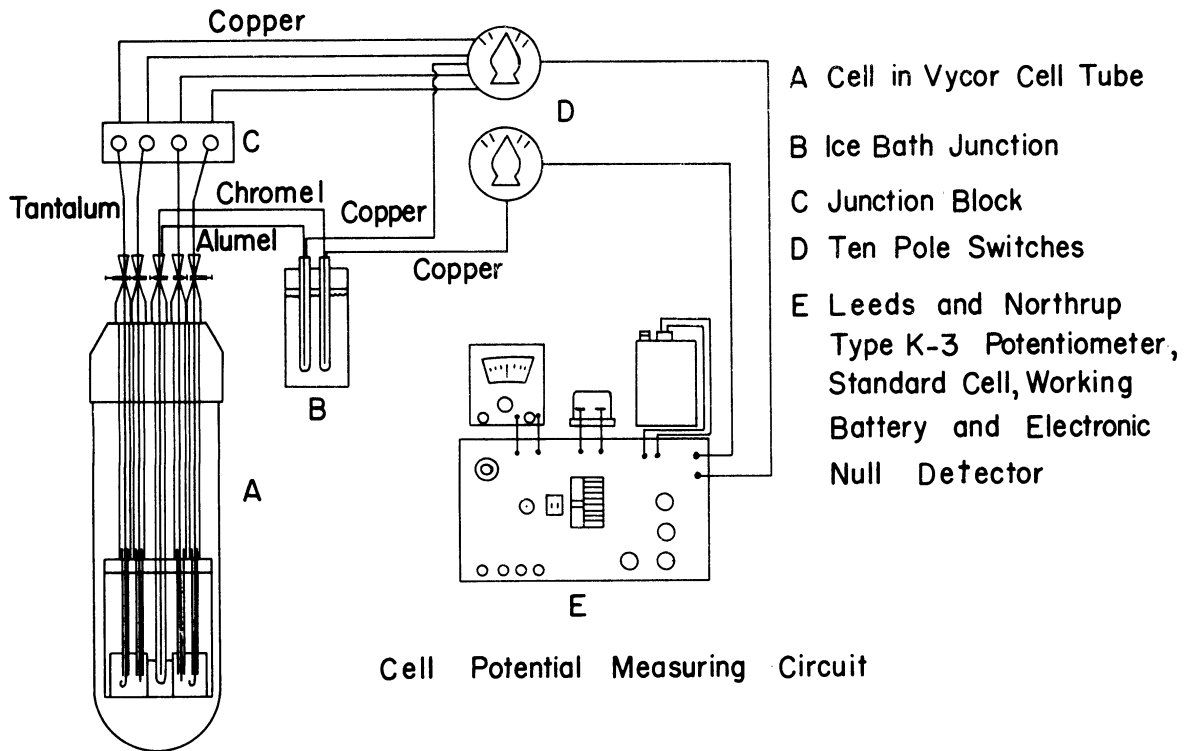


FIGURE 5 SCHEMATIC DIAGRAM OF TEMPERATURE CONTROL AND POTENTIAL MEASUREMENT CIRCUITS

c. Atmosphere System

The atmosphere system was designed so that the cell tube could be evacuated and flushed before establishing the helium atmosphere which was maintained throughout the experimental runs. A line diagram of the system is shown in Figure 6.

A Cenco "Hyvac 2" mechanical vacuum pump was used for evacuating the system, with an acetone-dry ice cold trap placed ahead of the pump. Pressure measurement was by means of a mercury filled U-tube manometer.

The helium, which was obtained in purified form from the University of Michigan Plant Department, was passed through a drying train before entering the cell tube. The train consisted of a tube containing "indicating" anhydrous calcium sulfate, a tube filled with copper gauze that was maintained at 500°C in a small auxiliary resistance furnace, and a second calcium sulfate drying tube. Fore- and back-bubblers were used to maintain a helium pressure of 35 mm of mercury throughout the cell operation.

d. Potential and Temperature Measuring Equipment

The circuit used for the electrode potential and temperature measurements is shown in Figure 5. The tantalum leads from the electrodes were connected through a junction block to a pair of inter-connected ten-pole gang switches. The thermocouple was attached to compensating leads, which led to an ice-bath cold junction; copper leads then connected the cold junction to a junction point on the unit which also led to the gang switches. Common leads from the gang switches to the potentiometer completed the circuitry. The arrangement allowed rapid measurement of both

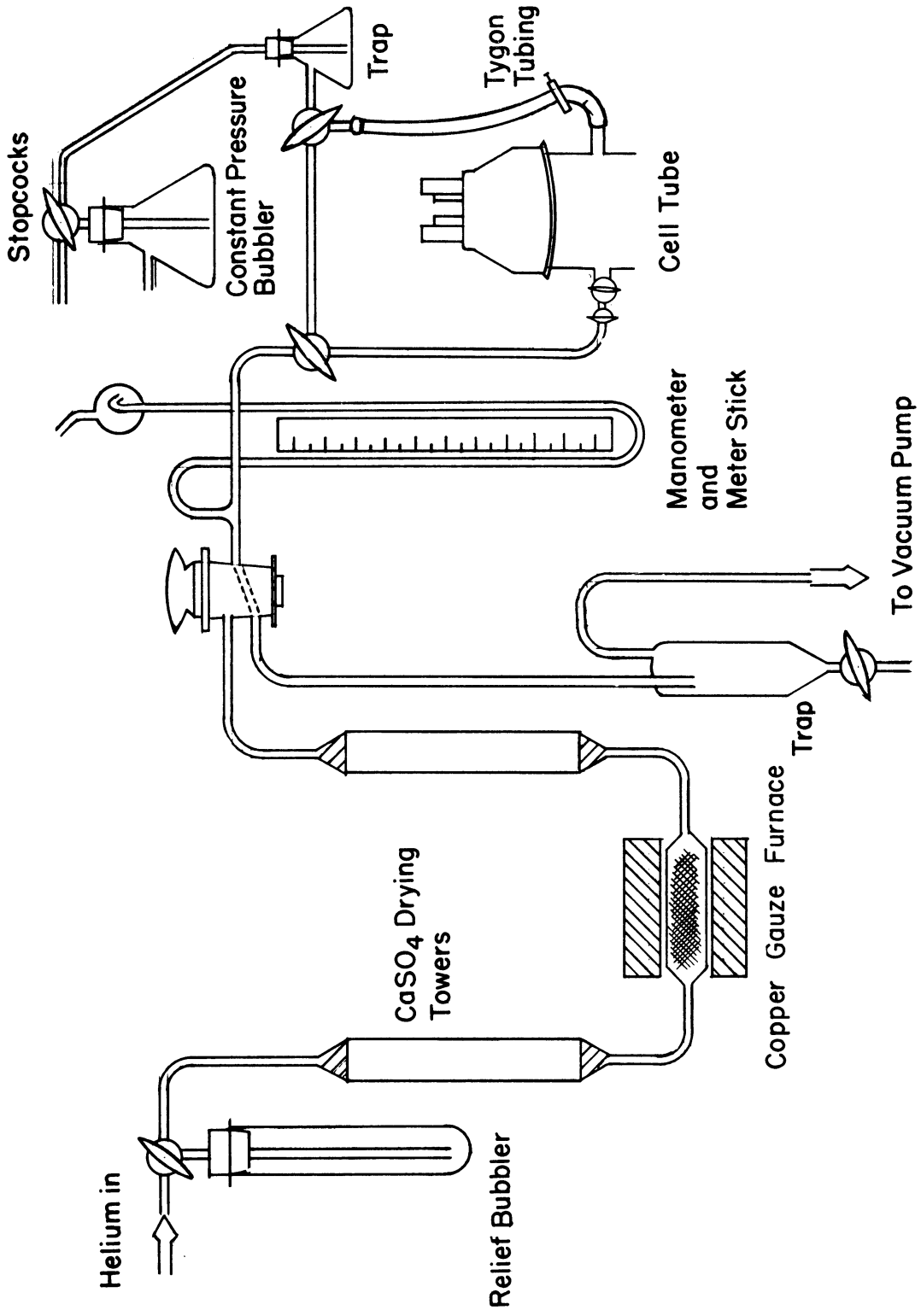


FIGURE 6 ATMOSPHERE SYSTEM

the temperature and electrode potential since any alloy electrode could be compared with the standard electrode, with alternate switching to the thermocouple if desired.

For the first 20 runs, a Leeds and Northrup No. 8687 Volt Potentiometer was used for the potential measurements. A Leeds and Northrup Type K-3 Potentiometer with a fresh standard cell then became available and was used in the remaining 65 runs. An electronic null detector was used with the Type K-3 instrument. The Volt Potentiometer was standardized against the Type K-3 Potentiometer and was found to have been in excellent agreement with the K-3.

All thermocouples used in the galvanic cell runs were made from the same spools of 26 gauge Chromel and Alumel wire. The wires were insulated with two-hole ceramic tubing. The thermocouples were checked for calibration against the melting points of pure bismuth and zinc. Both virgin and used thermocouples checked in this manner were found to be accurate to within 1°C.

e. Electrolyte Preparation Equipment

Prior to its use, the electrolyte was fused, with continuous evacuation for several hours. This process was carried out in a separate 110-volt powered auxiliary resistance furnace similar in construction to the main-unit furnace. "On-off" temperature control was maintained by a Pyro-Vane Electronic Temperature Controller.

The electrolyte was melted in a 40 mm diameter Vycor tube that was lowered to the bottom of a 64 mm diameter Vycor tube extending into

the furnace. The large Vycor tube was similar to the main-unit cell tube but had only one side arm, connected by a ball joint to a U-tube filled with glass wool. In turn, the U-tube was attached by heavy-wall rubber tubing to a tapered joint connection with the vacuum pump. An acetone-dry ice cold trap was placed ahead of the pump. The large Vycor tube was closed at the top by a Pyrex glass blind head which mated to a tapered joint.

2. Materials

High-purity metals were used for the alloy and standard electrodes. The source of each metal and its quoted purity are summarized in Table V. The various alloying elements were cut into convenient-sized pieces with thoroughly cleaned wire cutters or shears, and any surface oxidation was removed with appropriate etchants.

The tantalum lead wires were obtained from the Fansteel Metallurgical Corp. in 25 meter spools of 99.9+ per cent pure annealed wire. Both .040- and .025- inch diameter wires were used during the investigation.

The recrystallized alumina crucibles and insulators were obtained from Morganite, Inc. as their Triangle RR Grade, while the Norton Company supplied the alundum sheet used for the crucible lid.

Commercially prepared Reagent Grade chemicals were used for the electrolyte.

TABLE V
EXPERIMENTAL MATERIALS

<u>Material</u>	<u>Source</u>	<u>Grade</u>	<u>Quoted Purity-%</u>	<u>Form as Received</u>
<u>Metals</u>				
Zn	ASARCO*	A-58	99.999+	Splatters
Bi	ASARCO	A-59	99.999+	Shot
Ag	ASARCO	A-59	99.999+	Splatters
Au	Donated by Ford Motor Co.	--	99.995+	Powder
Cu	ASARCO	A-58	99.999+	Rod
Cd	ASARCO	A-60	99.999+	Splatters
Ga	Fisher Scientific Co.	Electronic	99.9999	Liquid
Hg	"	Instrument	99.999+	Liquid
In	ASARCO	A-58	99.999+	Extruded Stick
Pb	ASARCO	A-59	99.999+	Extruded Bar
Sb	ASARCO	A-60	99.999+	Fragments
Sn	Vulcan Detinning Co.	Extra Pure	99.998+	Cast Bars
<u>Chemicals</u>				
ZnCl ₂	Baker & Adamson	Reagent	95 (min)	
LiCl	J. T. Baker	Reagent	99.0	
KCl	Baker & Adamson	Reagent	99.5	

*ASARCO - American Smelting and Refining Company

3. Cell Operation Procedures

The operation of the galvanic cell was a two-step procedure. The first step consisted of the preparation of the alloy, the standard electrodes, and electrolyte. The second step was the operation of the cell to obtain electromotive force values for the alloys over a range of temperatures. Approximately one week per run was required for the preparation and operation.

a. Electrode Preparation

Both the alloy and standard electrodes were pre-melted under a helium atmosphere in the absence of the electrolyte in order to freeze the tantalum leads in place for ease in subsequent handling, to insure proper positioning, and to homogenize the alloys. The total charge per electrode, approximately 17-18 grams, was dictated primarily by the amount of the elongated bismuth shot that could be packed into the electrode crucibles. When melted and solidified, the crucibles were about 60 per cent filled. The charge calculations were based on about 17.5 grams of bismuth per electrode and were normalized in terms of the most difficulty divisible constituent. Thus, the first weighing was of the element most difficult to divide into proper-size small pieces, i.e., copper, silver, or zinc. A convenient amount was weighed to $\pm .0001$ gram, and the weights of the other constituents required to obtain the desired mole fractions were then calculated from this base. The additional elements were also weighed to $\pm .0001$ gram, but it should be realized that while the first weight was that of an actual piece of material, the succeeding weights

represented the best attempt to add material to a balance pan to match a desired weight. This rather subtle point has been discussed in more detail by Acton.⁽⁶⁶⁾ All the weighings were made on an Ainsworth Type LC Analytical Balance using Class S weights. The electrode compositions calculated from the weighed-in amounts were generally within .0001 mole fraction of the desired values.

Fresh crucibles and insulators were used for each run. The ends of the tantalum leads were cleaned with silicon carbide abrasive paper and washed in acetone prior to inserting them into the insulators and bending the tip to the circular shape.

Following the weighings, the cell was pre-assembled outside the tube but with the leads extending through the head, using a stainless steel cup in place of the large recrystallized alumina crucible. A metal fixture was wired to the top of the cup to hold the assembly together and to ensure correct lead positioning. Finally, titanium shavings were placed on top of the positioning fixture to serve as a "getter" during the lead-sinking operation.

The entire assembly was lowered into the Vycor cell tube by a hook through a wire loop at the top of the positioning fixture. The pinch clamps at the cell head were then closed and the tube was placed in the cold furnace and connected to the atmosphere system. The tube was evacuated and flushed several times with dried helium before turning on the furnace, and several additional flushing cycles were conducted after the furnace temperature had risen slightly. During the flushing sequence,

the pinch clamp on the tube outlet line was kept closed. Finally the clamp was opened and a slightly flowing helium atmosphere at 35 mm of mercury was established. The furnace temperature was then brought to 450°C in about 2-3 hours, after which the gas flow rate was increased and the pinch clamps were released and retightened individually to permit the leads to be pushed down into the now-molten electrodes. The leads were oscillated about 50 times to aid in mixing the alloy and wetting the leads, but care was taken that the final position of the leads was such that they did not touch the crucible bottoms. After all the leads had been positioned, the cell was held for an additional hour at 450°C for further homogenization.

The cell tube stop-cock was then closed and the gas flow reversed to provide a static atmosphere. The tube was removed from the furnace and air-cooled (while maintaining the helium atmosphere within) in order to freeze the leads in place.

The pre-sunk electrodes and head assembly were then removed from the cell tube, inspected, and the cell was re-assembled - this time in the large recrystallized alumina crucible with the alundum spacing disc as the cover. The 6 mm diameter Vycor insulating tubes were exchanged for those cut to the proper length for the actual running of the cell.

Additional pieces of zinc were added to the standard electrode crucible to fill the space made available by the melting and solidification of the initial zinc charge. This was done so that the volume of the zinc

standard was as large as possible, thus minimizing effects of impurities that might be introduced during lead sinking. Since the diameter of the standard crucibles was 10 mm, the alloy electrodes in their 15 mm diameter crucibles were considerably greater in volume. The total weight of the small zinc standards was about 5.5 grams - in contrast to the 17-18 grams of the alloy electrodes. In several runs one of the alloy electrodes was replaced by an additional pure zinc standard in a 15 mm diameter crucible. No difference was found between electromotive force measurements using this larger standard or the normal 10 mm diameter standard as a reference. Finally, the Vycor thermocouple well was placed in position and the entire cell and head assembly was mounted on a ring stand adjacent to the cell tube.

b. Electrolyte Preparation

While the electrode leads were being pre-sunk, the electrolyte was under preparation in the auxiliary furnace. The electrolyte consisted of 165 grams of the eutectic mixture of LiCl and KCl (42 mole per cent LiCl and 58 mole per cent KCl) plus 1.5 mole per cent of ZnCl₂. Previously, the electrolyte had been mixed in a large batch and evacuated continuously at room temperature in a vacuum dessicator for at least three days to remove moisture. The pre-treated electrolyte was then stored prior to use in a tightly closed jar in a dessicator. This procedure was adapted from the method of Laitinen, Ferguson, and Osteryoung.⁽⁶⁷⁾

The zinc chloride was vacuum dried separately for 4-6 hours at 250°C and then stored in a closed jar in a separate dessicator.

Approximately 1.5 mole per cent zinc chloride was added to the electrolyte in two ways during the experimental program. Initially, in about half of the runs, the zinc chloride was added to the molten electrolyte as it was being poured into the cell crucible. Later the procedure was changed and the dried zinc chloride was added to the eutectic mixture prior to its fusion. The entire mixture was then fused under continuous evacuation for four hours at 600°C. The purpose of the prolonged vacuum treatment of the electrolyte was to further remove any absorbed water. The vacuum treatment caused no significant loss of any of the electrolyte constituents, since a dummy batch carried through the entire preparation procedure was found unchanged in weight.

c. Starting of Runs

Before starting the run, the leads and the head were carefully checked to insure that each was in proper position and that the Vycor insulating tubes properly indexed with the openings in the head. The entire atmosphere supply system was purged with flowing helium. A Vycor funnel was positioned so the electrolyte could be poured into the large crucible.

When everything was in place, the vacuum pump was disconnected from the auxiliary salt purification equipment and connected to the main unit. The Vycor funnel was heated with a gas-oxygen welding torch, and the molten electrolyte mixture was removed from the auxiliary unit and poured through the heated funnel. For those runs where the zinc chloride was not added at the start of the electrolyte preparation, the zinc

chloride was melted in the Vycor funnel and allowed to run into the large crucible with the LiCl-KCl eutectic.

When all the electrolyte had been added to the crucible, the alundum disc was pushed down in its place as the crucible cover. Some of the electrolyte immediately solidified in contact with the large crucible and the electrode crucibles. This served to "cement" the electrode crucibles in position and allowed the entire assembly to be lifted by the lead wires and lowered into the cell tube. The cell tube was then placed in the furnace, sealed, and connected to the atmosphere system. In some of the earlier runs, the furnace was started cold. Later it was found more convenient to have the furnace temperature at about 550°C at the start of the run, which insured that the electrolyte was molten during the initial flushing operations, thus facilitating the removal of air bubbles that might have been trapped during the electrolyte transfer. In addition, there was less chance for moisture and oxygen absorption at the electrolyte surface.

The total time between the start of the electrolyte transfer and the sealing of the system was usually less than 30 seconds.

The cell tube was evacuated and flushed at least six times before the positive helium atmosphere was finally established. By this time the alloy and standard electrodes were molten and therefore the lead positions could be rechecked and adjusted so that the electrodes did not contact the crucible bottoms. When the system was thoroughly flushed, the pinch clamp on the outlet tube was opened and a slight flow of helium was established against the fore-bubbler. The internal pressure during

the runs was maintained at about 35 mm of mercury. The system was then allowed to equilibrate for several hours.

d. Operation During Experimental Runs

Before meaningful data could be obtained it was necessary that compositional equilibrium be established both in the electrodes and the electrolyte, and that thermal equilibrium be achieved in the entire system. For those runs where the furnace was started cold this required from 24 to 48 hours. When the procedure was changed so that the furnace was almost at the operating temperature when the run was started, the initial equilibrium period was considerably reduced. Depending on the alloy system under investigation, this was as little as 4 to 6 hours and generally within 12 to 16 hours.

The criterion adopted for satisfactory equilibrium was that the electrode potentials should vary only randomly over a range of about .2 mv in four or five sets of readings made during the course of an hour. If the variation was within this range but was systematic rather than random, it was assumed that equilibrium was still slowly being established. Once equilibrium had been attained, the cell responded only to temperature fluctuations which were normally within a range of one or two degrees. In a few cases, a systematic drift was noted in the potentials for a more prolonged period. In these instances, the potentials were measured with respect to the reference binary alloy composition included in most runs. It was found in virtually all such cases that the potential differences (i.e., the interaction effect) between a series of alloy electrodes (of

constant zinc content and variable amounts of added solutes) were constant and independent of the absolute level of the potentials. The drift in the absolute potentials was assumed to be related to some extraneous reaction involving the standard and the electrolyte, and perhaps represented the effects of residual amounts of moisture and oxides in the electrolyte. (This point is discussed in greater detail in the section on Alleviation of Errors, p. 37).

When it was determined that the cell had reached equilibrium or that a state of "dynamic" equilibrium could be assumed, the potential measurements were started. The electrode potentials were determined at a series of from four to eight temperatures within the range 450°C to 650°C. An effort was made to establish thermal equilibrium temperatures at close to even 50° temperature increments. The sequence of temperature measurements was random, some points being approached from above and some from below. In some instances, a set of readings would be made at a sequence of rising temperatures such as 500°, 550°, 600°, and 625°C. Following this, a similar sequence of falling temperatures would be investigated at the intermediate values, i.e., 575°, 525°, and 475°C. A set of readings was accepted if it met the general criterion of less than .2 mv variation over one hour. When the furnace temperature was changed, the establishment of a new thermal equilibrium required about two hours.

In making a set of potential readings, the cell temperature was read and then the individual electrode potentials were read in sequence. The cell temperature was then re-read and the average between the initial

and final temperatures was used as the temperature of the particular set of readings. The variation in indicated temperature, if any, was invariably in the range .2 to .4°C. During the potential readings, care was taken that the circuit was not completed for more than a fraction of a second. Since the readings were approached from both directions, mass transport in the cells was assumed negligible.

The total operating time of each cell was from three to six days, depending mainly on the time to reach initial equilibrium. It was generally possible to investigate five or six temperatures in a day of running. Although an effort was made to vary the pattern of the runs, since it was necessary to leave the cell unattended during the late night and early morning hours, the usual procedure was to take the highest temperature readings late during the evening and then set the temperature to a low value and allow it to cool during the night. In any event, repeated excursions to a given temperature were made during the course of a run. Throughout each run, a running plot of temperature versus potential was made and a linear relationship was normally found.

Reversibility in a given run was inferred from the linearity and the low standard deviation of the emf-temperature relations and the general stability of the potential readings with time. A special experiment was also conducted to confirm the reversibility of the cells.

e. Conclusion of the Run

When a sufficient amount of data had been obtained, or it became evident that the cell was no longer stable, the run was concluded by quenching the cell with water. It was necessary to adopt this procedure because of the corrosive nature of the electrolyte. During the cell operation, electrolyte occasionally collected at the bottom of the Vycor cell tube either from condensation on the tube walls or because of leakage through cracks that could develop in the large electrolyte crucible. If the molten electrolyte was allowed to solidify in contact with the Vycor tube, this invariably caused the tube bottom to crack.

A procedure was adopted to minimize this risk. The thermocouple and its protection tube were withdrawn from the cell. The head of the cell and the tantalum leads in their Vycor protection tubes were withdrawn as a unit and quenched in water. The alundum crucible cover was removed with a hook. A long stainless-steel rod was then immersed in the electrolyte. The Vycor tube was removed from the furnace, clamped in place and allowed to cool slightly; water was then poured down the inner walls of the Vycor tube to dissolve any spilled electrolyte before it had a chance to solidify in contact with the walls. The quenching froze the rod into the salt remaining in the cell crucible, and it was then possible to withdraw the crucible. Hot water was used to dissolve the salt away from the alloy electrodes, while all components of the cell were cleaned by boiling in hot HCl. The portions of the leads that had been in contact with the alloys were clipped off and the remaining parts of the leads were cleaned with silicon carbide abrasive paper. For the

next run, the leads were reversed and the "fresh" ends of the leads were used as the portion that contacted the alloys.

In the initial runs, .040-inch diameter tantalum wire was used for the leads. However, it was soon noted that after several runs, the portion of the leads exposed to the vapor above the salt melt became severely embrittled. Consequently, the change was made to .025-inch lead wire, the wires were reversed after the first run, and then the leads were usually discarded after only two runs. The smaller wire diameter also allowed better closure of the Tygon head tubes with the pinch clamps.

4. Treatment of Data

a. Reduction of Raw Data

Once it had been established graphically that the emf-temperature relationship of the electrodes was linear, equations of slope-intercept form were fitted to the data by the method of least squares.⁽⁶⁸⁾ The electrode potentials at the five integral temperatures at intervals of 50°C over the range from 450° to 650°C were determined from the regression equation. All computations were made on an IBM 7090 computer using a program that had been written in MAD language. The program averaged the raw data at each temperature, if desired, and determined the slope and intercept of the least squares regression line. The standard error of estimate of the actual data was computed, together with the correlation coefficient. The standard deviation of the slope of the line was also computed.

From the interpolated potentials, the program then calculated the activity of zinc, the activity coefficient, and the natural logarithm of the activity coefficient of zinc in each alloy at each of the five integral temperatures. The program also calculated from the weighed-in values the mole fraction of each of the solute elements.

Since the data consisted of sets of several readings taken at relatively fixed values of temperatures, two procedures were tried in the calculations. In one, the computer was instructed to average the temperature and potential data and then proceed with the average values for the further calculations. That is, the four sets of readings made, for example, at 499.6, 499.5, 500.1, and 500.2°C were averaged and then treated as one data point at 499.8°C. The later procedure adopted was to treat each point separately as an independent reading, as indeed it was. Data for several runs were calculated in both ways and the interpolated potentials were identical. The statistical estimates of data scatter were somewhat improved by the second technique since the sample size had been considerably increased. The use of the individual data points also made it unnecessary to take an equal number of readings at each temperature.

As noted previously (p. 28), suitable manipulation of the activity equation allows the logarithm of the activity coefficient to be obtained directly from the electrode potentials with no need of computing the activities and activity coefficients as intermediate steps. A second computer program was written for this purpose to be used with the data

that had been corrected to the standard potentials of the reference binary alloys.

A linear regression program was also written that could be used for the determination of the self-interaction and ternary interactions if it appeared that the data were linear.

b. Determination of Interaction Parameters

Once the natural logarithm of the zinc activity coefficient had been obtained for each alloy electrode, the interaction parameter was usually determined graphically by Method I (p.19). For each temperature and each constant mole fraction of zinc, a plot was made of the \ln activity coefficient versus the mole fraction of added solute. Weighed-in values were used for all compositions. The limiting slopes of these plots were the values

$$\left(\frac{\partial \ln \gamma_{Zn}}{\partial X_j} \right)_{\substack{X_j=0 \\ X_{Zn} = \text{const.}}} .$$

The set of values determined for the third element at limiting dilution were then cross-plotted versus the mole fraction of zinc and extrapolated to $x_{Zn} = 0$, where the intercept is the ternary interaction parameter

$$\epsilon_{Zn}^j = \left(\frac{\partial \ln \gamma_{Zn}}{\partial X_j} \right)_{\substack{X_j=0 \\ X_{Zn}=0}} \quad (2a)$$

The limiting slope from this plot is the second-order interaction parameter

$$\epsilon_{z_n}^j = \left(\frac{\partial^2 \ln \gamma_{z_n}}{\partial X_j \partial X_{z_n}} \right)_{X_j=0, X_{z_n}=0}$$

In addition to graphical determination, a computer program was written to determine the parameters by least squares analysis of the matrix of activity coefficient data. The program performed the analysis by Methods I and II, and it was found that identical values of the interaction parameter were obtained by either method, however, statistical estimates of the confidence level of the parameters were better for the Method I calculations (Appendix C). The least squares method had the disadvantage that equal weight was placed on each data point. Since the binary data were known from repeated runs to better accuracy than the ternary data, it was desired to place more reliance on them in fitting the relation to determine the intermediate slopes. Consequently, the graphical method was used to determine the parameters reported in the next section.

IV. EXPERIMENTAL RESULTS

The experimental results of this investigation and the calculation of the interaction parameters are discussed in the section which follows. The order of presentation is: the zinc-bismuth binary system, ternary systems based on zinc-bismuth, and the test of the additivity hypothesis by means of multi-component solution studies. This section also includes the experiments confirming the assumptions on which the galvanic cell method is based and an estimation of the errors involved. The correlation of the results and the rationale for the observed interactions is reserved for the following Discussion Section.

A. Zinc-Bismuth Binary System

The binary alloys of zinc in bismuth were studied primarily to determine the self-interaction, if any, of zinc and to provide a basis for assessing multi-component interaction effects. However, the experiments also provided a verification of the experimental technique and a means for estimating the experimental uncertainties. Consequently, these results are discussed in this section in detail.

A total Of 63 successful binary electrodes were run at five concentration levels of zinc. In one run (Run 3) only binary alloys were studied, while in most of the remaining runs a binary alloy was included as an additional reference electrode with the ternary or higher-order alloys.

The replication of compositions was the following:

<u>X_{Zn}-Mole Fraction</u>	<u>No. of Electrodes Run</u>
.015	25
.025	14
.0375	10
.050	13
.075	1

Previous studies of the zinc-bismuth system at 600°C have been made by Kleppa^(45,46) and Lantratov and Tsarenko.⁽⁴⁷⁾ The most dilute solutions studied by Kleppa were .0639 and .1284 mole fraction zinc, while Lantratov and Tsarenko's most dilute compositions were .144 and .2611 mole fraction zinc.

Therefore, the composition of .075 mole fraction zinc was included in this investigation in order to overlap Kleppa's range and to provide an indication of the consistency of the results of the three studies.

The binary electrode results are summarized in Table VI. The values of the electromotive force (emf) were obtained by least squares analysis of the experimental data⁽⁶⁸⁾(see pp. 71-72). The results presented are the interpolated potential at 550°C, the slope of the least squares line relating the emf and temperature, the standard error of estimate of the emf's from the least squares line, and the natural logarithm of the activity coefficient of zinc at 550°C.

The standard error of estimate provides an indication of the scatter of data within an individual run, while the other quantities are affected by differences between runs.

TABLE VI
EXPERIMENTAL DATA FOR BINARY BISMUTH-ZINC ALLOYS

Run No.	EMF at 550°C	$(\frac{\partial \epsilon}{\partial t})$	σ	ln γ	Run No.	EMF at 550°C	$(\frac{\partial \epsilon}{\partial t})$	σ	ln γ
X Zn = .015					X Zn = .0375				
3	109.36	.221	.16	1.116	9	75.78	.184	.06	1.147
18	109.05	.218	.20	1.125	19	77.84	.182	.08	1.089
25	109.92	.214	.39	1.100	34	76.48	.179	.18	1.127
37	109.63	.212	.29	1.108	42	76.80	.179	.18	1.118
38	110.51	.217	.21	1.084	44	75.66	.174	.42	1.150
41	110.04	.216	.21	1.097	45	76.16	.175	.06	1.136
47	107.66	.219	.15	1.164	46	75.85	.174	.13	1.145
48	109.34	.216	.08	1.117	54	75.67	.175	.07	1.150
52	109.72	.220	.04	1.106	55	75.17	.175	.32	1.164
57	108.23	.214	.37	1.148	70	75.24	.175	.16	1.162
58	108.75	.219	.25	1.133	Average	76.06	.177	.17	1.140
64	110.48	.219	.25	1.084	X Zn = .050				
65	109.13	.219	.10	1.123	3	67.50	.164	.20	1.092
68	111.96	.229	.07	1.043	17	67.38	.170	.23	1.096
71	110.03	.213	.24	1.097	23	66.17	.165	.06	1.130
72	108.10	.225	.24	1.152	28	66.24	.165	.81	1.128
73	108.33	.217	.18	1.145	29	66.63	.179	.37	1.117
75	109.38	.225	.27	1.116	39	66.47	.163	.14	1.122
76	110.44	.220	.25	1.086	50	66.18	.160	.16	1.130
77	109.52	.219	.08	1.112	51	66.12	.167	.09	1.132
78	110.45	.227	.20	1.084	56	66.61	.161	.15	1.118
79	108.61	.210	.12	1.137	69	66.03	.161	.10	1.134
80	108.32	.220	.19	1.145	81	65.76	.157	.44	1.142
83	109.71	.230	.20	1.106	81B	65.96	.162	.15	1.136
85	111.53	.220	.38	1.055	84	66.62	.162	.14	1.117
Average	109.53	.219	.20	1.111	Average	66.43	.164	.23	1.120
X Zn = .025					X Zn = .075				
3	92.08	.197	.20	1.092	3	52.82	.143	.18	1.101
16	94.58	.199	.34	1.022					
20	92.22	.194	.57	1.088					
27	91.63	.197	.32	1.105					
32	93.04	.198	.24	1.065					
33	91.20	.198	.11	1.117					
40	91.61	.194	.20	1.106					
43	89.62	.191	.16	1.156					
49	90.23	.194	.16	1.145					
53	89.86	.192	.27	1.155					
58	90.62	.196	.12	1.134					
61	90.95	.187	.28	1.124					
66	92.20	.190	.38	1.089					
67	91.84	.189	.46	1.099					
Average	91.56	.194	.27	1.107					

Note: EMF, millivolts

$(\frac{\partial \epsilon}{\partial t})$, millivolts/°C

σ , standard error of estimate of emf values from least-squares line, mv.

X_{Zn}, mole fraction

The average potential at 550°C and average emf-versus-temperature slope were calculated from the replicate data for each composition. (Table VI). To test the consistency with the other investigators, the activity of zinc was calculated at 550°C and 600°C from the average values. In addition, the 600°C data of Kleppa and Lantratov and Tsarenko were extrapolated to 550°C using their emf-temperature slopes. The results of these comparisons are shown in Figures 7 and 8 as plots of zinc activity versus zinc mole fraction at 550 and 600°C respectively. Figure 9 presents a plot of $\partial E/\partial t$ versus mole fraction zinc. In all cases, a smooth curve encompasses the data and shows that the present dilute solution results are consistent with the data taken on more concentrated solutions. This agreement, together with the general stability of the cell behavior, was taken as evidence that the present experimental apparatus was reliable and that there was apparently no significant alteration of zinc content during the runs. Figures 7 and 8 show that the zinc-bismuth system exhibits a strong positive deviation from Raoult's Law.

Examination of Figures 7 and 8 and the data at other temperatures also revealed that the activity-versus-concentration relation was linear in the region below approximately .075 mole fraction, thus indicating that Henry's Law applies. The limiting slope of the 550°C line is 3.04 and is the Henry's Law constant or γ^0 , the activity coefficient at infinite dilution. Therefore, on this basis it can be concluded that the self-interaction coefficient of zinc is zero.

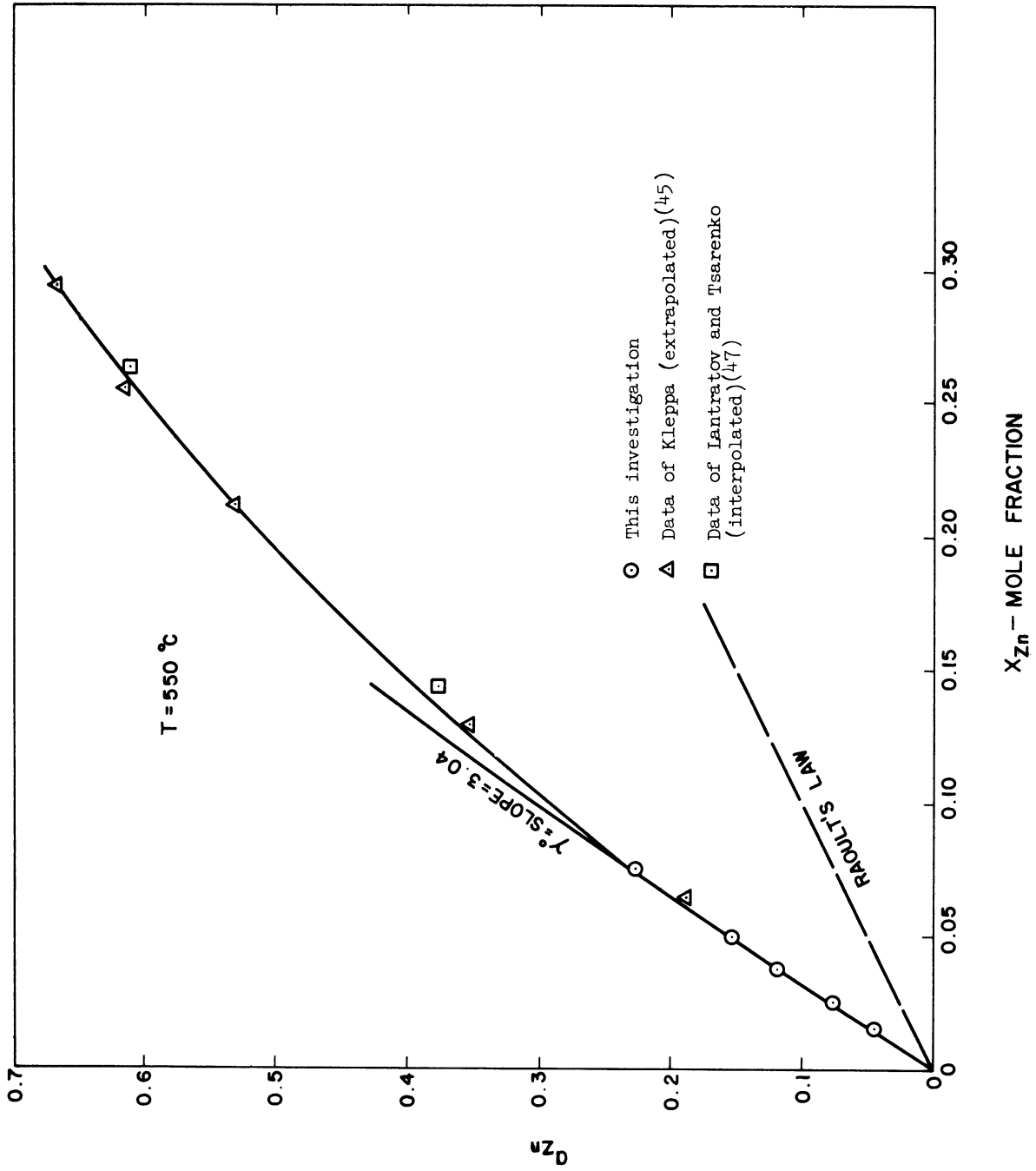


Figure 7. Activity of Zinc versus Mole Fraction of Zinc in Bismuth at $550^\circ C$

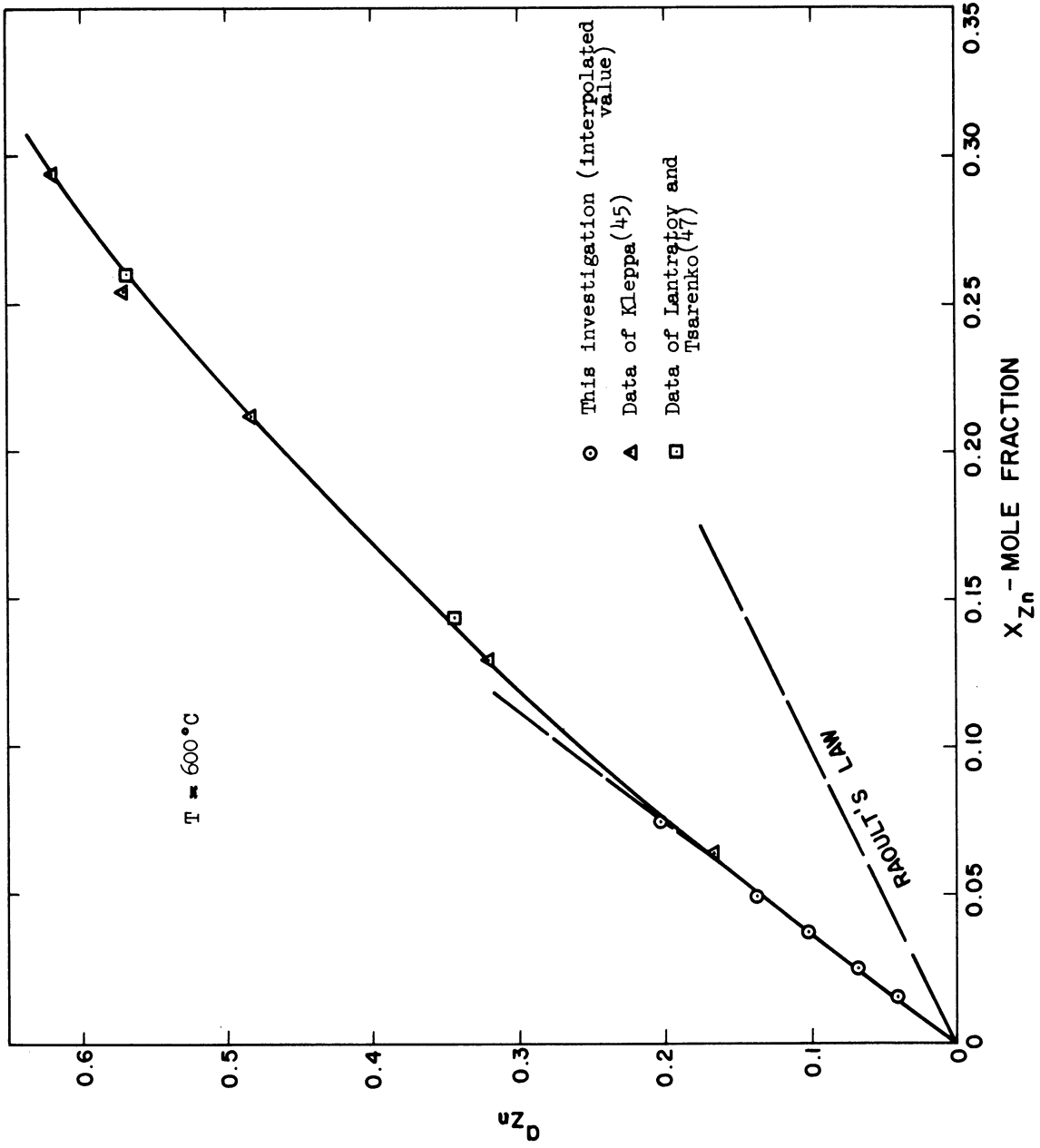


Figure 8. Activity of Zinc versus Mole Fraction of Zinc in Bismuth at 600°C.

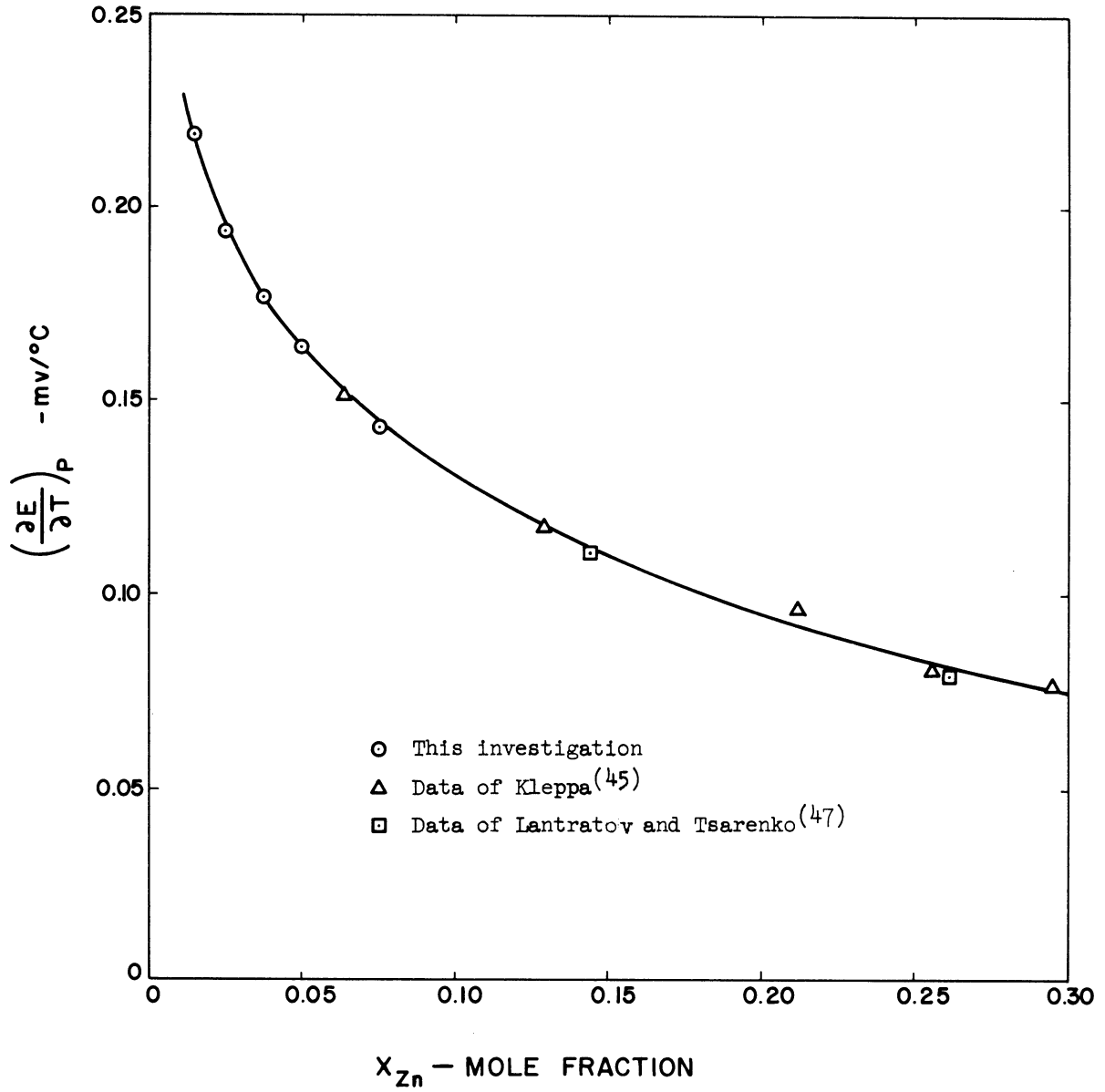


Figure 9. Slope of EMF-Temperature Curves $(\partial E/\partial T)$ versus Mole Fraction of Zinc in Bismuth.

However, a more sensitive test is to consider the behavior of either the activity coefficient or the logarithm of the activity coefficient, since both of these quantities must be constant in the Henry's Law region.

Figure 10 presents a plot of the natural logarithm of the activity coefficient versus the mole fraction of zinc, with the values calculated from the average potentials indicated as circles, and the scatter in the actual log values indicated as superimposed frequency distribution bar graphs for each composition level. A horizontal line is also drawn at $\ln \gamma = 1.110$, the value corresponding to the Henry's Law constant taken from Figure 7. The average values appeared to be in reasonable agreement with the horizontal line with the exception of the data for .0375 mole fraction. In addition, the experimental values appeared to be fairly randomly distributed about the average values, again with the exception of the .0375 mole fraction results. Here it appeared that experimental results might be skewed towards high values.

In order to further study these results, several linear regression analyses were run on the experimental values of $\ln \gamma$. A computer program was employed to determine the slope of the regression line, its intercept, the standard error of estimate, the standard deviation of the slope, and to calculate the value of "t" for the hypothesis that the slope is not significantly different from zero.⁽⁶⁸⁾ The results of the calculations are summarized below:

STATISTICAL ANALYSIS OF BINARY DATA AT 550°C

Data Considered	For Linear Relation Between $\ln \gamma_{Zn}$ and x_{Zn}		Std. Error of Est.	$t_{calc.}$	(From Table in Ref. 68) $t_{.95, n}$
	Slope	Intercept			
All 64 data points	.275	1.108	.029	1.151	2.000
54 points (excludes data for $x_{Zn} = .0375$)	.140	1.108	.029	.578	2.005
52 points (excludes data for $x_{Zn} = .0375,$.064, .075)	.337	1.104	.029	1.203	2.005
39 points (only includes the data for $x_{Zn} = .015,$.025)	-.439	1.118	.032	-.410	2.020

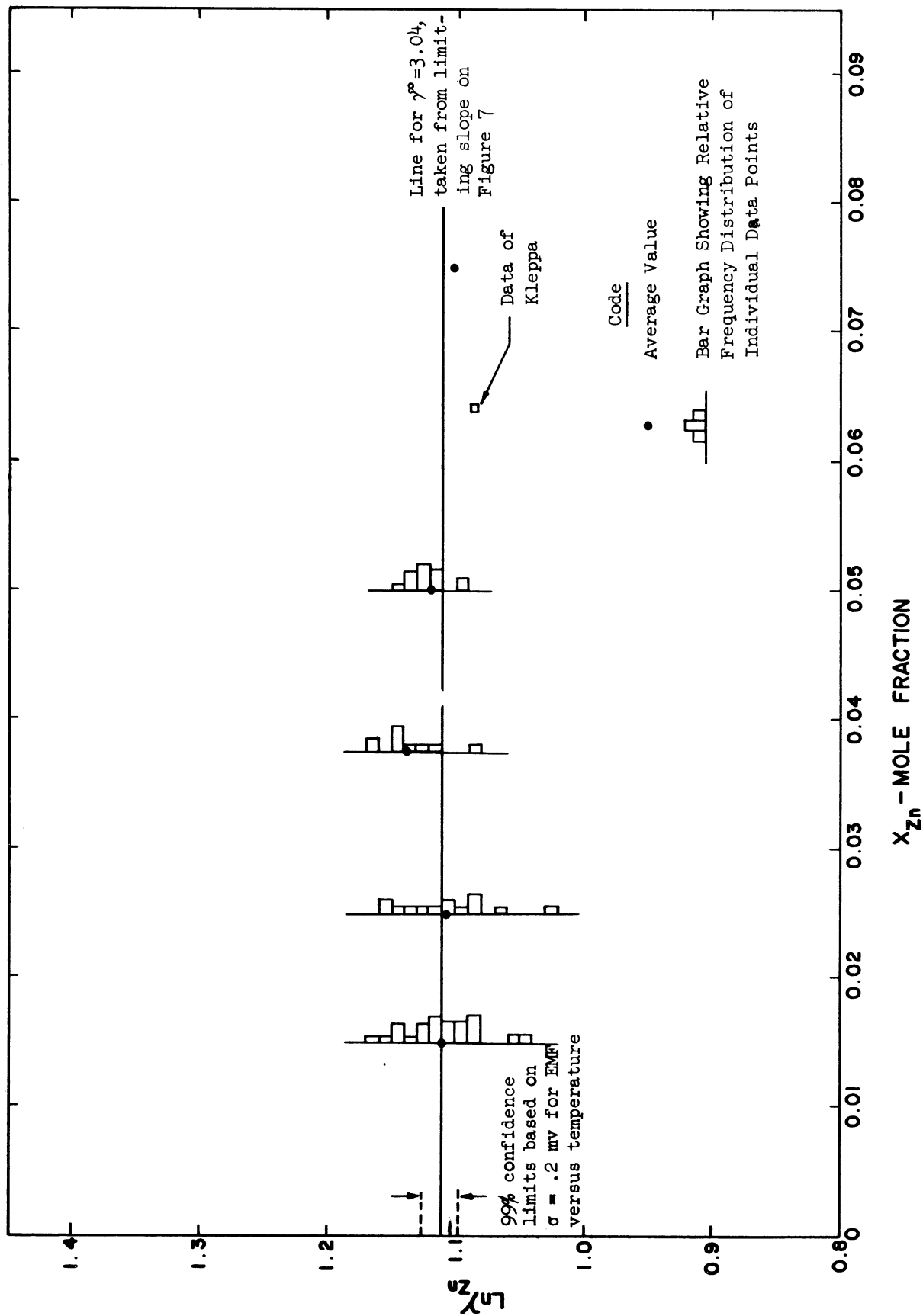


Figure 10. Determination of Zinc Self-Interaction in Dilute Solution with Molten Bismuth.

The tabulation shows that although the various least squares lines have slight slopes (i.e., the interaction parameter might not be zero), in no case was this slope significantly different from zero. Therefore, it was concluded that the self-interaction of zinc is essentially zero.

The extent of the Henry's Law region depends on what interpretation is placed on the data at .0375 mole fraction zinc. It appears most reasonable to conclude that these data are skewed, since if the data are accepted at face value, the activity-versus-concentration curve calculated from average potentials would have a point of inflection between .025 and .0375 mole fraction zinc, an occurrence that would be possible but unlikely. Since the average potentials for .015, .025, and .050 mole fraction yield $\ln \gamma$ values that are in close agreement, the conclusion reached is that the Henry's Law region extends to at least .050 mole fraction and might go to .075 mole fraction, although at this point some curvature does appear to be developing in the activity-concentration line.

A further point to be considered is the within-run scatter as opposed to the between-run scatter. Without using the formal technique of analysis of variance, it is still possible to assess these effects by a statistical argument.⁽⁶⁸⁾ Table VI shows that the standard error of estimate is approximately the same for all compositions at an average value of .20 millivolts. Strictly speaking, this cannot be considered as a standard deviation, since by using linear regression, the confidence

limit placed on the value for the emf at a given temperature depends on where that temperature is in relation to the entire range of temperatures studied. For a point at the middle of the range, which is the case for the 550° data, the variance of estimate is the standard error of estimate divided by the square root of the number of observations.⁽⁶⁸⁾

However, for the present discussion, it would be desirable to have a number that would express the variance of potential for a run as a whole, and as a conservative value, the standard error of estimate can be used. Assuming that .20 millivolts is a reasonable figure, then the application of 99 per cent confidence limits to the average potential for $x_{Zn} = .015$ would suggest the range of $\ln\gamma$ at 550°C from 1.093 to 1.127 as reflecting all the expected variation due to temperature and other uncertainties within a run. When these limits are applied to Figure 10, it is seen that some experimental values for $\ln\gamma$ fall outside this range and that a portion of the variation shown by the bar graphs must be due to differences between runs. These differences are most likely caused by slight compositional differences and residual impurities and/or moisture in the electrolyte, since in the ternary runs the potentials of all electrodes appeared to be affected to the same extent.

On this basis, the majority of the scatter shown in the bar graphs of Figure 10 has been assigned to a "cell factor". Corrections for the "cell factor" were made in the following manner. Based on the regression analysis and the limiting slope drawn on Figure 7, $\ln\gamma = 1.110$ was adopted as the "best" or "most probable" value for the zinc-bismuth

system at 550°C. The potential corresponding to this value was calculated for each of the compositions studied. Extrapolations to the other temperatures, 450, 500, 600, and 650°C were made using the average values of the emf-temperature slopes. The result was a set of "standard" electrode potentials for binary alloys which are summarized in Table VII together with the average values from the original data. In most cases, the adjustment was quite small, ranging from a few hundredths of a millivolt to approximately one millivolt for the .0375 mole fraction data.

The implications of this procedure are that all the uncertainties between electrodes have been combined in one correction factor. By using average values of emf-versus-temperature slopes, compositional variation, if any, has been subordinated to the absolute factors such as residual impurities or moisture in the electrolyte or junction potentials at the standard/electrolyte interface, etc. By applying the "cell factor", which is determined from the binary electrode results, to the absolute potentials of the multi-component electrodes in the same cell the results of several runs can be compared on a common basis. Since the interaction parameters are relative quantities, this merely means that the comparisons are made to a common base point, and that (hopefully) the remaining variation in the multi-component electrode results is due to factors associated with the added solutes and not to the factors resulting from the operation of a particular cell. The statistical analysis was confined to the 550°C data, since the confidence in interpolated potentials from least squares analysis is best at the mid-point of the temperature range studied.

TABLE VII

SUMMARY OF BINARY ELECTRODE POTENTIALS AND ACTIVITY
COEFFICIENTS FOR BISMUTH-ZINC ALLOYS

Electrode Potential	"Average Values" X_{Zn} -Mole Fraction					"Standard Values" ^a X_{Zn} -Mole Fraction				
	Temp. °C	.015	.025	.0375	.050	.015	.025	.0375	.050	.050
450	87.63	72.16	58.36	50.03	87.67	72.05	59.39	50.48		
500	98.58	81.86	67.21	58.23	98.62	81.75	68.24	58.68		
550	109.53	91.56	76.06	66.43	109.57	91.45	77.09	66.88		
600	120.48	101.26	84.91	74.63	120.52	101.15	85.94	75.08		
650	131.43	110.96	93.76	82.83	131.47	110.85	94.74	83.28		
$(\partial \epsilon / \partial t)_p$.219	.194	.177	.164	.219	.194	.177	.164		
Activity Coefficient	$\gamma_{Zn}^0 = 3.96$	3.96	3.44	3.02	2.70	2.43				
					$\gamma_{Zn}^{**} = 3.96$	3.42	3.04	2.72	2.46	

* By visual fit of slope to plots of a_{Zn} vs X_{Zn}

**Value corresponding to $\ln \gamma$ calculated for $X_{Zn} = .015$

a, Standard values obtained by normalizing 550° emfs to be equivalent to $\ln \gamma = 1.110$ (obtained from 64-point linear regression) and then applying $(\frac{\partial \epsilon}{\partial t})_p$ values from "average values."

b) Electrode potential, millivolts

If .20 millivolts is used as a conservative estimate of the standard deviation of the potential within a run, then it can be said at the 99 per cent confidence level that uncertainties within a run are in the order of $\pm .5$ to 1.0 per cent of the absolute potential. The "cell factors" used to correct the data in multi-component runs depend on the temperature under consideration and thus it is difficult to fix an over-all estimate of the uncertainties removed by using the standard potentials. However, in most cases, the corrections were less than one per cent of the absolute level of the potential, and in only a very few cases was the correction much larger than one per cent.

The Henry's Law constants for the binary alloys were determined for both the average potentials and the standard potentials for the range 450 to 650°C and are summarized in Table VII. The values for the average potentials were obtained by visual fit of the best slope to large scale plots of activity versus concentration, with less weight placed on the average data for .0375 mole fraction zinc than on the .015, .025, and .050 mole fraction data. The values for the standard potentials correspond to $\ln \gamma$ for $x_{Zn} = .015$. The differences between the two sets of values are slight, although it is felt that a slight uncertainty exists in the second decimal place. The preferred values are those obtained from the standard potentials. Since the interaction parameters for the ternary studies are determined from $\ln \gamma$ values, three decimal places were carried forward to the $\ln \gamma$ calculations.

The temperature dependence of the Henry's Law constant was found to fit the following type of relationship as suggested by Dealy and Pehlke⁽⁸⁶⁾

$$\ln \gamma_{zn}^0 = -0.79 + \frac{1568}{T (^{\circ}K)}$$

Using this equation, γ^0 at 352°C is 5.6. The value of γ^0 calculated from the vapor pressure data of Yokokawa et al.⁽⁶¹⁾ at this temperature was 5.4.

The detailed analysis of the binary alloy results thus showed that the self-interaction of zinc in bismuth is essentially zero, that the Henry's Law region extends to at least .050 mole fraction zinc, and that the system exhibits a strong positive deviation from Raoult's Law. Also, the experimental procedures have been verified, and a basis has been laid for assessing the confidence to be placed on the results from multi-component runs.

B. Zinc-Bismuth-j Ternary Systems

The zinc-bismuth-j ternary systems were studied to determine the interaction parameter between the solute elements, Zn and j, and to investigate the possible periodicity of such interactions. The data are presented separately for each system studied. The presentation of the results in this section is primarily factual; the interpretation of the effects and the significance of temperature dependence are discussed in a later section on the Rationale of the Observed Interactions (pp. 166-176).

The order of presentation of the systems studied is by increasing atomic number of the solute j . The data are presented in form of tabulations of the electrode potential at 550°C, the slope of the emf-versus-temperature relation, the standard error of estimate for the least squares relation between emf and temperature, and the natural logarithm of the activity coefficient at 550°C. Before calculating the activity coefficient the electrode potential was corrected by the "cell factor", where the cell factor is the difference between the measured and standard values for the potential of the binary electrode included in the cell.

The interaction parameters were determined graphically by Method I (pp.19-21). They were obtained by cross-plotting the limiting slopes of plots of $\ln\gamma_{Zn}$ versus x_j for various constant contents of zinc. The calculations were carried out at 450, 500, 550, 600, and 650°C. For each system, a plot is presented defining the temperature dependence of the interaction parameters. The intermediate slopes and the final values for the first-and second-order interaction parameters are summarized in Table IX.

1. Bismuth-Zinc-Copper System

The results showing the effect of copper on the activity of zinc are presented in Table VIII and Figures 11 through 13. Additional data defining the single-phase liquidus boundary in the bismuth-rich corner of the system are presented in a later section (p.128). Here it will be mentioned that in the first runs on this system, a marked

TABLE VIII
EXPERIMENTAL DATA FOR BISMUTH-ZINC-j TERNARY ALLOYS

Run No	X _{Zn} *	0		.0075		.015		.025		.0375		.050												
		EMF at 550°C	(∂E/∂t) _t	σ	lny	EMF at 550°C	(∂E/∂t) _t	σ	lny	EMF at 550°C	(∂E/∂t) _t	σ	lny	EMF at 550°C	(∂E/∂t) _t	σ	lny							
Bi-Zn-Cu Alloys j = Cu																								
5	.015	109.57						109.66	.208	.37	1.108	110.77	.205	.56	1.076	119.92 e	.208	.46	1.044	114.83 e	.218	.39	.962	
68	C		112.49	.223	.58	1.110		114.49	.219	.36	1.054	115.41	.215	.19	1.028	115.09 e	.213	.23	1.037					
7	.025	91.45						U	-	-	-	93.06 e	.179	.09	1.065	95.11 e	.188	.25	1.007	95.86 e	.206	.33	.986	
22	C							97.41	.202	.05	.992	98.71 e	.193	.19	.905	99.51 e	.201	.06	-	U				
66	C		92.20	.190	.38	1.110		93.24	.187	.26	1.081	95.25 e	.185	.26	1.024	97.13 e	.185	.19	.971	96.80 e	.200	.06	.979	
67	C		91.84	.189	.46	1.110		93.77	.186	.29	1.056	94.90 e	.183	.26	1.024	97.02 e	.180	.25	.964	98.68 e	.173	.18	.917	
8	.0375	77.09						78.38	.172	.06	1.074	82.06 e	.163	.08	.970	83.84 e	.159	.62	.920	83.32 e	.154	.96	.934	
9	C		75.78	.184	.06	1.110		U	-	-	-	83.55 e	.167	.13	.852	82.08 e	.168	.66	.993	U				
22	C							N	-	-	-	80.72 e	.173	.09	1.008	N				N				
70	C		75.04	.174	.36	1.110		77.00	.169	.28	1.065	72.33 e	.151	.30	1.186	78.72 e	.180	.26	1.002	N				
2	.050	66.88						69.05 e	.158	.06	1.049	70.71 e	.155	.11	1.002	72.12 e	.159	.10	.962	73.88 e	.155	.10	.613	
69	C		66.25	.159	.29	1.110		68.31 e	.155	.26	1.052	69.68 e	.152	.26	1.013	71.39 e	.155	.39	.965	N				
Bi-Zn-Ga Alloys j = Ga																								
52A	.015	109.57						107.09	.216	.05	1.192	106.56	.221	.11	1.207	106.08	.213	.04	1.220	106.88	.213	.04	1.198	
52B	C		109.48	.221	.04	1.109		107.08	.211	.05	1.178	107.05	.207	.09	1.179	107.47	.200	.20	1.167	108.13	.201	.16	1.148	
58	C		108.75	.219	.16	1.109		107.42	.214	.14	1.148	107.53	.215	.09	1.145	107.62	.213	.18	1.142	N				
58	.025	91.45						N	-	-	-	89.47		-	-	N				N				
53	C		90.62	.196	.12	1.109		89.26	.190	.15	1.127	89.47	.189	.11	1.121	89.96	.188	.11	1.107	U				
57	C		(90.11)					89.48	.190	.22	1.128	N		-	-	N				N				
61	C		90.90	.187	.28	1.109		89.56	.186	.24	1.148	89.69	.185	.22	1.144	90.06	.185	.19	1.134	N				
61	C		90.86	.187	.28	1.111		N	-	-	-	N		-	-	N				N				
55	.0375	77.09						75.08	.175	.35	1.112	75.83	.176	.38	1.092	75.74	.175	.40	1.094	72.05	.169	.42	1.199	
56	.050	66.88						66.21	.162	.09	1.121	U		-	-	67.19	.159	.10	1.094	67.93	.159	.09	1.073	

TABLE VIII (CONT'D)

X_j*

Run No	X _{Zn} *	STD EMF for Binary	0			.015			.025			.0375			.050							
			EMF at 550°C	($\frac{\partial E}{\partial t}$)	σ	ln γ	EMF at 550°C	($\frac{\partial E}{\partial t}$)	σ	ln γ	EMF at 550°C	($\frac{\partial E}{\partial t}$)	σ	ln γ	EMF at 550°C	($\frac{\partial E}{\partial t}$)	σ	ln γ				
Bi-Zn-Ag Alloys j = Ag																						
18	.015	109.57 c	109.05	.218	.20	1.110	111.22	.218	.14	1.049	111.22	.216	.15	1.049	112.72	.215	.08	1.006	113.92	.214	.12	.973
16	.025	91.45	94.64	.199	.34	-	93.64	.196	.28	1.048	94.82	.193	.48	1.014	97.49	.197	.45	.938	97.23	.190	.41	.945
21							94.30	.191	.18	1.028	94.30	.191	.18	1.028	96.52	.190	.18	.967	N	-	-	-
19	.0375	77.09	77.84	.182	.08	1.111	80.24	.181	.10	1.043	84.21	.183	.09	.931	84.83	.182	.16	.914	83.80	.178	.08	.943
21							N	-	-	-	79.09	.170	.06	1.057	82.38	.173	.07	.965	N	-	-	-
17	.050	66.88	67.38	.170	.23	1.110	69.22	.168	.24	1.058	71.17	.169	.20	1.003	71.58	.167	.25	.991	73.37	.166	.24	.941
Bi-Zn-Cd Alloys j = Cd																						
12	.015	109.57	N	-	-	-	109.74	.227	.05	1.105	110.39	.224	.01	1.087	U	-	-	-	U	-	-	-
15			111.89	.221	.23	1.109	N	-	-	-	N	-	-	-	109.35	.216	.09	1.174	113.38	.222	.08	1.068
65			109.06	.221	.10	1.109	U	-	-	-	U	-	-	-	109.18	.218	.14	1.112	109.21	.217	.17	1.113
10	.025	91.45	N	-	-	-	92.96	.201	.13	1.068	93.10	.199	.05	1.064	91.09	.196	.08	1.120	91.09	.195	.06	1.120
14			N	-	-	-	92.54	.198	.14	1.074	92.29	.197	.12	1.087	90.31	.194	.10	1.142	92.91	.197	.06	1.069
13	.0375	77.09	N	-	-	-	77.32	.178	.16	1.104	77.57	.178	.12	1.097	77.81	.178	.17	1.090	78.08	.178	.09	1.082
11	.050	66.88	N	-	-	-	68.06	.167	.11	1.077	67.94	.166	.06	1.080	67.58	.164	.09	1.090	66.68	.163	.04	1.116
15			N	-	-	-	N	-	-	-	N	-	-	-	69.01	.166	.10	1.115	68.41	.166	.07	1.132
Bi-Zn-In Alloys j = In																						
48	.015	109.57	109.13	.226	.32	1.110	107.79	.223	.33	1.148	107.22	.219	.34	1.164	107.08	.215	.33	1.168	106.54	.211	.32	1.183
43	.025	91.45	89.82	.191	.16	1.110	U	-	-	-	U	-	-	-	87.95	.191	.26	1.163	87.91	.191	.28	1.164
49			90.41	.191	.25	1.110	89.69	.190	.22	1.131	89.52	.190	.21	1.135	89.72	.191	.16	1.130	90.09	.190	.14	1.149
44	.0375	77.09	75.66	.174	.42	1.110	76.08	.175	.26	1.100	75.85	.175	.21	1.106	75.84	.175	.12	1.106	75.73	.175	.08	1.110
54A			75.45	.175	.05	1.110	75.94	.176	.05	1.096	75.77	.176	.05	1.101	75.60	.175	.05	1.106	75.27	.175	.05	1.115
54B			75.89	.175	.09	1.110	75.92	.174	.07	1.143	75.90	.175	.07	1.110	75.56	.175	.06	1.119	75.06	.174	.05	1.134
50	.050	66.88	66.18	.160	.16	1.110	65.86	.159	.13	1.119	U	-	-	-	U	-	-	-	64.32	.158	.19	1.162
51			66.12	-	-	1.110	N	-	-	-	65.76	.168	.16	1.120	65.43	.168	.20	1.130	N	-	-	-

TABLE VIII (CONT'D)

X_j^*

Run No	X_{Zn}	STD EMF for Binary	0			.015			.025			.0375			.050							
			EMF at 550°C	$\frac{\partial \epsilon}{\partial t}$	σ	EMF at 550°C	$\frac{\partial \epsilon}{\partial t}$	σ	EMF at 550°C	$\frac{\partial \epsilon}{\partial t}$	σ	EMF at 550°C	$\frac{\partial \epsilon}{\partial t}$	σ	EMF at 550°C	$\frac{\partial \epsilon}{\partial t}$	σ					
Bi-Zn-Sn Alloys $j = Sn$																						
25	.015	109.57	109.92	1.110	110.66	1.089	110.22	1.102	111.62	1.062	111.52	1.065	111.52	1.062	111.52	1.065						
47	C,D	C	108.01	.216	.18	1.110	108.64	.216	.18	1.092	108.91	.216	.18	1.085	109.52	.216	.18	1.068	110.16	.216	.18	1.049
20	.025	91.45	92.21	.194	.57	1.110	95.85	.197	.62	1.007	95.39	.196	.58	1.023	94.64	.195	.69	1.042	94.40	.194	.57	1.098
27	C	C	91.63	.197	.32	1.110	92.03	.196	.23	1.099	91.49	.193	.58	1.114	93.97	.198	.41	1.044	92.14	.195	.35	1.096
26	.0375	77.09	77.84	.183	.03	1.110	U	-	-	-	U	-	-	-	79.58	.183	.06	1.061	80.40	.183	.04	1.038
45	C	C	76.16	.175	.06	1.110	76.57	.175	.06	1.098	U	-	-	-	U	-	-	-	U	-	-	-
46	C	C	75.58	.174	.15	1.110	76.08	.174	.13	1.096	76.21	.174	.14	1.092	76.61	.174	.14	1.081	U	-	-	-
23	.050	66.88	66.17	.165	.06	1.110	67.08	.165	.08	1.084	68.91	.167	.09	1.033	U	-	-	-	69.03	.166	.12	1.029
24	C	C	67.26	.164	.21	1.110	67.28	.164	.18	1.109	67.54	.164	.18	1.102	67.83	.164	.18	1.094	67.96	.165	.22	1.090
Bi-Zn-Sb Alloys $j = Sb$																						
36	.015	109.57	N	-	-	-	111.54	.217	.34	1.055	114.73	.217	.30	.965	N	-	-	-	N	-	-	-
37	C	C	109.63	.212	.29	1.110	111.15	.210	.28	1.067	113.82	.210	.29	.922	115.88	.209	.30	.934	117.66	.209	.27	.884
32	.025	91.45	93.04	.198	.24	-	93.69	.194	.20	1.046	95.81	.195	.16	.986	97.71	.194	.22	.933	99.76	.194	.20	.875
34	.0375	77.09	76.48	.179	.18	1.110	79.29	.178	.18	1.030	80.68	.176	.12	.991	82.49	.176	.12	.940	84.38	.175	.12	.887
28	.050	66.88	66.64	.158	.97	1.109	U	-	-	-	70.70	.161	.21	.994	71.85	.160	.24	.962	75.18	.161	.28	.868
36	C	C	N	-	-	-	68.89	.162	.20	1.093	N	-	-	-	72.57	.161	.24	.950	N	-	-	-
Bi-Zn-Hg Alloys $j = Hg$																						
59	.015	109.57	103.52	.209	.37	1.110	104.39	.210	.32	1.086	103.78	.209	.36	1.103	U	-	-	-	U	-	-	-
60	.025	91.45	91.61	.194	-	1.110	92.57	-	-	1.083	93.57	-	-	1.055	94.38	-	-	1.032	95.35	-	-	1.005
Bi-Zn-Pb Alloys $j = Pb$																						
38	.015	109.57	110.51	.217	.21	1.110	110.68	.218	.18	1.105	110.35	.218	.19	1.115	107.87	.215	.25	1.185	112.19	.221	.26	1.063
64	C	C	110.48	.219	.25	1.110	109.80	.218	.37	1.129	109.29	.217	.42	1.144	108.64	.217	.38	1.162	108.73	.219	.30	1.159
40	.025	91.45	91.61	.194	.20	1.110	91.14	.194	.24	1.123	90.47	.194	.26	1.142	90.04	.193	.27	1.154	89.22	.193	.19	1.178
42	.0375	77.09	77.07	.176	.34	1.110	76.27	.175	.34	1.132	75.51	.174	.23	1.154	75.69	.175	.38	1.149	75.04	.175	.36	1.167
39	.050	66.88	66.47	.163	.14	1.110	65.68	.162	.09	1.132	65.10	.162	.18	1.149	64.98	.162	.14	1.152	64.68	.162	.19	1.160

TABLE VIII (CONT'D)

Run No	* X_{Zn}	STD EMF for Binary	X_j^*											
			EMF at 550°C	$(\frac{\partial \epsilon}{\partial t})_0$	σ	lny	EMF at 550°C	$(\frac{\partial \epsilon}{\partial t})_0$	σ	lny	EMF at 550°C	$(\frac{\partial \epsilon}{\partial t})_0$	σ	lny
Bi-Zn-Au Alloys $j = Au$														
			0		.005		.010		.015		.020			
31	.015	109.51 C,D	110.00 N	.225	-	1.110	N	114.49	.228	.05	.971	116.75	-	-
35			N	-	-	-								
33	.025	91.45 C	91.20	.198	.11	1.110	93.84	.196	.16	1.036	98.71 e	.190	.31	.927
29	.050	66.88 C	66.66 N	.179	.37	1.110	70.60	.155	.29	1.005	74.15 e	.140	.08	.905
35			N	-	-	-								
Bi-Zn-Au Alloys $j = Au$ (cont'd)														
			.025		.0375		.050							
31	.015	109.51 C,D	U	-	-	-	127.41e	.225	.18	.619	133.66 e	.222	.08	.443
35			N	-	-	-	N	-	-	-	N	-	-	-
33	.025	91.45 C	N	-	-	-	N	-	-	-	N	-	-	-
29	.050	66.88 C	84.07e	.129	.29	.619	U	-	-	-	U	-	-	-
35			N	-	-	-	N	-	-	-	N	-	-	-

* Mole Fraction weighed-in basis
 EMF = mv; $(\frac{\partial \epsilon}{\partial t})_0$ = mv/°C for range 450°-650°C; σ = Standard error of estimate of EMF data from least squares line, mv
 lny = log activity coefficient, based on corrected EMF if so indicated in second column
 C = All EMF's corrected using difference of binary EMF from standard EMF as the cell correction factor
 D = Unstable standard, EMF obtained as difference from standard value assumed for binary
 N = Composition not run
 U = Discarded because EMF's were unstable or grossly in error
 e = Extrapolated value, obtained from data taken in single phase region at higher temperatures

TABLE IX
SUMMARY OF INTERACTIONS WITH ZINC IN DILUTE SOLUTION WITH MOLTEN BISMUTH

Added Solute-j	Temp. °C	$\left(\frac{\partial \ln \gamma_{Zn}}{\partial X_j}\right)_{X_j=0, X_{Zn}=\text{const}}$				$\epsilon_{Zn}^j = \left(\frac{\partial \ln \gamma_{Zn}}{\partial X_j}\right)_{X_{Zn}=0, X_j=0}$	$\epsilon_{Zn}^j = \left(\frac{\partial^2 \ln \gamma_{Zn}}{\partial X_j \partial X_{Zn}}\right)_{X_{Zn}=0, X_j=0}$
		$X_{Zn}^* = .015$.025	.0375	.050		
Cu	450	-3.2	-3.4	-3.7	-4.3	-2.95	-19
	500	-3.0	-3.2	-3.4	-4.0	-2.7	-19
	550	-2.7	-2.9	-3.1	-3.6	-2.4	-19
	600	-2.5	-2.7	-2.9	-3.3	-2.2	-19
	650	-2.3	-2.5	-2.7	-2.9	-2.05	-18
Ga	450-650	+3.6 ±0.6	+2.7 ±.4	+0.7	+0.5	+5.0 ±.7	-100 ±20
Ag	450	-3.5	-3.7	-4.0	-4.2	-3.3	-17
	500	-3.1	-3.4	-3.6	-3.8	-2.8	-20
	550	-2.8	-3.0	-3.2	-3.5	-2.5	-20
	600	-2.5	-2.8	-3.0	-3.2	-2.2	-21
	650	-2.2	-2.5	-2.7	-3.0	-1.9	-22
Cd	450-650	-0.3	-0.3	-0.5	0	-0.3	0
In	450-650	+1.7	+1.0	+0.3	+0.5	+2.2	-40
Sn	450-650	-0.8	-0.7	-1.1	-1.0 ±0.6	-0.5	-12
Sb	450	-5.4	-5.4	-5.5	-5.3	-5.4	0
	500	-4.9	-5.1	-4.9	-4.9	-4.9	0
	550	-4.4	-4.5	-4.4	-4.5	-4.45	0
	600	-4.2	-4.4	-4.1	-4.3	-4.2	0
	650	-4.0	-3.8	-3.8	-4.0	-3.9	0
Au	450	-22	-25	-	-32	-19	-220
	500	-21	-22	-	-27	-18.5	-140
	550	-19	-19.5	-	-21	-18	-50
	600	-18	-17.5	-	-17	-17.5	0
	650	-16	-15	-	-13	-17	+80
Hg	550	-.5 to -2.0	-2.0	-	-	-1 to -2	?
Pb	450	+1.4	+1.5	+1.4	+1.4	+1.4	0
	550	+1.3	+1.3	+1.3	+1.3	+1.3	0
	650	+1.2	+1.2	+1.2	+1.1	+1.2	0

*Mole fraction

discontinuity was noted in the emf-versus-temperature relations between 500 and 600°C for some of the compositions studied. These discontinuities were the temperatures of transition from two- or three-phase regions to the single phase liquid region.⁽⁵⁶⁾ The emf's reported in Table VIII where 550°C is below the transition point were obtained by extrapolation from the single phase region. The potentials thus determined apply to the so-called "super-cooled" liquid. In the single-phase region, the slopes of the emf-temperature relations were decreased slightly by the addition of copper, thus indicating that the entropy of mixing was decreased.

This system was the first one studied and the results of several runs were questionable. In addition, the reference binary electrode was not routinely included with each cell at the time of these runs. Consequently, the system was later reinvestigated and most reliance is placed on the results of the later runs.

The individual plots of $\ln \gamma_{\text{Zn}}$ versus x_{Cu} (Figure 11) are quite consistent. In all cases, the addition of copper increased the electrode potential at constant zinc content, thus causing a decrease in both the activity and activity coefficient. Over the range studied to .050 mole fraction copper, the effect on $\ln \gamma_{\text{Zn}}$ was linear with the mole fraction of copper.

The limiting slopes from these plots were a linear function of the mole fraction of zinc in the region below .0375 mole fraction. (Figure 12) The interaction parameters ranged from about -2.1 to -2.9 and

varied linearly with the reciprocal of the absolute temperature (Figure 13). The second-order interaction parameter (the limiting slope of the lines in Figure 12) appeared to be almost constant with temperature and was -19.

2. Bismuth-Zinc-Gallium System

The experimental results for the bismuth zinc gallium system are presented in Table VIII and Figures 14 through 16.

The emf-versus-temperature relations were linear throughout the entire temperature range studied and their slopes were generally unchanged by the gallium addition. Thus, a single-phase liquid was present at all temperatures studied. The small additions of gallium increased the activity of zinc when the zinc content was low. However, the effect of the gallium addition became less as both the zinc and gallium contents were increased. In contrast to the bismuth-zinc-copper system, the effect of the added element was not linear.

Replicate runs performed at .015 mole fraction zinc were not in complete agreement. During Run 52, the effect due to gallium appeared to have become less at lower temperatures during the latter portion of the run. This occurred during one late-night period when the apparatus was left unattended. Consequently, the run was divided into parts A and B at this point and considered as two separate determinations. The two parts of Run 52 were in good agreement at the higher temperatures, but the agreement was poorer as the temperature was decreased. The agreement with the replicate run, Run 58, was variable, depending on the temperature considered.

Three determinations were made at .025 mole fraction zinc (Figure 14) and the agreement between runs was better. For the higher concentrations of zinc, the effect of gallium was very slight.

The interaction parameter was determined as $5.0 \pm .7$ from the median limiting slopes indicated on Figure 15. There was no conclusive evidence for temperature dependence of the interaction parameter. The estimated second-order parameter was -100 ± 20 .

3. Bismuth-Zinc-Silver System

The experimental results for the bismuth-zinc-silver system are presented in Table VIII and Figures 17 through 19.

Published phase diagrams for this system⁽⁵⁷⁾ indicated that a wide-range single phase liquid existed at the bismuth-rich corner. The experimental observations of linear, continuous emf-temperature relations confirmed that the alloys were single phase. All the electrodes were well-behaved.

The addition of silver raised the electrode potential, thus decreasing the activity and activity coefficient of zinc. The effect on $\ln \gamma_{Zn}$ was linear with the mole fraction of added silver. The entropy of mixing of zinc was decreased slightly by the silver additions.

The interaction parameters ranged from -1.8 to -3.3 and varied linearly with the reciprocal absolute temperature (Figure 19). The second-order interaction parameter at 550°C was determined as -20 and appeared to have a linear dependence on reciprocal absolute temperature.

4. Bismuth-Zinc-Cadmium System

The experimental results for the bismuth-zinc-cadmium system are presented in Table VIII and Figures 20 through 22.

The interaction between cadmium and zinc was very slight and at the border-line of the region of experimental accuracy. The most consistent interpretation of the plots of $\ln \gamma_{Zn}$ versus x_{Cd} was that the interaction was very slightly negative. The first-order parameter was estimated as $-.3$ and the second-order parameter was zero. No temperature dependence could be detected. The emf-temperature relations were linear and continuous and the slopes were little changed by the cadmium additions. All the solutions studied were single phase.⁽⁵¹⁾

The very slight negative interaction was consistent with the iso-activity data presented by Oleari and Fiorani⁽⁵¹⁾ for higher concentrations of zinc.

The most probable cause of the scatter in the experimental results for this system was the fact that the zinc-cadmium combination has free energies of chloride formation whose difference is close to the minimum value of ΔG_{II}° for Type II displacement. Chemical and spectrographic analysis showed that the zinc content in the ternary alloys did not change measurably during the runs, however, the accuracy of the analyses may not have been sufficiently good to detect slight changes in zinc content that could account for the scatter.

5. Bismuth-Zinc-Indium System

The results for the bismuth-zinc-indium system are presented in Table VIII and Figures 23 through 25.

The emf-temperature relations were well-behaved throughout the whole temperature range and the alloys were all single phase.

The addition of indium increased the activity and activity coefficient for all compositions studied. However, the effect was diminished as the concentration of zinc was increased. For .015 mole fraction zinc, the effect of the indium addition was not linear over the entire range to .050 mole fraction indium. For the higher concentrations of zinc, the effect did appear to be linear. No measurable temperature dependence was found for the interaction parameter which was determined as +2.2. The second-order parameter was -40 and was also appeared independent of temperature.

The agreement between replicate runs was generally quite good. In Run 54, at .0375 mole fraction zinc, there was a shift in the potential of the binary reference electrode during one over-night period. The run was separated at this point and treated as two determinations. When the "cell factor" was applied to the two sets of data the corrected emf's of the ternary electrodes were found in good agreement. This emphasized the value of the "cell factor" for referring the interactions to a common base point.

The positive first-order interaction parameter was consistent with the observations of Yokokawa et al.⁽³⁶⁾ that indium additions increased the activity of zinc at higher concentrations of zinc.

6. Bismuth-Zinc-Tin System

The results of the study of the effect of tin on the activity of zinc in molten bismuth are summarized in Table VIII and Figures 26 through 28. The published data⁽⁵²⁾ and the experimental observations were that a single-phase liquid existed at all temperatures and compositions studied in this investigation.

The effect of the zinc additions was to increase the electrode potential, thus decreasing the activity and activity coefficient of zinc. The effect appeared to be linear with the mole fraction of added tin.

In the determination of the interaction parameter, most reliance was placed on the data taken at .015 and .0375 mole fraction zinc. The replicate runs for these compositions were in good agreement, while data taken at the other zinc contents exhibited some scatter. There was no significant temperature dependence to the interactions.

The first-order interaction parameter was fixed at $-.5$ and the second order parameter at -12 .

The experimental results were qualitatively consistent with the observations of Yokokawa et al,⁽³⁶⁾ and Oleari and Fiorani⁽⁵²⁾ for more concentrated solutions.

7. Bismuth-Zinc-Antimony System

The experimental results for the bismuth-zinc-antimony system are summarized in Table VIII and Figures 29 through 31.

All the compositions studied were single-phase throughout the experimental temperature range.⁽⁵⁷⁾ The addition of antimony decreased

the activity and activity coefficient and the effect on $\ln \gamma_{Zn}$ was linear. The agreement between replicate runs was excellent.

For .025 mole fraction zinc (Run 32), the cell factor correction was not applied since it was found that the values of $\ln \gamma_{Zn}$ calculated from the uncorrected emf's for the ternary alloys fell on a line intersecting the ordinate ($x_{sb} = 0$) at the standard value of $\ln \gamma_{Zn}$ for $x_{Zn} = .025$. Apparently in this case, the binary electrode may have contained less zinc than intended, since its emf at 550°C and emf-versus-temperature slope were slightly high compared to the normal expectation.

The interaction parameters ranged from -3.9 to -5.4 and were linear with the reciprocal absolute temperature. Second-order effects in this system were negligible.

8. Bismuth-Zinc-Gold System

The results for the bismuth-zinc-gold system are summarized in Table VIII and Figures 32 through 34.

The addition of gold was found to cause a marked decrease in the activity of zinc. In addition, discontinuities were observed in the emf-temperature relations, thus indicating that the transition to the single-phase liquid solution occurred within the normal range of compositions studied. By reducing the gold additions to the range from .005 to .020 mole fraction it was possible to obtain sufficient data in the single-phase region in the temperature range from 450 to 650°C to establish the limiting relations between $\ln \gamma_{Zn}$ and x_{Au} . Estimates were also made of the position of the liquidus surface at the bismuth-rich corner of this system (pp. 128-134).

The interaction parameter ranged from -17 to -19 and appeared to be linear with reciprocal absolute temperature. The second-order parameters ranged from +80 at 650°C to -220 at 450°C and also appeared to be linear with reciprocal absolute temperature. Since the interaction effects were well-defined by the data obtained at .015, .025, and .050 mole fraction zinc, no runs were made at .0375 mole fraction zinc.

9. Bismuth-Zinc-Mercury System

The results obtained for the bismuth-zinc-mercury system are summarized in Table VIII and Figure 35.

Due to the volatility of mercury and the potential health hazard, it had been decided to make only enough runs on this system to define the interaction effect and, if possible, estimate its extent. The experimental system was maintained closed to avoid mercury loss and the runs were discontinued as soon as the trend of the mercury additions became evident.

In Run 59 (.015 mole fraction zinc), the electrodes containing .015 and .025 mole fraction mercury had increased potentials, while the results for the electrodes containing .0375 and .050 mole fraction mercury were rejected due to instability.

In Run 60 (.025 mole fraction zinc) a consistent effect was found over the entire composition range studied. A linear decrease in $\ln \gamma_{Zn}$ was observed as x_{Hg} was increased.

The interaction parameter was estimated as -1 to -2 with most reliance placed on the data from Run 60. There appeared to be no temperature dependence to the interaction. The second-order effects, if any, were uncertain.

From the two runs, the evidence was that mercury is a moderate negative interactor with zinc. The study of the system was discontinued at that point.

10. Bismuth-Zinc-Lead System

The results obtained on the bismuth-zinc-lead system are summarized in Table VIII and Figures 36 through 38.

The published information and the experimental observations of emf-versus-temperature behavior were that this system was composed of a single-phase liquid at all temperatures and compositions studied in the present investigation.⁽⁵⁰⁾

The addition of lead caused a decrease in the electrode potentials, thus raising the activity and activity coefficient of zinc. The effect of lead on $\ln\gamma_{Zn}$ was to cause a linear increase with increasing mole fraction of lead. Only a very slight temperature dependence was found for the first-order interaction parameter and the second-order effects were negligible.

The interaction parameter ranged from +1.2 at 650 to +1.4 at 450°C.

The iso-activity plot of Valenti et al.⁽⁵⁰⁾ indicated that lead tended to increase the activity of zinc. The present results in dilute solution were consistent with those observations.

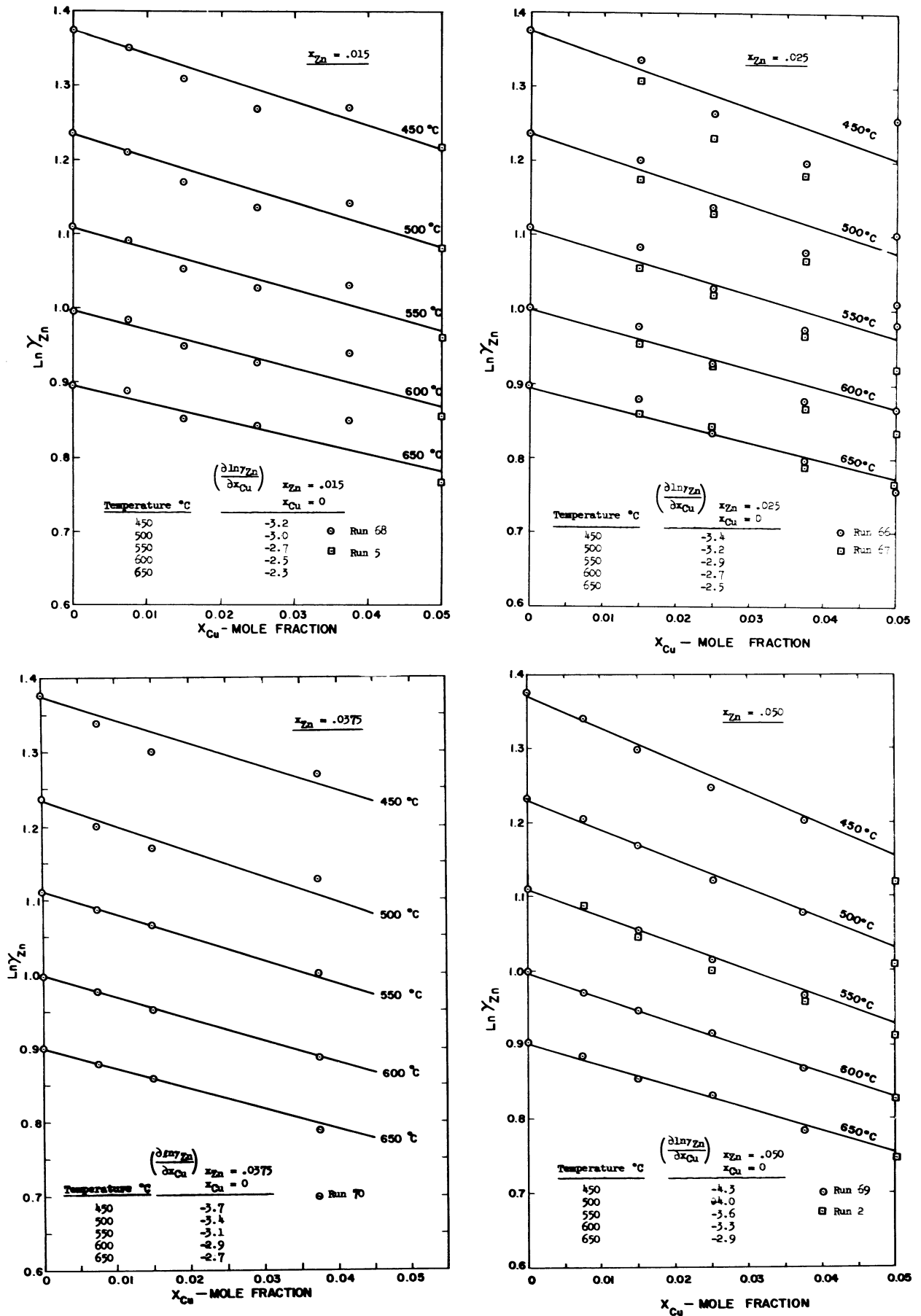


Figure 11. Natural Logarithm of Zinc Activity Coefficient versus Mole Fraction Copper - for Indicated Constant Mole Fractions of Zinc.

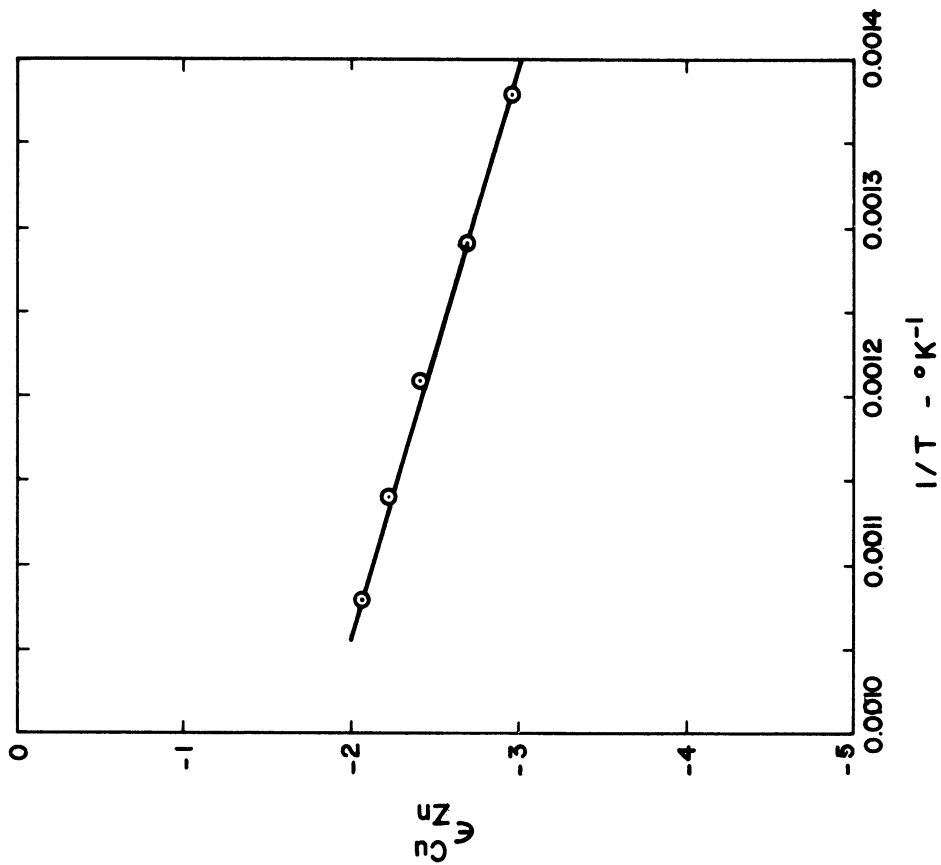


Figure 13. Temperature Dependence of First-Order Cu-Zn Interaction Parameter.

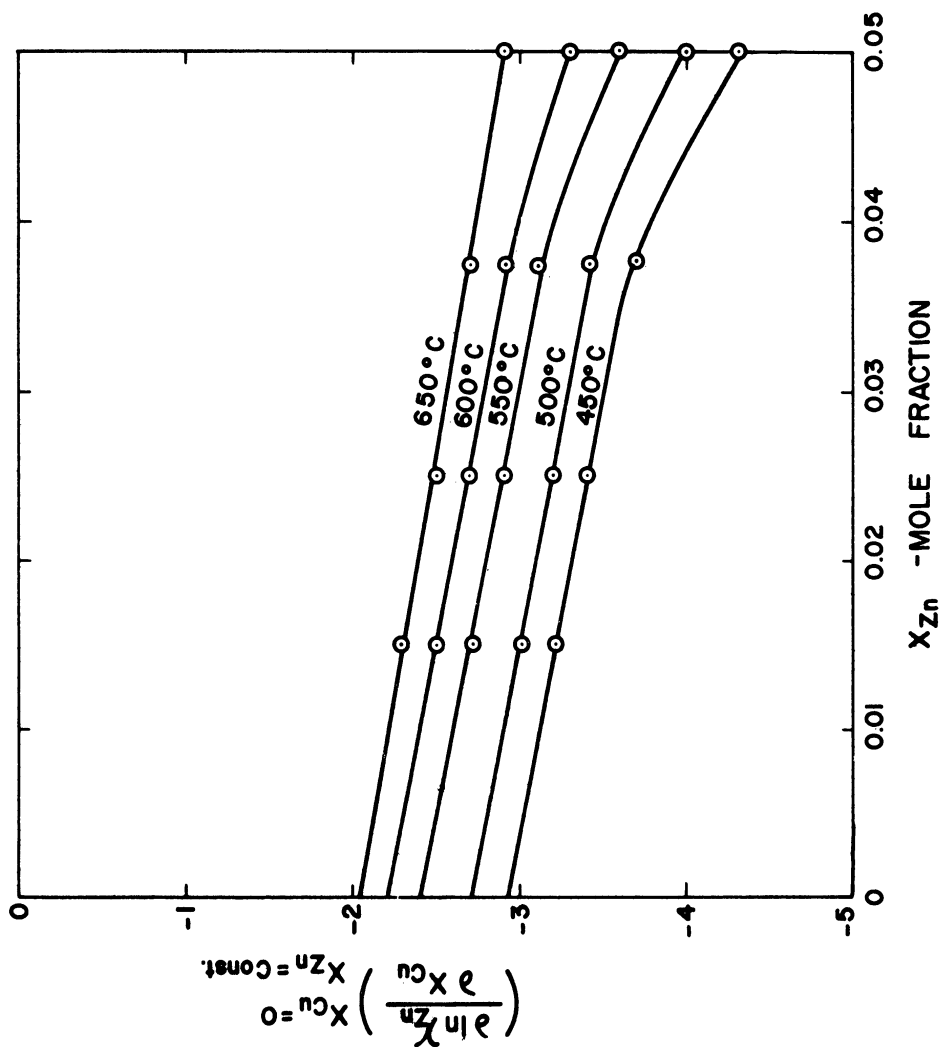


Figure 12. Determination of Cu-Zn Interactions in Molten Bismuth.

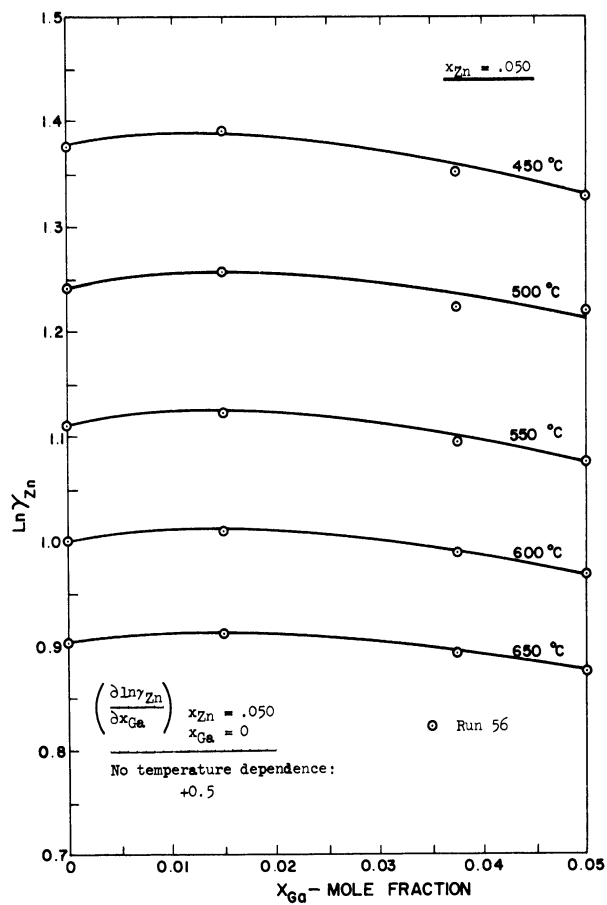
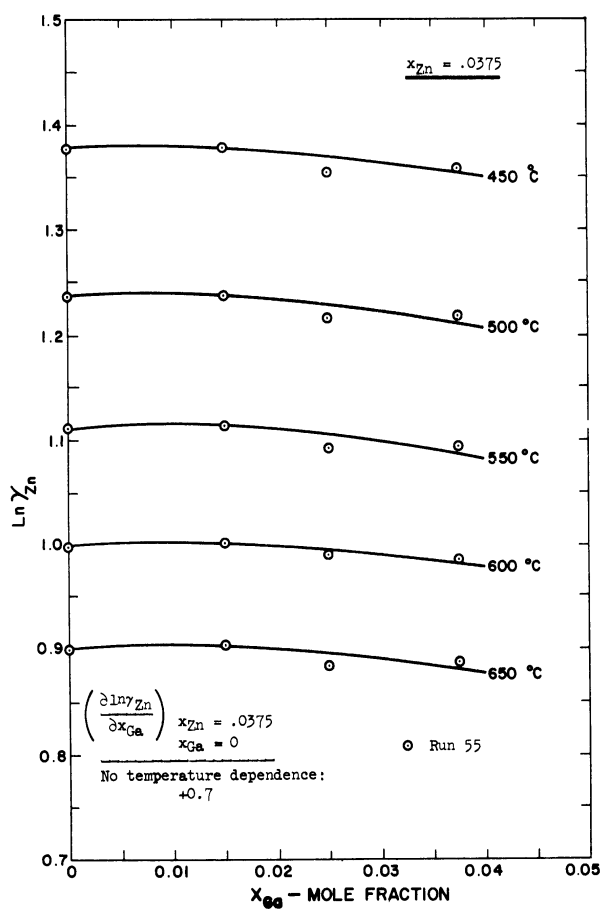
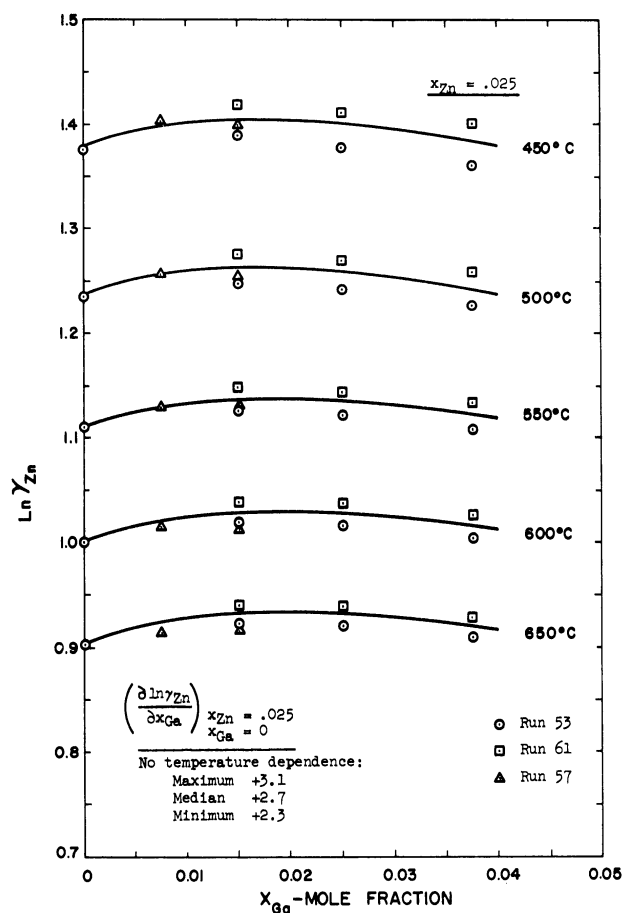
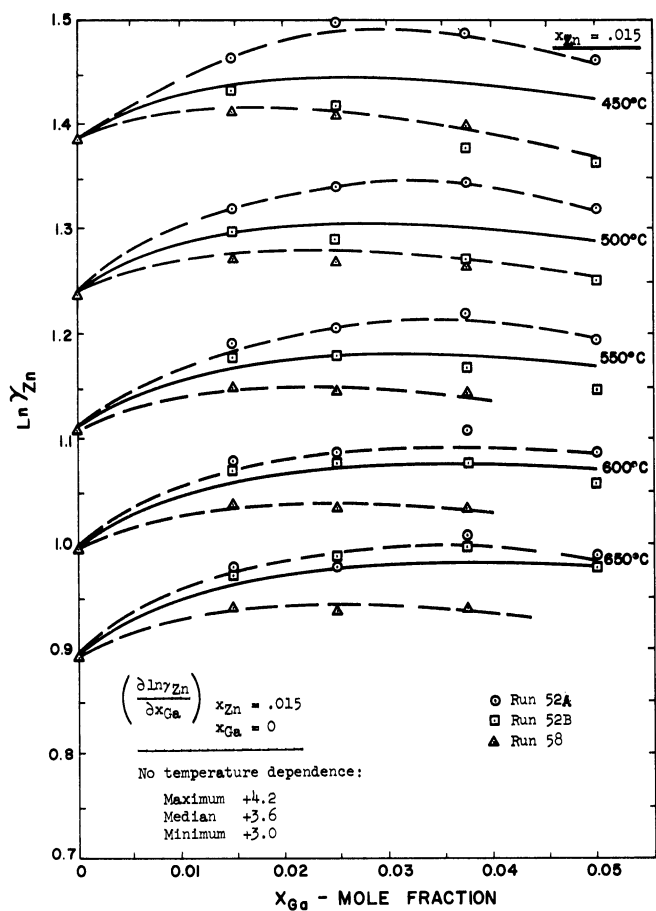


Figure 14. Natural Logarithm of Zinc Activity Coefficient versus Mole Fraction Gallium - for Indicated Constant Mole Fractions of Zinc.

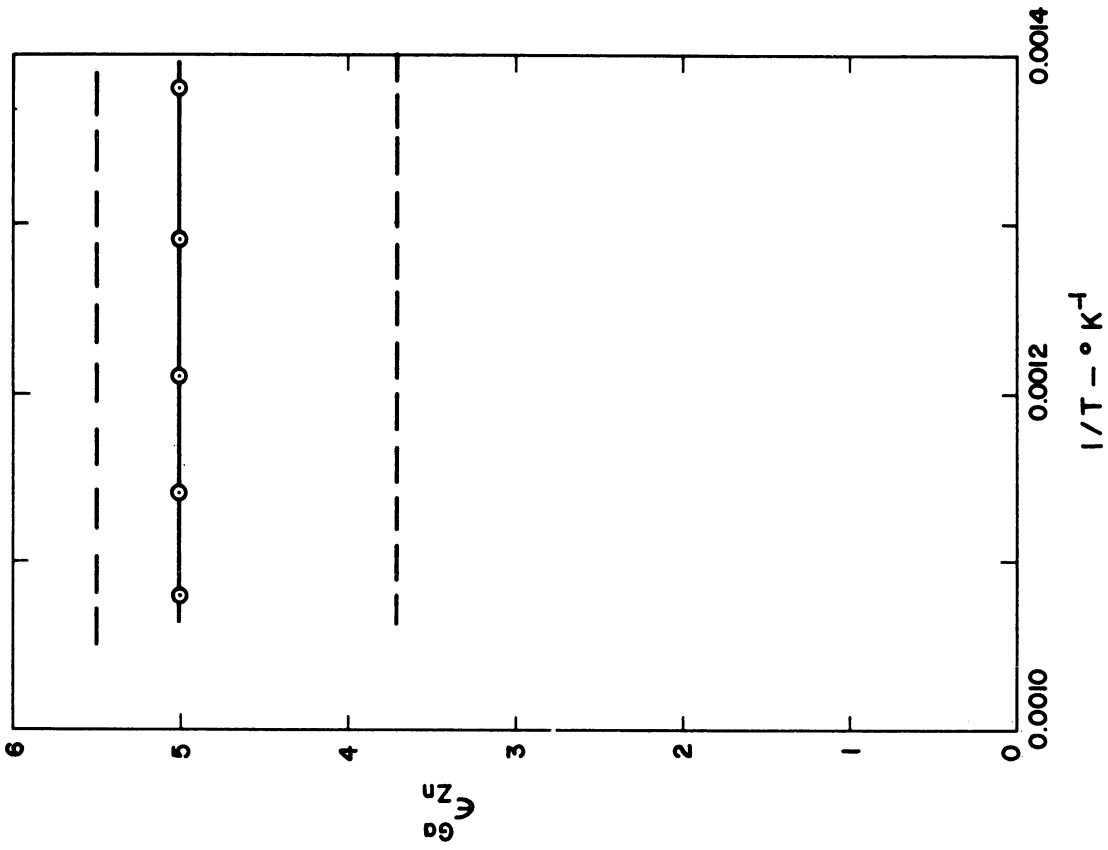


Figure 16. Temperature Dependence of First-Order Ga-Zn Interaction Parameter.

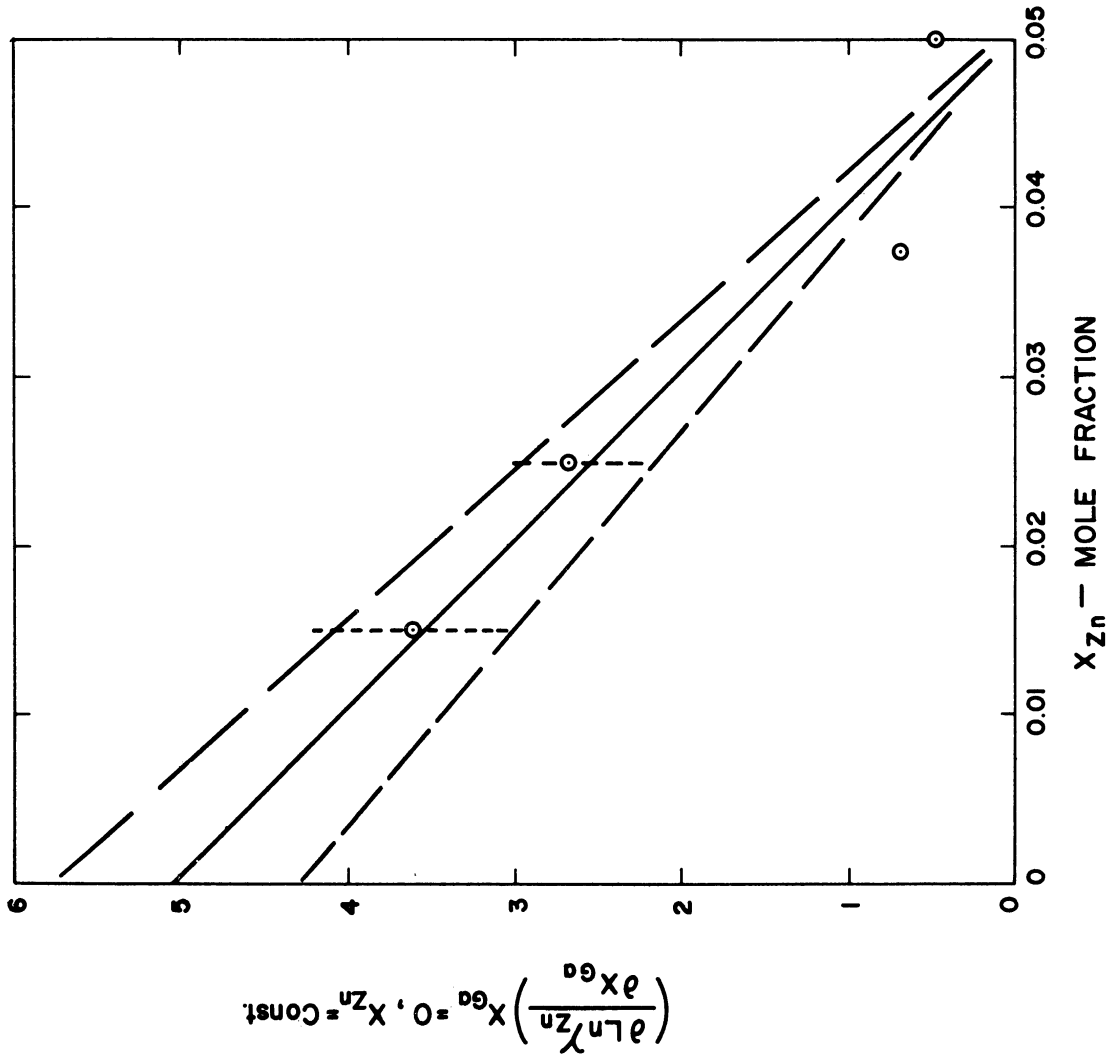


Figure 15. Determination of Ga-Zn Interactions in Molten Bismuth.

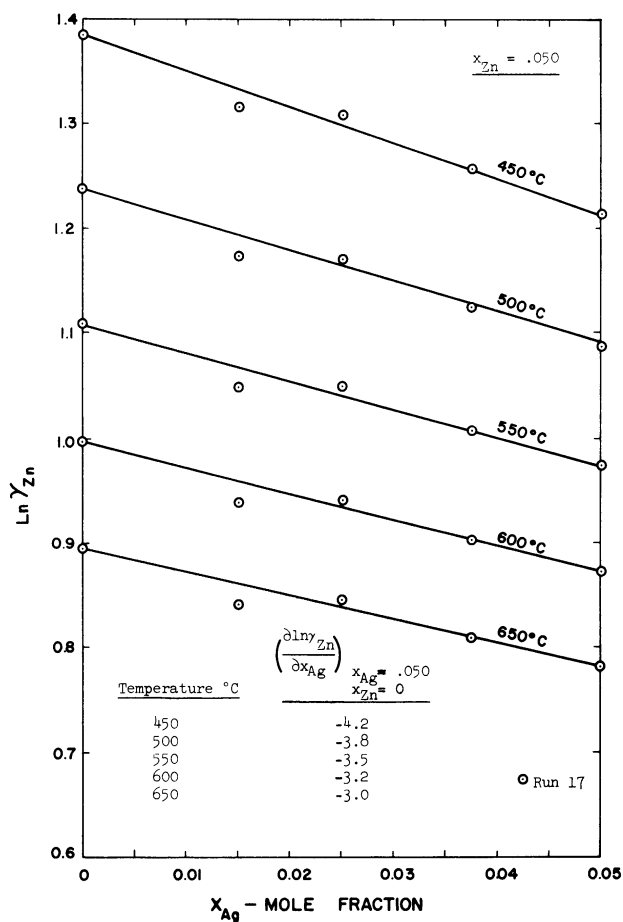
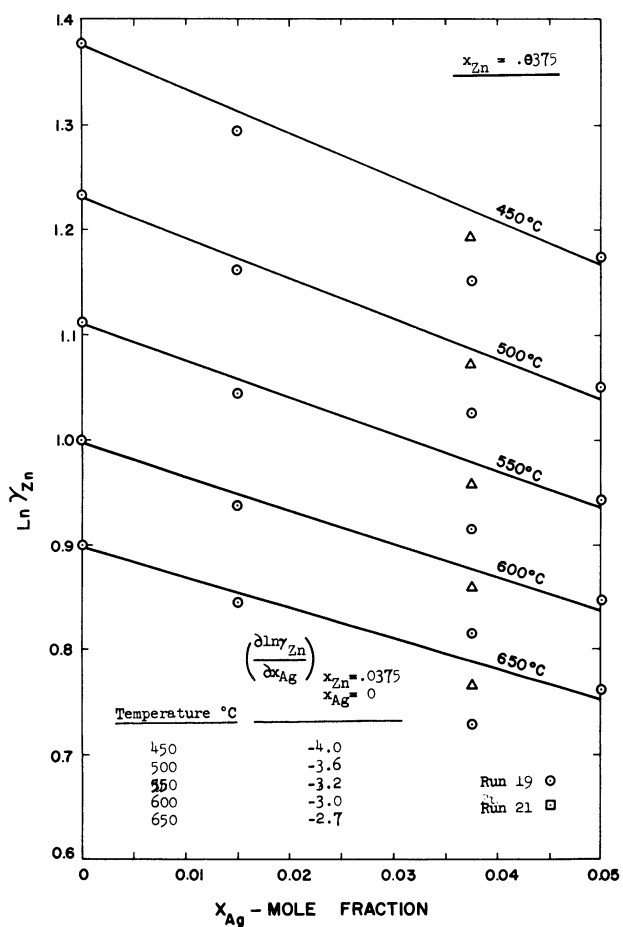
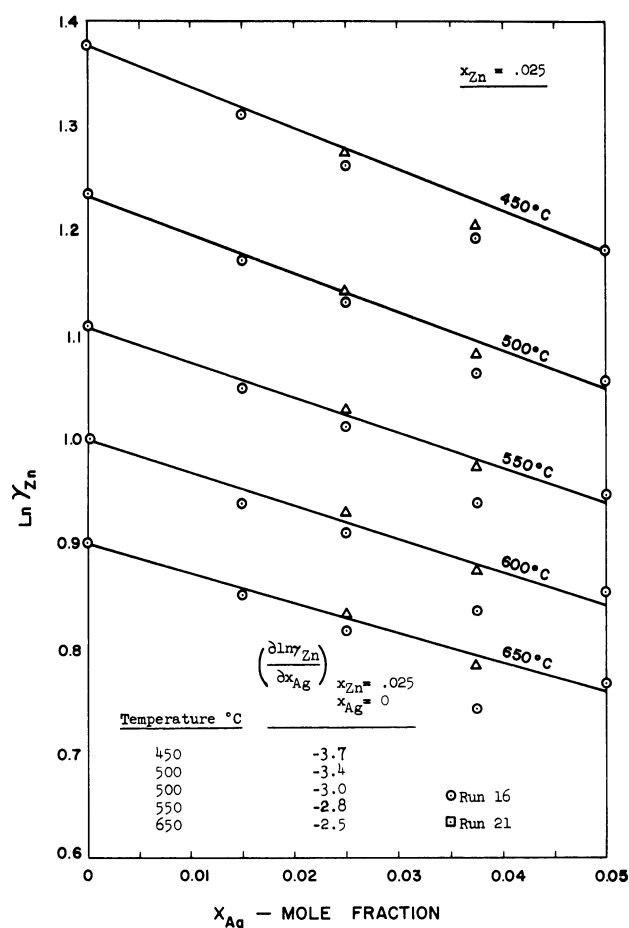
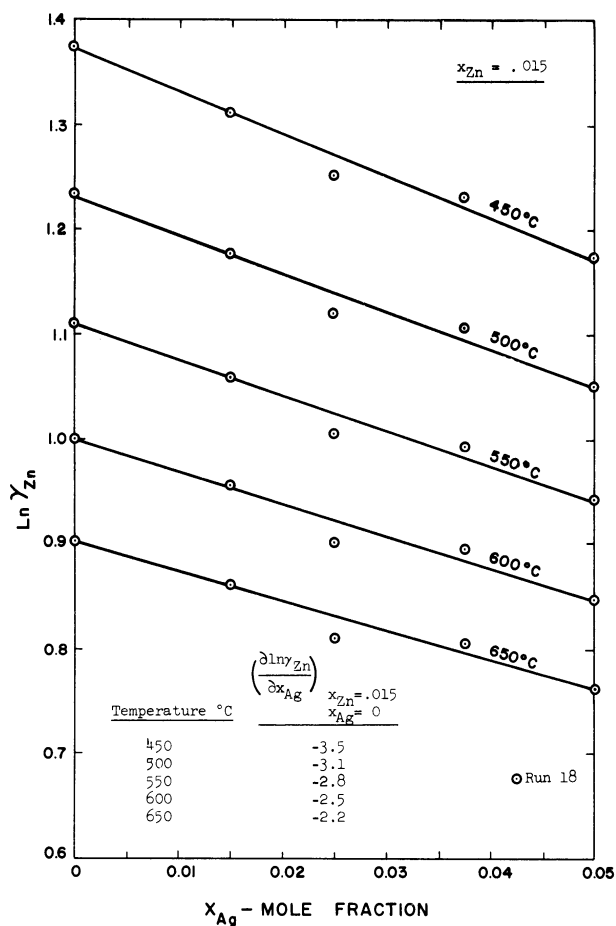


Figure 17. Natural Logarithm of Zinc Activity Coefficient versus Mole Fraction Silver - for Indicated Constant Mole Fractions of Zinc.

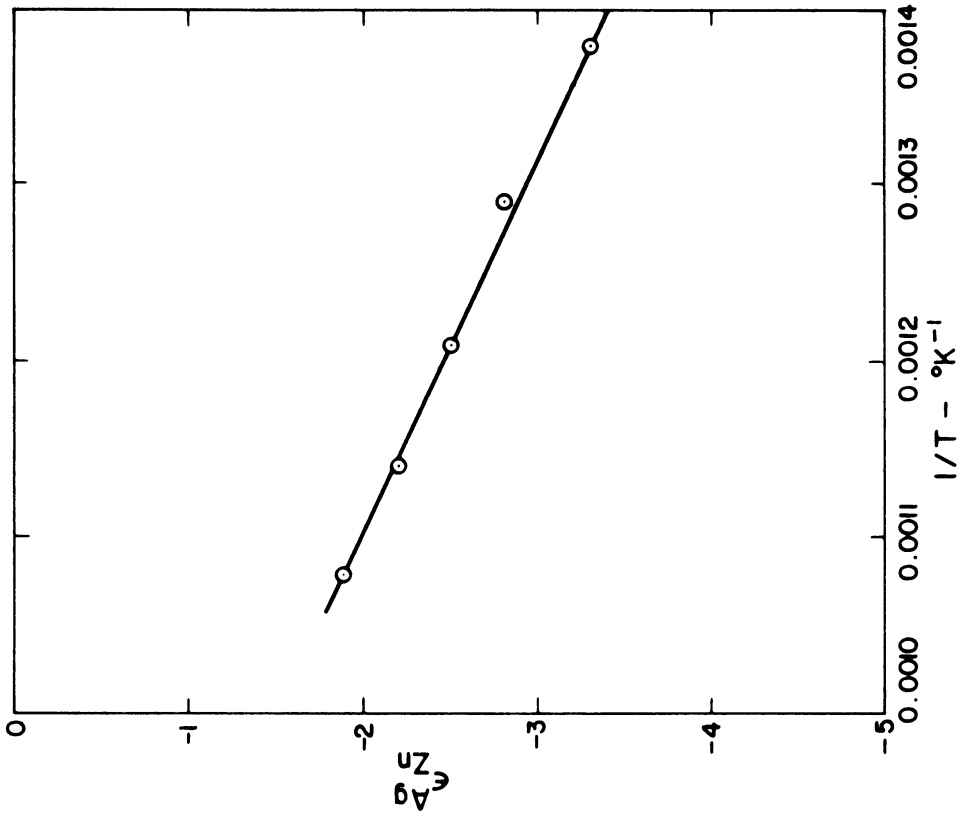


Figure 19. Temperature Dependence of First-Order Ag-Zn Interaction Parameter.

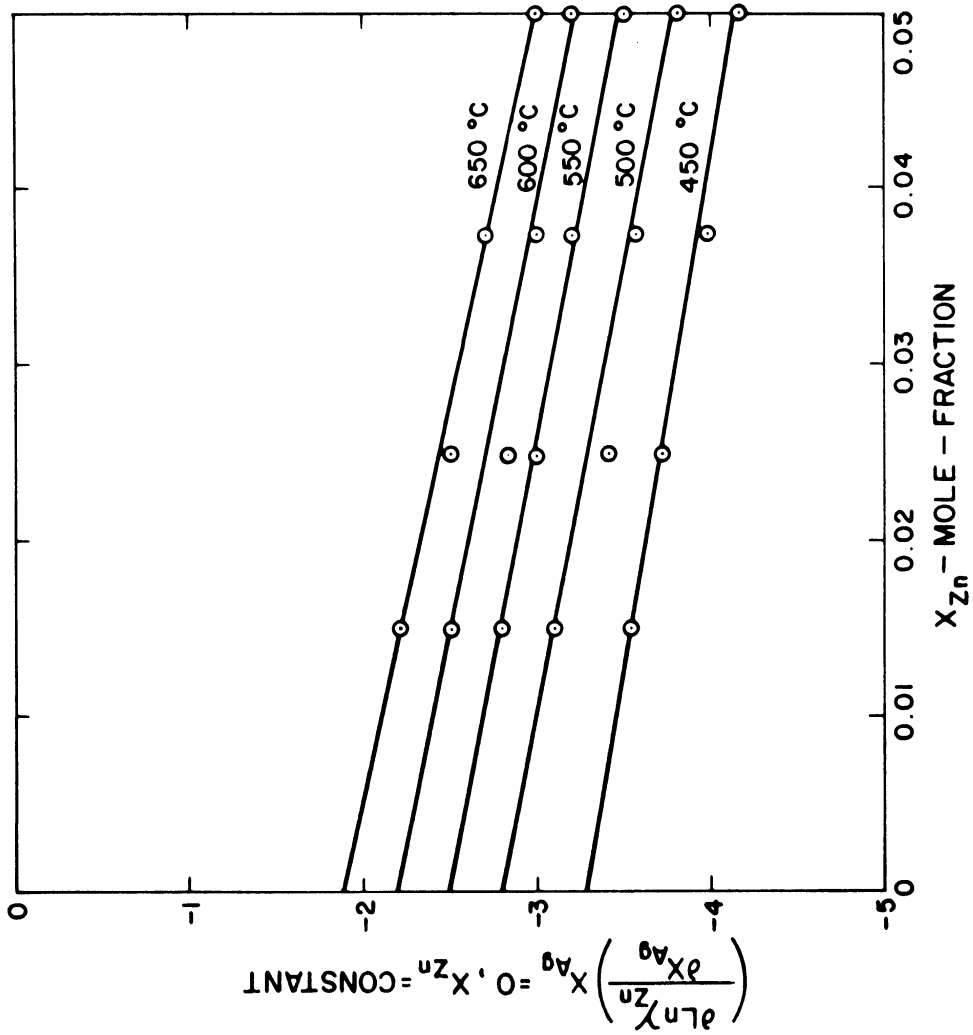


Figure 18. Determination of Ag-Zn Interactions in Molten Bismuth.

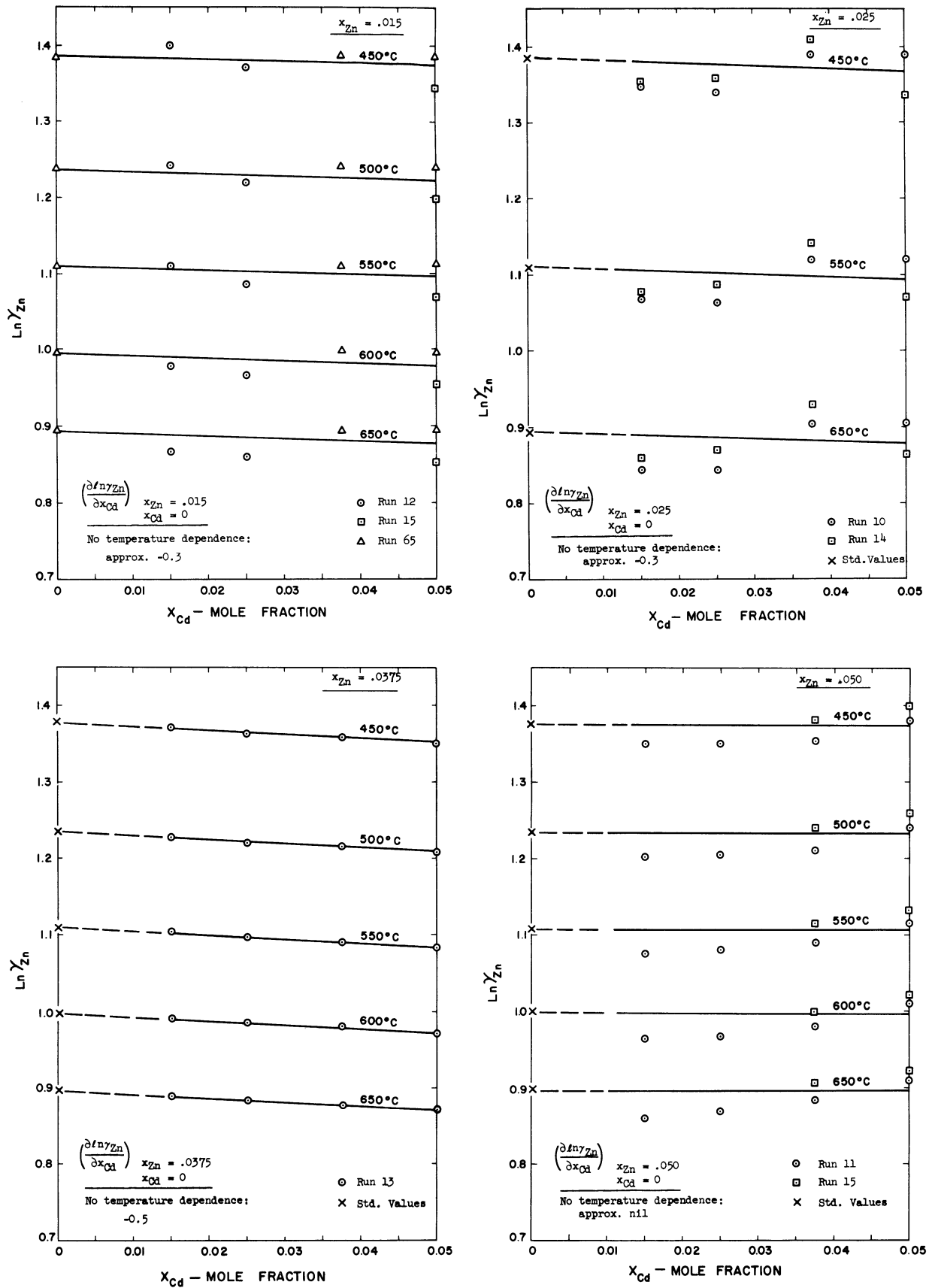


Figure 20. Natural Logarithm of Zinc Activity Coefficient versus Mole Fraction Cadmium - for Indicated Constant Mole Fractions of Zinc.

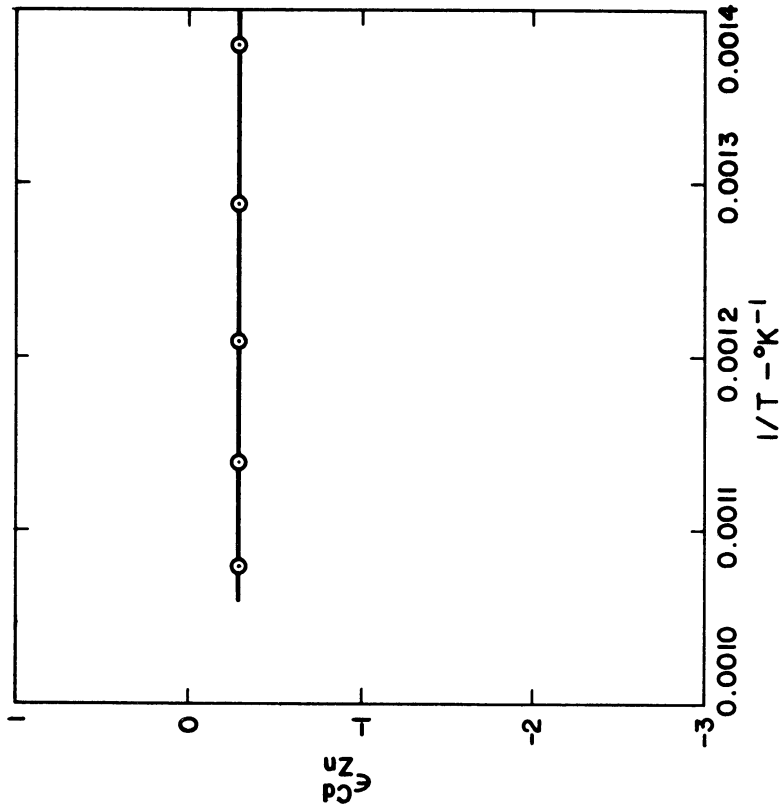


Figure 22. Temperature Dependence of First-Order Cd-Zn Interaction Parameter.

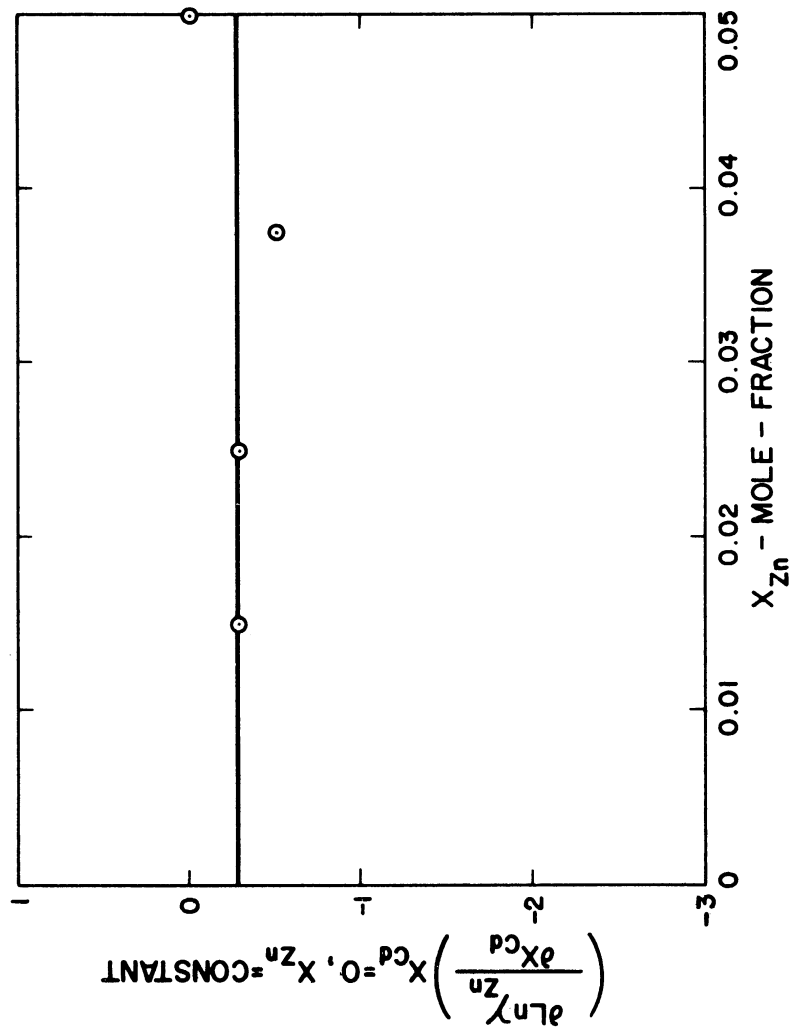


Figure 21. Determination of Cd-Zn Interactions in Molten Bismuth.

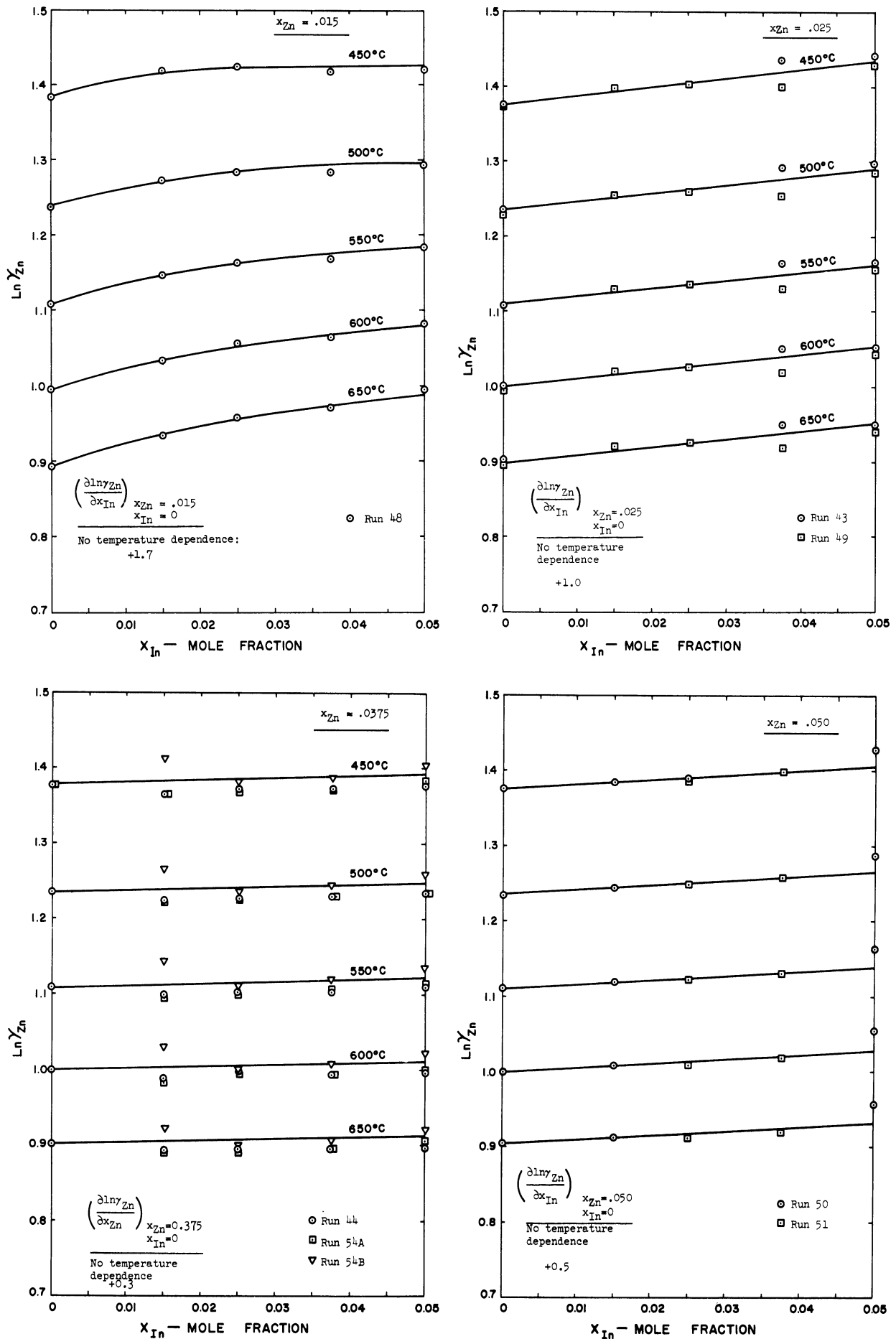


Figure 23. Natural Logarithm of Zinc Activity Coefficient versus Mole Fraction Indium - for Indicated Constant Mole Fraction of Zinc.

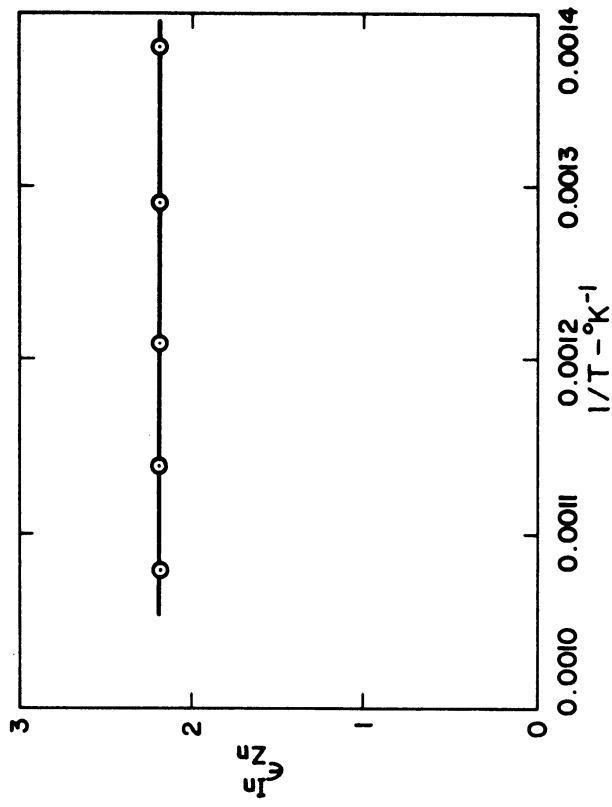


Figure 25. Temperature Dependence of First-Order In-Zn Interaction Parameter.

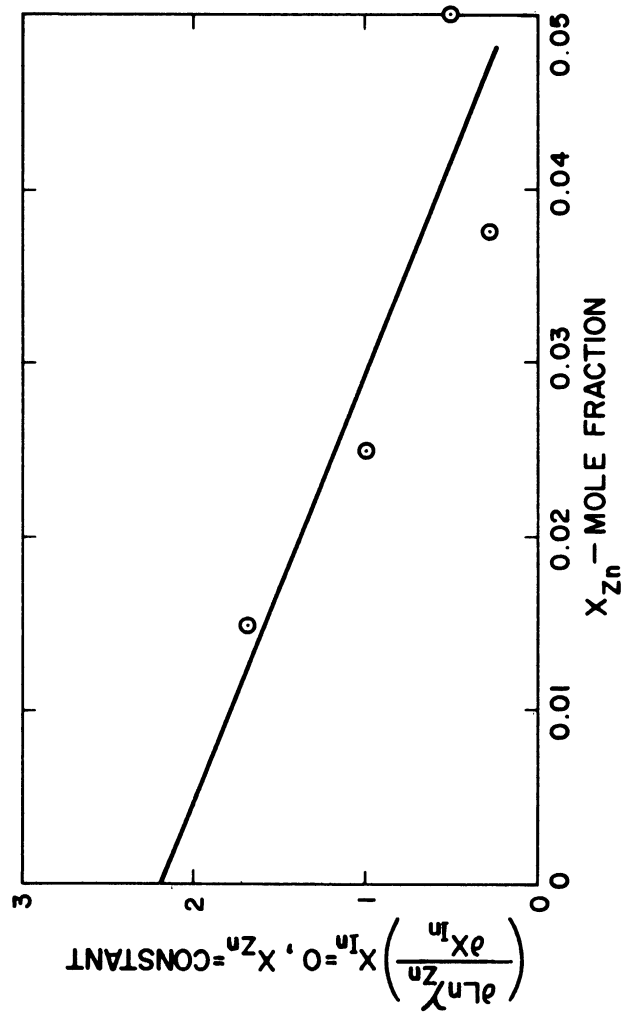


Figure 24. Determination of In-Zn Interactions in Molten Bismuth.

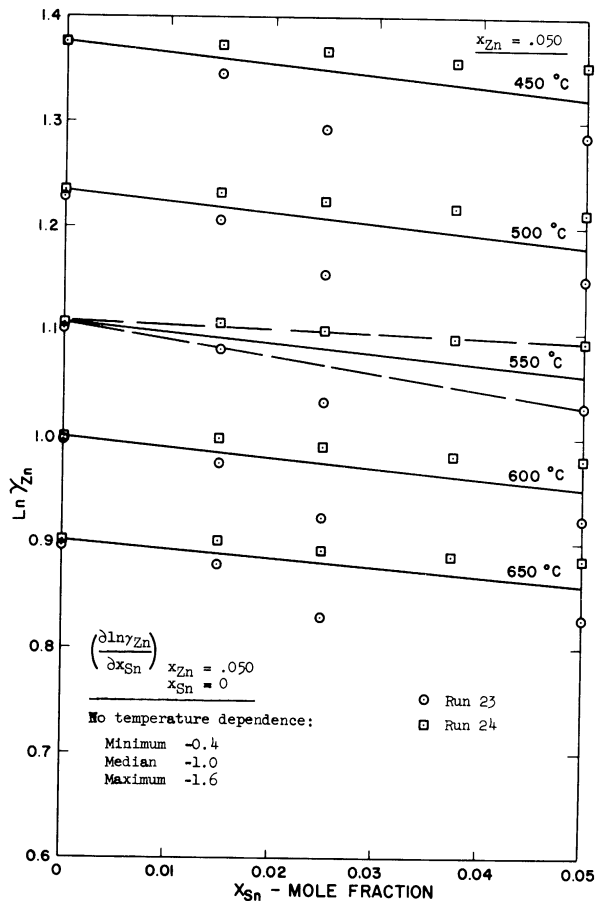
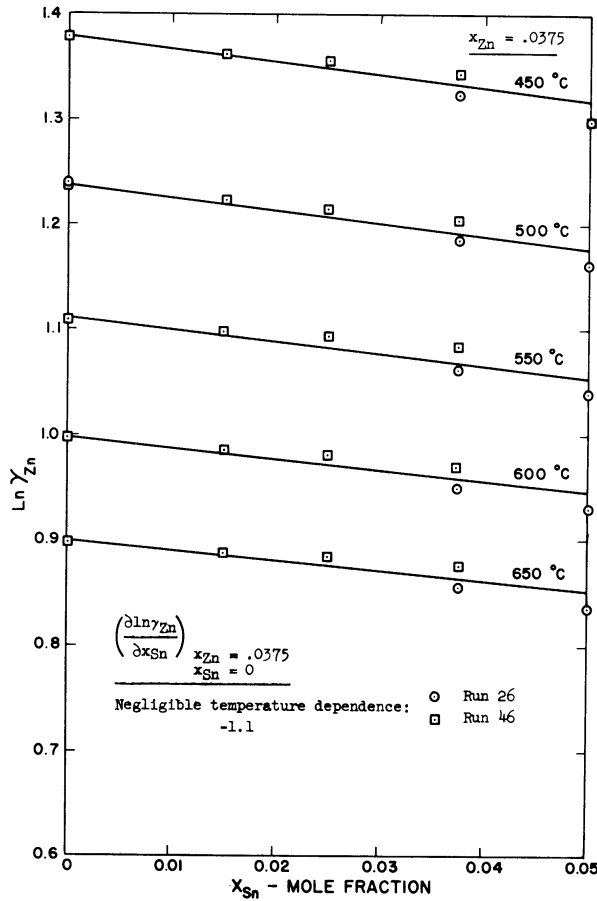
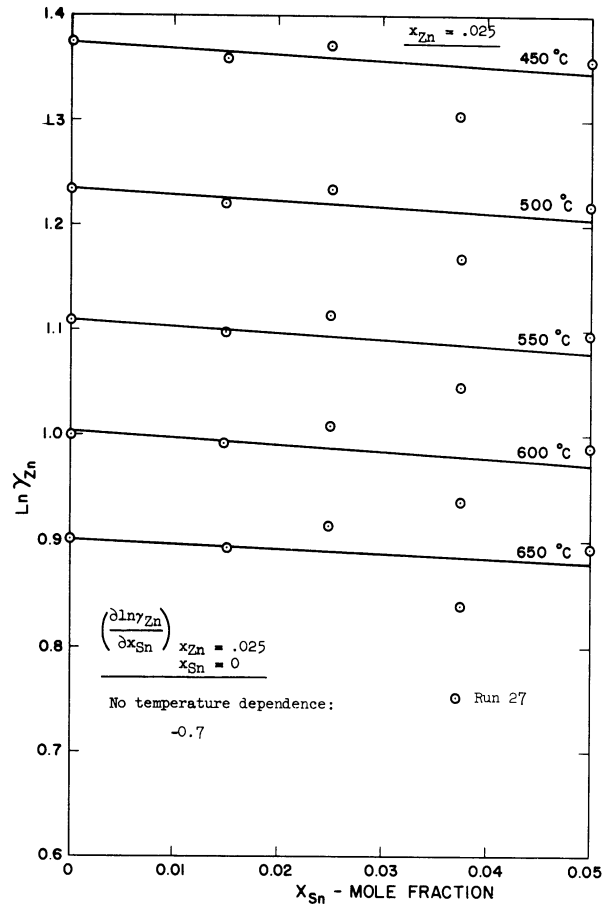
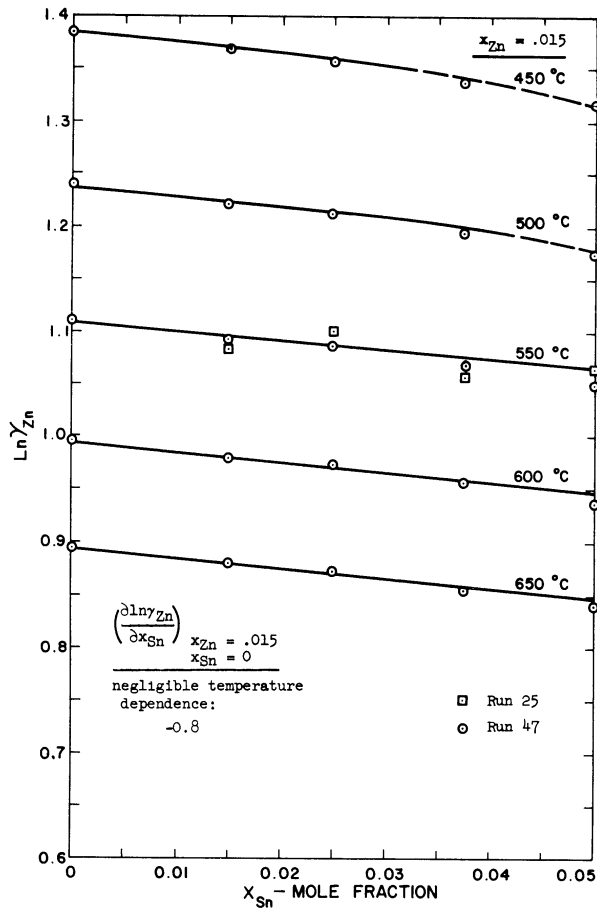


Figure 26. Natural Logarithm of Zinc Activity Coefficient versus Mole Fraction Tin - for Indicated Constant Mole Fractions of Zinc.

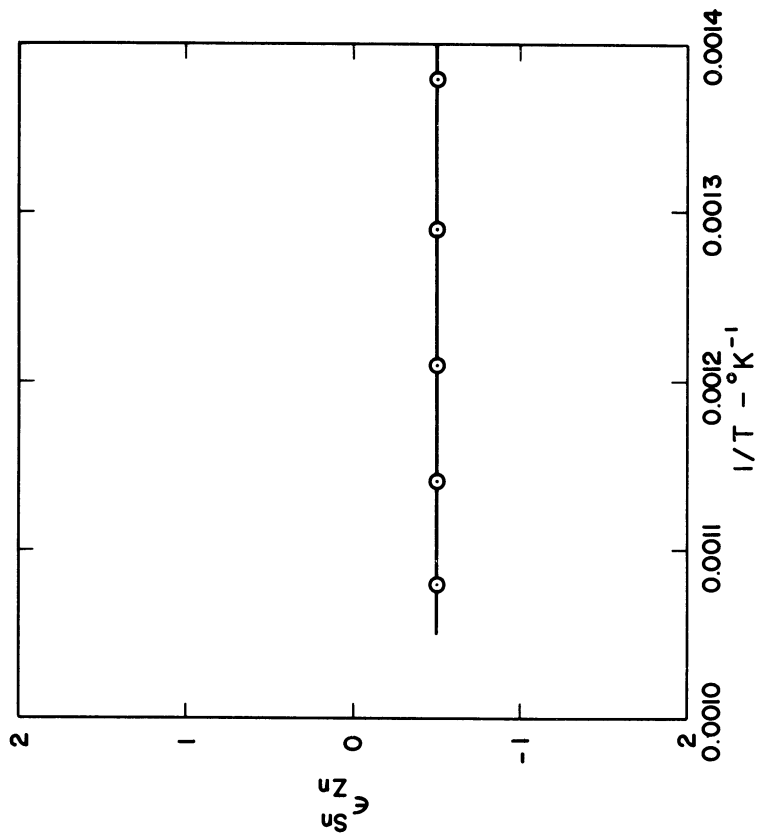


Figure 28. Temperature Dependence on First-Order Sn-Zn Interaction Parameter.

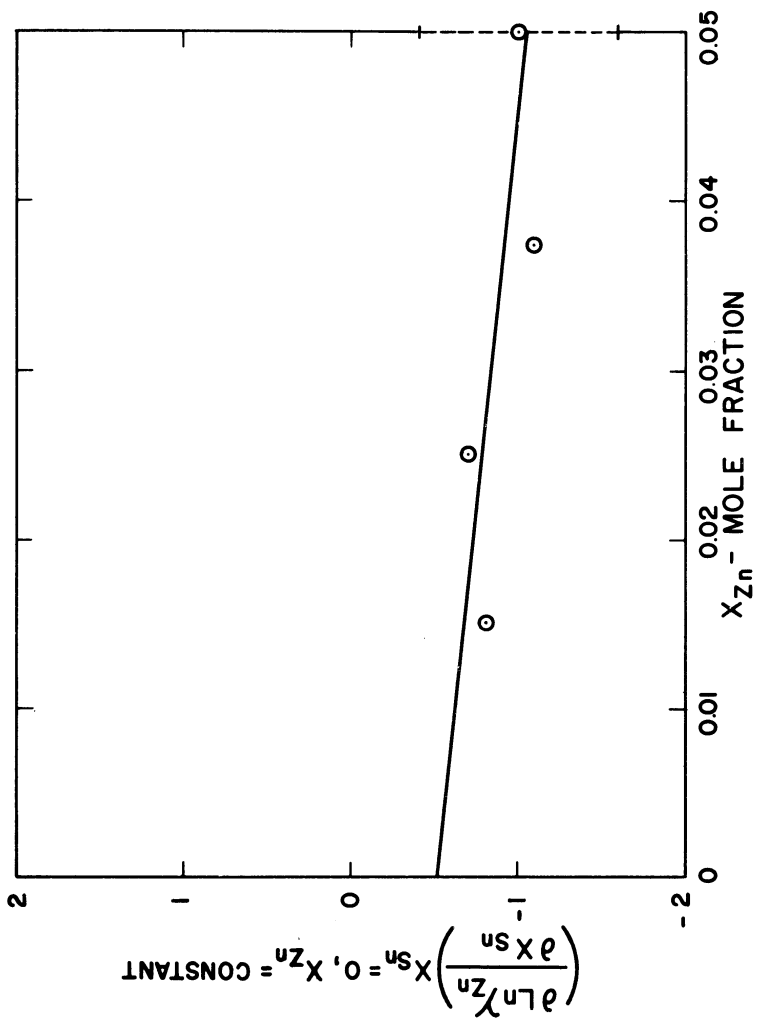


Figure 27. Determination of Sn-Zn Interactions in Molten Bismuth.

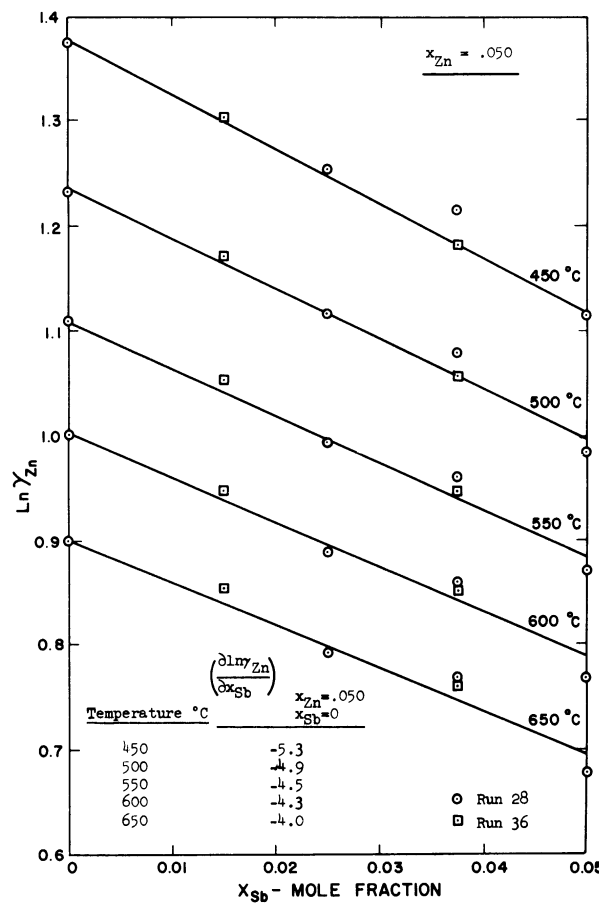
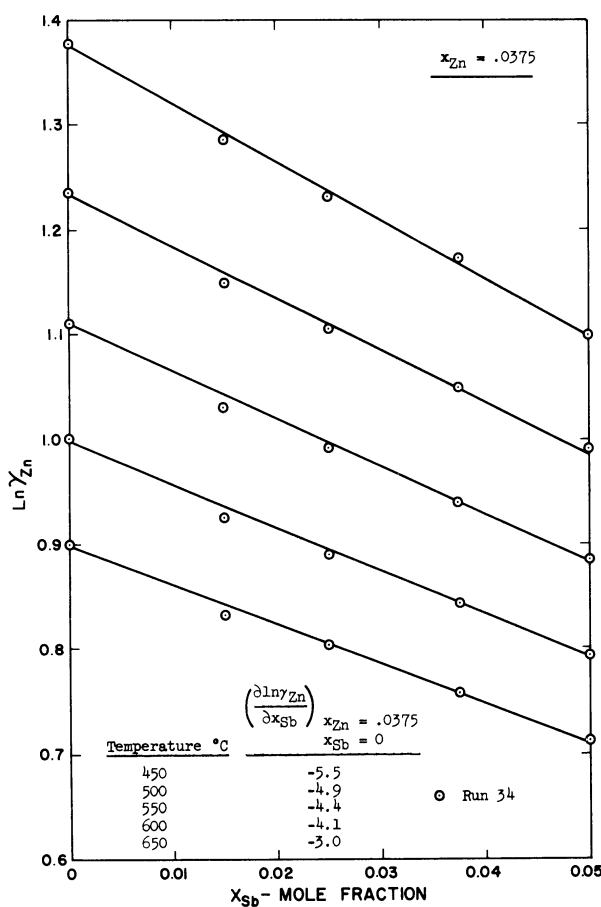
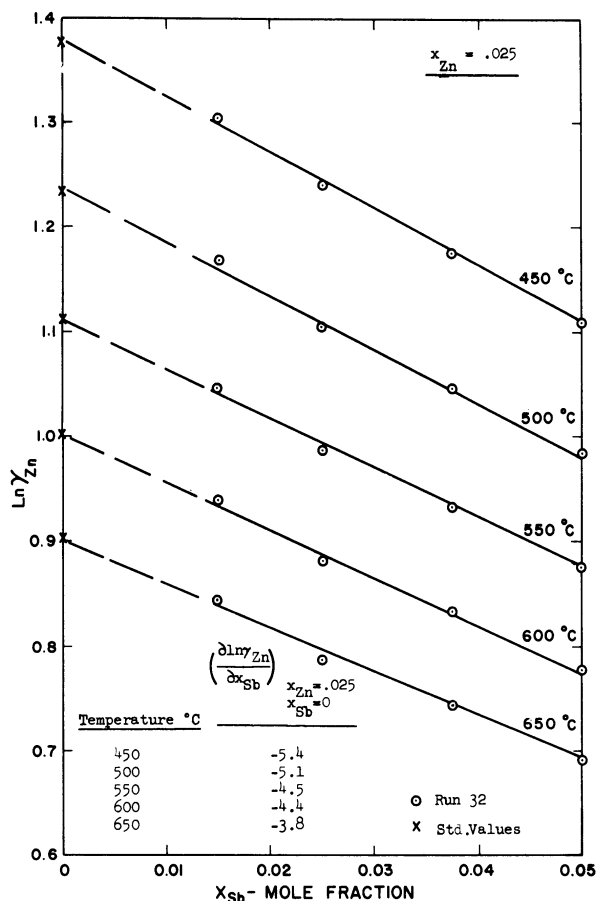
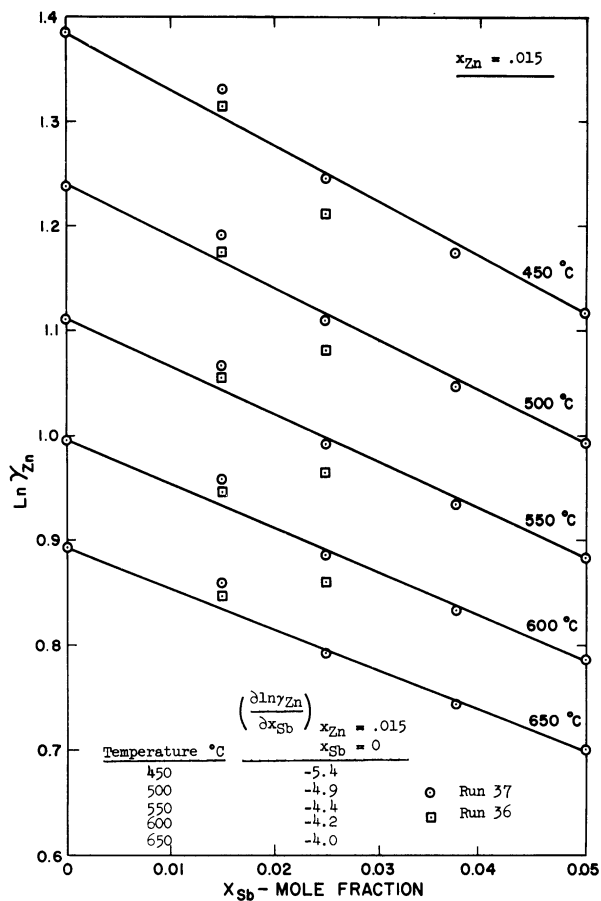


Figure 29. Natural Logarithm of Zinc Activity Coefficient versus Mole Fraction Antimony - for Indicated Constant Mole Fractions of Zinc.

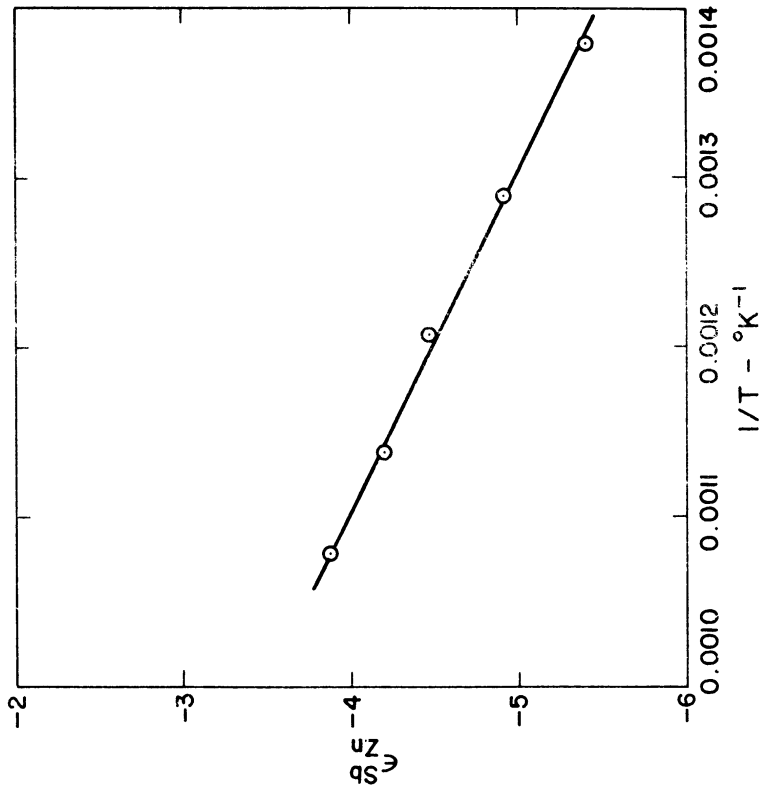


Figure 31. Temperature Dependence of First-Order Sb-Zn Interaction Parameter.

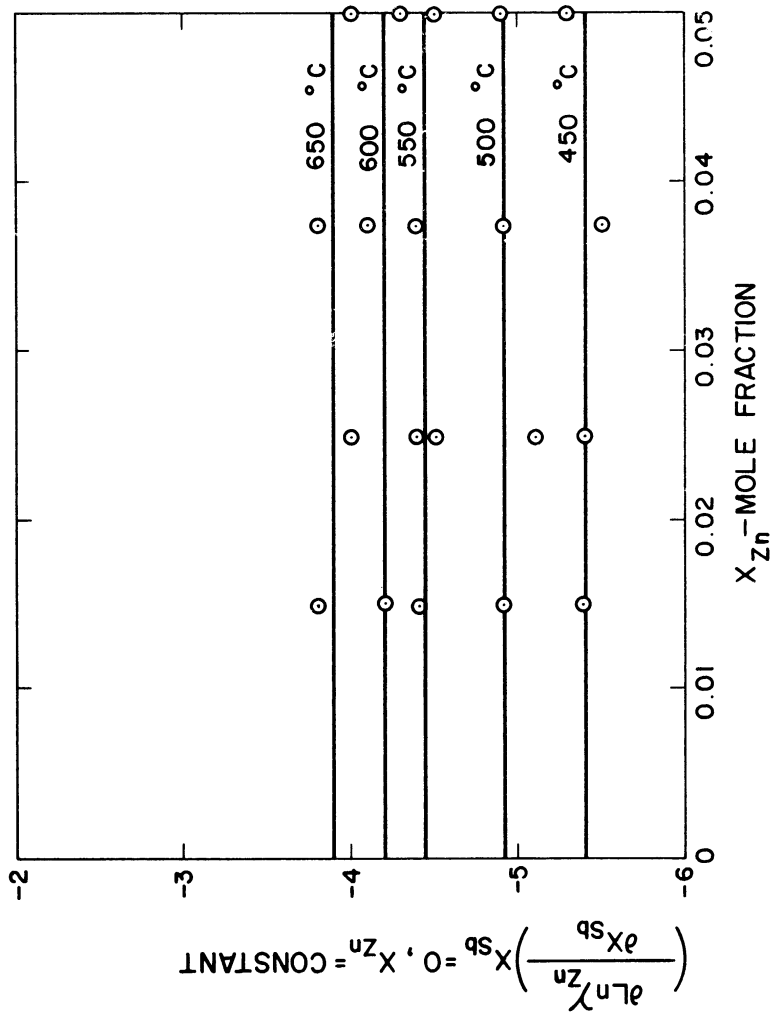


Figure 30. Determination of Sb-Zn Interactions in Molten Bismuth.

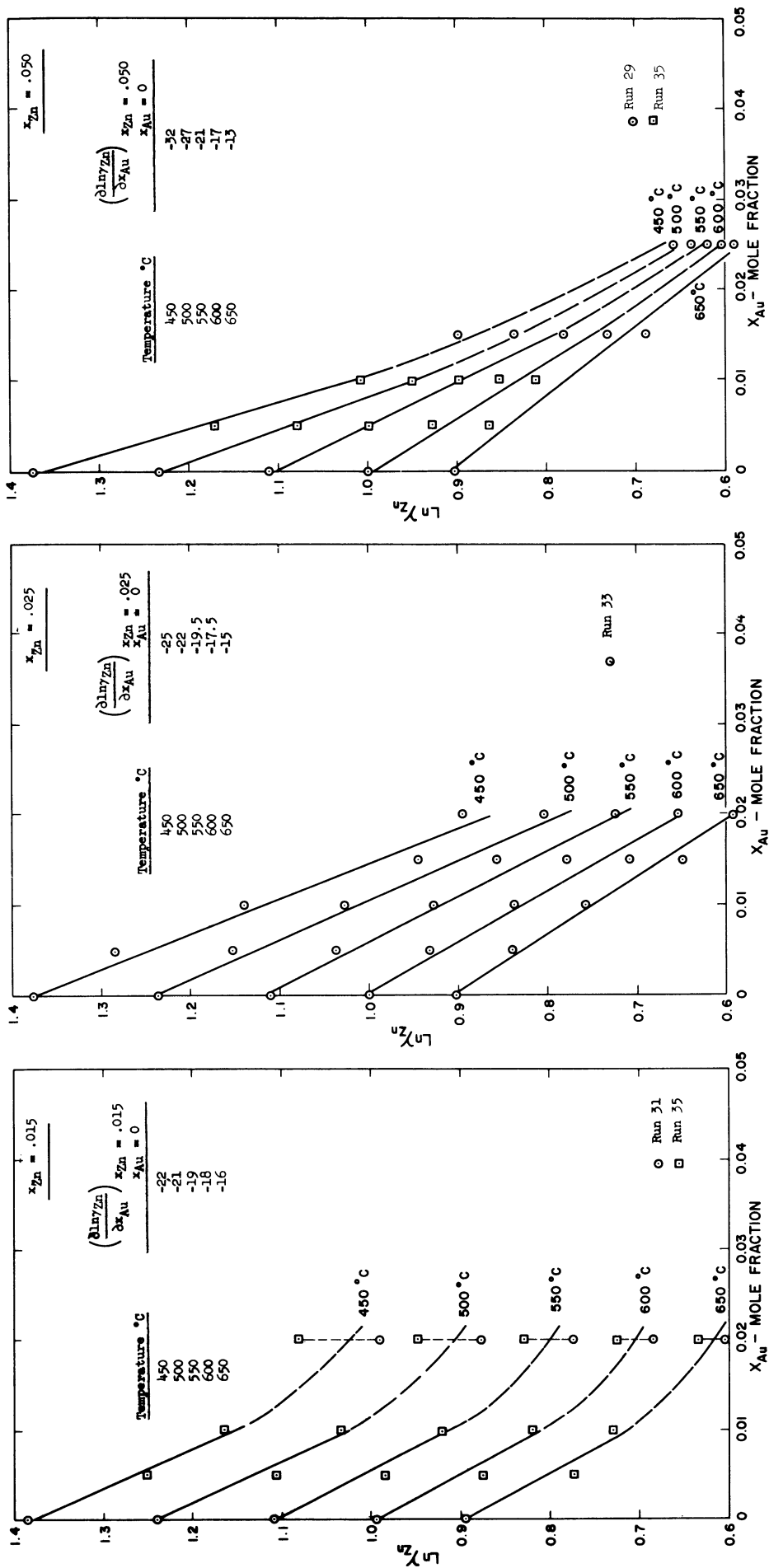


Figure 32. Natural Logarithm of Zinc Activity Coefficient versus Mole Fraction Gold -
for Indicated Constant Mole Fraction of Zinc.

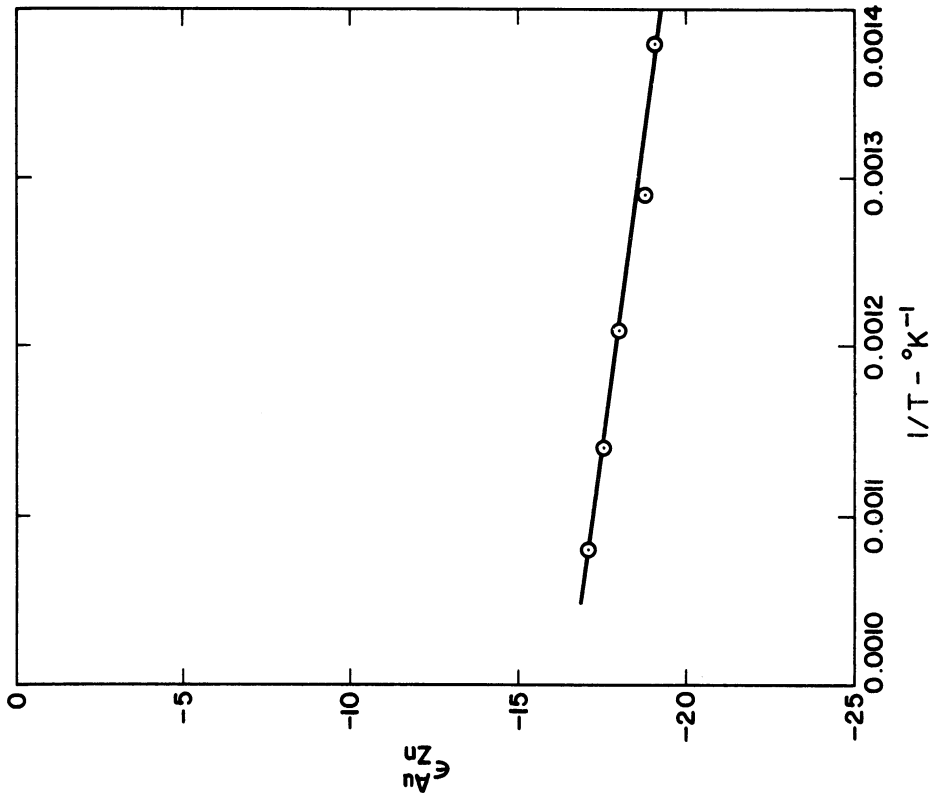


Figure 34. Temperature Dependence of First-Order Au-Zn Interaction Parameter.

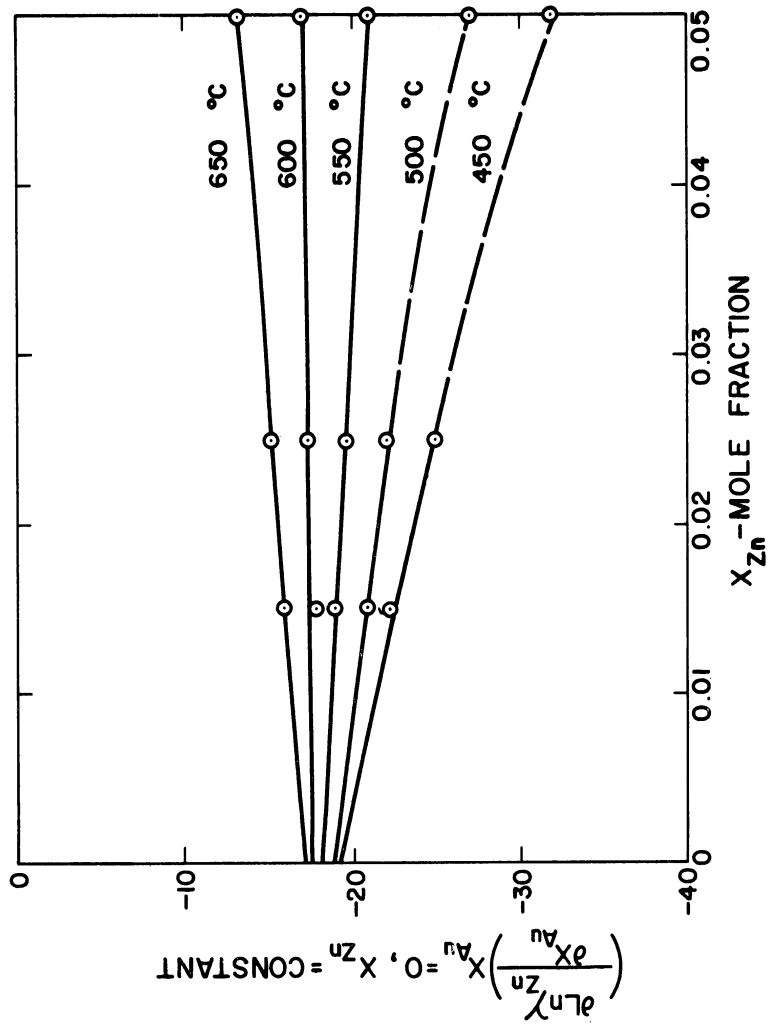


Figure 33. Determination of Au-Zn Interaction in Molten Bismuth.

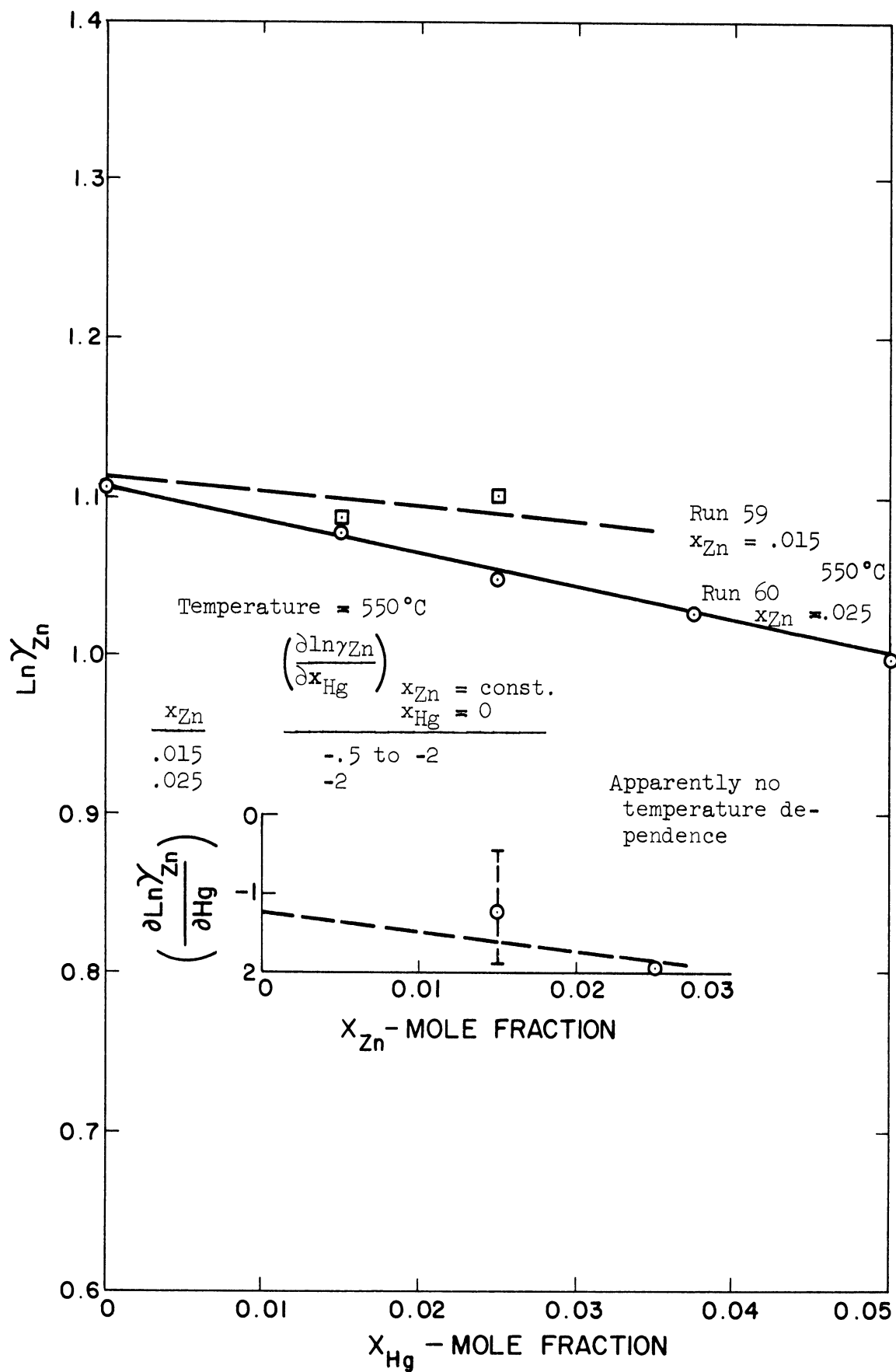


Figure 35. Natural Logarithm of Zinc Activity Coefficient versus Mole Fraction Mercury--for indicated constant mole fractions of zinc.

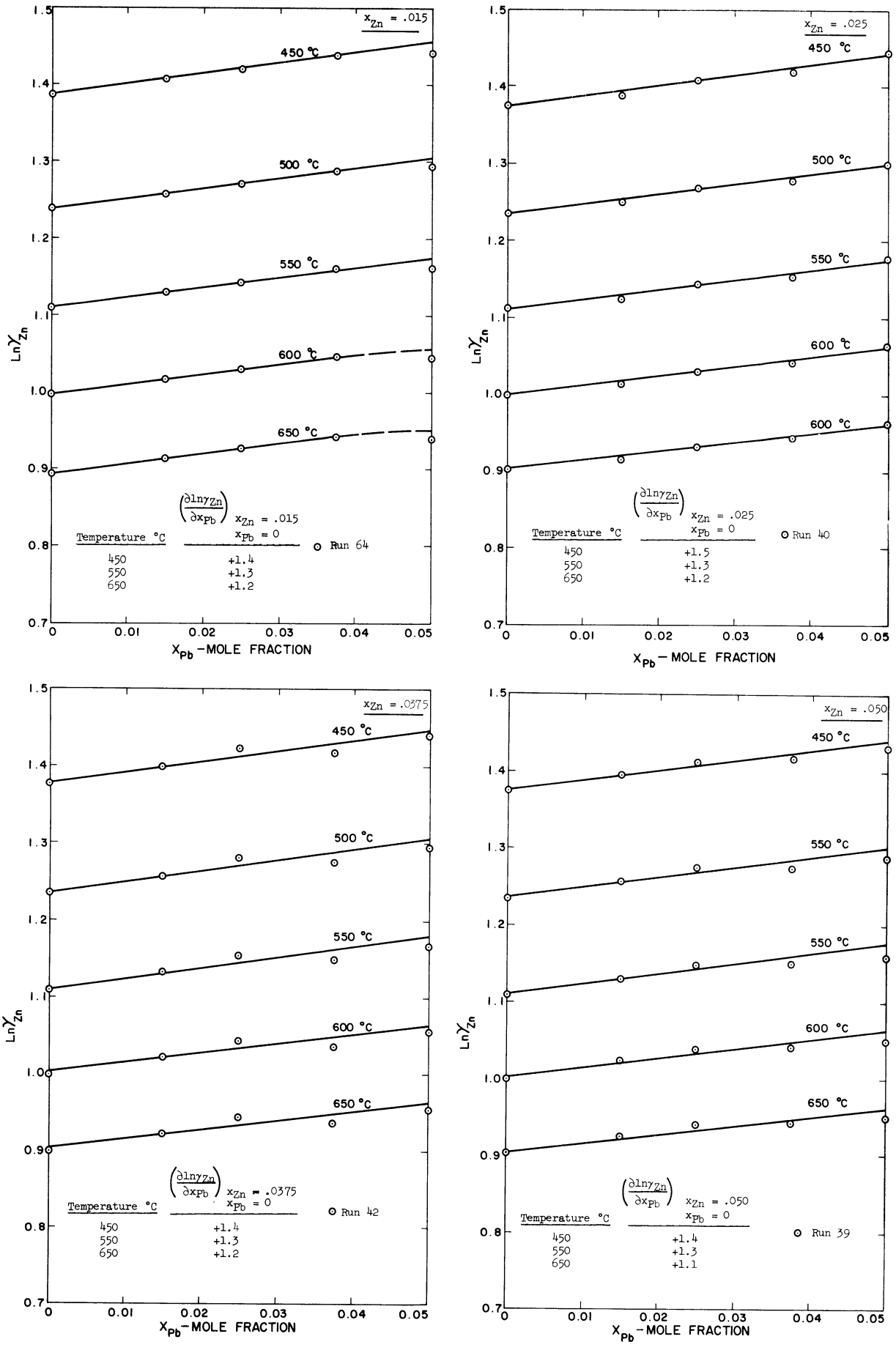


Figure 36. Natural Logarithm of Zinc Activity Coefficient versus Mole Fraction Lead - for Indicated Constant Mole Fractions of Zinc.

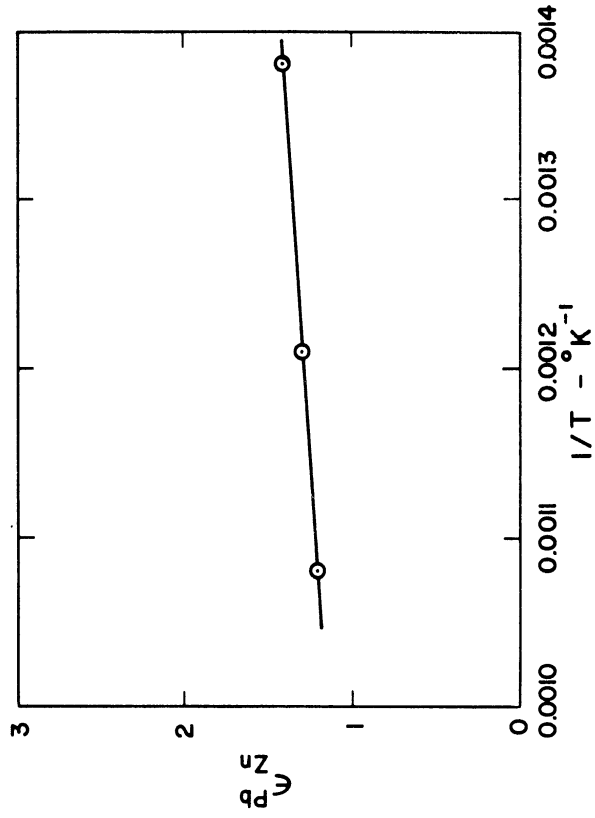


Figure 38. Temperature Dependence of First-Order Pb-Zn Interaction Parameter.

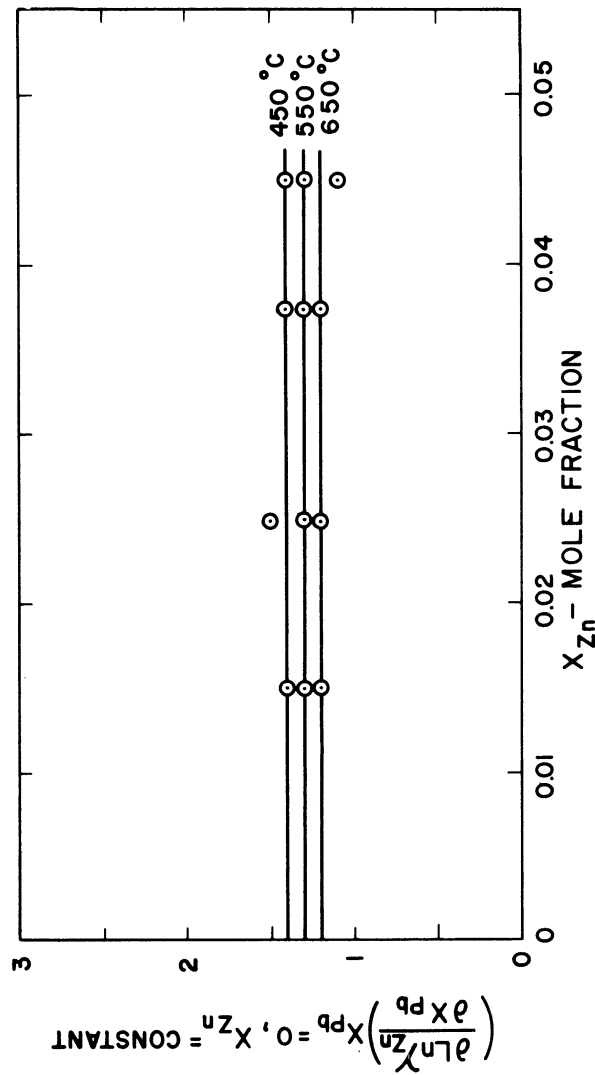


Figure 37. Determination of Pb-Zn Interactions in Molten Bismuth.

11. Summary of Ternary Interaction Results

The experimental results for the ten ternary systems studied are summarized in Table IX. The parameters included in this table are the intermediate slopes and the first- and second-order interaction parameters between zinc and the added solute at temperatures between 450° and 650°C.

The elements having positive interaction parameters, that is, those whose additions caused an increase in the activity of zinc were gallium, indium, and lead. Cadmium and tin produced slightly negative interaction parameters. Silver, copper, mercury, and antimony caused moderately negative effects, while gold had a strongly negative effect.

Where a significant temperature dependence was found for the first-order interaction parameter (copper, silver, gold, antimony, or lead), the variation was linear with respect to reciprocal absolute temperature over the range studied. A summary plot of these relations is given in Figure 39. The first-order parameter could be represented by analytical expressions of slope-intercept form, $\epsilon_j^1 = A_j + B_j/T$. All the second-order interaction parameters were found to be essentially independent of temperature except those for silver or gold. For these additions, a similar linear relation with reciprocal absolute temperature was found. The constants for the temperature dependence relations are summarized in Table X. The significance of the temperature dependence and the slopes and intercepts of the relations is discussed in detail on pp.208-217. It is sufficient to mention here that they represent the changes in the entropy and enthalpy of zinc due to the ternary interaction.

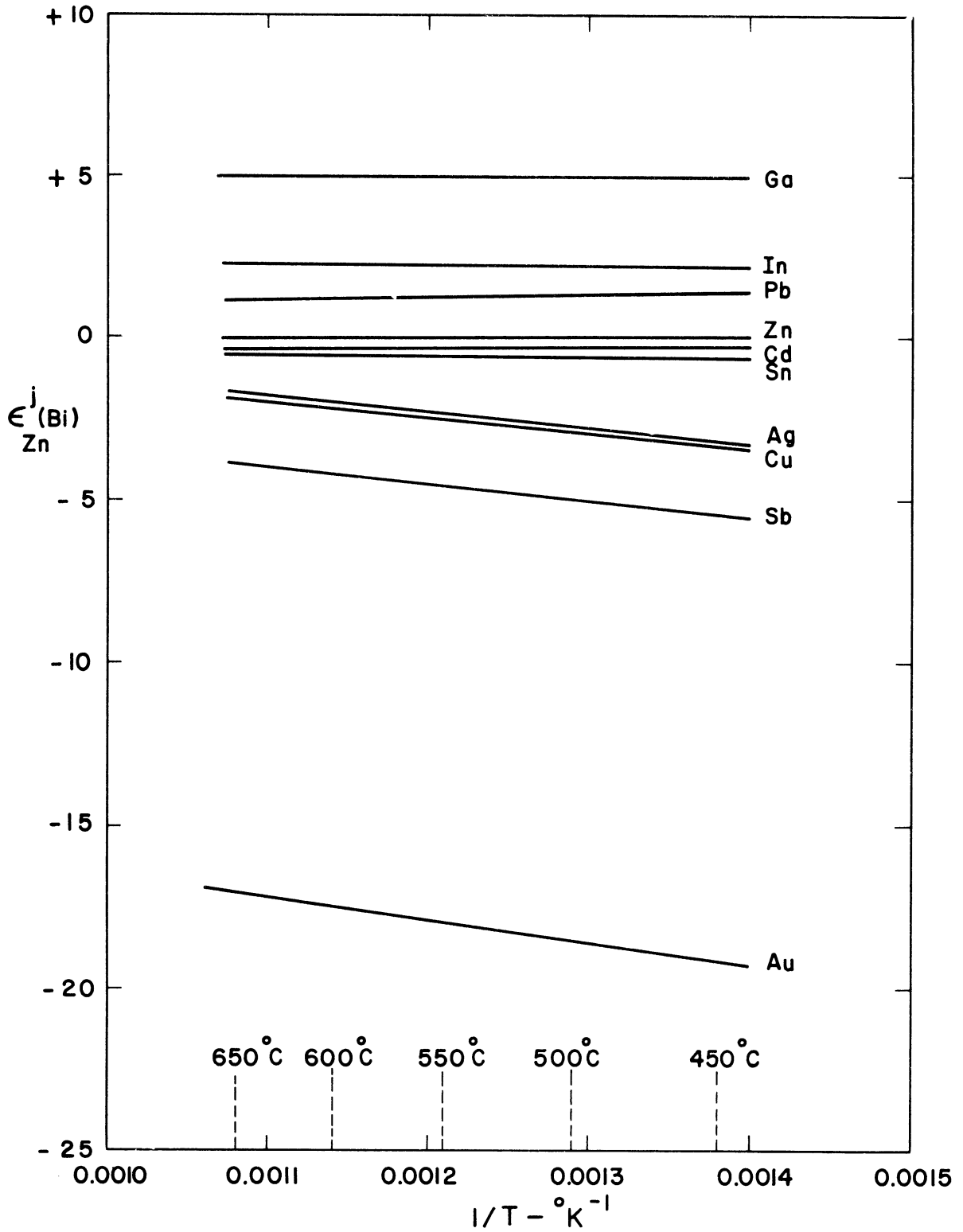


Figure 39. Summary Plot of Temperature Dependence of Interaction Parameters.

TABLE X

TEMPERATURE DEPENDENCE CONSTANTS FOR INTERACTIONS
WITH ZINC IN DILUTE SOLUTION WITH MOLTEN
BISMUTH IN THE RANGE 450 TO 650°C

Temperature Dependence Equation: $\epsilon = A_j + \frac{B_j}{T(^{\circ}\text{K})}$

Element	First-Order Interaction, ϵ_{Zn}^j		Second-Order Interaction, ϵ_{Zn}^j	
	A_j	B_j	A'_j	B'_j
Cu	1.292	-3070	-19	~0
Ga	5.0 ± 0.7	0	-100 ± 20	0
Ag	3.012	-4543	-31.2	14,872
Cd	-0.3	0	0	0
In	+2.2	0	0	0
Sn	-0.5	0	-12	0
Sb	1.473	-4945	0	0
Au	-9.886	-6640	1140	-1,000,000
Hg	-1 to -2	0	-	-
Pb	0.483	666	0	0

Note: See page 213.

$$A_j = -\frac{\sigma}{R}, \text{ where } \sigma_1 = \frac{\partial^2 S}{\partial X_i \partial X_j}$$

$$B_j = \frac{\eta}{R}, \text{ where } \eta_1 = \frac{\partial^2 H}{\partial X_i \partial X_j}$$

$$A'_j = -\frac{\sigma_2^*}{R}, \text{ where } \sigma_2^* = \frac{\partial^3 S}{\partial X_i^2 \partial X_j}$$

$$B'_j = \frac{\eta_2^*}{R}, \text{ where } \eta_2^* = \frac{\partial^3 H}{\partial X_i^2 \partial X_j}$$

12. Confidence Limits for Interaction Parameters

The standard error of estimate of potential within a given run was about .2 millivolts for cells run from 50 to 150 hours at temperatures in the range from 450-650°C. The difference between the absolute potentials of replicate cells was usually less than one per cent. A previous discussion (p. 37) covered the use of the reference binary electrode for determining a "cell factor" for the correction of the multi-component alloy results to the same base points.

It is difficult to fix precise confidence limits for the interaction parameters because of the several steps involved in their determination. A formal statistical analysis was run on data for the Bi-Zn-Sb system since the relations between $\ln y_{Zn}$ and x_{Sb} appeared to be well defined and the points could be given equal weight.⁽⁶⁸⁾ At the 90 per cent confidence level it was possible to fix the limits for the first-order interaction parameter at approximately +10 per cent of its absolute value (see Appendix C). Visual examination of the data for the other systems suggested that closer limits could be placed on some, while the same or greater limits could be applied to other systems. However, with the exception of the systems involving mercury or gallium, it can be said with reasonable certainty that the accuracy of the measured values of the interaction parameters is about +7-10 per cent of their absolute values.

13. Determination of Phase Boundaries for Ternaries with Cu or Au

In the experimental runs on the Bi-Zn-Cu and Bi-Zn-Au systems marked discontinuities were observed in the emf-versus-temperature

relations for a number of the experimental alloys. Above the point of discontinuity the slopes of the relations were very similar to those of the binary alloy of the same mole fraction zinc. Below the discontinuity, the slopes were markedly different and varied according to the amount of third element present.

The occurrence of such discontinuities is interpreted as the transition between the single phase liquid region, and underlying two- or three-phase regions. A number of investigators^(63,69-71) have used such observations to determine liquidus boundaries. Figure 40 shows emf-temperature relations for the alloys of Bi-Zn-Au and Figure 42 shows relations for the Bi-Zn-Cu alloys. The lower parts of Figures 40 and 42 are plots of the temperature of discontinuity in the emf-temperature relations versus the mole fraction of solute j for which they were observed, with the zinc content as the parameter. A cross-plot from these curves at constant temperature permitted the construction of the liquidus surface isotherms shown in Figures 41 and 43.

The complete isotherms for these systems at intermediate temperatures cannot be constructed from the limited experimental data, however, their general features may be readily deduced (Figure 41). At both the bismuth and zinc-rich corners, small regions of single phase liquids exist. These are denoted as L_1 and L_2 . The remainder of the isotherm consists of a succession of two and three-phase regions which radiate from the liquidus surface at the bismuth corner towards the Zn-Au or Zn-Cu side of the diagram. The two-phase regions correspond to the various solid solutions and/or intermetallic phases which occur in the Zn-Cu or Zn-Au binary systems.⁽⁵⁵⁾

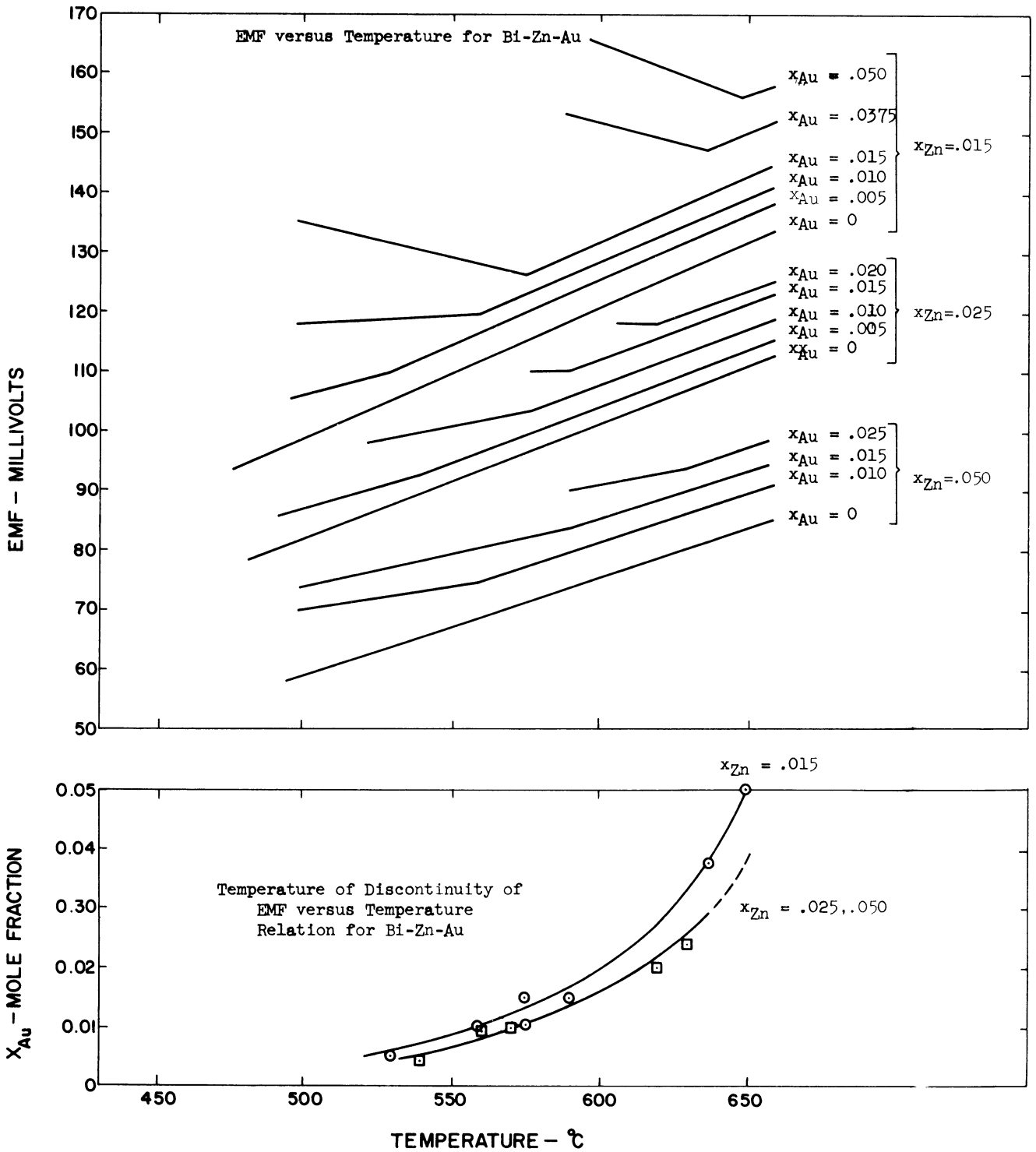
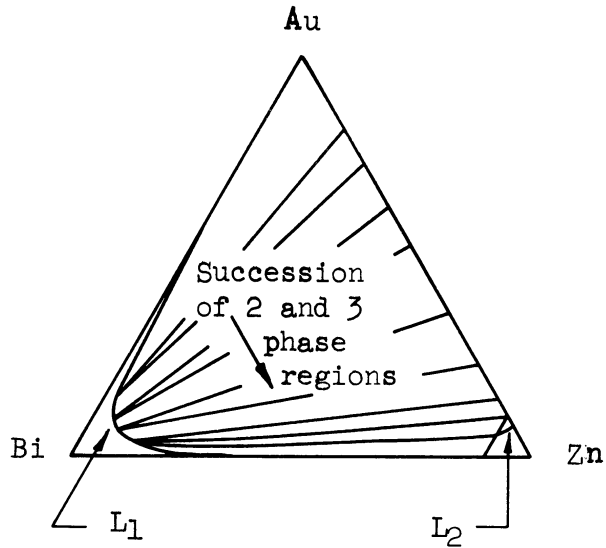


Figure 40. Electrode Potentials versus Temperature for Bi-Zn-Au Alloys.



Idealized schematic view of isotherms in the range 450-650°C

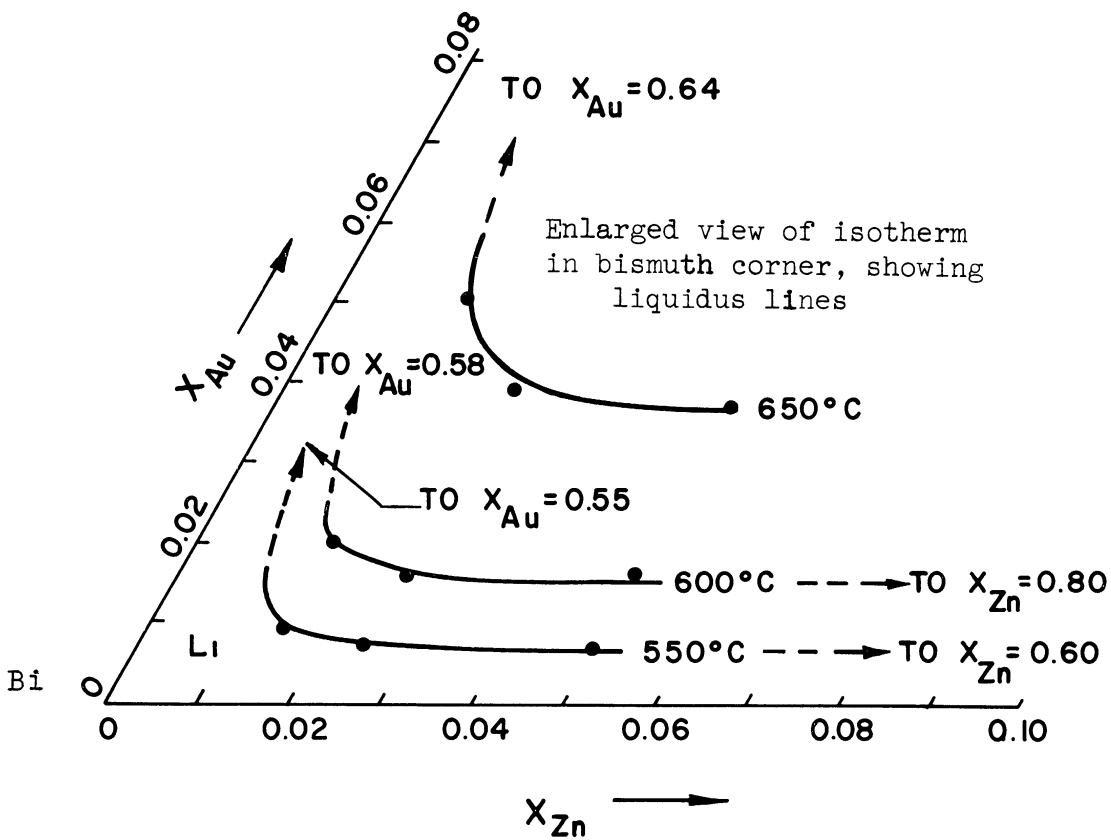


Figure 41. Isotherms for Bi-Zn-Au System Showing Liquidus Boundaries in the Bismuth Corner.

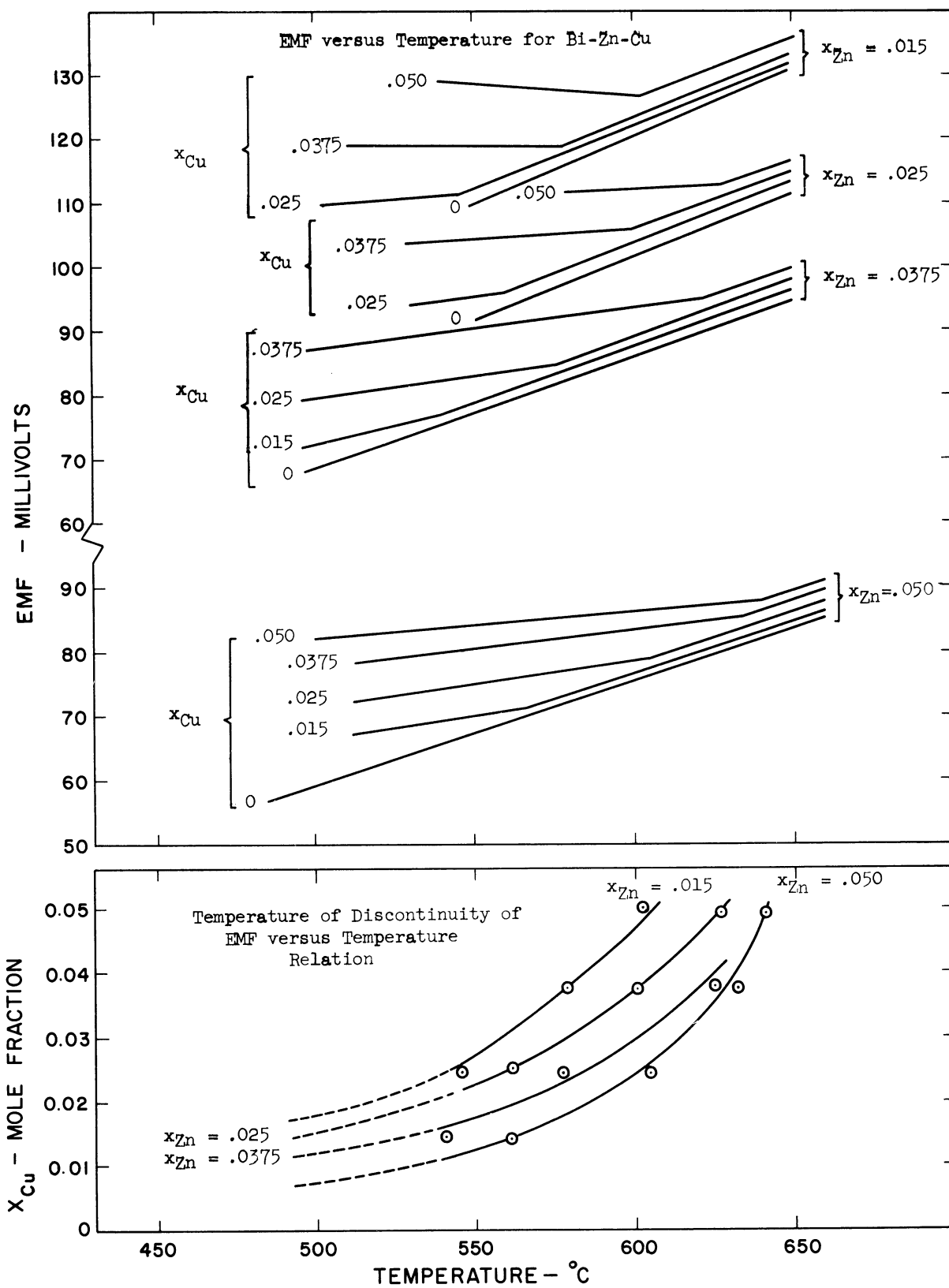


Figure 42. Electrode Potentials versus Temperature for Bi-Zn-Cu Alloys.

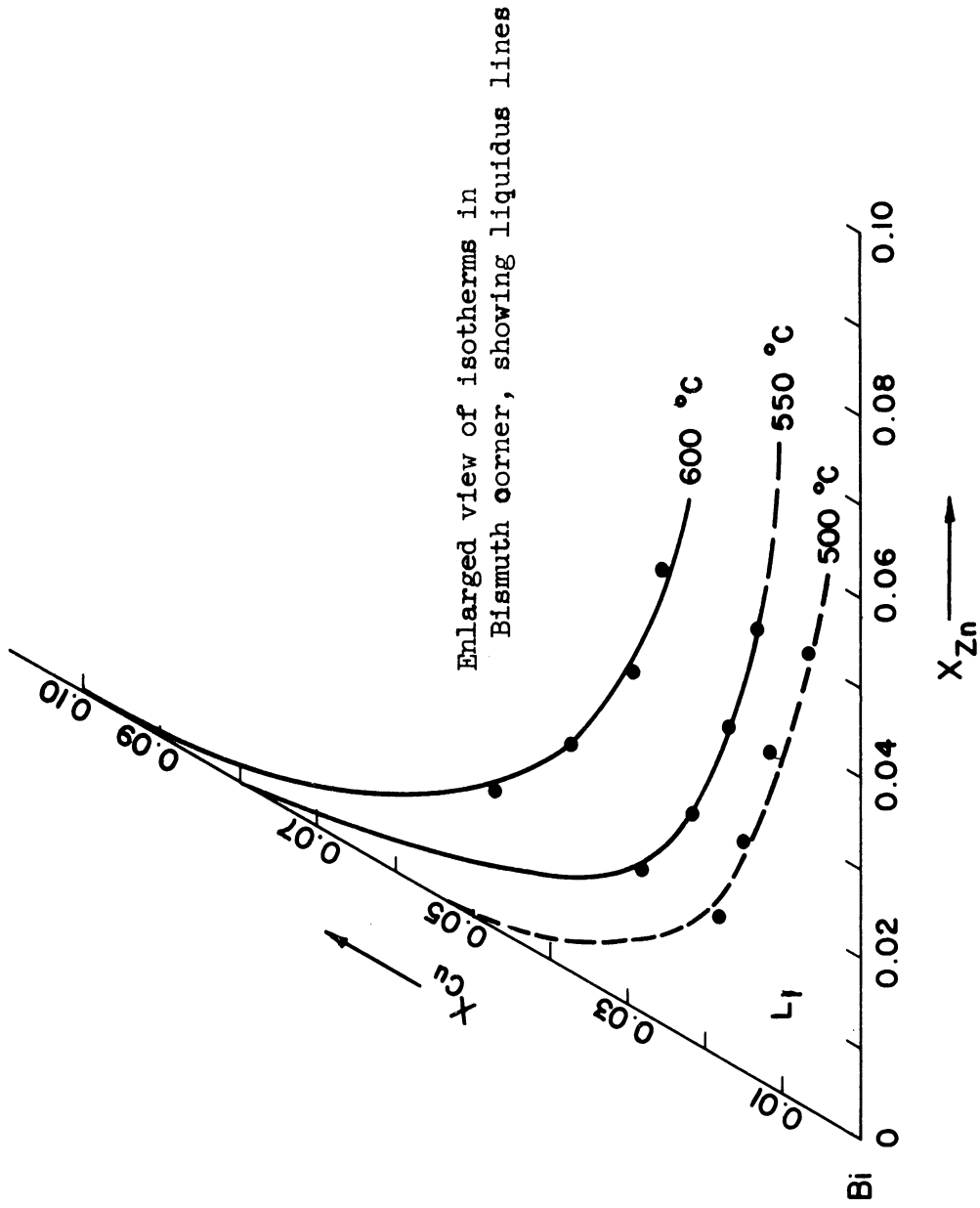


Figure 43. Isotherms for Bi-Zn-Cu System Showing Liquidus Boundaries in the Bismuth Corner.

The extent of the L_1 region increases as the temperature increases. In the present study, the experimental temperatures coincided with limited single-phase area for these two systems. If the experimental temperatures had been lower, similar discontinuities might have been observed for some of the other ternary systems studied. In three dimensions, the single-phase liquid area extends upward and outward from the melting point of pure bismuth (271°C).

C. Prediction of Zinc Activity in Multi-Component Solutions

With the establishment of the interaction parameters describing the various third element effects on the activity of zinc in dilute solution with molten bismuth, the next portion of the investigation was designed to test the applicability of these parameters in the prediction of zinc activity in higher-order solutions. A previous semi-quantitative study with limited success had been made by Okajima and Pehlke⁽⁷³⁾ for several solute additions to cadmium in lead.

The Taylor series expansion suggested by Wagner⁽⁵⁾ for the logarithm of the activity coefficient may be applied to any order solution, providing the expansion is made about the point of infinite dilution with respect to the solutes. By ignoring effects beyond the first order, the usual form of the expansion is

$$\ln \gamma_{zn}^I = \ln \gamma_{zn}^{I0} + X_{zn} \left(\frac{\partial \ln \gamma_{zn}^I}{\partial X_{zn}} \right)_{\substack{X_{zn}=0 \\ X_{jn}^I=0}} + \sum_{n=1}^n X_{jn}^0 \left(\frac{\partial \ln \gamma_{zn}^I}{\partial X_{jn}^I} \right)_{\substack{X_{zn}=0 \\ X_{jn}^I=0}} \quad (3)$$

$$\ln \gamma_{Zn}^I = \ln \gamma_{Zn}^{I0} + X_{Zn} \epsilon_{Zn}^{Zn} + \sum_{j=1}^n X_j \epsilon_{Zn}^{jZn} \quad (21)$$

The inclusion of the second-order effects for a quaternary system increases the number of terms in the expansion: (72)

$$\begin{aligned} \ln \gamma_{Zn}^I = \ln \gamma_{Zn}^{I0} + & \left[X_{Zn} \left(\frac{\partial \ln \gamma_{Zn}^I}{\partial X_{Zn}} \right) + X_{j_1} \left(\frac{\partial \ln \gamma_{Zn}^I}{\partial X_{j_1}} \right) + X_{j_2} \left(\frac{\partial \ln \gamma_{Zn}^I}{\partial X_{j_2}} \right) \right] \\ & + \left[\frac{1}{2} X_{Zn}^2 \left(\frac{\partial^2 \ln \gamma_{Zn}^I}{\partial X_{Zn}^2} \right) + X_{Zn} X_{j_1} \left(\frac{\partial^2 \ln \gamma_{Zn}^I}{\partial X_{j_1} \partial X_{Zn}} \right) + X_{Zn} X_{j_2} \left(\frac{\partial^2 \ln \gamma_{Zn}^I}{\partial X_{j_2} \partial X_{Zn}} \right) + \frac{1}{2} X_{j_1}^2 \left(\frac{\partial^2 \ln \gamma_{Zn}^I}{\partial X_{j_1}^2} \right) + \dots \right] \end{aligned} \quad (22)$$

(all derivatives at infinite dilution of solutes).

In the general case, the inclusion of the second order effects would require knowledge of all the additional terms. However, in the case of the zinc-bismuth system the self-interaction parameter is zero and hence the terms $\left(\frac{\partial \ln \gamma_{Zn}}{\partial x_{Zn}} \right)$ and $\left(\frac{\partial^2 \ln \gamma_{Zn}}{\partial x_{Zn}^2} \right)$ are eliminated. (Even if they were not zero, they could be evaluated from the binary data.)

Furthermore, in evaluating the first-order interactions for ternary alloys based on the zinc-bismuth system, it was noted in most cases that the relations between $\ln \gamma_{Zn}$ and x_j were linear. Thus, terms above the first order involving x_j would vanish (that is, $\left(\frac{\partial^2 \ln \gamma_{Zn}}{\partial x_j^2} \right)$ is zero).

Therefore, for ternary systems of bismuth-zinc-j obeying this condition, the expression for the logarithm of the activity coefficient reduces to

$$\ln \gamma'_{zn} = \ln \gamma'_{zn}{}^0 + X_j \left(\frac{\partial \ln \gamma'_{zn}}{\partial X_j} \right)_{X_{zn}=0, X_j=0} + X_{zn} X_j \left(\frac{\partial^2 \ln \gamma'_{zn}}{\partial X_j \partial X_{zn}} \right)_{X_j=0, X_{zn}=0} \quad (23)$$

$$\ln \gamma'_{zn} = \ln \gamma'_{zn}{}^0 + X_j \epsilon'_{zn}{}^j + X_{zn} X_j \epsilon'_{zn}{}^j \quad (24)$$

For a quaternary system, that is, zinc in bismuth plus two additional solutes, the Taylor series expansion through the second order terms becomes:

$$\begin{aligned} \ln \gamma'_{zn} = & \ln \gamma'_{zn}{}^0 + X_{j_1} \left(\frac{\partial \ln \gamma'_{zn}}{\partial X_{j_1}} \right)_{X_{zn}=0, X_{j_1}=0} + X_{j_2} \left(\frac{\partial \ln \gamma'_{zn}}{\partial X_{j_2}} \right) \\ & + X_{zn} X_{j_1} \left(\frac{\partial^2 \ln \gamma'_{zn}}{\partial X_{j_1} \partial X_{zn}} \right)_{X_{zn}=0, X_{j_1}=0} + X_{zn} X_{j_2} \left(\frac{\partial^2 \ln \gamma'_{zn}}{\partial X_{j_2} \partial X_{zn}} \right)_{X_{zn}=0, X_{j_2}=0} \\ & + X_{j_1} X_{j_2} \left(\frac{\partial^2 \ln \gamma'_{zn}}{\partial X_{j_1} \partial X_{j_2}} \right)_{X_{zn}=0, X_{j_1}, X_{j_2}=0} \end{aligned} \quad (25)$$

From ternary data it is relatively easy to evaluate the parameters $\left(\frac{\partial \ln \gamma_{zn}}{\partial x_{j_n}} \right)$ and $\left(\frac{\partial^2 \ln \gamma_{zn}}{\partial x_{j_n} x_{zn}} \right)$ and both of these terms may be readily included in the calculation of the activity coefficient. However, the term $\left(\frac{\partial^2 \ln \gamma_{zn}}{\partial x_{j_1} \partial x_{j_2}} \right)$ cannot be evaluated unless data are taken on the quaternary system. In the present case where four alloy electrodes are included per run, a minimum of four runs are needed to evaluate the first- and second-order coefficients for a ternary alloy. In a quaternary

alloy, 16 runs would be required to similarly determine the term $\left(\frac{\partial^2 \ln \gamma_{Zn}}{\partial x_{j_1} \partial x_{j_2}}\right)$. Therefore, for a highly complex alloy, the number of runs

to define all the second order terms would be prohibitive. Nevertheless, the second-order terms from the ternary studies appear in the expression for higher order solutions and their inclusion should improve the calculation of the logarithm of the activity coefficient.

The expressions available for calculation of activity coefficients in multi-component alloys may be termed the first-order and second-order solution interaction models.

The first-order model is the familiar equation of Wagner⁽⁵⁾

$$\ln \gamma_{Zn}^I = \ln \gamma_{Zn}^{I0} + \sum_{j=1}^m X_j \epsilon_{Zn}^j \quad (21)$$

where m is the number of additional solutes besides Zn .

The second-order model adds the cross-partial term $\left(\frac{\partial^2 \ln \gamma_{Zn}}{\partial x_{j_n} \partial x_{Zn}}\right) = \epsilon_{Zn}^j$ and is written as

$$\ln \gamma_{Zn}^I = \ln \gamma_{Zn}^{I0} + \sum_{j=1}^m X_j \epsilon_{Zn}^j + \sum_{j=1}^m X_{Zn} X_j \epsilon_{Zn}^j \quad (24)$$

For ternary systems where $\ln \gamma_i$ is a linear function of x_j and the self-interaction parameter of i is zero, the second-order model is rigorous. For solutions of quaternary or higher order, the second-order model can no longer be rigorous but should nevertheless provide a better representation for $\ln \gamma_i$ than the first-order model.

The assumption implicit in both models is that the interactions affecting the activity of a given solute in a dilute solution are primarily those between that solute and the others present. The cross-interactions between the extra solutes are taken as negligible.

In order to test the hypothesis of the additivity of the interaction effects and to compare the utility of the two solution interaction models, a series of experiments were run on quaternary, quinary, hexadic, and septenary solutions based on the zinc-bismuth system. The aims of these experiments were as follows:

1. To test the validity of the prediction models for increasing numbers of solute elements.
2. To test the validity of the prediction models for various combinations of positively and negatively interacting solutes.
3. To test the applicability of the prediction models as solute concentrations increased away from the dilute region.

The experimental procedure was to determine the activity coefficient of zinc in a given multi-component solution over the temperature range from 450° to 650°C and then to compare the observed value with the activity coefficient calculated from either of the prediction models. The base point for the comparison was the value of $\ln \gamma_{\text{Zn}}$ corresponding to the standard potential for that mole fraction of zinc. A reference binary electrode was included with each multi-component run so that a "cell factor" could be determined to bring the observed potentials to the same value as used in the prediction model.

The emf-versus-temperature relation for the multi-component alloy was compared with the one for the reference binary alloy in order to confirm that the solution was single phase in the experimental temperature region. In multi-component solutions containing gold or copper, marked discontinuities were observed similar to the case of the ternary alloys (Figures 41 and 43). Above the temperature of discontinuity, the slopes for the binary and multi-component alloys were very similar. Electrode potentials for the temperatures below the discontinuity point were obtained by extrapolation as the "super cooled" liquid. All the other multi-component alloys were single phase in the experimental region, as evidenced by the similarity for the temperature dependence of potential.

Neither gallium nor mercury were used in these studies since some uncertainty existed in the measured interaction parameters with zinc for these elements. Since the possible number of alloys and compositions that could be studied was quite large, the experiments were simplified as follows:

1. Equal mole fraction additions of the extra solutes were used.
2. Most of the experiments were run with $x_{Zn} = .015$, the most dilute compositions used in the binary and ternary studies. A few runs were made with $x_{Zn} = .050$ in order to check the validity of the models over the Henry's Law region for zinc.

3. Representative combinations of interactors were used; not all combinations and compositions were attempted.

By using the equal mole fraction additions, the equations for the solution interaction models could be reduced further to the following forms:

First Order Prediction Model:

$$\ln \gamma_{Zn_I}^I = \ln \gamma_{Zn}^{I0} + X_{j_n} \sum_{n=1}^m \epsilon_{Zn}^{j_n} \quad (X_{j_n} = \text{const.}) \quad (26)$$

Second Order Prediction Model:

$$\ln \gamma_{Zn_{II}}^I = \ln \gamma_{Zn}^{I0} + X_{j_n} \sum_{n=1}^m \epsilon_{Zn}^{j_n} + X_{Zn} X_{j_n} \sum_{n=1}^m \epsilon_{Zn}^{j_n} \quad (27)$$

$$\ln \gamma_{Zn_{II}}^I = \ln \gamma_{Zn}^{I0} + X_{j_n} \left(\sum_{n=1}^m \epsilon_{Zn}^{j_n} + X_{Zn} \sum_{n=1}^m \epsilon_{Zn}^{j_n} \right) \quad (28)$$

The base point for making the comparisons were the following activity coefficient values for the zinc-bismuth binary system:

Temperature °C	γ_{Zn}^0	$\ln \gamma_{Zn}^0$
450	4.00	1.386
550	3.03	1.110
650	2.46	.900

The interaction parameter values were taken from Table IX.

For the purpose of selecting the various combinations of interacting solutes, the elements were classified as follows:

Type of Interaction with Zinc	Element	Symbol for Interaction
Positive	In	+
	Pb	+
Slight Negative	Cd	~
	Sn	~
Moderate Negative	Cu	-
	Ag	-
	Sb	-
Strong Negative	Au	=

The final results of these studies are summarized in Table XI, while the experimental data are included in Appendix A. The tabulated results are grouped according to the type of solution, the type of interactors present, and the level of the zinc and added solute concentrations. The observed activity coefficient is then compared with activity coefficients calculated using the First-Order or the Second-Order Solution Interaction Prediction Model. The comparisons are made at 450, 550, and 650°C. In those cases where a range of compositions were studied for a given alloy system, the results are plotted to show the region of validity of the interaction model. The sections which follow are devoted to factual presentation of the results. A more general discussion of the multi-component alloy studies is reserved for the Discussion section (pp.239-246).

1. Quaternary Alloys

A total of eleven different combinations of two added solutes were studied in the investigation of quaternary alloys. All alloys were studied in the "dilute" condition, i.e., where the mole fraction of zinc and both solutes was .015. In addition, three combinations were studied under "non-dilute" conditions, i.e., where the mole fraction of zinc was .050, or where the mole fraction of zinc was .015 and the total added solute concentration was increased up to .215 mole fraction. In addition, replicate runs were made on six of the dilute compositions.

The agreement between the measured and predicted activity coefficients was very good in all cases where the solutes were dilute. The agreement became better as the temperature was increased. In almost all the cases, the second-order model yielded a slightly improved prediction over the first-order model. No significant influence due to the particular combination of the interacting elements could be detected with certainty in the dilute solution results. (Table XI)

However, when the mole fraction of zinc was held constant and the total added solute concentration increased beyond .030 mole fraction, the prediction models were completely successful in only one of the three cases studied. For clarity these results are plotted in Figures 44 and 45 as $\ln \gamma_{Zn}$ versus $\sum x_j$ since (under the conditions of these studies) Equations (26) and (28) predicted a linear relation with $\ln \gamma_{Zn}$. For the solutions containing antimony and silver (both negative interactors with zinc) the experimental and predicted values agreed excellently

TABLE XI
RESULTS OF MULTI-COMPONENT SOLUTION STUDIES OF ADDITIVITY HYPOTHESIS

Type of Solution	Types of** Interactor	x _{Zn} x _j * x _{Bi}			Added Solute Elements		Activity Coefficient of Zinc at 450°C			Activity Coefficient of Zinc at 550°C			Activity Coefficient of Zinc at 650°C						
							Observed			Predicted			Observed			Predicted			
							γ _{observed}	γ _{calc.} Model I	γ _{calc.} Model II	γ _{observed}	γ _{calc.} Model I	γ _{calc.} Model II	γ _{observed}	γ _{calc.} Model I	γ _{calc.} Model II				
Binary	(Basis for Comparison for All Following Alloys)						4.00				3.04				2.46				
Quaternary	+ +	.015	.015	.955	Pb In		4.32	4.24	4.19	3.21	3.20	3.17	2.56	2.59	2.59				
		.015	.015	.955	Pb In		4.12			3.14			2.55						
	~ ~	.015	.015	.955	Cd Sn		4.20	3.96	3.94	3.06	3.00	2.99	2.47	2.95	2.42				
		.015	.015	.955	Cd Sn		3.96			3.02			2.45						
	+ -	.015	.015	.955	Pb Sb		3.76	3.76	3.76	2.82	2.90	2.90	2.27	2.36	2.36				
		.015	.015	.955	Pb Sb		3.70			2.84			2.29						
	+ ~	.015	.015	.955	Pb Sn		4.06	4.05	4.04	3.08	3.07	3.05	2.49	2.49	2.48				
		.015	.015	.955	Pb Sn		3.96			2.99			2.46						
	~ -	.015	.015	.955	Sn Ag		3.78	3.77	3.76	2.90	2.90	2.88	2.49	2.37	2.36				
		.015	.015	.955	Sn Ag		3.76			2.88			2.47						
	- -	.015	.015	.955	Cu Ag		3.74	3.62	3.61	2.80	2.82	2.79	2.31	2.32	2.30				
	- =	.015	.015	.955	Sb Au		2.61	2.75	2.65	2.17	2.17	2.15	1.84	1.80	1.83				
	.015	.015	.955	Ag Au		2.60	2.86	2.72	2.19	2.23	2.20	1.85	1.85	1.87					
Quaternary	- -	.015	.015	.955	Ag Sb		3.72	3.51	3.50	2.77	2.73	2.72	2.27	2.25	2.24				
		.015	.025	.935	Ag Sb		3.25	3.21	3.20	2.58	2.55	2.53	2.15	2.12	2.11				
		.015	.0375	.910	Ag Sb		2.86	2.88	2.86	2.28	2.33	2.31	1.92	1.98	1.95				
		.015	.050	.885	Ag Sb		2.70	2.58	2.56	2.20	2.14	2.11	1.88	1.84	1.81				
		.015	.100	.785	Ag Sb		1.73	1.67	1.64	1.51	1.51	1.48	1.37	1.37	1.33				
		.050	.015	.920	Ag Sb		3.49	3.48	3.46	2.74	2.73	2.70	2.26	2.27	2.22				
		.050	.050	.850	Ag Sb		2.58	2.53	2.48	2.13	2.14	2.06	1.84	1.85	1.92				
	+ -	.015	.015	.955	Pb Ag		3.84	3.88	3.88	2.89	2.98	2.96	2.36	2.43	2.42				
		.015	.015	.955	Pb Ag		3.82			2.90			2.33						
		.015	.025	.935	Pb Ag		3.68	3.81	3.80	2.83	2.94	2.92	2.32	2.42	2.49				
		.015	.0375	.910	Pb Ag		3.58	3.72	3.69	2.72	2.90	2.87	2.25	2.49	2.36				
		.015	.050	.885	Pb Ag		3.60	3.62	3.60	2.80	2.86	2.82	2.52	2.37	2.33				
		.015	.100	.785	Pb Ag		3.17	3.29	3.24	2.53	2.69	2.62	2.17	2.28	2.20				
	+ -	.015	.015	.955	In Sb		3.70	3.81	3.78	2.87	2.93	2.90	2.37	2.39	2.37				
		.015	.025	.935	In Sb		3.46	3.70	3.64	2.73	2.86	2.82	2.28	2.46	2.32				
		.015	.050	.885	In Sb		2.98	3.41	3.31	2.45	2.70	2.64	2.11	2.26	2.19				
		.015	.100	.785	In Sb		2.41	2.90	2.74	2.10	2.41	2.29	1.90	2.15	1.95				
		.050	.015	.920	In Sb		3.69	3.77	3.70	2.94	2.93	2.86	2.35	2.41	2.33				
		.050	.050	.850	In Sb		3.14	3.38	3.36	2.50	2.70	2.49	2.09	2.28	2.26				
	Quinary	- - -	.015	.015	.940	Cu Ag Sb		3.24	3.36	3.34	2.59	2.63	2.62	2.17	2.18	2.17			
			.015	.015	.940	Cd Sn Sb		3.67			2.85			2.34					
		~ ~ -	.015	.015	.940	Cd Sn Sb		3.88	3.65	3.65	2.90	2.82	2.80	2.43	2.29	2.29			
		+ ~ ~	.015	.015	.940	Pb Cd Sn		3.96	4.04	4.03	3.02	3.06	3.05	2.44	2.46	2.44			
			.015	.015	.940	Pb Cd Sn		4.02			3.04			2.44					
+ + -		.015	.015	.940	In Pb Ag		3.92	3.99	3.92	3.04	3.08	3.04	2.49	2.52	2.48				
		.015	.030	.895	In Pb Ag		4.08	3.96	3.86	3.11	3.12	3.05	2.52	2.56	2.50				
		.015	.050	.855	In Pb Ag		4.25	3.94	3.77	3.24	3.19	3.06	2.64	2.65	2.53				
		.050	.030	.860	In Pb Ag		3.72	3.96	3.64	2.91	3.12	2.87	2.40	2.57	2.39				
~ ~ -		.015	.015	.940	Cd Sn Ag		3.96	3.76	3.73	2.96	2.89	2.87	2.40	2.36	2.35				
		.015	.030	.895	Cd Sn Ag		3.54	3.54	3.49	2.73	2.75	2.72	2.24	2.27	2.23				
+ ~ -		.015	.015	.940	Pb Cd Ag		3.94	3.88	3.85	3.00	2.96	2.96	2.43	2.42	2.41				
		.015	.030	.895	Pb Cd Ag		3.63	3.74	3.72	2.79	2.90	2.88	2.28	2.39	2.36				
		.050	.030	.860	Pb Cd Ag		3.62	3.74	3.65	2.83	2.90	2.82	2.33	2.39	2.31				
Hexadic		+ + ~ -	.015	.015	.925	In Pb Sn Sb		3.84	3.87	3.82	2.96	2.97	2.96	2.40	2.42	2.39			
			.015	.015	.925	Cd Sn Ag Sb		3.54	3.47	3.44	2.74	2.70	2.68	2.24	2.23	2.21			
	+ + - -	.015	.015	.925	In Pb Ag Sb		3.77	3.70	3.66	2.86	2.88	2.84	2.30	2.37	2.34				
		.015	.015	.925	In Cd Ag Sb		3.62	3.62	3.57	2.84	2.81	2.78	2.35	2.34	2.29				
		.050	.015	.890	In Cd Ag Sb		3.46	3.62	3.46	2.72	2.81	2.78	2.35	2.32	2.21				
	+ + ~ ~	.015	.015	.925	In Pb Cd Sn		4.12	4.16	4.11	3.15	3.17	3.14	2.56	2.56	2.52				
	.050	.015	.890	In Pb Cd Sn		3.92	4.16	4.00	3.02	3.17	3.05	2.45	2.56	2.46					
Septenary	+ ~ ~ - -	.015	.015	.910	In Cd Sn Sb Ag		3.96	3.58	3.52	3.02	2.79	2.74	2.44	2.30	2.27				
		.015	.015	.910	In Pb Sb Ag Cu		3.80	3.54	3.48	2.95	2.78	2.73	2.42	2.30	2.26				
	+ + ~ ~ -	.015	.015	.910	In Pb Cd Sn Sb		3.80	3.85	3.80	2.87	2.96	2.92	2.31	2.41	2.38				

* Equal mole fraction addition of extra solute.

** See p 141 for classification of interactions.

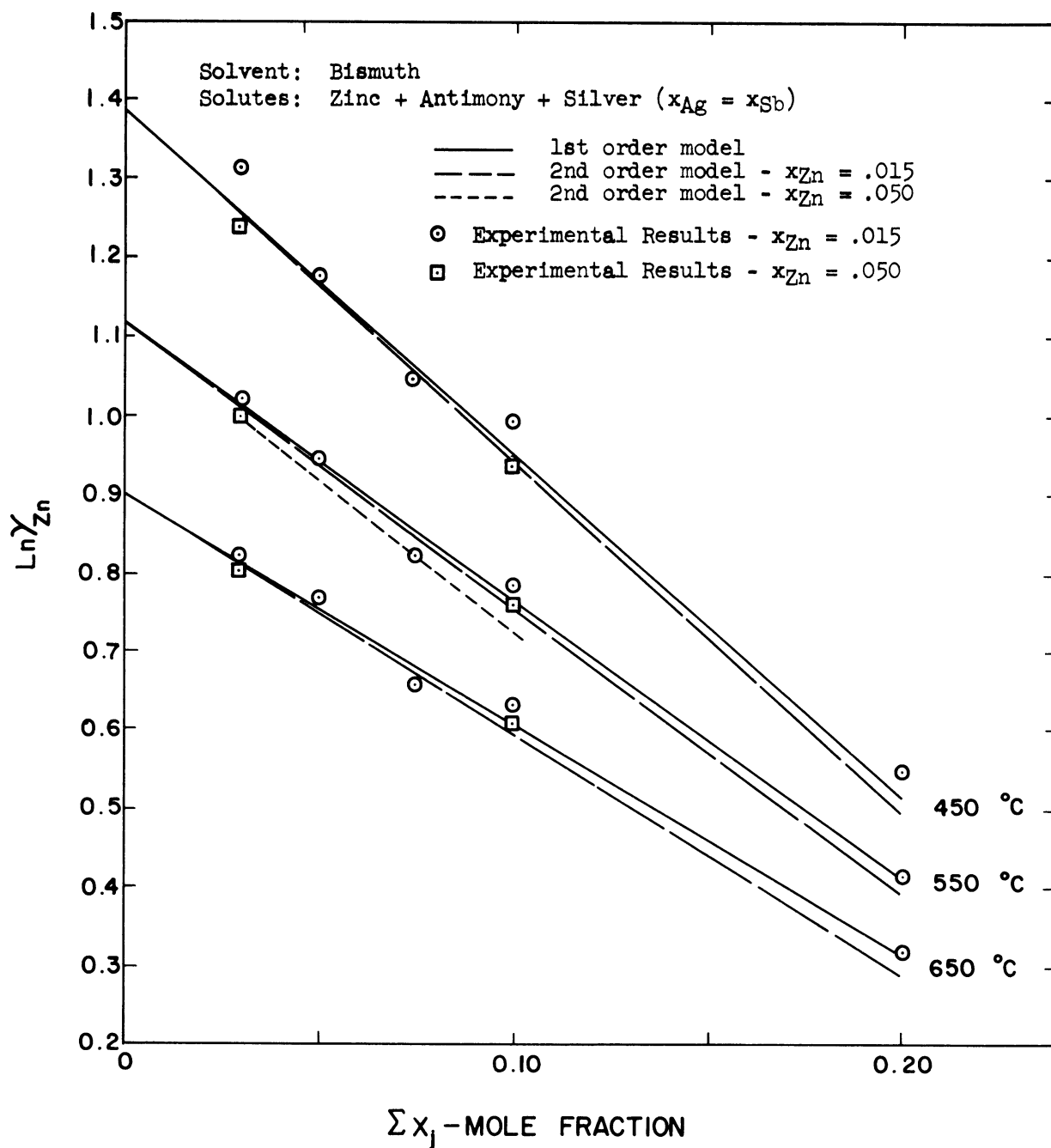


Figure 44. Logarithm of Zinc Activity Coefficient versus Total Mole Fraction of Added Solutes for Quaternary Alloys of Bi-Zn-Ag-Sb--comparison of observed and predicted values.

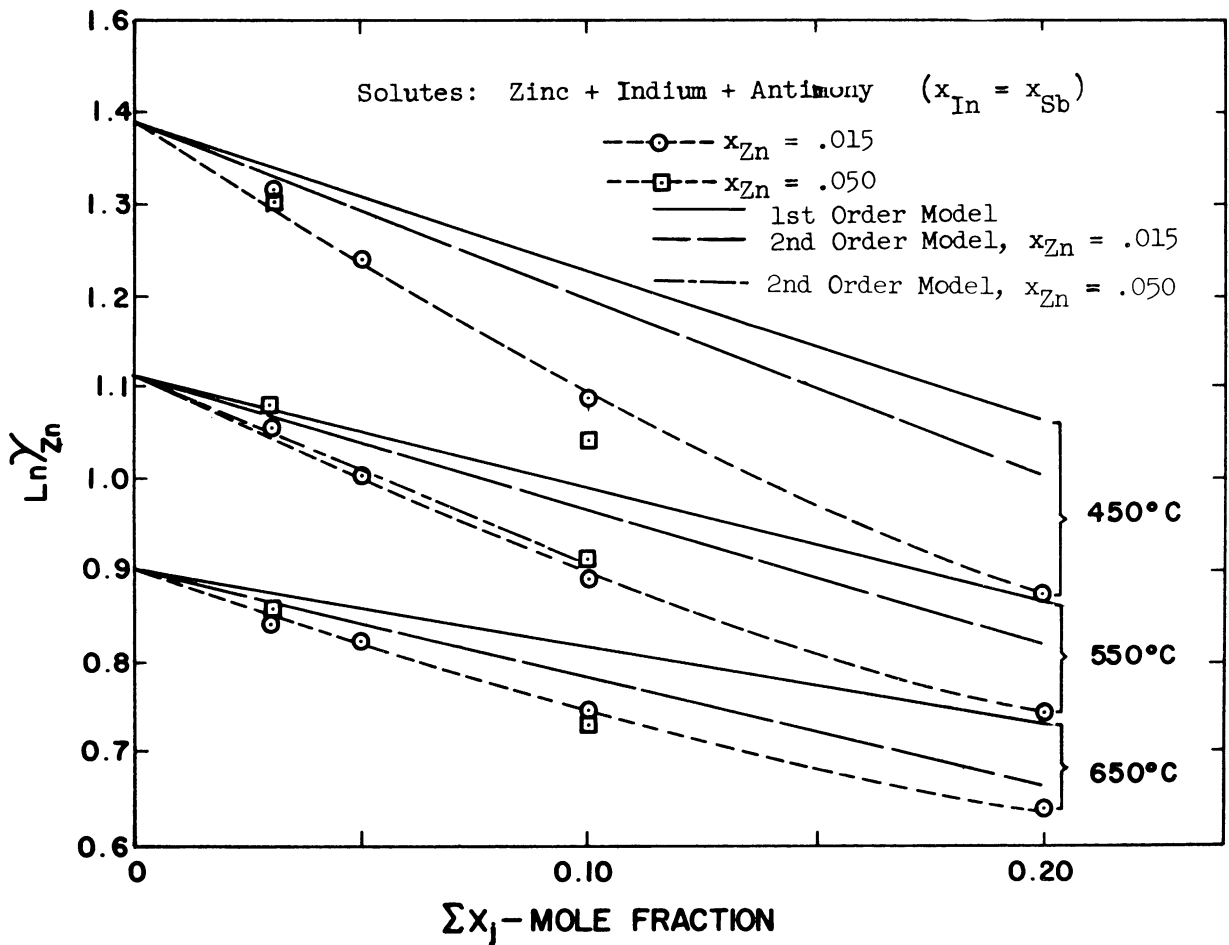
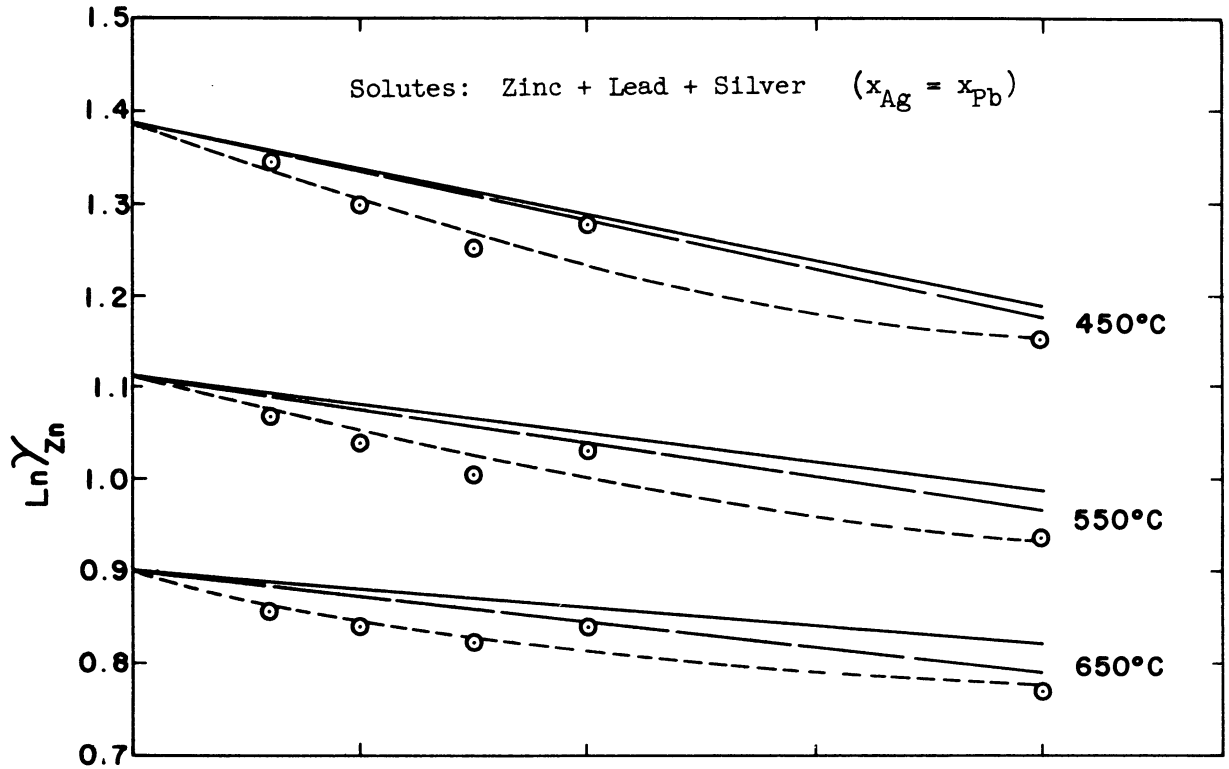


Figure 45. Logarithm of Zinc Activity Coefficient versus Total Mole Fraction of Added Solutes for Quaternary Alloys of Bi-Zn-In-Sb and Bi-Zn-Ag-Pb - Comparison of Observed and Predicted Values.

even out to a total solute concentration of .215. This is considerably away from the dilute region in which the ternary parameters were measured, however, it will be recalled that many of the ternary results were linear up to the highest concentration of solute studied (.10 mole fraction). The agreement was not so good for additional total solute concentrations beyond .03 mole fraction for the solutions containing lead plus silver or antimony plus indium. In both these cases a positive interactor was combined with a negative interactor. Although the agreement became better as the temperature was increased, the experimental values of $\ln\gamma_{Zn}$ were always less than the predicted values. The second-order model was closer to the experimental results, but only began to achieve fairly good agreement at 650°C. However, in both cases, the effect of the combination of solutes was less than if the negative interactor alone had been present at the same total concentration. For example, the value of $\ln\gamma_{Zn}$ for the case where indium and antimony were both present was greater than if antimony had been present alone at the same mole fraction and considerably less than if indium alone had been present. Therefore, the positive interactor moderated the effect of the negative interactor, yet the net effect on $\ln\gamma_{Zn}$ in these cases was not the algebraic sum of the individual interactions.

An increase in the zinc content to .050 mole fraction did not result in significantly different effects in the quaternary solutions.

2. Quinary Alloys

Six compositions were investigated where three additional solutes were added to the zinc-bismuth system. A limited study of "non-dilute" compositions was made on three alloys, while replicate runs were made on two of the dilute compositions. For the case where each of the solutes were present at .015 mole fraction the predicted values agreed quite well with the experimental results. The second-order model produced slightly better results than the first-order model. The agreement between the predicted values and the measured values was better as the temperature was increased. (Table XI)

For the "non-dilute" solutions the results were mixed. In the system where indium, lead, and silver were the added elements, Figure 46 shows that the experimental results for $x_{Zn} = .015$ agreed well with the first-order model but not the second-order model. However, for the one alloy where $x_{Zn} = .050$, the second-order model yielded very good agreement with the experimental result. For the two systems containing cadmium, tin, and silver or lead, cadmium, and silver the predictions from either model were in fair agreement with the experimental results.

3. Hexadic Alloys

Five examples of alloys were studied where four solute elements were added to the zinc-bismuth system. For two of the compositions, zinc mole fractions of .015 and .050 were studied. In the other systems, the zinc was held at .015 mole fraction. In all alloys, the added solutes were kept at .015 mole fraction each.

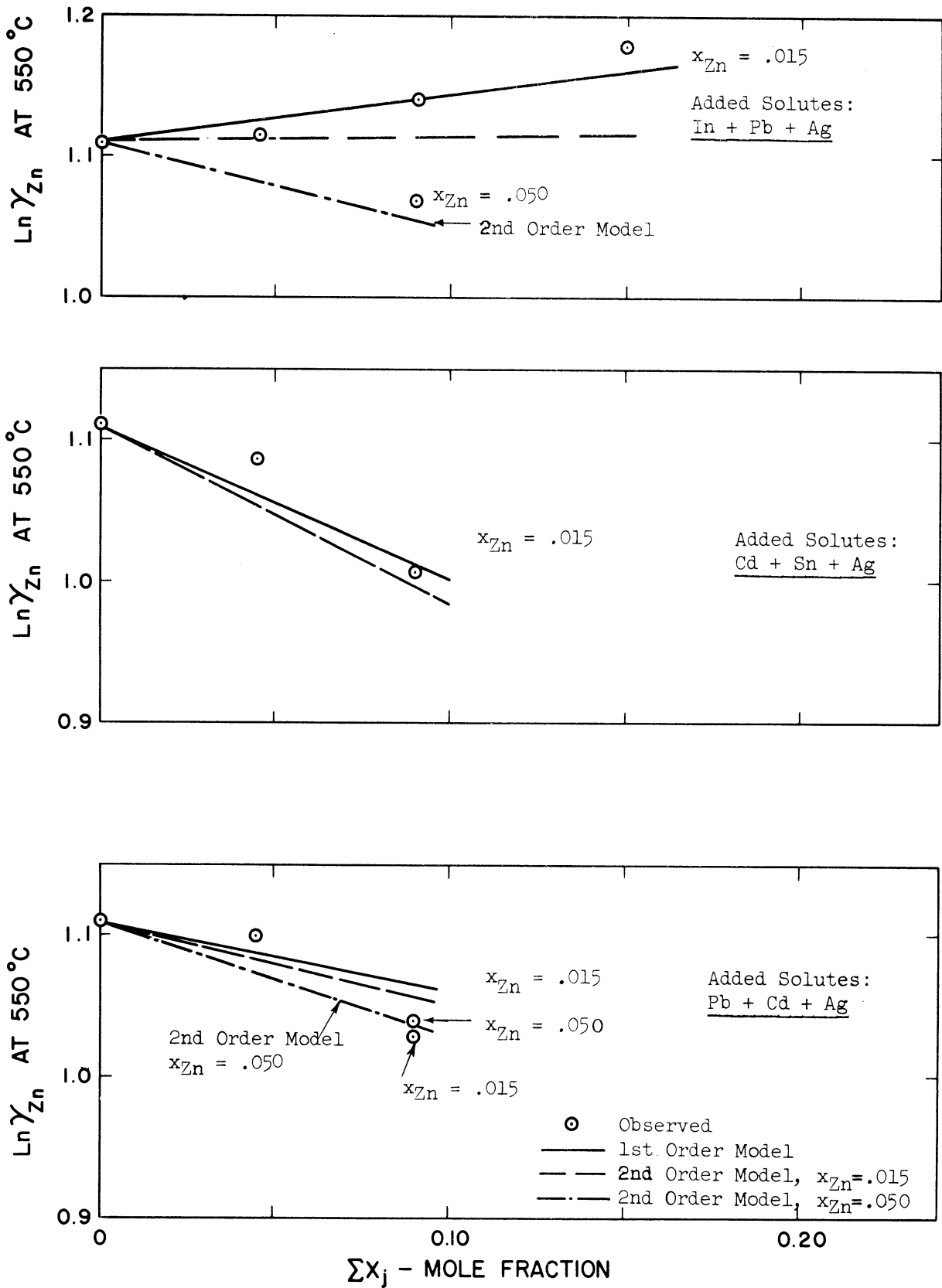


Figure 46. Logarithm of Zinc Activity Coefficient versus Total Mole Fraction of Added Solutes for Quinary Alloys Based on Bi-Zn - comparison of observed and predicted values.

In virtually all cases, the observed and predicted values were in very good agreement at all temperatures considered. The second-order model yielded better predictions for most of the alloys. Increasing the mole fraction of zinc did not appear to affect the validity of the predictions. (Table XI)

4. Septenary Alloys

Three alloys were studied where five solute elements were added to the zinc-bismuth system. All the solute concentrations were held at .015 mole fraction. For one alloy the measured and predicted values were in fairly good agreement over the whole range of temperatures considered. However, in the other two cases the observed values for the activity coefficient were distinctly higher than the predicted values, although the difference was less at 650°C than at the lower temperatures. The disagreements were associated with the alloys having two or three negative interactors, while the alloy producing fair agreement had only one negative interactor. (Table XI)

5. Summary of Multi-Component Interaction Effects

The experimental results of the multi-component solution studies may be summarized as follows:

1) Test of the effect of increased number of solute elements:

- a) For $x_{Zn} = .015$ and $x_{Bi} > .9$: For solutions up to hexadic, the agreement between observed and predicted values was excellent at all temperatures. For the septenary alloys, the

agreement was only fair in two cases, and moderately good in the other case.

b) For $x_{Zn} = .05$ and $x_{Bi} \approx .9$: The agreement was good to excellent for the quaternaries, and fair to good for the quaternaries and hexadics.

2) Test of the effect of the departure from the "dilute" solution region:

a) For $x_{Zn} = .015$ and $\sum x_j \rightarrow .20$: The agreement in the quaternary solution for silver plus antimony was excellent at all temperatures. For the systems with lead plus silver or indium plus antimony, the observed activity coefficients were significantly less than the predicted values, however, the positively interacting component did moderate the effect of the negative interactor. The agreement improved somewhat as the temperature was increased but only became fair at best.

b) In the quinary alloys, the results were fairly good in two out of three cases.

c) For the hexadic alloys the limited evidence was that the agreement became slightly poorer as x_{Zn} was increased at a constant level of the total solute concentration.

3) Test of the effect of various combinations of positive and negative on the activity coefficient of zinc:

In the dilute solutions, ($x_{Bi} \approx .9$) the effect of different combinations of interacting elements was not significant for any of the

solution types studied. In the non-dilute quaternaries, two systems where positive and negative interactors were combined resulted in lower than expected values for γ_{Zn} . In the case where both the interactors were negative, the predicted and observed activity coefficients were in excellent agreement throughout the entire range of compositions studied. The second-order model yielded improved predictions but did not completely account for the observed effects. The divergence between observed and predicted values became less at the highest temperature studied.

D. Confirmation of Basic Assumptions

In the discussion of the experimental method, mention was made of the basic assumptions inherent in utilizing the galvanic cell method for activity determination. These included the reversibility of the cell, the ionic conductance of the electrolyte, the valence of the element whose activity is being measured, the absence of significant side reactions, and the verification of the alloy compositions and that the alloys were single-phase liquids.

Several methods are available for the verification that these assumptions were actually realized in the experimental process. Probably most important is the behavior of the galvanic cells themselves. Another direct procedure is chemical analysis of the electrodes. It is also possible to perform a direct experiment to verify the conductance of the electrolyte, the question of the metal valence, and the reversibility of the cells. Indirect verification is also possible by comparing the experimental results with those of independent investigations. Ideally, such comparisons should be made with data obtained by different experimental techniques. This was not completely possible for the present results since the only activity studies reported in the literature for the zinc-bismuth system in the range 450-650°C had also been conducted by the galvanic cell method for higher concentrations of zinc. However, it was possible to compare the independent use of the galvanic cell method at these temperatures. In addition, the present results could be extrapolated to a temperature where data had been taken by a dynamic vapor pressure method.⁽³⁶⁾

The behavior of the cells has been previously discussed in detail. In general, all the cells were quite stable. The relations between electrode potential and temperature were linear over the range studied, except where discontinuities were noted because of transition to a single phase liquid. For those systems where published phase diagrams indicated existence of a single phase liquid the slopes of the emf-temperature relations for binary and ternary alloys were almost

identical. Where transition to a single phase liquid did occur, the change in slope was quite marked (see Figures 40 and 42). Hence, the fact that the slopes for the binary and multi-component alloys for which no phase diagrams were available were almost identical and had no discontinuities could be taken as evidence that a given system was composed of a single-phase liquid at the temperature under consideration.

The activity data obtained in the present studies of the binary alloys were shown to be logical extensions to the dilute region of the previous galvanic cell results of Kleppa⁽⁴⁵⁾ and Iantratov and Tsarenko⁽⁴⁷⁾ obtained at higher levels of zinc. Where the present experimental compositions overlapped those of Kleppa's investigation, the activity versus concentration relations were in good agreement. The present results were also extrapolated to 352°C by use of the temperature dependence relation for $\ln \gamma^0$ (see p. 90). This was the temperature at which Yokokawa et al.⁽¹⁶⁾ had used a dynamic vapor pressure method to determine the activity of zinc. The value of γ^0 calculated from Yokokawa's data was 5.4, while the extrapolated value from these studies was 5.6.

Kleppa⁽⁴⁵⁾ reported that chemical analysis of his samples showed no change in composition from the weighed-in values within the accuracy of the method of analysis (which was unstated). He also noted that the electrode weights before and after the runs differed by only a few milligrams (the total weights were not reported).

As part of the present investigation, chemical analyses were made on the electrodes from several binary and ternary alloy runs. In

addition, an attempt was made to determine the weight change of the electrodes. The results of these studies are reported separately, but in general they showed that negligible compositional and weight changes occurred from the weighed-in values.

In addition to the chemical analyses, weight-change studies, and the inferences drawn from cell behavior, a special experiment was conducted to verify the reversibility of the cell, the electrolyte conductance, and the valence of zinc. This procedure was termed the Faraday Yield experiment and is described below.

1. Faraday Yield Experiment

This experiment was conducted after the emf-temperature relations had been established for Run 53 (Bi-Zn-Ga system, $x_{Zn} = .025$). The intent of the experiment was to change the composition of the binary reference electrode by deliberate transference of zinc from the standard electrode. When the new composition had been established and its potential determined, the procedure would be reversed and the zinc transferred back to the standard. If the cell was reversible, the potential should return to the original value. The transfer would be by passing a constant current between the standard and the binary electrode for a measured period of time - thus a specified number of coulombs of electricity would have been passed. By Faraday's Law, the electrochemical equivalent of zinc is given by

$$\frac{\text{Mol. Wt.}}{\text{Valence}} \times \frac{1}{f} = \frac{65.38}{2(96,500)} = .338 \text{ mg./coulomb}$$

This expression gives the weight of zinc that will be transferred per coulomb.

The mole fraction of zinc in the binary electrode was .025 and the electrode contained .1404 grams of zinc plus 17.5037 grams of bismuth. To raise the content of zinc to .0375 mole fraction, it was necessary to increase the weight of zinc to .2132 grams. Thus it was necessary to transfer .0728 grams of zinc. Using the Faraday equivalent, and assuming a valence of two for the zinc, the amount of electricity required is 216 coulombs. At a current of 150 milli-amps, 24 minutes are required.

At the start of the run, the temperature of the cell was equilibrated at 500°C (and maintained at this value throughout the experiment) and the potentials of all the electrodes were measured. (The values will be summarized later.) The power source was a small electrolytic etching unit containing several fresh dry cells wired in series, and incorporating a DC voltmeter and a milli-ammeter. The positive terminal from the power source was connected to the lead from the pure zinc standard in the cell and the negative terminal to the alloy lead. The current within the cell passed from the standard electrode to the alloy and was maintained at 150 milli-amps by means of a rheostat. As current flowed and some polarization occurred, it was necessary to raise the voltage slightly. The initial voltage was about .5 volts and the final voltage reached .7 volts. Following the passage of 216 coulombs, the leads were disconnected and the cell allowed to equilibrate. The behavior of the electrode potentials is shown schematically in Figure 47.

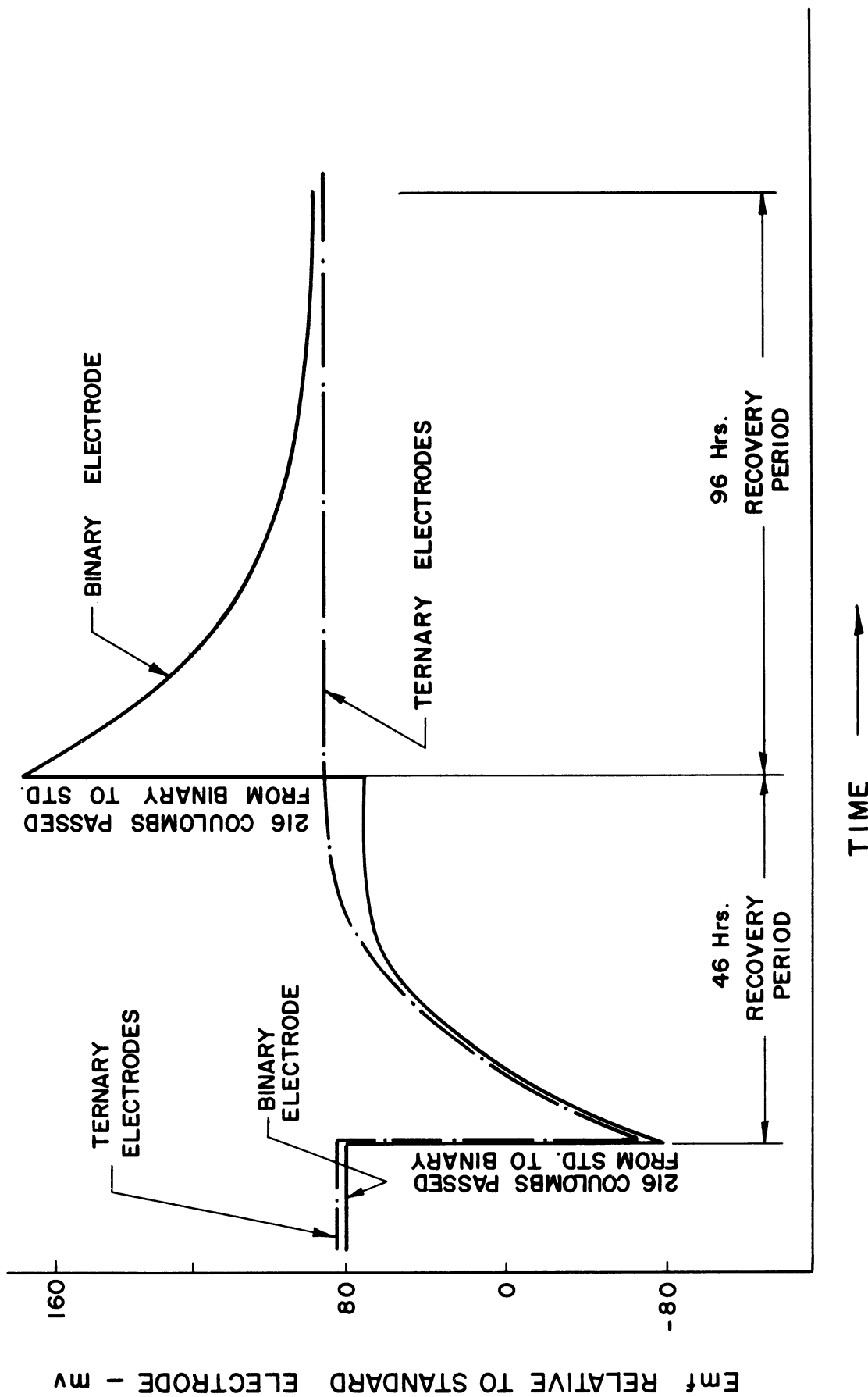


Figure 47. Schematic Diagram of Electrode Potential Behavior During the Faraday Yield Experiment.

About 46 hours were required for the electrode potentials to recover from polarization to a constant value. The point of complete recovery was taken as the time when the emf's became stable and the emf of the ternary alloy electrodes had returned to the values noted immediately before the passage of the current. At this point, the potential of the binary electrode had settled out at a value quite close to that expected for an alloy containing .0375 mole fraction zinc at 500°C.

The external power source was then re-connected, this time in the reverse manner, and 216 coulombs were passed through the cell. The current was monitored manually to remain at 150 milli-amps. This time the initial voltage was about .6 volts. It was necessary to raise the voltage to about 1.1 volts at one point, but then it was reduced to about .7 volts in the latter stages of the experiment. Following the passage of the current, approximately 96 hours were required for recovery of the binary electrode to a constant potential. The indicated emf's of the ternary electrodes were unaffected by the re-transfer operation. The run was discontinued when it was noted that no further change in the binary potential had occurred over a 16 hour period.

At this point the potential of the binary electrode had returned to a value characteristic of a .025 mole fraction zinc alloy at 500°C, while the alloy electrodes over the entire time of the experiment had changed by only .1 to .2 millivolts.

A condensation of the experimental observations follows:

Time	Temperature	Electrode Potentials-mv			
		Binary	Alloy ¹	Alloy ²	Alloy ³
Before current transfer	500°C	80.55	79.88	80.04	80.41
12 hours after current transfer	499.6	45.38	57.46	57.63	58.00
46 hours after current transfer (upon completion of recovery)	500.0	67.86	79.89	80.03	80.31
13 hours after current re-transfer	499.4	101.97	80.05	80.20	80.47
96 hours after current re-transfer	500.0	81.29	80.00	80.09	80.64

Binary Electrode ($x_{Zn} = .025$ weighed-in)	Nominal Composition	Expected Emf (Std. Value)
Initial Emf	$x_{Zn} = .025$	81.75mv
After Current Passage and Recovery	$x_{Zn} = .0375$	68.24
Change in Emf	Expected Change	13.51
After Second Current Passage and Recovery		
Change from Intermediate Value		
Average change in EMF =		13.06mv or 96.5 per cent of expected change.

Change in Alloy Electrodes Over 144 hours of the Experiment	Alloy ¹	Alloy ²	Alloy ³
	+0.12mv	+0.05	+0.23

The behavior of the observed electrode potentials during the recovery periods is consistent with the assumption that the polarization took place at the surface of the electrode where the reaction $Zn \rightleftharpoons Zn^{++} + 2e$ took place. When zinc was transferred out of the standard

and into the binary electrode, all the potentials of the ternary alloys were affected with respect to the standard electrode. However, when full recovery from the polarization had taken place and the current was reversed to transfer zinc out of the binary electrode and back to the standard, only the potential of the binary electrode was affected relative to the standard.

The average change in potential of the binary electrode for the two steps of the Faraday Yield experiment was 96.5 per cent of the expected change for the planned alteration of zinc from .025 mole fraction to .0375 mole fraction and back. The theoretical or expected change was based on the assumptions of cell reversibility, ionic conductance of the electrolyte and a valence of two for zinc. It was concluded that the experimental results were well within the expected accuracy of the experiment and that the validity of the experimental assumptions was adequately verified.

2. Electrode Weight Changes

An attempt was made to remove the electrodes from several cells in as quantitative a manner as possible to determine their weight change, if any. The usual method of concluding the run was to water quench the cell to avoid the danger of the Vycor tube bottom cracking on contact with any solidifying electrolyte that might have condensed outside the cell crucible. The water quench usually caused some splashing of the liquid alloys and thus weight change determinations from normally concluded runs were not attempted.

The procedure for "quantitative" electrode removal was to withdraw the tantalum leads as carefully as possible, remove the Vycor cell tube from the furnace, and allow the entire assembly to cool in air with a rod extending into the salt melt. The salt solidified at about 350°C while the alloys, being almost pure bismuth, did not freeze completely until about 270°C. As soon as the salt had solidified sufficiently to hold the rod in place, the cell crucible was withdrawn by the rod and the Vycor tube filled with water. Of the two attempts to use this procedure, one of them ended with a cracked tube bottom.

When it was certain that the electrodes were solid under their blanket of salt, the salt was dissolved in a stream of hot water. The electrode crucibles were then dried and weighed. Slight weight losses, ranging from .2 to 1.5 per cent were noted from the alloy electrodes (17-18 grams total weight). Of the two zinc standard electrodes, one apparently gained about .5 per cent and the other lost about .5 per cent in weight.

The results are considered good within the expected accuracy but inconclusive since there was the possibility of losing material as the electrode leads were withdrawn and in washing out some other material with the salt.

3. Chemical Analysis

Chemical analysis was conducted on a number of the electrodes for runs concluded by the normal "quenching" procedure. Both wet chemical procedures and emission spectroscopy were employed. The spectrographic

analysis was conducted on an ARL Spectrograph in the Department of Chemical and Metallurgical Engineering, University of Michigan, while the wet chemical analysis was done by an outside laboratory (Ledoux and Co., Teaneck, New Jersey). Several samples were analyzed by both means.

The primary purpose of the analyses was to verify that no significant transfer of zinc had taken place during the operation of the cell. Since the effect of the displacement reactions (if they occurred) would be expected to be greatest for alloys low in zinc and high in the amount of third element, the emphasis in the analysis was on these types of alloys. In addition, displacement due to the third element might be expected most likely for cadmium, tin, or lead-containing alloys.

The results obtained by emission spectroscopy are summarized in Table XII. In addition to the alloys reported, attempts were also made to analyze for zinc in the presence of copper or tin. In these alloys it was very evident that the presence of the third element interfered with the zinc analysis. The results for the cadmium-containing alloys appeared to be free of interferences, while there was some indication of a very slight interference by lead.

However, for the binary alloys the spectrographic determinations were not subject to third element interferences and the results appeared to be fairly good. The standards for the spectrographic analysis were a series of binary zinc-bismuth alloys from .0075 to .050 mole fraction zinc that had been sealed in evacuated glass tubes, held molten in a furnace at 450°C for several hours, air cooled, and then removed from

TABLE XII

RESULTS OF CHEMICAL ANALYSES OF ALLOY ELECTRODES
(Analysis Made After Completion of Run)

Type of Alloy	Run No.	Nominal Composition (Weighed-In Value)			by Emission Spectroscopy			Analyzed Composition			by Wet Chemistry	
		x _{Zn} Mole Frac.	% Zn Weight	x _j Mole Frac.	x _{Zn} Mole Frac.	x _{Zn} Mole Frac.	x _j Mole Frac.	% Zn* Weight	x _j Mole Frac.	% Zn* Weight	x _j Mole Frac.	
Spectroscopic Standards (not run as electrodes)	G-1	.015	.47	-	-	.0152	.48	-	-	-	-	
	G-4	.050	1.62	-	-	.0547	1.78	-	-	-	-	
	47	.015	.47	-	.014/.016	.0155	.49	-	-	-	-	
	64	.015	.47	-	.013	-	-	-	-	-	-	
	65	.015	.47	-	.016	.0152	.48	-	-	-	-	
	68	.015	.47	-	.012	.0127	.40	-	-	-	-	
	71	.015	.47	-	.0145	-	-	-	-	-	-	
	77	.015	.47	-	.016	-	-	-	-	-	-	
Binary Alloys	67	.025	.79	-	.0255	.0239	.76	-	-	-	-	
	70	.0375	1.20	-	.032	-	-	-	-	-	-	
	81	.050	1.62	-	.065	.0502	1.63	-	-	-	-	
Ternary Alloys	64	.015	.47	.015 Pb(1.50 wt. %)	.017	.0127	.40	.0152(1.52 wt. %)	-	-	-	
		.015	.47	.025 Pb	.014	-	-	-	-	-	-	
		.015	.47	.0375 Pb	.0155	-	-	-	-	-	-	
		.015	.47	.050 Pb	.018	-	-	-	-	-	-	
65		.015	.47	.0375 Cd	.015	-	-	-	-	-	-	
		.015	.47	.050 Cd	.0145/.015	-	-	-	-	-	-	
47	.015	.47	.050 Sn(2.93 wt. %)	-	.0138	.45	.0489(2.88 wt. %)	-	-	-		
70	.0375	1.20	.015 Cu(.47 wt. %)	-	.0298	.96	.0118(.37 wt. %)	-	-	-		
83	.015	.47	.015 each; In, Pb, Cd, Sn	-	-	.35	-	-	-	-		

* Stated to be average of two determinations; reported as weight percent and then converted to mole fraction.

the tubes. The samples analyzed from the completed electrodes had been water quenched from approximately 450°C, washed free of salt, broken out of their small crucibles, and then ground flat on one face.

The spectrographic calibration curves prepared from the standards were generally good at the lower concentrations of zinc, but some scatter was evident about $x_{Zn} = .025$. Since the solid solubility of zinc in bismuth is very small⁽⁵⁵⁾ the samples with larger amounts of zinc may have experienced some segregation. The spectrographic results for nominal zinc contents of .0375 and .050 may have thus been influenced by non-uniform zinc distribution in the solid standard, the unknown sample, or both.

The results obtained on the sample containing .015 mole fraction nominal zinc content appeared to be randomly distributed about .015. The accuracy for commercial spectrographic analysis is quoted as from five to seven per cent of the element present.⁽¹⁹⁾ At $x_{Zn} = .015$, this would imply that $\pm .001$ mole fraction accuracy is the best that could be expected. The present results appear to be in this range and it can be concluded, at least from the spectrographic data, that alteration of the zinc content was slight and that if it did occur, it was within the range of accuracy of analysis.

The results of the wet chemical analyses are also summarized in Table XII. In general these results agreed very well with the spectrographic analyses. Two of the spectrographic standards were included with the specimens sent for wet chemical analysis in order to confirm

their composition and the consistency of the two types of analysis. The wet analyses were the average of two determinations. Their accuracy was not specified, however, the wet results obtained on the spectrographic standards suggest that it was probably at least +10 per cent.

There was no evidence from any of the chemical analyses that a significant increase in the zinc content had occurred in any of the alloy electrodes as a result of the galvanic cell runs. Consequently, the absence of significant displacement reactions, diffusion, or transference of zinc by current flow was confirmed, since all of these processes would have led to an increase in the zinc content.

In several of the alloy electrodes the analyses indicated a slight decrease in the zinc content from the weighed-in value. It is possible that the wet analyses may have been biased towards low values, particularly if complete gravimetric separation of zinc was difficult. However, it is also possible that some zinc could have been lost by volatilization or by preferential solution into the molten-salt electrolyte. Studies by Yamagishi and Kamemoto⁽⁶¹⁾ had indicated the latter possibility, however, if either effect had been significant it would have been evidenced by a noticeable increase in the electrode potentials (see Figure 9). Since the electrode potentials were generally quite steady over the running time of the cell, the loss of zinc by these or any other process during the runs was small.

Analysis was also made for the third element content in three of the ternary electrodes. The results generally confirmed that there

was no substantial alteration of x_j from the weighed-in values. The copper and zinc analyses in the Bi-Zn-Cu ternary sample were both lower than expected, however, they were low in the same proportion. This may have been due to segregation in the portion of the electrode analyzed since this system tended towards limited single-phase solubility at the low temperature from which the electrode had been quenched at the conclusion of the run.

V. DISCUSSION

The discussion of the experimental results is divided into four main categories. The first considers the rationale for the observed interactions in the ternary alloys. The general approach is to consider explanations based on the structure and physical properties of the elements involved. The second category covers the applicability of simple solution models for the prediction of interactions. The approach of such theories is partly phenomenological and partly based on statistical thermodynamics. The third topic discussed is the validity of using ternary data for the prediction of activity in higher-order solutions. This stems from Wagner's suggestion of the Taylor series expansion for \ln activity coefficient and is thus a phenomenological approach. The last topic considered includes the limitations of the present results and suggestions for further work.

A. Rationale for the Observed Interactions in Ternary Alloys

One of the major premises on which this investigation was based is that substantial evidence existed from studies conducted in molten iron that the interactions of various third elements with a given primary solute were a periodic function of the atomic number of the added solute. The experimental results were fairly conclusive for non-metallic primary solutes such as carbon, hydrogen, nitrogen, or oxygen, as affected by additional metallic elements. However, the data were limited and inconclusive in the case where the primary solute was also metallic (such as chromium or nickel).

This investigation was designed to study the premise of periodicity for the case where both solutes were metals. Third-element additions from the 4th, 5th, and 6th Periods (Group B) were made to the basic system of zinc dissolved in molten bismuth. The results of these studies will first be discussed on the basis of periodicity, however, since this explanation did not completely account for the experimental observations a number of other possibilities are considered. Among these are included the electronegativities of the elements, thermodynamic interactions between the solutes alone, and atomic size factors.

1. Evidence for Periodic Behavior of Interaction Parameters

Attempts were made to correlate the first- and second-order interaction parameters determined at 550°C with the position of the added solute elements in the Periodic Table. The attempted correlations were both by Period (Figures 48 and 50) and by Sub-Group (Figure 49).

With the notable exceptions of tin and antimony, the first-order parameters almost obeyed a periodic rule. Within each period considered, the trend was for the first-order parameter to become less negative with increasing atomic number of the solute. However, in the 5th Period (the most complete sequence studied), the sequence of increasing parameter values showed an abrupt reversal in the middle.

Considering the results by sub-groups (Figure 49); in three cases (Groups Ib, IIb, and IIIb) there was some tendency for the parameter values to decrease as the atomic number increased. However, the results for Group IVb (tin and lead) were in the opposite direction.

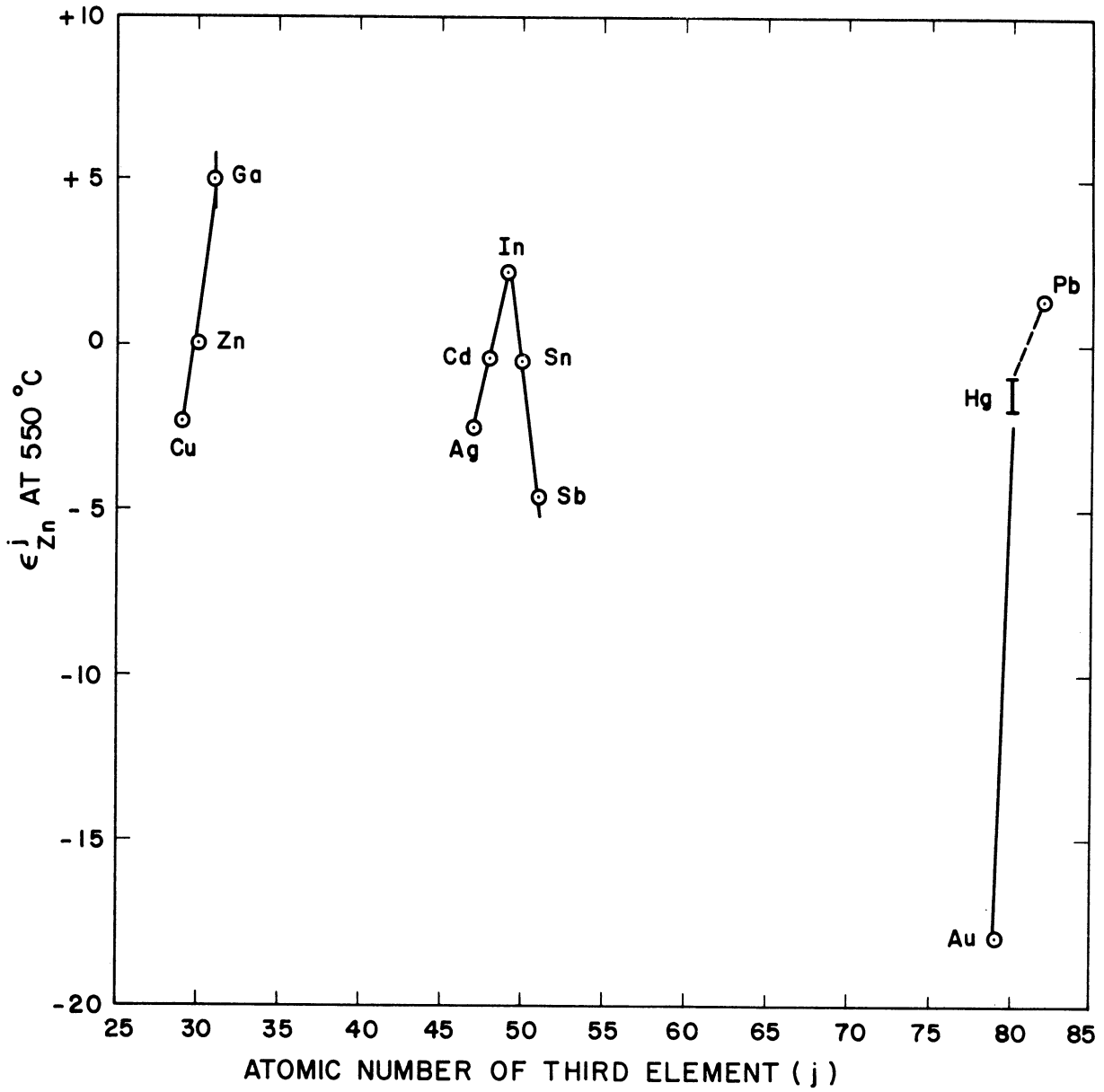


Figure 48. First-Order Zinc- j Interaction Parameters versus Atomic Number of j - correlation by period.

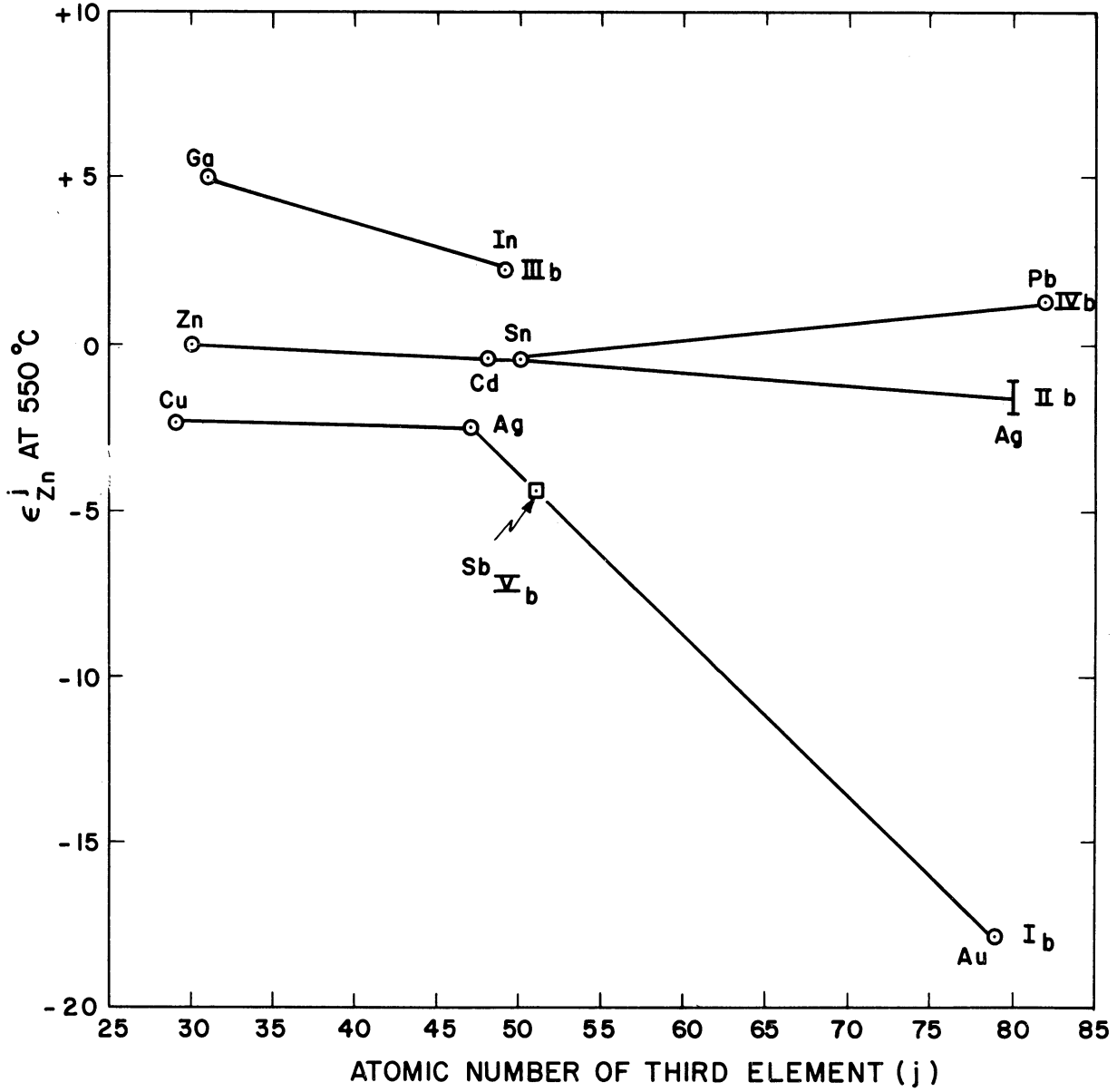


Figure 49. First-Order Zinc- j Interaction Parameters versus Atomic Number of j - correlation by sub-group.

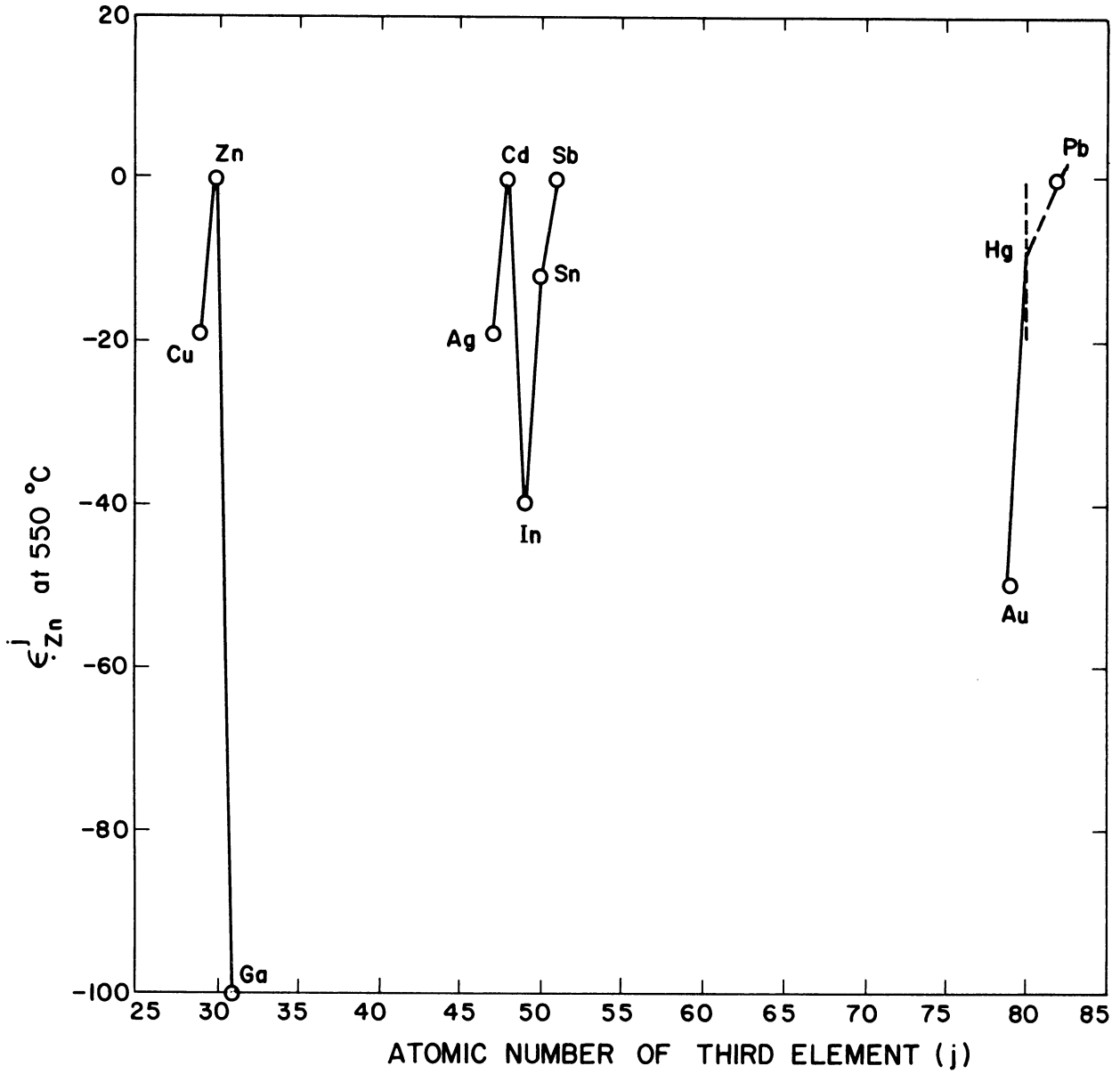


Figure 50. Second-Order Zinc-j Interaction Parameters versus Atomic Number of j - correlation by period.

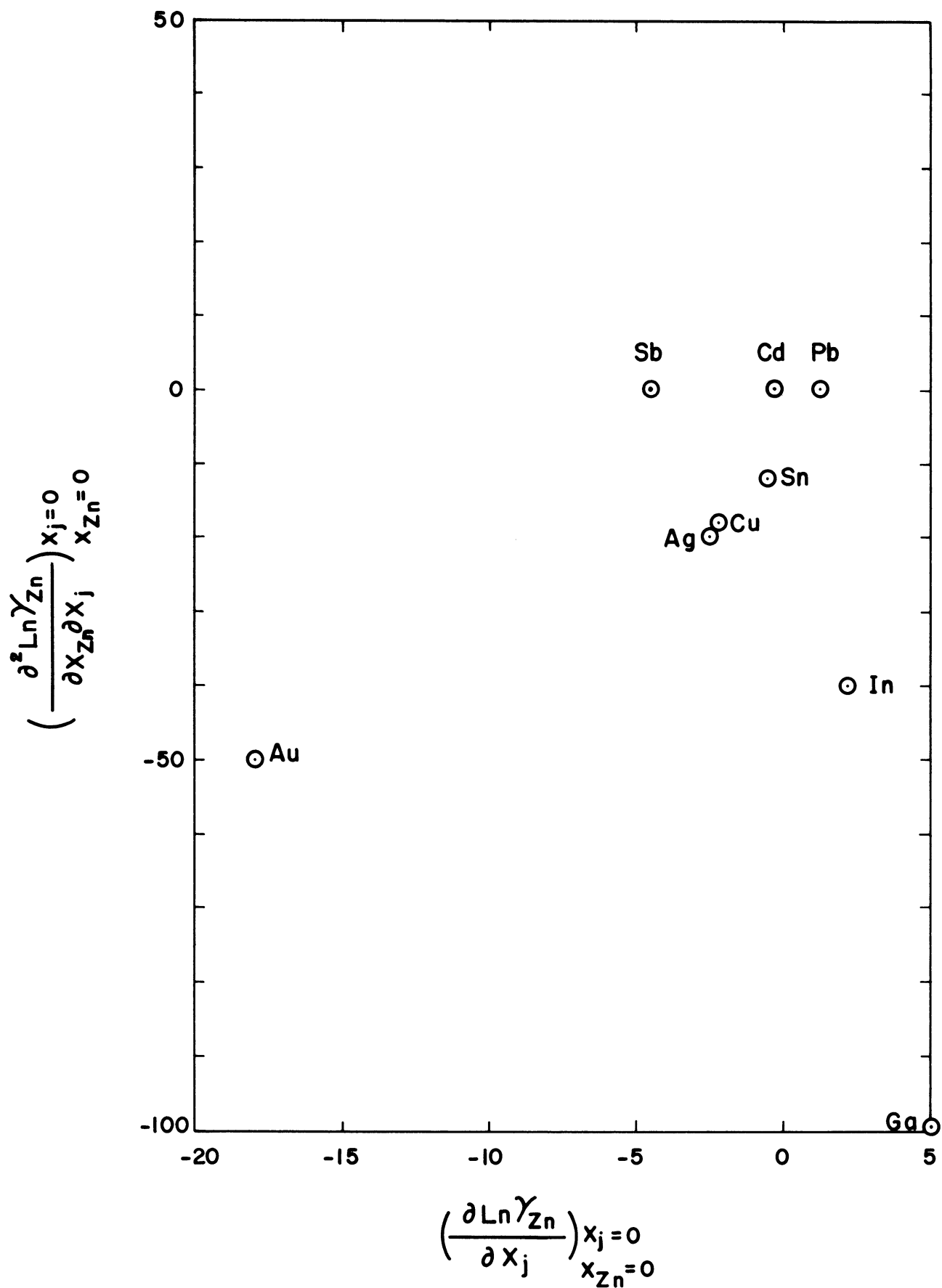


Figure 51. First-Order Zinc-j Interaction Parameters versus Second-Order Zinc-j Interaction Parameters.

There appeared to be no periodicity in the values of the second-order parameters (Figure 50) nor was there any discernible correlation between the first and second-order parameters involving a given solute element. (Figure 51)

The primary basis for assuming periodic behavior is that many of the physical and chemical properties of elements can be explained on the basis of electronic configuration.⁽⁷⁴⁾ As the atomic number is increased, the total number of electrons increase and the number of outer shell electrons vary cyclically. Schenck, Froberg, and Steinmetz⁽¹³⁾ noted that periodicity of interactions leads to the supposition that the activity of the dissolved element is related to the number of valence electrons of the ternary elements or to the number of their electrons in unfilled shells.

The electronic arrangement of the solute elements and the ternary interaction parameters are summarized below in periodic form. (Page 173)

On examining this table it is noted that the elements copper, silver, and gold, all with an unfilled (s) shell, behave similarly and the interaction becomes stronger (more negative) as the total number of electrons (or Atomic Number) increases. The sequence zinc, cadmium, and mercury contains elements with a filled outer (s) shell. These elements also obey a similar sequence of decreasing interaction parameter as the atomic number increases. Gallium and indium each contain one electron in their outermost (unfilled) shell (this time a p-shell) and similarly show a relative decrease in the interaction parameter with atomic number.

Subgroup

Period	I _b		II _b		III _b		IV _b		V _b	
	A.N.	s ¹ e*	A.N.	s ² e	A.N.	p ¹ e	A.N.	p ² e	A.N.	p ³ e
1				2		3		4		5
	Total Outer Shell Electrons (s + p)									
	Atomic No., Outermost Shell, Interaction Parameter									
4	29	Cu	-2.4	30	Zn	0	31	Ga	+5 ±.7	-
5	47	Ag	-2.5	48	Cd	-.3	49	In	+2.2	50 Sn - .5
6	79	Au	-18.0	80	Hg	-1, -2	-	-	-	81 Pb +1.3
										82 (Bi)

* ε^j_{Zn} at 550°C; A.N. -Atomic Number; s¹, s², p¹, p², p³ -outer shell configuration

Thus far, the "rule" would appear to be the following: a "deficiency" of (s) electrons relative to zinc results in a negative interaction, a "surplus" of (p) electrons causes a positive interaction, while the absolute value of the effect is moderated by the total number of electrons of the solute.

However, when the interaction parameters and electron configurations of tin, lead, and antimony are considered, the "rule" breaks down. There is no way to account either for the negative interaction parameters of antimony or tin, or the relative increase in the parameter on going from tin to lead. Furthermore, there is no plausible way from this tabulation to explain the "rule" of why a "surplus" or "deficiency" of electrons in the outermost shell should account for a given direction of interaction.

Wagner⁽²³⁾ suggested that the chemical potential of a solute could be separated into a portion μ_i due to its ions of valence z_i and a portion which is the product of the valence and the chemical potential of the electrons, $z_i\mu_e$.

In discussing the marked periodicity for ternary metallic interactions with carbon or various gases dissolved in liquid iron, cobalt, or manganese (all transition metals with unfilled inner shells), Schenck, Froberg, and Steinmetz⁽¹³⁾ employed Wagner's concept and argued that the primary solute was dissolved as a positive, electron-donor ion. The electron liberated by such ionization then contributed partly to the chemical potential of free electrons, $z_i\mu_e$, and partly to fill the unfilled inner shell of the solvent. A metallic third element addition can either provide electrons to the solution or complete its own shells. When ionized, the

third element might also affect the chemical potential of the free electrons. It might be expected that those additional solute elements with almost empty inner shells would be able to capture more electrons than the solvent, and thus the sign of the interaction would be negative since the chemical potential (or concentration) of free electrons would be decreased. A linear relation between interaction parameter and atomic number could then be explained by the fact that, inside a given period, the number of electrons given up or the degree of shell-filling would increase with the atomic number. The interaction would become more positive as the filling increases. The effect of the ions on the free electrons would either remain constant or also increase with the atomic number. The interaction thus would result from the competition between the solvent and the added solute for the electrons given up by the carbon, etc.

Presumably (although not discussed by Schenck, et al.), the argument might be capable of extension to the case where the primary solute is a metallic transition element dissolved under the above conditions. However, virtually no experimental data are available for such systems involving transition metal solvents.

The extension of the above argument to the case of zinc dissolved in bismuth does not appear possible. Although the zinc could be considered as dissolved as positive ions of charge two, bismuth has no unfilled inner shells and thus the electrons given up by the zinc would go only to increase the chemical potential of free electrons since there would be no competition for electrons between bismuth and the added solute. On the basis of

the relative shell-filling tendencies for the solutes considered in this investigation, a reversal of the interaction effect within a period (such as noted for the 5th Period in these studies) also could not be accounted for. The explanation would have to be constructed in terms of the outermost or valence electrons. Such a correlation by sub-group might provide a basis for assigning an "individuality" of behavior to antimony, however, the available data provide no basis for explaining why the subgroups behave as they do.

It would appear that periodicity or electronic configuration per se does not provide a tenable explanation for the observed interactions. The partial periodicity shown in Figure 48 probably reflects only the fact that some other mechanism controls the interactions and that one of the factors in such a mechanism may have a periodic basis.

2. Alloying Considerations

If purely periodic considerations are ruled out as the factors governing the solute interactions in the ternary systems, the explanation must be sought in some other property less directly related to atomic structure. We thus turn to the general field of alloying theory, solution thermodynamics and bonding between unlike atoms.

A convenient approach to solution thermodynamics is in terms of the excess properties, that is, the deviations by which the thermodynamic properties of a real solution differ from those of an ideal solution of the same relative concentration. Indeed, the excess free energy of solution is given by the expression

$$\Delta \bar{G}_{zn}^{xs} = RT \ln \gamma'_{zn}$$

Hence, the interaction parameters $\left(\frac{\partial \ln \gamma'_{zn}}{\partial x_j} \right)$, etc. merely express the relative change in the excess free energy due to solute additions.

In a recent discussion of the thermodynamics of metallic solutions, Kleppa⁽²⁵⁾ recalled from the work on the theory of alloying and binary-phase diagram studies by Hume-Rothery et al., that such systems reflect the interplay on the excess properties by at least three important factors: the electrochemical or electronegativity factor, the size factor, and the valence factor. Usually the size factor causes a positive contribution to the excess properties, a difference in electronegativities causes a negative contribution, while a difference in valence can often produce an asymmetry in the excess functions over the range of solution of i in j or j in i.

a. Electronegativities

The role of electronegativities in solution interactions as applied to Wagner's electron model has recently been discussed in detail by Sponsellor^(77,89) and Obenchain.⁽¹⁹⁾ The general basis of these discussions was to consider that electronegativities can be related to changes in the electron/atom ratio that take place in the alloying process. Wagner^(5,23) had proposed that the activity of a solute will be increased by addition of a second solute if both solutes change the electron/atom

ratio in the same direction, or decreased if the solutes change the electron/atom ratio in opposite directions.

The electronegativity itself represents the relative attraction of an atom for valence electrons in a covalent bond.^(75,76) A number of investigators^(75,78,79) have derived electronegativity values for the elements based on the relative heats of formation and dissociation for various compounds that could be formed. The electronegativity is regarded as a fundamental quantity of arbitrary and approximately known absolute value, but whose relative values express in a general way the electron affinity of an element. To some extent, the electronegativity increases with increasing valence. Thus it can be termed a measure of the effective valence. Furthermore, a change in electronegativity can be interpreted as a difference in effective valence depending on the environment the element finds itself in.

In its application to the solution of a particular element in a liquid metal solvent, the electronegativity difference can be used as a measure of the relative transfer of electrons between solute and solvent. Elements which are more metallic than the solute will give up valence electrons, while those less metallic than the solvent will gain electrons. The free electron concentration in a particular solution may thus be increased or decreased by a solute addition.

Thus far, the discussion is similar to the previously cited one of Schenck et al.⁽¹³⁾ regarding the electron capture competition between solutes and solvent. However, Sponsellor^(77,89) and later Obenchain⁽¹⁹⁾

suggested the use of the electronegativity concept, thus allowing an "effective" valence or electron affinity to be employed rather than the more limited concept of the outermost shell electrons.

Considering the chemical potential of a component in solution, Obenchain⁽¹⁹⁾ used the arguments of Wagner⁽²³⁾ and Himmler.⁽²⁴⁾ If the chemical potential is separated into that part due to the ions and that part due to the electrons, the activity of a component i in solution may be written as

$$a_i = \exp \left[\frac{1}{RT} \left(\mu_i(+ \text{ion}) + z_i \mu_e - \mu_i^0 \right) \right] \quad (29)$$

where $\mu_i^0 =$ constant at temperature T .

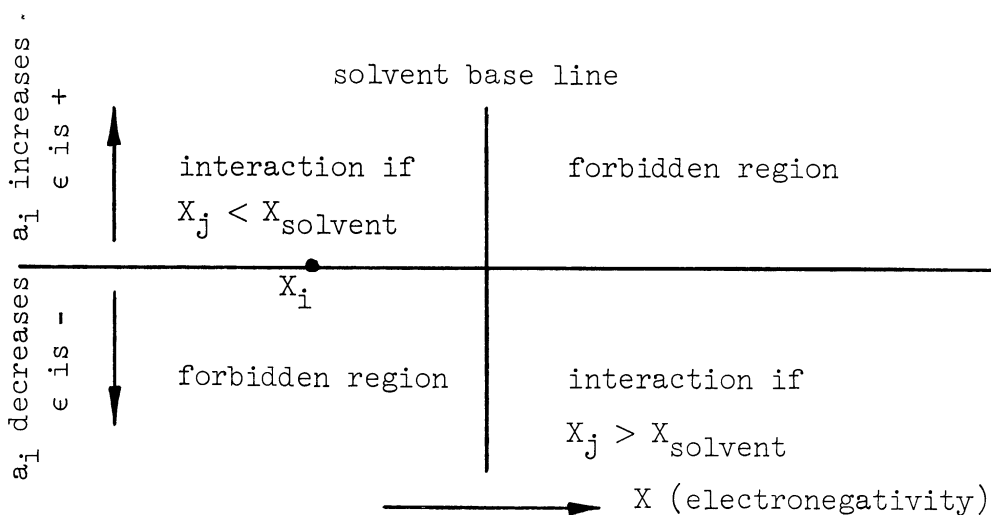
If $\mu_i(+ \text{ion})$ is taken as essentially constant, then changes in μ_e govern the activity of the constituent i , and it is assumed that μ_e increases as the ratio of free electrons to atoms is increased or decreases as the ratio is decreased. Finally, if the electronegativities are taken as a measure of the electron affinity or "effective electrons per atom", then it is possible to predict the effect of a given solute addition on the activity of constituent i . The basis for the prediction is what effect the addition of solute j has on the electron/atom ratio already established by the solution of constituent i in the solvent.

By considering the various cases to be encountered in Equation (29) for a third element addition to a given binary solution, Obenchain systematized Wagner's proposal and summarized a set of rules for predicting the sign of the interaction parameter. Without reproducing the

reasoning in detail, they are:

1. If the added solute j affects the electron/atom ratio in the same way as did solute i in the binary, then the activity is increased and the interaction effect will be positive.
2. If the added solute affects the electron/atom ratio opposite to the case of the binary, then the activity is decreased and the interaction will be negative.

The employment of electronegativities in conjunction with these rules may be clarified somewhat by referring to the diagram below:



Thus, for a solvent of given electronegativity, the position of the primary solute i fixes the manner in which the interaction parameter should behave as another solute is added. Those added solutes whose electronegativities fall to the same side of the base line as i should

(according to these rules) increase the activity of i and thus the interaction parameter should lie in the upper left (positive) quadrant of the diagram. Conversely, when the electronegativity of solute j falls on the opposite side of the base line from that of i , then the interaction parameter occupies the lower right (negative) quadrant. The other two quadrants are thus "forbidden" regions for the interaction parameters with solute i . In the case where the electronegativity of i is to the opposite side of the base line in the diagram, the roles of the quadrants are reversed. The previously "forbidden" regions then become the permissible regions and vice versa.

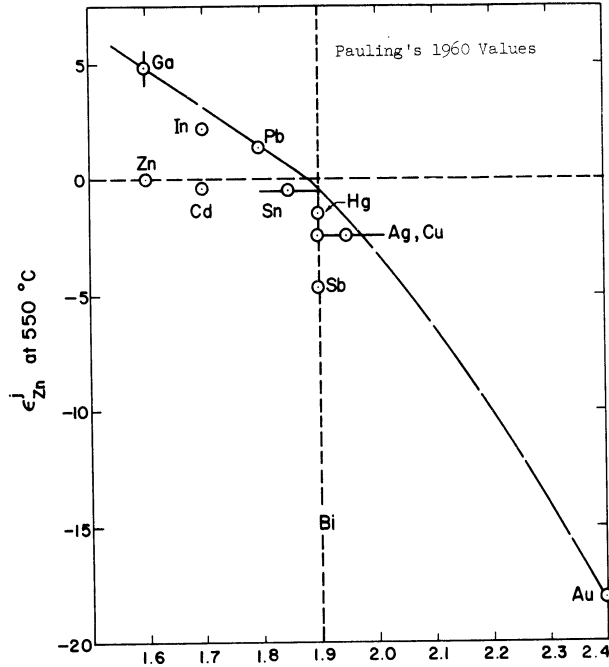
Obenchain qualitatively tested these concepts for 80 systems for which interaction parameter data were available from the literature. In slightly over 80 percent of the cases considered, the correct sign of the interaction could be predicted. Considering the assumptions involved in establishing the model and the fact that the electronegativities are known only approximately and may vary depending on the environment, the results of this approach were remarkably good. Sponcellor^(77,89) had used this method to predict the sign of third element interactions with calcium dissolved in liquid iron and was successful for three out of the four added solutes for which he had experimental data.

Using these concepts, the first-order interaction parameter results of the present investigation are presented in Figure 52 as a function of the electronegativity of the elements involved. The test was made using the electronegativity values of several authors (which

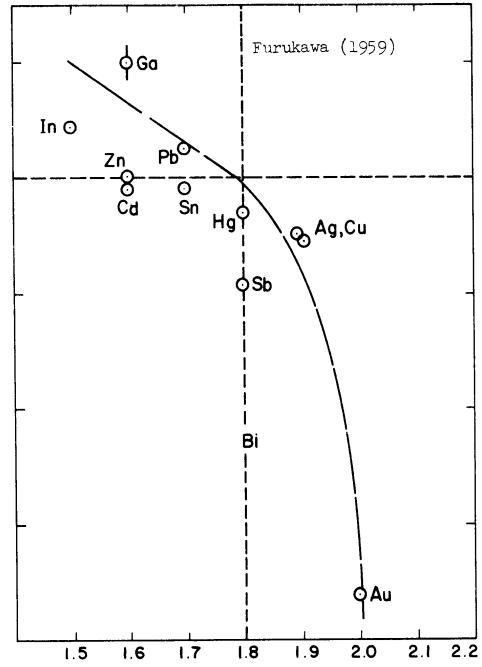
TABLE XIII

ELECTRONEGATIVITY VALUES FOR ELEMENTS INTERACTING
WITH ZINC IN BISMUTH

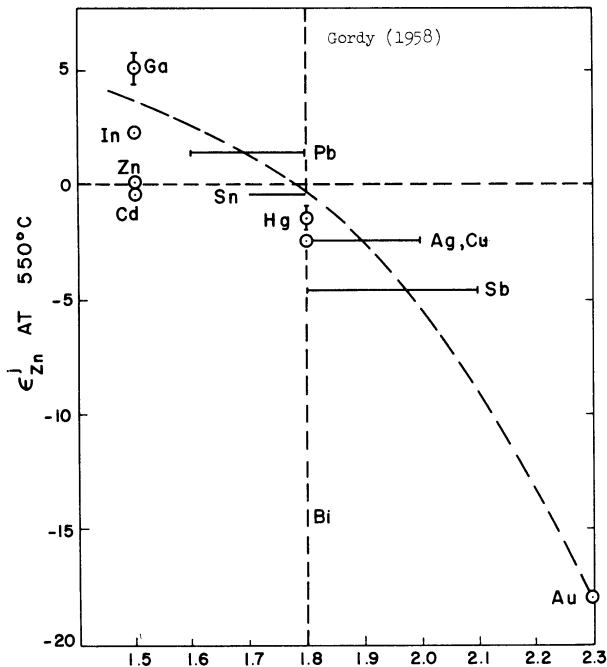
Element	<u>Electronegativity - (electron-volts/bond)^{1/2}</u>			
	Pauling ⁽⁷⁵⁾	Gordy ⁽⁷⁶⁾	Furukawa ⁽⁷⁸⁾	Allred ⁽⁷⁹⁾
Bi	1.9	1.8	1.8	2.0 ₂
Zn	1.6	1.5	1.6	1.6 ₅
Cu	1.9, 2.0	1.8, 2.0	1.9	1.9 ₀
Ga	1.6	1.5	1.6	1.8 ₁
Ag	1.9	1.8	1.9	1.9 ₃
Cd	1.7	1.5	1.6	1.6 ₈
In	1.7	1.5	1.5	1.7 ₈
Sn	1.8, 1.9	1.7, 1.8	1.7	1.9 ₆
Sb	1.9	1.8, 2.1	1.8	2.0 ₅
Au	2.4	2.3	2.0	2.5 ₄
Hg	1.9	1.8	1.8	2.0 ₀
Pb	1.8	1.6, 1.8	1.7	2.3 ₃



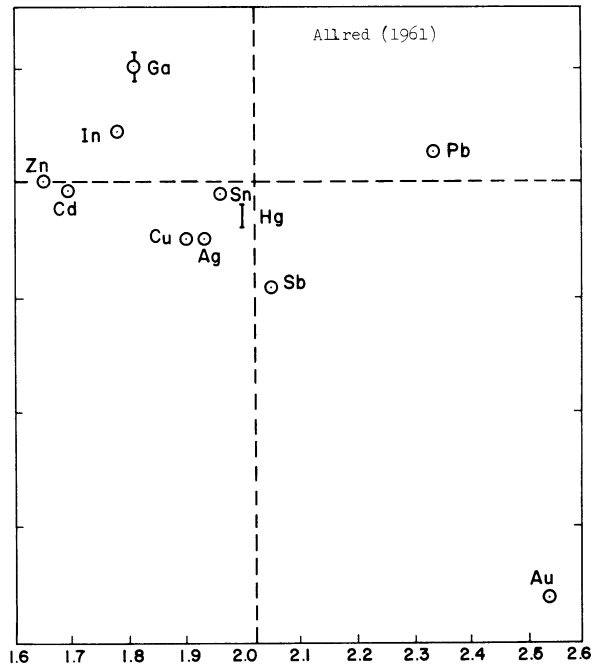
(a) ELECTRONEGATIVITY



(b) ELECTRONEGATIVITY



(c) ELECTRONEGATIVITY



(d) ELECTRONEGATIVITY

Figure 52. First-Order Interaction Parameters for Zinc-j versus Electronegativities of the Added Solute j.

are summarized in Table XIII). Since the electronegativity of zinc is less than that of the solvent bismuth, it would be expected that positive interactions would be found with elements whose electronegativities were also less than that of bismuth and vice versa for those solutes with larger electronegativities than bismuth.

If the values given by Pauling⁽⁷⁵⁾ (Figure 52a), Furukawa⁽⁷⁸⁾ (Figure 52b), and Gordy⁽⁷⁶⁾ (Figure 52c) are used, the results are generally similar. The interaction parameters for most elements fell in the permissible regions, the only clear exceptions being the cases of tin and cadmium. However, the "penetration" of the "forbidden" region was only slight. The electronegativities of mercury and antimony were close enough to that of bismuth so that some ambiguity existed as to what the prediction should have been. When Allred's values were used⁽⁷⁹⁾ (Figure 52d), the interaction parameters for lead, copper, silver, and mercury fell in the "forbidden" regions, but the parameter for antimony was clearly in a permissible region.

The success of the electronegativity model for interaction prediction is summarized below:

	<u>Electronegativity Scale Used</u>			
	<u>Pauling</u>	<u>Furukawa</u>	<u>Gordy</u>	<u>Allred</u>
Total Third Elements	10	10	10	10
Number of Unambiguous Predictions Possible	7	8	8	10
Number of Correct Predictions	5	6	6	4
Percentage of Success	71%	75%	75%	40%

Disregarding the results obtained using Allred's electronegativities, the percentage of successful predictions compares favorably with that of Obenchain who used Pauling's and Furukawa's values primarily.

Figures 52a, b, and c also indicate that there is some quantitative basis to the electronegativity prediction model. The interaction parameters for those elements where a successful prediction can be made as to the sign of the interaction also tend to lie on a single line which passes through a value of zero interaction at the electronegativity of the bismuth solvent.

The apparent quantitative nature of the result is quite interesting, however, additional data would be desirable on other systems before it could be termed conclusive. However, it does appear that a considerable number of the observed interactions can be accounted for on the basis of electronegativity difference, and furthermore, that the greater the difference, the greater the numerical value of the interaction parameter. Before an unequivocal interpretation could be placed on the "correlation", some theoretical explanation would have to be found for the slope or shape of the line, and for the penetration, even though slight, of the interaction parameters for tin and cadmium into the "forbidden" regions.

b. Size Factors

If electronegativities do not completely account for the observed interactions it would be logical, continuing the analysis summarized by Kleppa,⁽²⁵⁾ to consider size factors - either alone or as moderating the electronegativities.

It was noted by Kleppa that differences in atomic size should give rise to positive contributions to excess properties. Accordingly, the experimental values for first-order interaction parameters with zinc in bismuth were studied with respect to a number of size-related factors. The quantities used were the Goldschmidt atomic radius, the atomic volume, and the ionic radii of Pauling and Goldschmidt.⁽⁷⁶⁾ The attempted correlations are shown in Figures 53 through 55. The results were completely negative. There appeared to be no regularity to the interaction parameters when size factors alone were considered. Attempts to group the size-factor plots by Periodic Table considerations were also unsuccessful.

In a discussion of the influence of chemical factors on the extent of primary solid solubility, Darken and Gurry⁽⁷⁶⁾ used a plot of the atomic radius versus the electronegativity. In general, elements which had appreciable solid solubility in a given solvent tended to be found in an ellipse of maximum width ± 15 percent of the value of the atomic radius and a height of $\pm .4$ electronegativity units. Waber et al.⁽⁸⁷⁾ later used this method to study solid solubilities in 1455 binary metallic combinations with about 77 percent reliability.

Since a plot of this type appeared to be useful for simultaneous consideration of size and electronegativity effects in alloying, the elements used in the present interaction investigation were plotted in this manner. It was noted (Figure 56) that if a line were drawn between the coordinate points for zinc and bismuth, the elements lying to the right of the line were positive interactors and those lying to the left

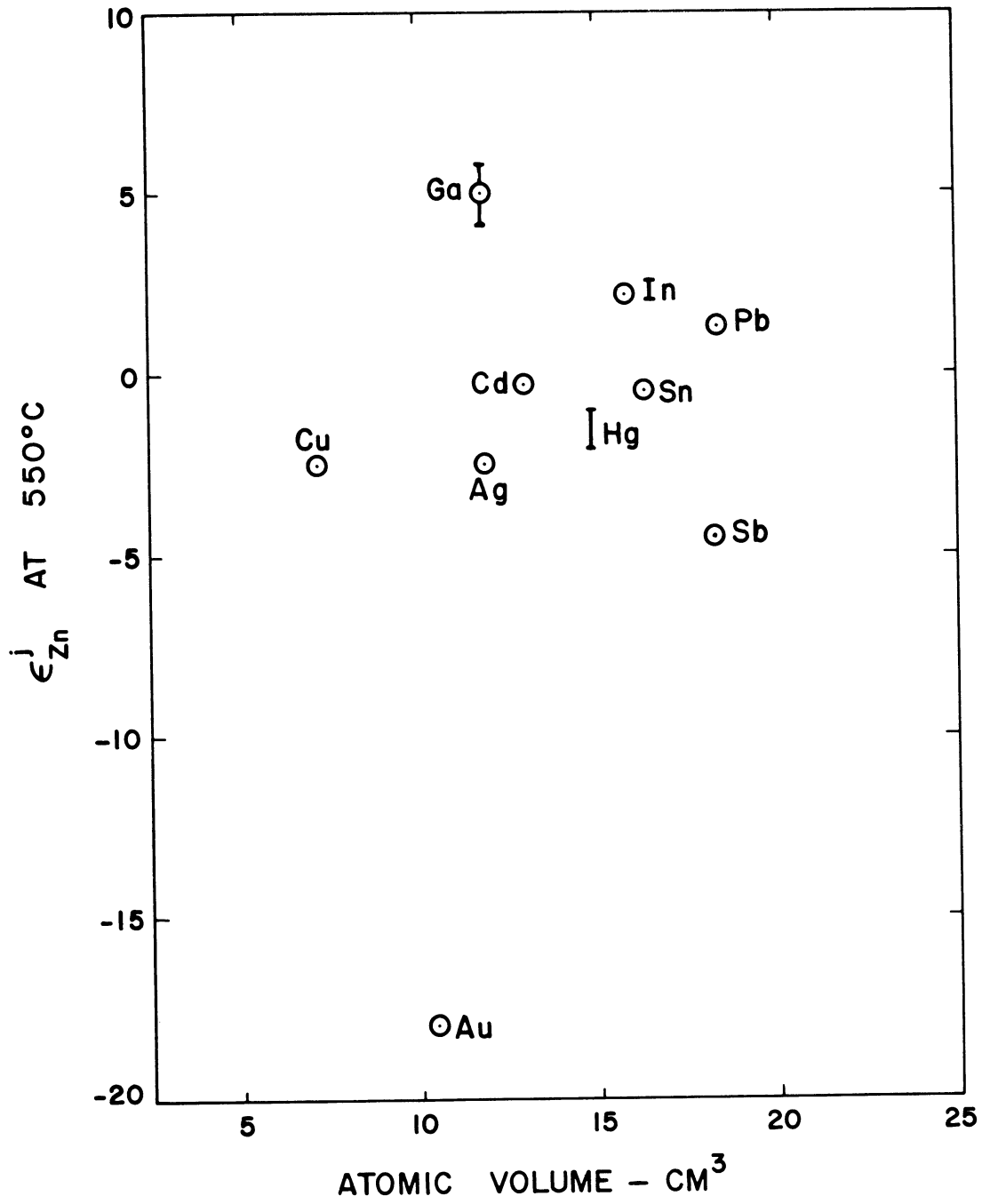


Figure 53. First-Order Zinc-j Interaction Parameters versus Atomic Volume of Added Solute j.

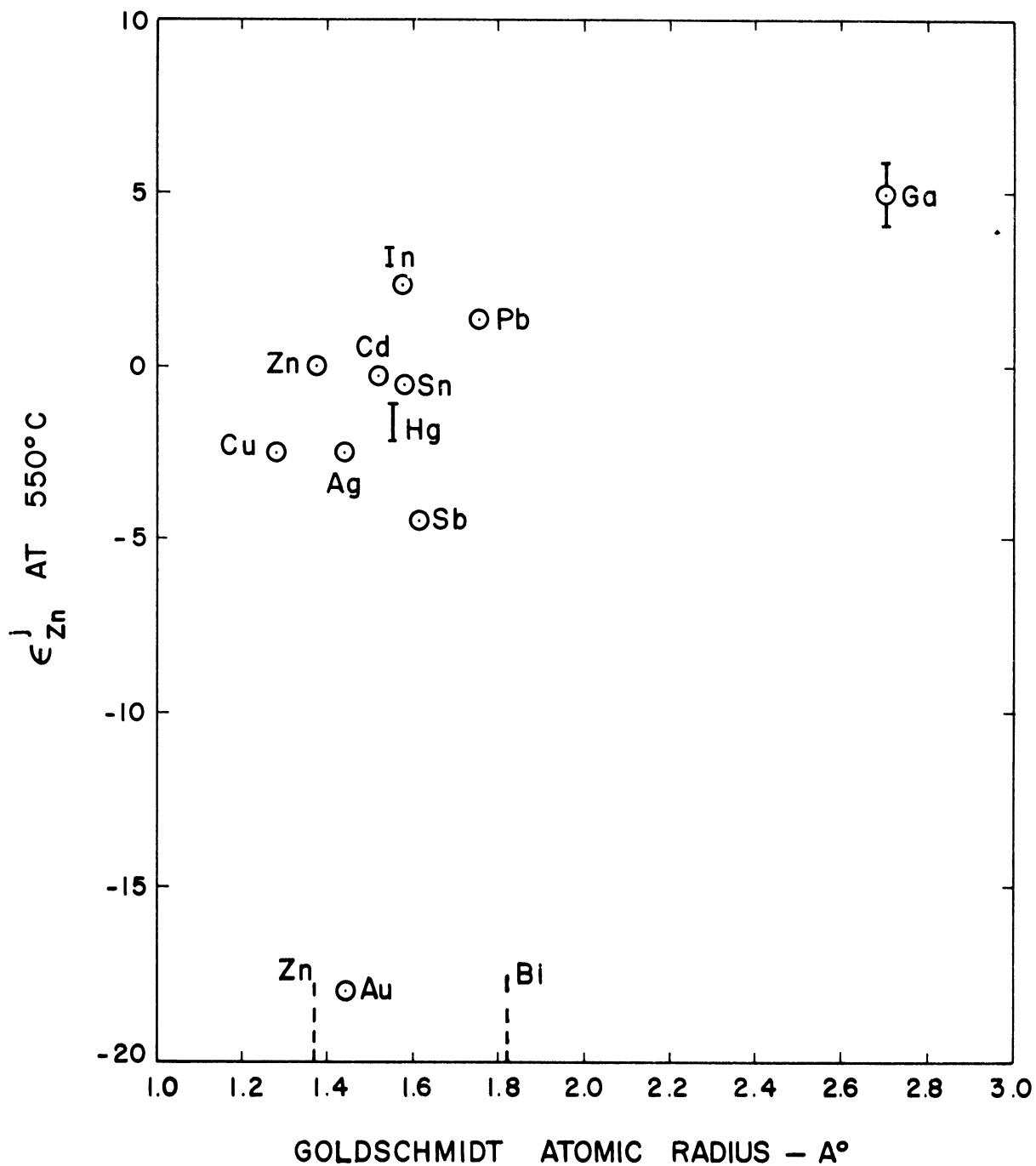


Figure 54. First-Order Zinc-j Interaction Parameters versus Atomic Radius of Added Solute j.

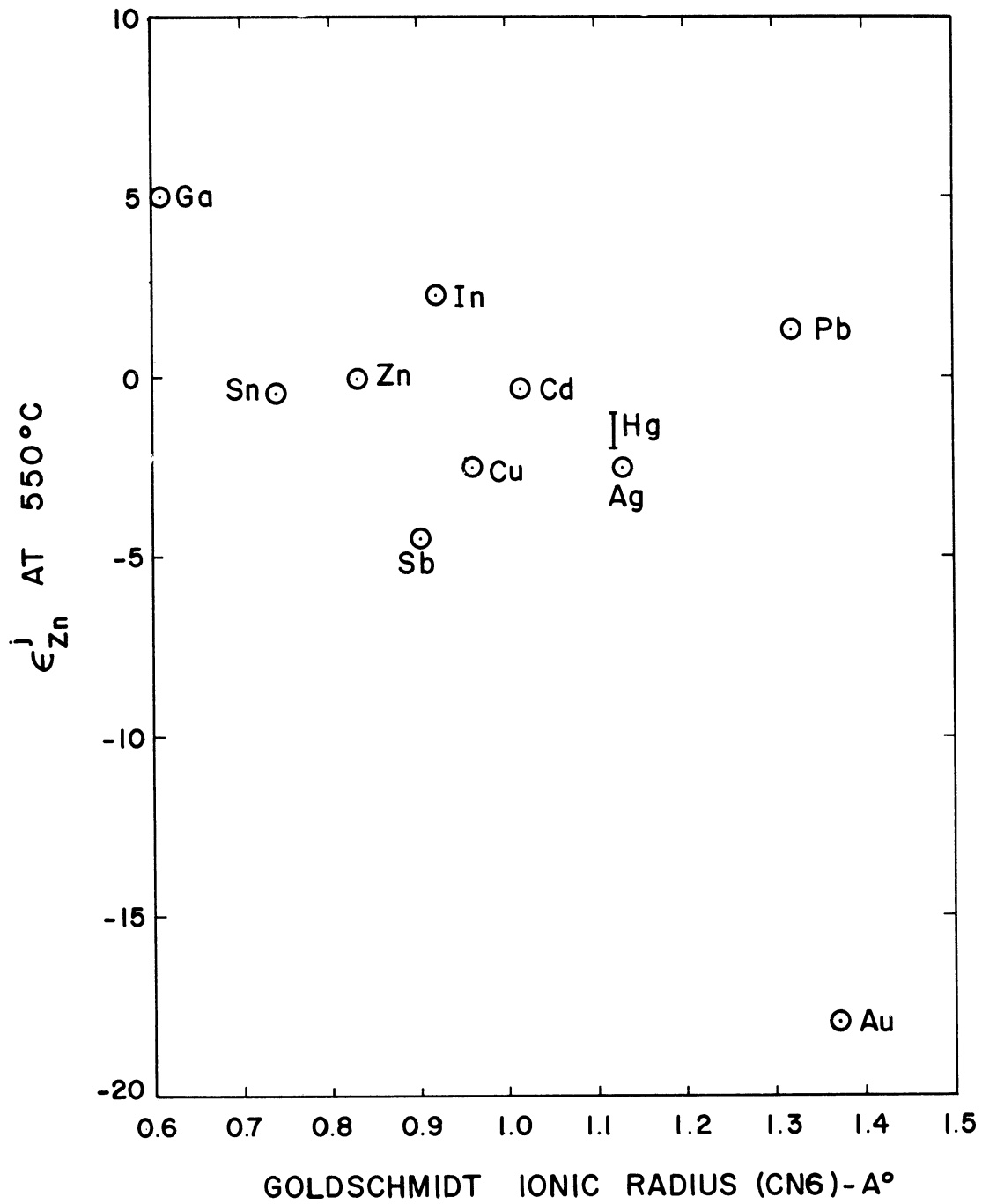


Figure 55. First-Order Zinc-j Interaction Parameters versus Ionic Radius of Added Solute j.

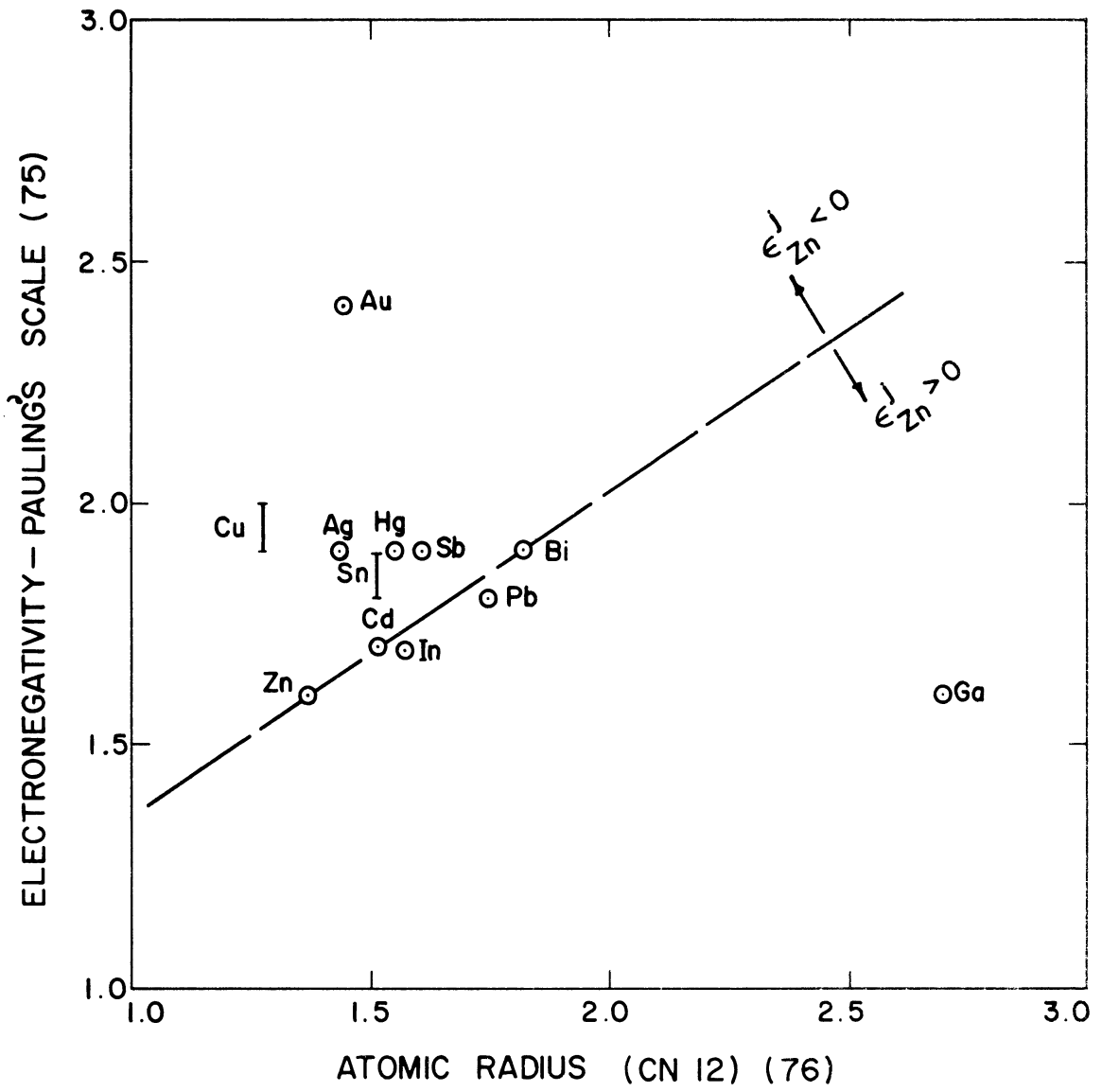


Figure 56. Darken-Gurry Plot of Atomic Radius and Electronegativity for Zinc, Bismuth, and Added Solutes.

of the line were negative interactors. In addition, the distance of each solute element from such a base line was roughly proportional to the numerical value of its interaction parameter with zinc in bismuth. In general, therefore, negative interactions were associated with large values of electronegativities and small atomic radii, while positive interactors were associated with an increase in the atomic radius. These observations are consistent with Kleppa's comments (p. 177). The "correlation" shown in Figure 56 depends on the values used for the electronegativities - best results were obtained with Pauling's values. The results are interesting but hardly conclusive.

A variation of this approach was then attempted on a basis that would combine both the electronegativity and the size factor. The method used was to divide the electronegativity for each element by a size factor. When atomic volume is used, the quotient is an "electronegativity per molar unit volume", while when the ionic radii or atomic radii are used, the quotient is a "hybrid" term that could be also considered as a measure of charge density or electron affinity density. Plots using these factors are shown in Figure 57. The only attempt that showed any promise was the plot of interaction parameter versus the quotient: electronegativity/atomic radius. The trend of results is similar to the plot versus electronegativity alone (Figure 52). However, an attempt to apply the prediction rules of page 180 to this plot did not succeed. Since zinc lies to the right of bismuth on the plot, the permissible regions would be expected to be the upper right and lower left quadrants. In Figure 57 only indium thus lies in the proper quadrant.

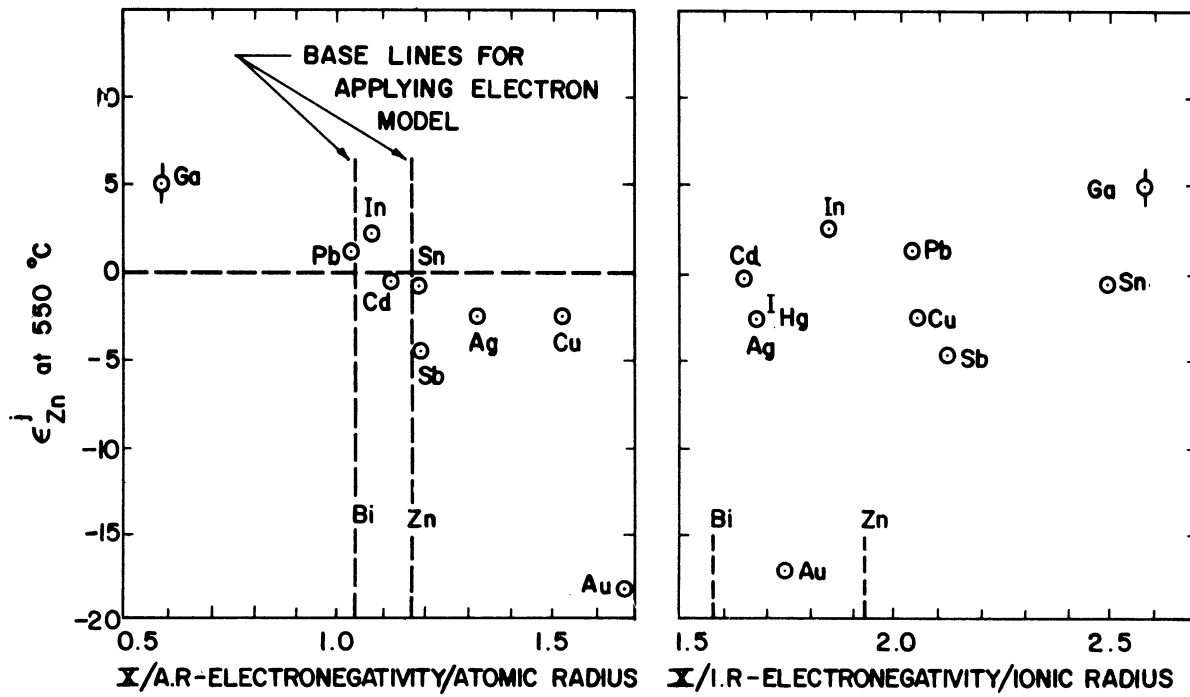
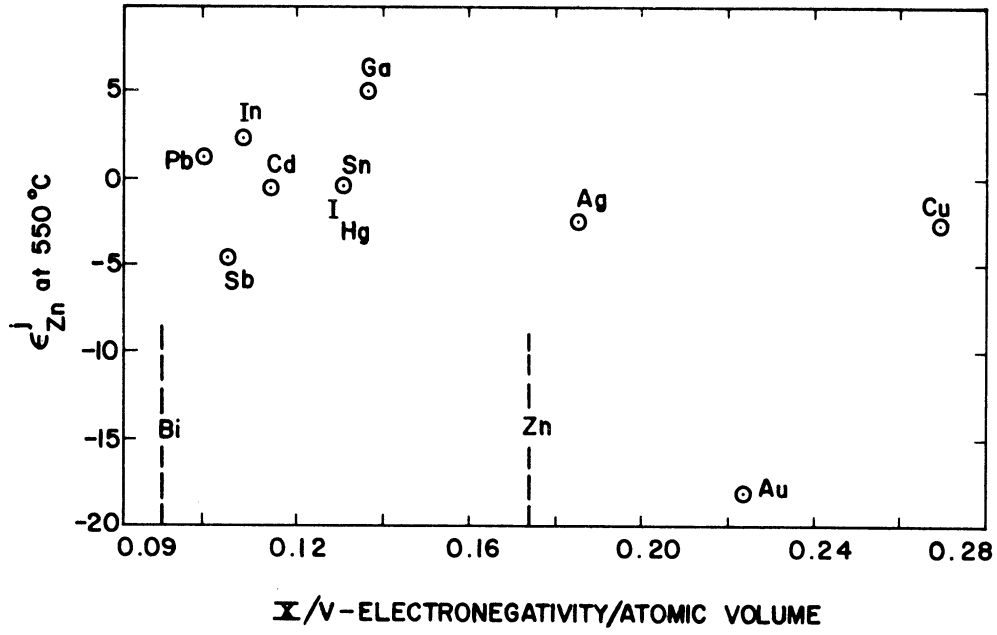


Figure 57. Electronegativity-Size Factor Correlation Attempts for First-Order Zinc-j Interaction Parameters.

However, if the plot is considered on the basis that the effect of a given third element rests in the difference in the "hybrid" or density factor from that of zinc, then three of the four elements lying to the left of the value for zinc (lower values of the hybrid factor) produce positive interactions, while all of the elements to the right of zinc produce negative interactions. Thus, the deviation can be removed for tin that occurred where the rules were applied to the plots of ϵ_{Zn}^j versus electronegativity alone. However, cadmium still remains anomalous. Furthermore, there is no theoretical justification for this correlation or why the atomic radius is the proper size factor to use. While an effective volume could be calculated from the atomic radius, the result would only be to spread the abscissa of the plot and would not change the relative position of the parameters. In effect, this interpretation calls for a reversal of the previous rule; implying that those elements with "hybrid" factor to the same side of the solute zinc as the solvent bismuth produce the positive interactions, while elements to the other side produce the negative interactions. The apparent correlation shown in Figure 57 must thus be considered primarily empirical, of questionable theoretical justification, and perhaps only coincidental. However, the value of the attempts at correlation by direct or semi-direct application of size factor is to show that if size effects enter into the interactions, their influence is secondary to the electronegativity effects.

Finally, in considering "hybrid" or energy density effects on interactions, it was noted that the solubility parameter of Hildebrand⁽³³⁾

also expresses such a quantity. The solubility parameter is the square root of the energy of vaporization or sublimation per unit volume, and is described by Hildebrand as a measure of "internal pressure." While this concept will be used later in considering the applicability of regular solution theory to the prediction of interaction parameters (p.220), it should be mentioned at this point in conjunction with the correlation attempts. A plot of the first-order interaction parameters versus the solubility parameter is presented in Figure 58. There is no correlation in this plot and furthermore, as will be shown later, only half of the interaction parameters have the correct algebraic sign that would be predicted by regular solution theory.

It would appear that the direct moderation of energy factors by size-factors does not lead to a reasonable explanation of the interactions for the systems studied, however, size effects undoubtedly play a part.

3. Thermodynamic Factors

With the inability of usual alloying concepts of electronegativity and size difference to completely account for the observed interactions, attention was directed to qualitative and possibly quantitative thermodynamic considerations. The approach used was primarily phenomenological and began with consideration of the zinc-bismuth binary system itself. Strong positive deviations from ideal solution behavior characterize liquid alloys of zinc plus bismuth. The activity coefficient of zinc in the dilute region is about three and there is a region of liquid

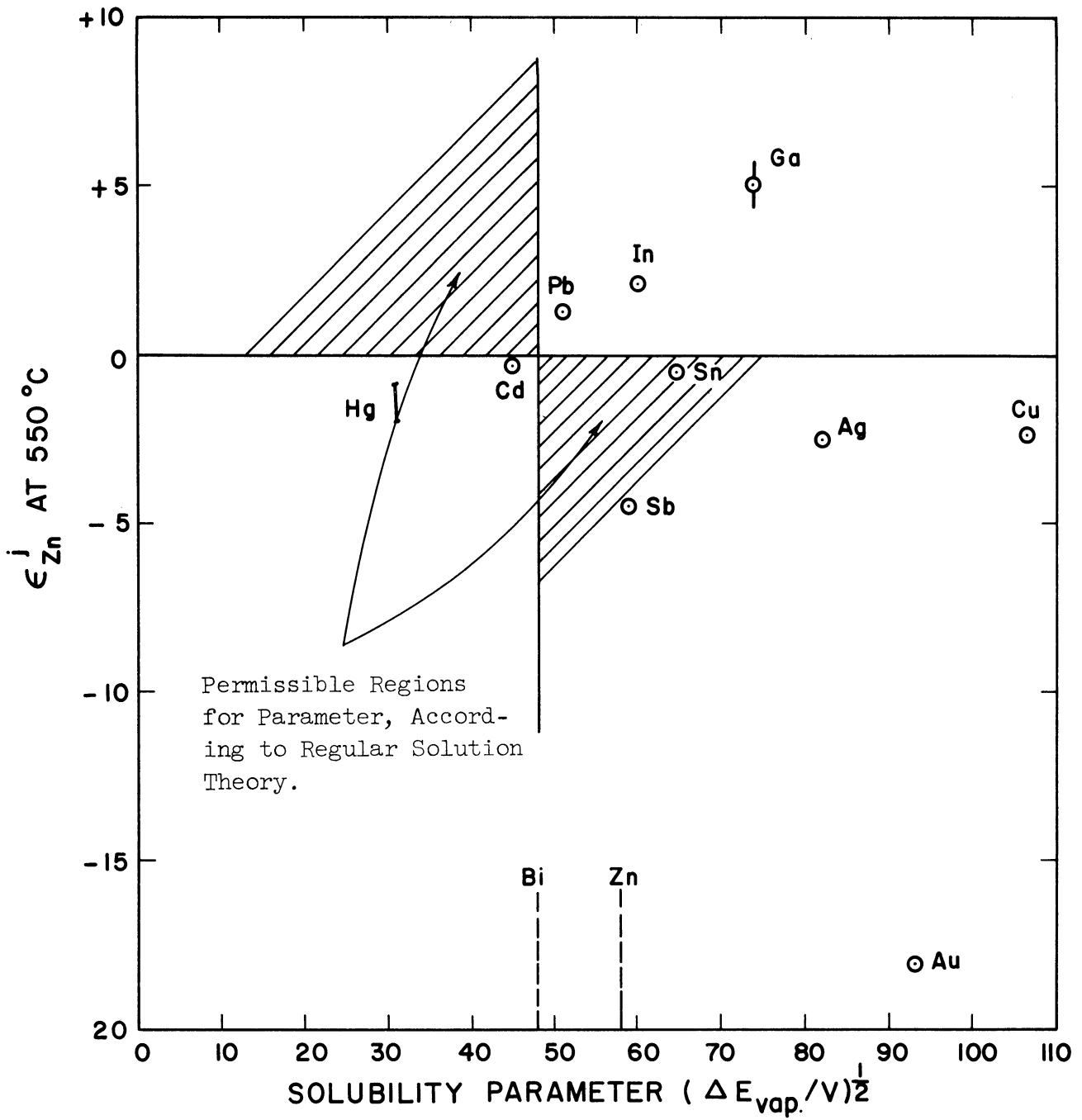


Figure 58. First-Order Zinc-j Interaction Parameters versus Solubility Parameter of Added Solute j.

immiscibility at higher zinc concentrations. Zinc and bismuth are only slightly, if at all, soluble in each other in the solid state.

Kubaschewski and Catterall⁽⁵³⁾ attributed positive excess entropies of mixing in the zinc-bismuth system to the destruction of covalent bonds. Kleppa⁽⁴⁵⁾ showed that the partial molal heat of mixing of zinc could be represented by an equation of the type $\Delta\bar{H}_{\text{Zn}} = \phi_{\text{Bi}}^2 \Delta\bar{H}_{\text{Zn}\infty}$, where $\Delta\bar{H}_{\text{Zn}\infty}$ is the relative partial molal heat content of zinc at high dilution and ϕ is the volume fraction of bismuth. This showed that the atomic sizes of zinc and bismuth, which differ by a factor of 2.1 (volume ratio) have a bearing on the number of bonds formed between them.

All of these observations are consistent with a liquid state where the mixing of zinc and bismuth is non-random. Therefore, it might be expected that when a solute is added that would tend to alloy with or form a miscible solution with zinc, the activity of the zinc would tend to decrease, since effectively the bismuth would "see" less zinc. Conversely, a solute that by itself would tend towards immiscibility with zinc might effectively increase the activity of zinc relative to bismuth.

Accordingly, an attempt was made to classify the experimental results by the type of solution formed by zinc plus the solute j . Table XIV qualitatively summarizes the solution behavior and also presents activity coefficient and excess free energy of mixing for zinc dissolved in an equi-molar solution of zinc with j . The data used were taken from Hultgren.⁽⁵⁴⁾

TABLE XIV
FACTORS FOR THERMODYNAMIC EVALUATION OF
ZINC-J BINARY SYSTEMS

Solute-j	Type of Solution Formed in Binary Alloy (deviation from ideality)		Calculated Activity Coefficient** and Excess Free Energy at 550°C
	Zinc + j	j + Bi	
Cu	neg*	pos	γ_{Zn} in Zn + j at $x_{Zn} = .5$ ΔG_{Zn}^{xs} in Zn + j at $x_{Zn} = .5$ (kcal/g atom)
Zn	-	pos	.37 -1610
Ga	pos*	?	- -
Ag	neg*	pos	1.14 +215
Cd	pos	neg	.88 -350
In	pos*	neg	1.40 +550
Sn	pos	pos	1.46 +625
Sb	neg*	?	1.33 +460
Au	neg*	neg	.54 -1000
Hg	pos	neg	.04 -5300
Pb	pos*	neg	1.20 +300
			2.53 +1530

* Direction of deviation from ideality consistent with sign of interaction parameter between Zn and j in Bi.

** Data from Hultgren et al. (54)

Considering only the type of solution formed by zinc in j , the expectation is that those elements forming a binary negative-deviating solution with zinc would also tend to produce negative interaction parameters with zinc in ternary solution with bismuth. Thus, the activity of zinc in solutions with copper, silver, antimony, or gold has a negative deviation from Raoult's Law (and there are many compounds formed in the solid alloys of these binaries). Negative interactions with zinc occurred in the ternary solutions formed by these metals in bismuth. Conversely, gallium, indium, and lead are positive interactors with zinc in bismuth, and the zinc activity in binary alloys with these metals exhibits a positive deviation from ideality. There is little tendency for solid solubility or compound formation in these binary systems. However, three of the solute elements, cadmium, tin, and mercury were slight negative interactors with zinc in bismuth yet the activity coefficient of zinc in binary alloys with these metals is greater than one, a positive deviation from ideality. The simple qualitative explanation based on the character of the solute binary systems is thus valid for seven of the ten cases considered. An attempt was made to extend the qualitative analysis to include the relative ideality of the solute j in bismuth (or the converse) but examination of the j -Bi solution behavior (Table XIV) failed to reveal any regularity that could be correlated with the interaction parameters.

The success of this explanation was about as good as obtained using Wagner's electron model in conjunction with electronegativities. Where the interactions were large, the effect was successfully predicted.

The unexplained elements were the same for both models. The slight cadmium and tin effects could not be explained with either model, while mercury's electronegativity was the same as bismuth, rendering that prediction ambiguous. Therefore, the same factors involved in the binary zinc-j interactions probably entered into the electronegativity model.

Considering the 70 percent qualitative success of the explanation, calculations were made to see if any quantitative basis existed. The premise was that the interaction between zinc and the solute j , in a ternary solution were both approach infinite dilution, might be governed by the excess free energy of mixing in a binary alloy of 50 mole percent zinc in j . The data in Hultgren⁽⁵⁴⁾ for $\Delta\bar{G}_{Zn}^{XS}$ were extrapolated to 550°C under the assumption that the heat of mixing remained essentially constant. The results are summarized in Table XIV and plotted in Figure 59 versus the interaction parameter.

The results show that there is a definite quantitative basis to the effect. Furthermore, and perhaps coincidentally, the results can be grouped by the position in the Periodic Table of the elements involved. In general, the less negative the $\Delta\bar{G}_{Zn}^{XS}$ in the binary zinc-j, the more positive the interaction in a ternary solution with bismuth. However, it will be noted that the exceptions to the qualitative rule, the slight negative interactions for cadmium, tin, and mercury, appear in the wrong quadrant of the quantitative diagram, and furthermore, while the 4th and 6th period elements appeared in order of atomic number going from left to right on the plot, the 5th period elements were not in order.

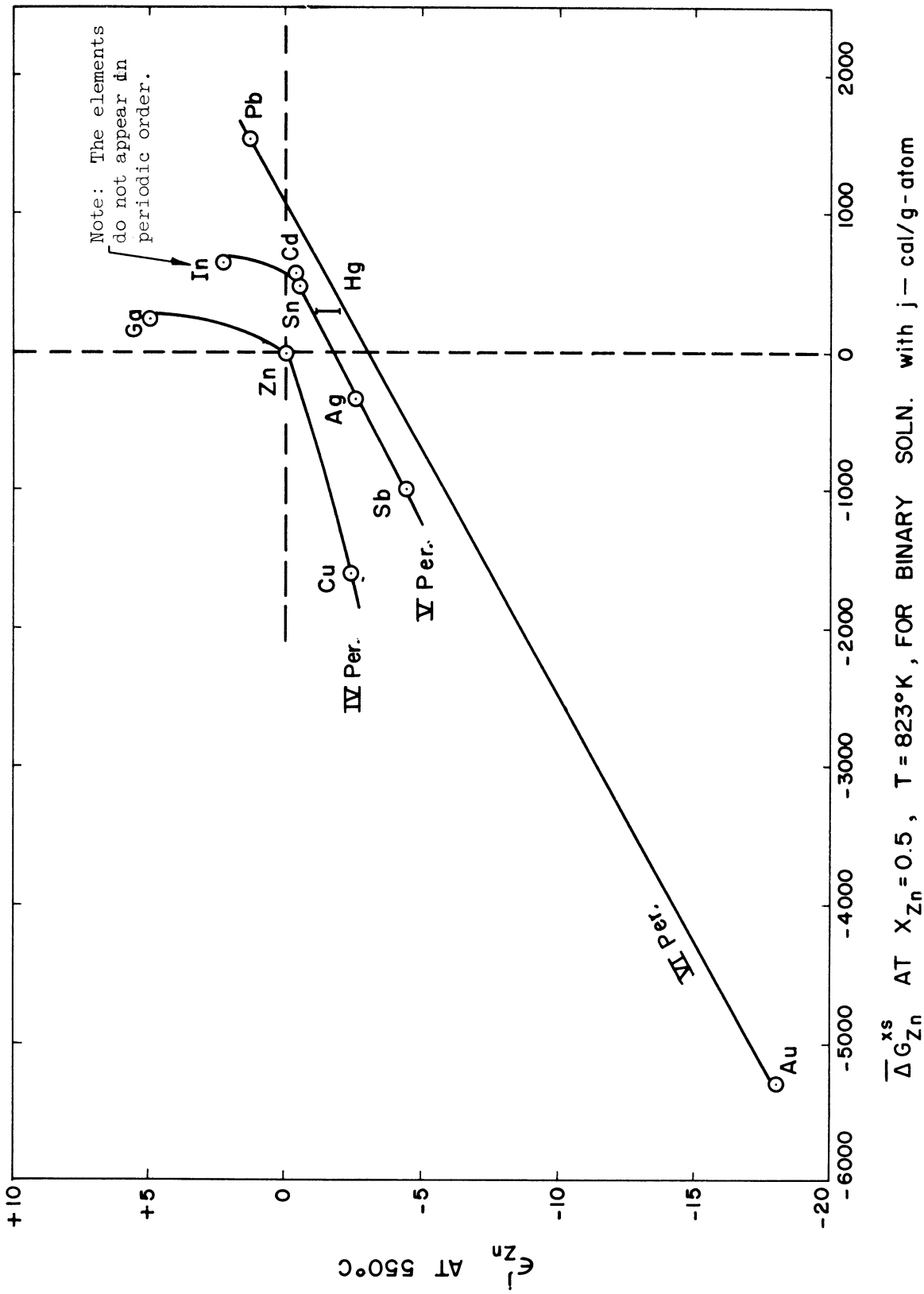


Figure 59. First-Order Zinc-j Interaction Parameters versus Excess Partial Molal Free Energy of Mixing of Zinc for Equimolar Mixture of Zinc and j.

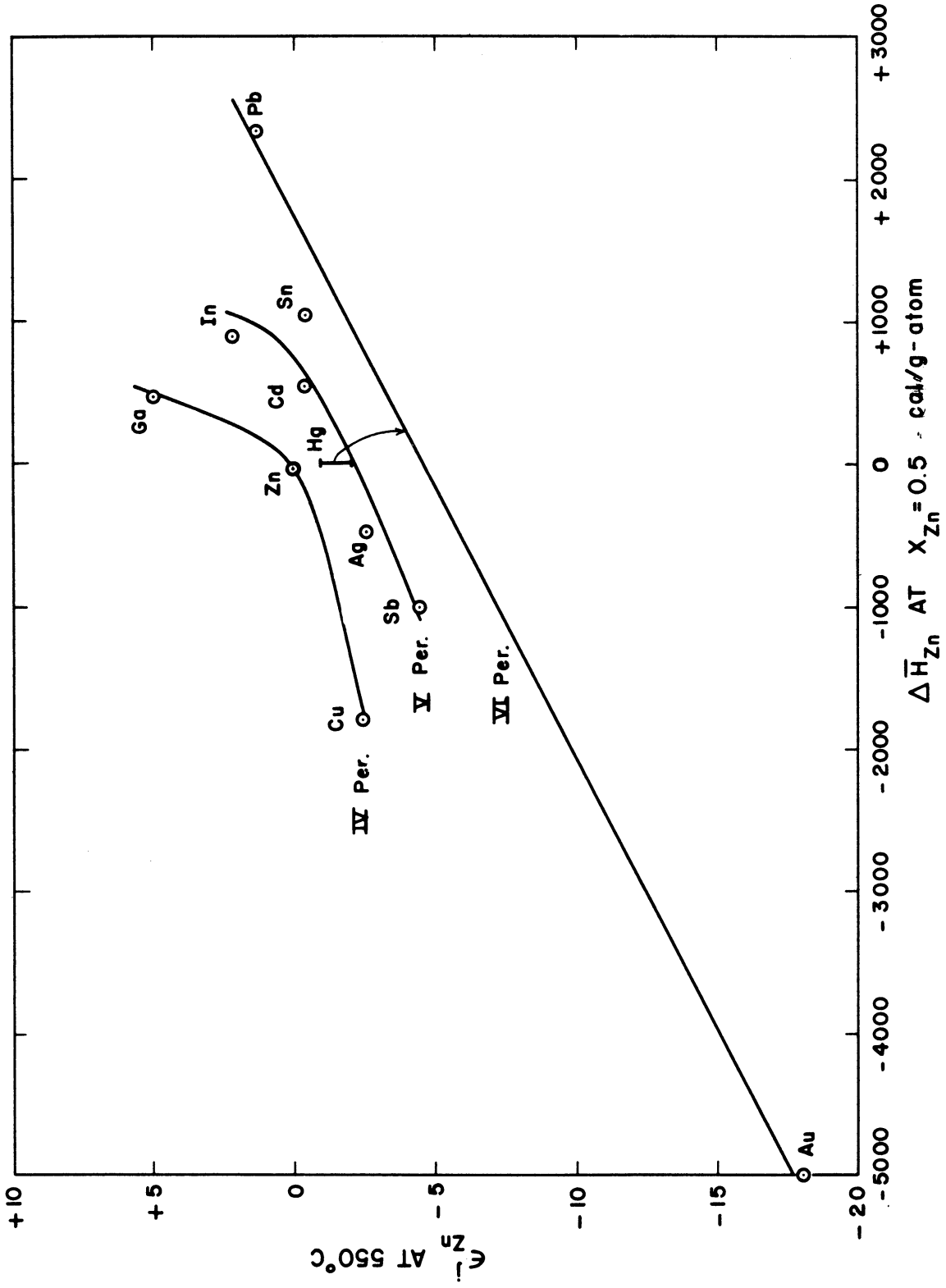


Figure 60. First-Order Zinc-j Interaction Parameters versus Partial Molal Heat of Mixing of Zinc in Equimolar Mixture of Zinc and j .

Since the assumption of constant heat of mixing was involved in the extrapolations of $\Delta\bar{G}_{Zn}^{XS}$ used in Figure 59, a similar plot of interaction parameter versus $\Delta\bar{H}_{Zn}$ was made. Figure 60 shows that the general form of the plots of ϵ_{Zn}^j versus $\Delta\bar{H}_{Zn}$ or $\Delta\bar{G}_{Zn}^{XS}$ was the same, however, there is a bit more scatter in the plot involving $\Delta\bar{H}_{Zn}$. Therefore the entropy term involved in $\Delta\bar{G}_{Zn}^{XS}$ contributes to the interaction effect. Since the entropy can be divided into the configurational and vibrational contributions, it is probable that, despite the undetermined nature of the size effect, it is the configurational entropy term that accounts for the smoother curves of Figure 59 as compared to Figure 60. The comments regarding size difference effects on bonding energy made by Kleppa⁽⁴⁵⁾ and Kubaschewski and Catterall⁽⁵³⁾ (cited on page 196) support this conclusion.

An attempt was made to relate the data of Figure 59 by subgroup in the Periodic Table but no regularity of behavior could be discerned.

The results of these correlation attempts showed that most of the observed first-order interaction in the ternary alloys could be accounted for on the basis of binary interactions between the solutes. However, the slight interactions due to tin, cadmium, or mercury additions did not fit any of the simple explanations.

4. Other Physical or Chemical Factors

In addition to the properties previously discussed, there are other physical or chemical properties that might be used to correlate the interaction effects. Where these properties may be within themselves

periodic in behavior, the result of the correlation will be only as good as the attempt shown in Figure 48 for a direct relationship with atomic number. For instance, Batsanov⁽⁸⁰⁾ recently derived a system of electronegativities based on geometric considerations. Covalent, metallic, and geometric electronegativities were given, however, the values are all periodic with atomic number and no meaningful correlation could be made with the observed interaction parameters.

As another example of a possible correlating factor, Figure 61 shows a plot of the first-order interaction parameters versus either the first or second ionization potentials of the solute elements.⁽⁸¹⁾ Turkdogan⁽¹⁰⁾ had previously shown that third element effects on the solubility of carbon in iron (which can be related to the interaction parameter) exhibited some linearity with the second ionization potential. The present results show no correlation with the second ionization potential and only a dubious relation with the first ionization potential. Sponsellor^(77,89) attempted to use the first ionization potential in the same way that electronegativities were used in the application of Wagner's electron model (p.180). His prediction of the sign of the interaction parameter for third element additions to calcium dissolved in liquid iron was correct in only two of four cases.

Another physical quantity giving a rough measure of how readily an element gives up electrons is the work function. Sponsellor also applied the photo-electric work function to his data mentioned above and was correct in predicting the algebraic sign of the interaction for three

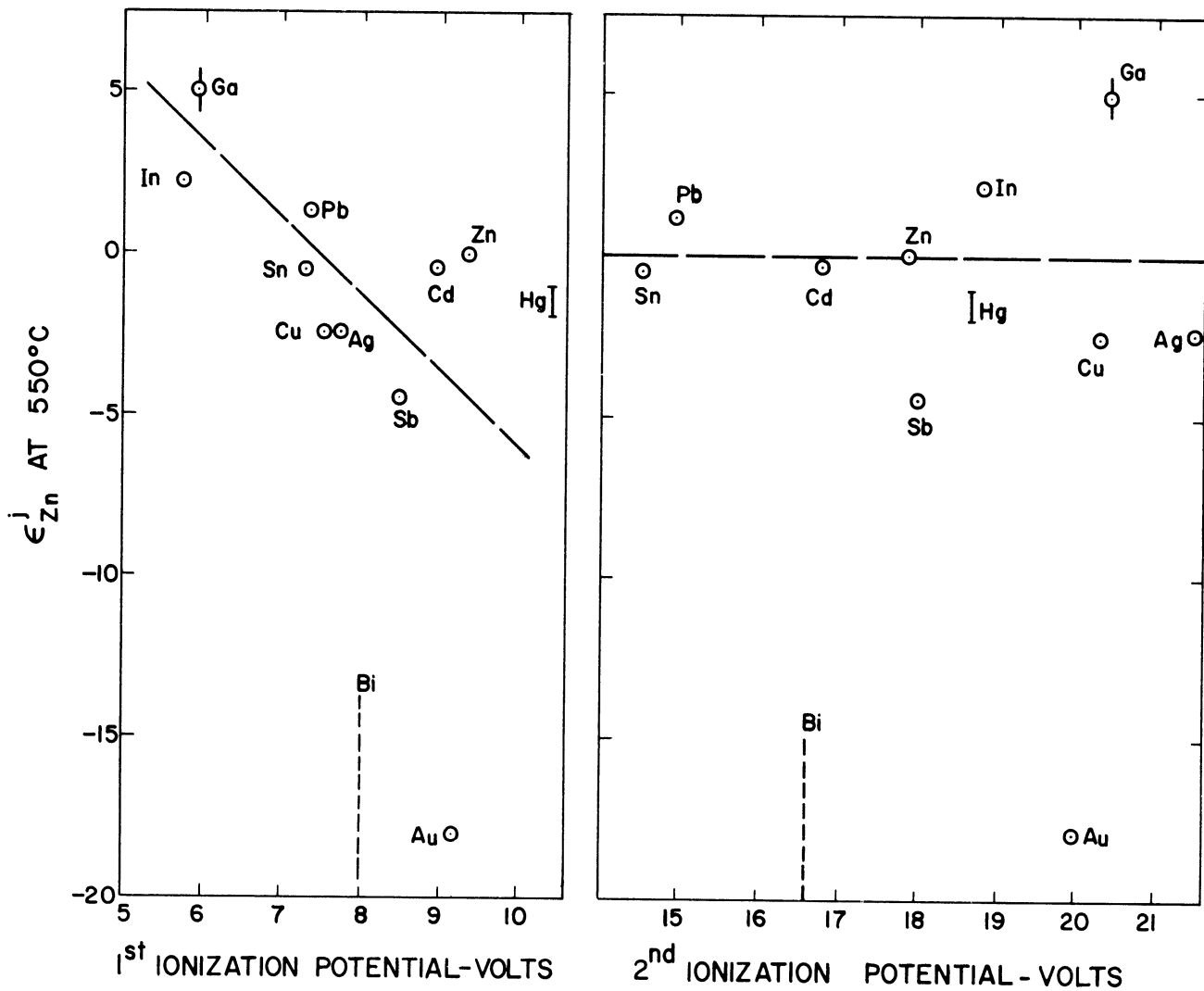


Figure 61. First-Order Zinc-j Interaction Parameters versus First and Second Ionization Potentials of Bismuth, Zinc, and Added Solutes j.

out of the four cases considered. The present results were tested against the work function, but the range of values given for the photoelectric work function⁽⁸¹⁾ made meaningful predictions impossible. However, using average values of work function determined by a contact potential method,⁽⁸¹⁾ the algebraic sign of the interaction was predicted correctly for eight out of nine solutes for which data were available, assuming that the value for zinc is less than for bismuth. A plot of the results of this correlation attempt is shown in Figure 62. The only element clearly falling in a "forbidden" region is antimony but the degree of penetration is slight. In addition, there is a fair quantitative relation between work function and the interaction parameter. The correlation thus accounts for the interaction parameters of tin and cadmium, but at the expense of losing agreement for antimony.

As another example, one might directly consider the relative chemical reactivity of the various solute elements. A correlation could be attempted using an electromotive force series or the free energy of formation for a series of similar compounds. Figure 63 shows such a relation in terms of the free energy of formation for chlorides.⁽⁶²⁾ The results appear to fit a two-branch curve which has its discontinuity at the free energy of formation of zinc chloride. However, Figure 63 is purely empirical since there is no basis for drawing a two-branch curve other than the fact that the three positive interactors and the seven negative interactors may be classified in this manner. The extent of the interaction, as might be expected, depends on the relative difference in

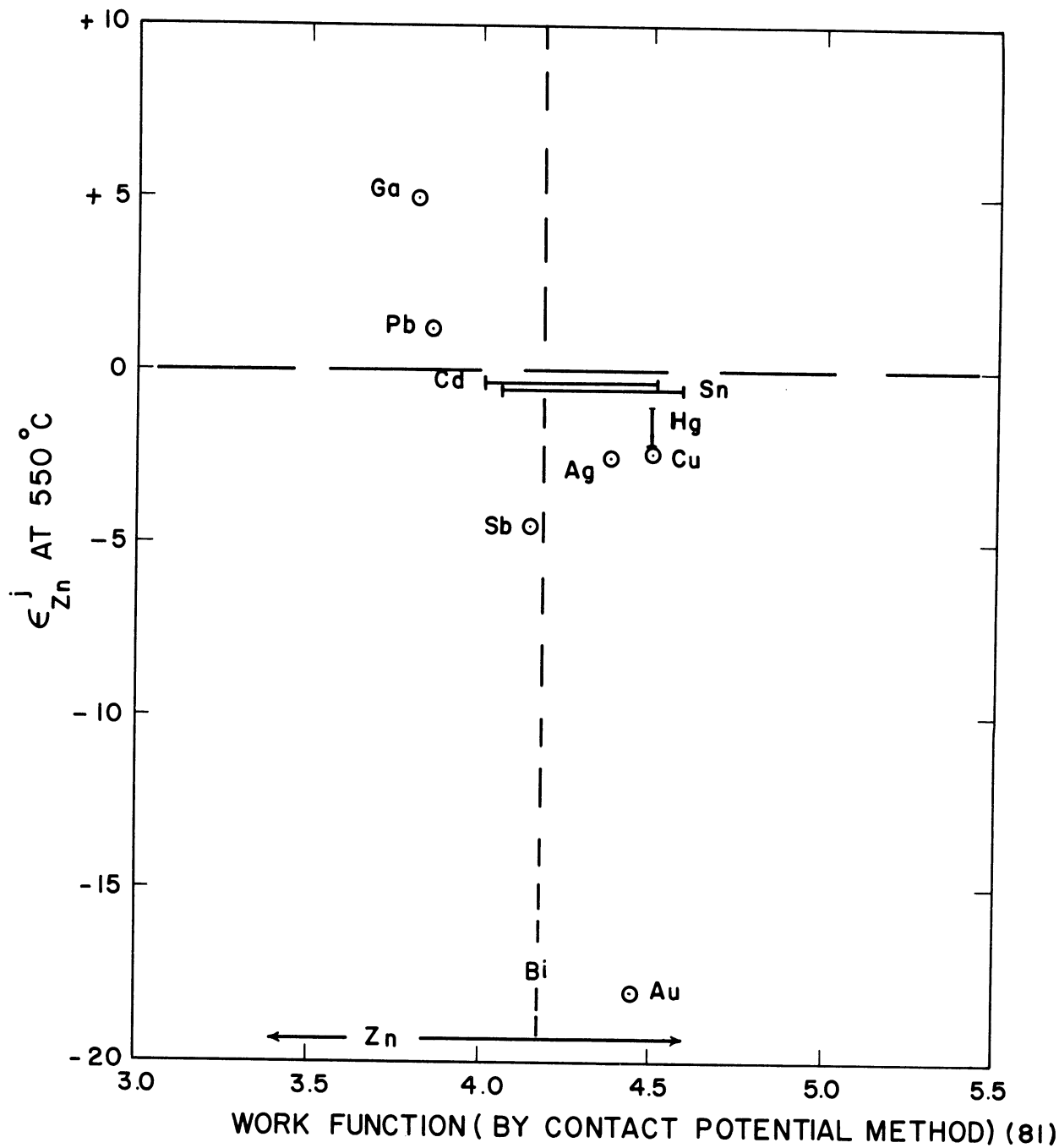


Figure 62. First-Order Zinc-j Interaction Parameters versus Work Function for Bismuth, Zinc, and Added Solutes j.

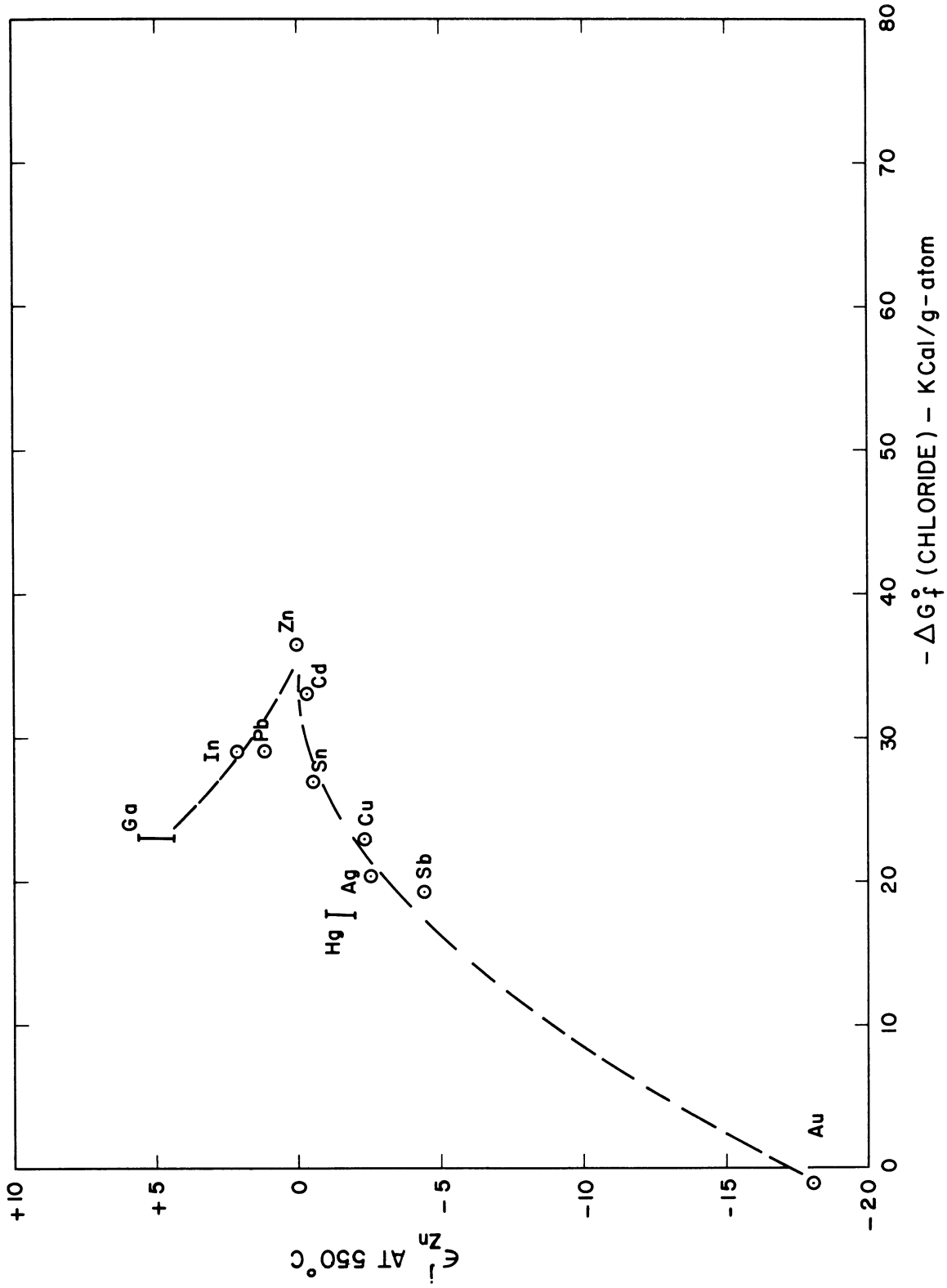


Figure 63. First-Order Zinc-j Interaction Parameters versus Standard Free Energy of Formation of Chlorides at 550°C.

ΔG_f° , much as the previous explanations based on electronegativities or $\Delta \bar{G}_{Zn}^{XS}$ for the binary systems formed by the solutes, however, the shape of the relation drawn in Figure 63 has no readily apparent theoretical basis. Weinstein and Elliott⁽⁸⁷⁾ attempted a correlation between the effective number of free electrons of the added solute and the interactions with hydrogen in liquid iron. Their correlation was only fair but there was some indication that the relation was a two-branch curve with a discontinuity at four effective free electrons. Due to a lack of data, it was not possible to apply this approach to the present results. Furthermore, there is no direct analogy between Weinstein and Elliott's curve and Figure 63.

In summary, it would appear that a good chance for a structure-related explanation of the interaction effects would lie in a model, such as Wagner's approach, which considers the chemical potential of the free electrons but which also incorporates some recognition of size-dependency.

In a later section (pp. 217-239) the prediction of interaction parameters is considered on the basis of some presently accepted general solution models having their primary basis in statistical thermodynamics.

5. Temperature Dependence of Interactions

The experimentally determined first and second-order interaction parameters were found to either be constant over the 450 to 650°C temperature range of this study, or else to exhibit a linear variation with the reciprocal absolute temperature. The data could be expressed in equations

of slope-intercept form, e.g.,

$$\epsilon_{z_n}^j = A_j + \frac{B_j}{T}$$

Dealy and Pehlke⁽¹⁶⁾ stated that by using thermodynamic relationships the variation of the first-order interaction parameter with temperature is given by the expression:

$$\frac{d\epsilon_i^j}{d\left(\frac{1}{T}\right)} = \frac{1}{R} \left(\frac{\partial^2 H}{\partial x_i \partial x_j} \right)_{x_i=x_j=0} \quad (30)$$

(The derivation of this equation, which has not been previously published, is given in Appendix B, together with an alternate version). Dealy and Pehlke further suggested that a useful extrapolation of interaction parameters could be accomplished by a linear plot, providing that the derivative of enthalpy was constant or else not a strong function of temperature.

Chipman and Corrigan⁽²²⁾ have also recently considered the question of the temperature dependence of interaction parameters and, under certain simplifying assumptions, derived an equation similar to that of Dealy and Pehlke. The assumption made was that the interaction parameter

$\left(\frac{\partial \ln \gamma_i}{\partial x_j} \right)_{x_i = x_j = 0}$, remains constant over a finite range of

concentration (at first glance this appears reasonable since it will be recalled that linear relations between $\ln \gamma_{z_n}$ and x_j were found for many of the solutes studied in this investigation). If the second-order effects

were neglected and the infinitely dilute solution was adopted as the reference state, then Wagner's Taylor series expansion reduces to:

$$\ln \gamma_i^1 = \epsilon_i^j x_j \quad (31)$$

(note that by the change of reference state, $\ln \gamma_i^0 = 0$)

Since the excess free energy of mixing is normally given by the expression

$$\Delta \bar{G}_i^{xs} = RT \ln \gamma_i^1 \quad (32)$$

a new free energy term was introduced as

$$G_i^{xj} = RT \ln \gamma_i^1 = RT \epsilon_i^j x_j \quad (33)$$

with the meaning that this expresses the "extra" free energy of component i due to the addition of component j and "within the limits of present-day experimental accuracy", is a linear function of concentration within a finite range. By defining "extra" terms for the entropy and enthalpy, Chipman and Corrigan then could write the following relations culminating in an expression for the temperature dependence of the interaction coefficient.

$$G_i^{xj} = RT \epsilon_i^j x_j = H_i^{xj} - TS_i^{xj} = \eta_i^j x_j - T \sigma_i^j x_j \quad (34)$$

where

$$\eta_i^j = \frac{H_i^{x_j}}{X_j} \quad , \quad \sigma_i^j = \frac{S_i^{x_j}}{X_j}$$

$$R X_j \frac{d\epsilon_i^j}{d\left(\frac{1}{T}\right)} = \frac{d\left(\frac{G_i^{x_j}}{T}\right)}{d\left(\frac{1}{T}\right)} = H_i^{x_j} \quad (35)$$

The interpretation placed on this result by Chipman and Corrigan if the heat of solution of component i in a ternary alloy was the same as in its binary alloy with the same solvent, then $H_i^{x_j} = 0$ and ϵ_i^j is independent of temperature. It was further stated that if the entropy change is the same for both cases, then

$$\frac{d\epsilon_i^j}{d\left(\frac{1}{T}\right)} = \frac{\epsilon_i^j}{T} \quad (\text{if } S_i^{x_j} = 0) \quad (36)$$

Thus a direct proportionality should exist between ϵ and $1/T$.

This approach to temperature dependence is interesting since it places a more readily grasped interpretation to the situation than Dealy and Pehlke's less familiar quantity $\left(\frac{\partial^2 H}{\partial x_i \partial x_j}\right)$. However, it is evident that the two approaches are really similar.

By restricting their treatment to first-order effects only, Chipman and Corrigan limited the generality of their results. Their approach may be extended to a more general consideration of the temperature dependence of dilute solute interactions by the following reasoning:

Writing the Taylor series expansion through the second-order terms and assuming the case of zinc-bismuth alloys where $\epsilon_i^i = \epsilon_i^i = \epsilon_i^j = 0$

$$\ln \gamma_i^j = \ln \gamma_i^{j0} + x_i \epsilon_i^j + x_j \epsilon_i^j + \frac{1}{2} x_i^2 \epsilon_i^j + \frac{1}{2} x_j^2 \epsilon_i^j + x_i x_j \epsilon_i^j \quad (22)$$

$$\ln \gamma_i^j - \ln \gamma_i^{j0} = x_j \epsilon_i^j + x_i x_j \epsilon_i^j \quad (37)$$

Since for a binary alloy, $\Delta \bar{G}_i^{\text{XS}} = RT \ln \gamma_i$

Then for a ternary or multicomponent alloy; multiplying (37) by RT

$$RT (\ln \gamma_i^j - \ln \gamma_i^{j0}) = \bar{G}_{i(j)}^{\text{ex}} \quad (38)$$

$\bar{G}_{i(j)}^{\text{ex}}$ is the "extra" excess free energy due to the addition of j (the same as defined by Chipman and Corrigan).

This quantity may be separated into enthalpy and entropy terms

$$\bar{G}_{i(j)}^{\text{ex}} = \bar{H}_{i(j)}^{\text{ex}} - T \bar{S}_{i(j)}^{\text{ex}} \quad (39)$$

Rewriting Equation (37)

$$\bar{G}_{i(j)}^{\text{ex}} = RT (\ln \gamma_i^j - \ln \gamma_i^{j0}) = RT [x_j \epsilon_i^j + x_i x_j \epsilon_i^j] \quad (40)$$

$$[\epsilon_i^j + x_i \epsilon_i^j] = \frac{1}{R x_j} \left[\frac{\bar{H}_{i(j)}^{\text{ex}}}{T} - \bar{S}_{i(j)}^{\text{ex}} \right] \quad (41)$$

If ϵ_{i1}^j is zero, or else merely neglected, then Chipman and Corrigan's expression (Equation 34) is obtained in slightly different form by using the definitions $\frac{\bar{H}^{ex}}{x_j} \equiv \eta$ and $\frac{\bar{S}^{ex}}{x_j} \equiv \sigma$.

$$\epsilon_{i1}^j = \frac{1}{R} \left[\frac{\eta}{T} - \sigma \right] \quad (42)$$

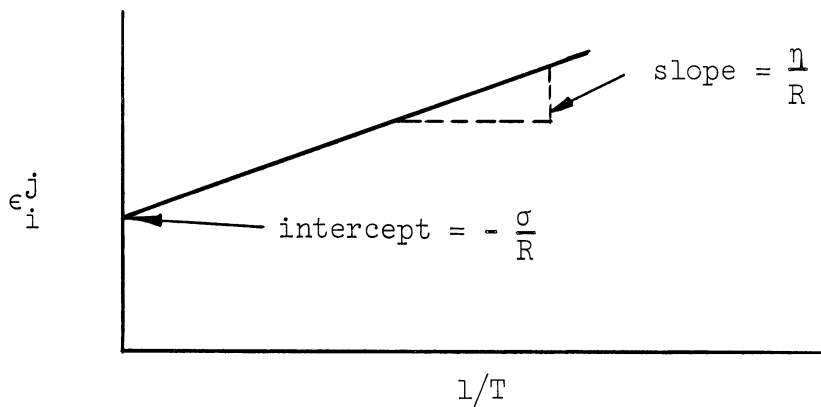
From this expression it can be seen directly that

if $\sigma = 0$, then ϵ_{i1}^j is directly proportional to $1/T$

if $\eta = 0$, then ϵ_{i1}^j is a constant independent of T and equal to $-\sigma/R$

However, this expression is more general since it also shows that a plot of ϵ_{i1}^j versus $1/T$ can have a finite slope and intercept, or if such a plot is a straight line, then η and σ are constant.

The slope is given by η/R and the intercept is $-\sigma/R$.



Furthermore, Dealy and Pehlke's term $\frac{\partial^2 H}{\partial x_i \partial x_j}$ is η and is a partial molar quantity. Its nature may be grasped more readily by the following definitions:

$$\frac{\partial H}{\partial x_i} \equiv \bar{H}_i ; \quad \eta = \frac{\partial \bar{H}_i}{\partial x_j} = \frac{\partial^2 H}{\partial x_i \partial x_j} , \text{ since } n_i = x_i \text{ if } n_T = 1$$

and thus it is the change in the partial molar enthalpy of i due to the addition of j i.e., the "extra" quantity defined by Chipman and Corrigan.

This analysis also shows that it is not possible to have a constant first-order interaction parameter and a constant entropy of mixing ($\bar{S}_i^{\text{ex}} = 0$) unless the interaction parameter is zero. For the case where ϵ_i^j appears to be constant (within experimental error) for a limited range of temperature, η is probably very small, and hence ϵ_i^j is also quite small. This is consistent with the observed behavior for the ternary additions of cadmium, tin, and indium. The expected slight temperature dependence was detectable only for the case of lead. In the more general case, such as with the present experimental results where the second-order interactions are large or are not neglected, they may be included in this analysis by the following process:

The "extra" enthalpy and entropy are divided into the first-order and second-order components.

$$\bar{H}_{i(j)}^{\text{ex}} = \bar{H}_1^{\text{ex}} + \bar{H}_2^{\text{ex}} \quad (43)$$

$$\bar{S}_{i(j)}^{\text{ex}} = \bar{S}_1^{\text{ex}} + \bar{S}_2^{\text{ex}} \quad (44)$$

Then using Equation (41)

$$(\epsilon_i^j + x_i \epsilon_i^j) = \frac{1}{R x_j} \left[\frac{\bar{H}_1^{ex} + \bar{H}_2^{ex}}{T} - (\bar{S}_1^{ex} + \bar{S}_2^{ex}) \right] \quad (45)$$

The equation can be separated as follows

$$(\epsilon_i^j + x_i \epsilon_i^j) = \frac{1}{R x_j} \left[\frac{\bar{H}_1^{ex}}{T} - \bar{S}_1^{ex} + \frac{\bar{H}_2^{ex}}{T} - \bar{S}_2^{ex} \right] \quad (46)$$

and can be written as two parts

$$\epsilon_i^j = \frac{1}{R x_j} \left[\frac{\bar{H}_1^{ex}}{T} - \bar{S}_1^{ex} \right] = \frac{1}{R} \left[\frac{\eta_1}{T} - \sigma_1 \right] \quad (47)$$

$$\epsilon_i^j = \frac{1}{R x_i x_j} \left[\frac{\bar{H}_2^{ex}}{T} - \bar{S}_2^{ex} \right] = \frac{1}{R} \left[\frac{\eta_2}{x_i T} - \frac{\sigma_2}{x_i} \right] = \frac{1}{R} \left[\frac{\eta_2^*}{T} - \sigma_2^* \right] \quad (48)$$

A linear relation, such as indicated in Table X, between ϵ_i^j and $1/T$ is predicted if the second-order "extra" terms are constant. Furthermore, additional equations could be obtained if the process were carried out through the third-order terms, etc. Experimentally in a galvanic cell at a given x_i and x_j it may be observed that

$$\bar{S}_{i(j)}^{ex} = n F \left[\left(\frac{\partial \epsilon}{\partial T} \right)_{i(j)} - \left(\frac{\partial \epsilon}{\partial T} \right)_i \right] \quad (49)$$

$$\bar{H}_{i(j)}^{ex} = -n F \left[(\epsilon_{i(j)} - \epsilon_i) - T \bar{S}_{i(j)}^{ex} \right] \quad (50)$$

By using Equations (43) through (48), the observed values can be expressed as the sums of the first and second-order contributions to the "extra" excess quantities:

$$\bar{S}_{i(j)}^{ex} = \sigma_1 X_j + X_i X_j \sigma_2^* \quad (51)$$

$$\bar{H}_{i(j)}^{ex} = \eta_1 X_j + X_i X_j \eta_2^* \quad (52)$$

In Chipman and Corrigan's second conclusion (Equation 36), a direct proportionality was expected between ϵ and $1/T$ if $\bar{S}_{i(j)}^{ex} = 0$; however, Equations (47) and (48) showed that proportionality may also be obtained when σ and σ_2^* are not zero.

Equation (49) was used to obtain values of $\bar{S}_{i(j)}^{ex}$ for several of the alloys studied in this investigation. The results which are tabulated below indicate that it is probably different from zero, while Table X had shown the proportionality between the interaction parameters and $1/T$.

X_{Zn}	\bar{S}_1 Zn-Bi Binary	$\bar{S}_{1(j)} (X_j = .015)$			$\bar{S}_{1(j)} - \bar{S}_1 = \bar{S}_{1(j)}^{ex}$		
		j = Cu	Ag	Au	Cu	Ag	Au
.015	9.95e.u.	9.85e.u.	10.05e.u.	10.80e.u.	-0.10e.u.	+0.10e.u.	+0.85e.u.
.025	9.05	8.90	8.85	8.35	-0.15	-0.20	-0.70
.0375	8.30	7.85	8.35	-	-0.45	+0.05	-
.050	7.60	7.25	7.75	6.85	-0.35	+0.15	-0.75

e.u. = entropy units, cal/°K/g. atom

The magnitude of $\overline{S}_{i(j)}^{ex}$ in the above tabulation is at the borderline of statistical significance. The estimated standard deviation of the slopes of the emf-versus-temperature curves had ranged from about .001 to .005 millivolts per °C. Applying 90 percent confidence limits to these values suggested that $\overline{S}_{i(j)}^{ex}$ as calculated from Equation (49) could range from $\pm .10$ to $\pm .40$ entropy units and still be interpreted as within the range of experimental uncertainty. Hence, it is believed that the tabulation of $\overline{S}_{i(j)}^{ex}$ on page 216 has qualitative, but not necessarily quantitative validity - as exemplified by the differences in algebraic sign for a few values.

Equation (51), in conjunction with the temperature dependence coefficients from Table X was also used to estimate $\overline{S}_{i(j)}^{ex}$ for several of these alloys. The results were of the same order of magnitude as the experimental values but the previously mentioned uncertainties precluded a quantitative comparison.

The consideration of the temperature dependence of the interaction parameters has thus led to a potentially useful extension of the "extra" terms introduced by Chipman and Corrigan. The present studies suggest that the possibility of second-order effects must be considered in any attempt to interpret solute interactions in terms of thermodynamic quantities such as enthalpy and entropy.

B. Prediction of Ternary Interactions From Simple Solution Models

Thus far the discussion has been concerned with attempts to account for the observed interactions on the basis of structure-related

physical or chemical criteria. The possible explanations were only semi-quantitative at best.

On the other hand, the general development of the field of thermodynamics has led to the formulation of several theories which attempt to account for solution behavior. Insofar as these theories lead to expressions for the excess free energy of mixing, it is possible to use them for calculations of interaction effects.

Oriani and Alcock⁽³¹⁾ recently discussed some simple models of solutions and pointed out that they are primarily statistical and based on assumptions regarding the energy of an assembly of atoms, molecules, or ions without regard to the physical basis of the interaction. The models considered were the regular solution, the subregular solution, and the quasi-chemical model. The principal assumption involved is that the total energy of a collection of molecules is the sum of the interaction energies between the individual molecules taken two at a time. In the simple solution models only nearest-neighbor interactions are considered.

The results of the present investigation were examined from the standpoint of the implications of these models and their utility for the prediction of interactions in ternary solutions.

1. Regular Solution Model

The regular solution concept, which was introduced by Hildebrand,⁽³³⁾ is that the entropy of solution is ideal, i.e., the mixing is random, while the enthalpy of solution has some finite value. Using the convenient

concepts of the excess thermodynamic quantities, the following relations apply:⁽⁴¹⁾

$$\Delta \bar{G}_i^{xs} = \Delta \bar{G}_i - \Delta \bar{G}_i^{ideal} = RT \ln \gamma_i \quad (53)$$

$$\Delta \bar{S}_i^{xs} = \Delta \bar{S}_i - \Delta \bar{S}_i^{ideal} = \Delta \bar{S}_i + R \ln X_i \quad (54)$$

$$\Delta \bar{H}_i^{xs} = \Delta \bar{H}_i - \cancel{\Delta \bar{H}_i^{ideal}} = \Delta \bar{H}_i \quad (55)$$

$$\Delta \bar{G}_i^{xs} = \Delta \bar{H}_i - T \Delta \bar{S}_i^{xs}; \text{ but if } \Delta \bar{S}_i = \Delta \bar{S}_i^{ideal} \quad (56)$$

then

$$RT \ln \gamma_i = \Delta \bar{H}_i \quad (\Delta \bar{S}_i^{xs} = 0) \quad (57)$$

The activity coefficients for regular solutions are thus directly related to the partial molal heats of mixing.

For the case of a regular ternary solution, Hildebrand and Scott⁽³³⁾ showed that the activity coefficient of component i is given by the expression

$$\ln \gamma_i = \frac{\Delta \bar{H}_i}{RT} = \frac{V_i}{RT} (\delta_i - \bar{\delta})^2 ; \bar{\delta} = \phi_k \delta_k + \phi_i \delta_i + \phi_j \delta_j \quad (58)$$

ϕ is the volume fraction, V is the molar volume and δ is the solubility parameter.

The solubility parameter is defined as $\left(\frac{\Delta E_{\text{vap}}}{V}\right)^{\frac{1}{2}}$, the square root of the energy of vaporization per cubic centimeter. The meaning attached to the solubility parameter is that it represents the "cohesive energy density" of an element. (33)

Equation (58) may be extended to the calculation of interaction parameters by differentiating with respect to the mole fraction of component j . When the limit is taken at infinite dilution of the solutes, the expression for the interaction parameter ϵ_i^j is given by:

$$\epsilon_i^j = \left(\frac{\partial \ln \gamma_i}{\partial x_j}\right)_{x_i=x_j=0} = -\frac{2}{RT} \left(\frac{V_i V_j}{V_k}\right) (\delta_k - \delta_i)(\delta_k - \delta_j) \quad (59)$$

A similar expression may be derived for the self-interaction parameter.

$$\epsilon_i^i = \left(\frac{\partial \ln \gamma_i}{\partial x_i}\right)_{x_i=0} = -\frac{2}{RT} \frac{V_i^2}{V_k} (\delta_i - \delta_k)^2 \quad (60)$$

The interaction parameters thus become only functions of the molar volume and the solubility parameters of the elements involved.

The subscripts for i and j may be interchanged to show that

$\epsilon_j^i = \epsilon_i^j$ and hence Wagner's reciprocity relation (Equation (3)) is

obtained directly. In addition, the form of the equation for ϵ_i^j predicts a linear relation with the reciprocal absolute temperature. Thus, depending on the validity of the assumption of regular solution behavior, the interaction parameters can be predicted from readily obtainable information. Hildebrand and Scott⁽³³⁾ tabulated values of V and δ for a number of metals at 298, 500, and 1000°K. The change in solubility parameter with increasing temperature was quite small "thanks to small coefficients of thermal expansion and small ΔC_p 's, as well as small volume changes and heats of fusion."

Before attempting to apply these equations to the present results for ternary solutions based on zinc in bismuth, their utility was tested by calculations for several systems where substantially regular behavior was expected. Hildebrand and Scott examined galvanic cell data for several binary systems and noted that the agreement with regular solution behavior was "excellent for zinc in cadmium, good for cadmium in tin and lead, and not so good for zinc in tin and thallium in tin."

Dealy and Pehlke's compilation of interaction parameters in non-ferrous systems⁽¹⁶⁾ gave the effect of several third elements on the activity of cadmium dissolved in tin or lead. In addition, Boorstein and Pehlke's⁽²¹⁾ results for tin additions to cadmium dissolved in bismuth were useful, since examination of their cadmium-bismuth binary data revealed that regular solution behavior was obeyed.

The calculated and observed interaction parameters for those systems where the binary solutions were regular are compared below:

Solvent	Solute _i	Solute _j	T°C	ϵ_1^j Predicted	ϵ_1^j Observed
Sn	Cd	Zn	700	-1.1	-1.6
Sn	Cd	Pb	500	-4.8	0
Pb	Cd	Sb	500	+ .8	-1.6
Pb	Cd	Sn	500	+1.6	-1.4
Pb	Cd	Bi	500	- .4	- .9
Bi	Cd	Sn	500	+ .8	+1.1

The algebraic sign of the interaction parameter was predicted correctly in only three of the six cases considered. Where the sign was predicted correctly, the numerical value of the interaction parameter was calculated with only fair success.

The present data for the bismuth-zinc-j systems were then examined, however, it was immediately noted that the behavior of the zinc-bismuth binary was not regular. The observed values for the mixing entropy of zinc were appreciably greater than the ideal values. Since the molar volumes of zinc and bismuth are widely different (9.2 cc/mole versus 21.3 cc/mole), an attempt was made to account for the excess entropy of zinc on the basis of the size effect. The calculation was made using an expression given by Hildebrand and Scott⁽³⁹⁾ for the ideal mixing entropy of unequal-size molecules.

$$\Delta \bar{S}_i^{ideal} = \bar{S}_i - S_i^{\circ} = -R \left[\ln \phi_i + \phi_k \left(1 - \frac{V_i}{V_k} \right) \right] \quad (61)$$

A comparison of the observed and calculated mixing entropies for zinc in bismuth is given below:

x_{Zn}	$\bar{S}_i - S_i^{\circ}$, Ideal		$\bar{S}_i - S_i^{\circ}$ Observed
	Equal-size Molecules	Unequal-size Molecules	
.015	8.35 eu.	8.95	9.95
.025	7.35	7.95	9.05
.0375	6.55	7.05	8.30
.050	5.95	6.45	7.60

(eu = entropy units, cal/°K/g-atom)

These results show that even if the size disparity is taken into account, the zinc-bismuth binary system is not regular. (Oriani and Alcock⁽³¹⁾ noted that an internal inconsistency in the definition of the regular solution can lead to an apparent $\Delta\bar{S}_i^{XS}$ of a few-tenths of an entropy unit. The results given above exceed this limit.)

It was therefore not expected that the prediction of interaction parameters for bismuth-zinc-j systems using the regular solution model would be particularly successful. The calculated and observed parameters are compared in Table XV. The algebraic sign of the interaction was predicted correctly in only five of the ten cases considered. None of the positive interactions were predicted correctly. For the cases where the qualitative prediction was correct, the numerical values were only in fair to poor agreement with the observed values at 550°C.

The regular solution model would thus seem to have limited usefulness in the prediction of interaction effects in metallic systems. The success of the model was only 50 per cent, regardless of whether the underlying binary solution conformed to regular solution behavior.

TABLE XV

COMPARISON OF OBSERVED INTERACTION PARAMETERS WITH VALUES CALCULATED USING SIMPLE SOLUTION MODELS

Solute	Observed ϵ_{Zn}^j	Regular Solution Model		Wada and Saito's Eqn.		Alcock and Richardson's Equations											
		Predicted ϵ_{Zn}^j at 823°K		Quasi-chemical Model		Factors Used with Alcock and Richardson's Equations					Alcock and Richardson's Equations						
		-		-		γ_j^0	γ_j^0	$\gamma_{Zn(j)}^0$	$\gamma_{Zn(j)}^0$	$\gamma_{Zn(Bi)}^0$	$\gamma_{Zn(Bi)}^0$	γ_{Zn}^0	γ_{Zn}^0	γ_{Zn}^0	γ_{Zn}^0	γ_{Zn}^0	γ_{Zn}^0
Cu	-2.4	-2.2	-5.2 to -6.5	850	5.1	1300	.6	1100	1.5	.078	1100	-1.8	-2.5	-3.0			
Ga	+5.0 to +.7	-1.6*	-.3 to -.9*	-	-	723	1.15	-	-	-	-	-	-	-			
Ag	-2.5	-1.8	-2.7 to -3.6	1000	2.6	1000	.6	1000	2.1	.11	1000	-1.6	-2.2	-2.6			
Cd	-.3	+.2*	+5.1 to +7.4*	773	1.0	800	1.4	790	3.4	.41	790	-.3	-.9	-.9			
In	+2.2	-1.0*	+2.6	623	.3 ^b	700	1.6	700	4.0	1.33	700	+2.2	+0.3	+0.3			
Sn	-.5	-2.3	-1.5	608	1.2	700	1.5	650	4.6	.27	650	-.5	-1.3	-1.4			
Sb	-4.5	-1.1	-1.6 to -2.1	-	-	823	.6	-	-	-	-	-	-	-			
Au	-18.0	-2.4	-3.7	973	.8	1048	.09	1000	2.1	.054	1000	-16.5	-2.9	-3.6			
Hg	-1 to -2	+1.3*	+2.7 to +3.3*	594	1.46	608	1.2	600	5.0	.16	600	-1 to -2	-1.8	-2.1			
Pb	+1.3*	-.3*	+3.0	773	.4	926	2.2	850	3.0	1.83	850	+1.3	+.6	+.6			

No. of systems for correct prediction of sign of interaction

5/10

7/10

8/8

8/8

* Systems where algebraic sign of ϵ was incorrectly predicted
 a Data from Hultgren et al. (54)
 b Calculated from ΔH_{Zn} assuming regular solution
 c At average temperature for data of $\gamma_j^0(Bi)$ and $\gamma_{Zn(j)}$
 d $Z = 7.5$

2. Sub-regular Solution Model

A variation of the regular solution model was proposed by Hardy⁽³⁵⁾ and termed the "sub-regular" model. In this formulation, the excess free energy of mixing is taken as a function of concentration. For a binary system, Yokokawa et al.⁽³⁶⁾ gave the sub-regular formulation for the excess free energy as

$$G^e = x_i x_j \left[A_{ij}^{\circ} + (x_i - x_j) A'_{ij} \right] = x_i x_j \left[A_{ij}^{\circ} + (1 - 2x_j) A'_{ij} \right] \quad (62)$$

A plot of $G^e/x_i x_j$ versus x_i should thus be linear and have finite slope.

The same treatment was extended to ternary systems by Yokokawa et al., and the following expression was obtained

$$G^e = x_j x_i A_{ij}^{\circ} - x_i x_k A_{ik}^{\circ} + x_k x_j A_{kj}^{\circ} + x_j x_i \frac{x_j - x_i}{x_j + x_i} A'_{ij} \quad (63)$$

$$+ x_i x_k \frac{x_i - x_k}{x_i + x_k} A'_{ik} + x_k x_j \frac{x_k - x_j}{x_k + x_j} A'_{jk}$$

where the A's are constants, characteristic of the appropriate binary system.

This equation was further used to obtain a rather complex relation for the excess chemical potential of constituent i . As part of the present investigation the latter expression was differentiated with respect to the mole fraction of component j in order to derive

an expression for the interaction parameter in terms of the constants of Yokokawa's formulation of the sub-regular model.

After considerable manipulation the final expression is given by

$$\epsilon_i^j = \frac{1}{RT} \left\{ (A_{ij}^{\circ} - A_{ik}^{\circ} - A_{jk}^{\circ}) + (A'_{ij} + A'_{ik} - A'_{jk}) \right\} \quad (64)$$

It is assumed that the interactions A° and A' are unaffected by the additional solutes and/or solvent. It will be noted that this relation predicts a linear relation between ϵ_i^j and reciprocal absolute temperature.

Thus, providing that the constants are known for sub-regular behavior of the three binary pairs in the ternary alloy, the interaction parameter may be calculated provided that the binary alloys are either sub-regular in behavior or regular (in which case the constant $A' = 0$).

Yokokawa et al. gave constants for binaries involving tin, zinc, indium, and bismuth and it was possible to compare experimental results from two systems studied in this investigation with calculated values from the sub-regular model. The calculations are given below:

<u>System</u>	<u>A_{Sn-Zn}°</u>	<u>A_{Zn-Bi}°</u>	<u>A_{Bi-Sn}°</u>	<u>A'_{Sn-Zn}</u>	<u>A'_{Zn-Bi}</u>	<u>A'_{Bi-Sn}</u>
Sn - Zn - Bi	1660	3100	-205	-430	1280	-125
	<u>A_{In-Zn}°</u>	<u>A_{Zn-Bi}°</u>	<u>A_{Bi-In}°</u>	<u>A'_{In-Zn}</u>	<u>A'_{Zn-Bi}</u>	<u>A'_{Bi-In}</u>
In - Zn - Bi	2320	3100	-700	-420	1280	0

(It was not possible to verify these constants; Yokokawa commented that the zinc systems could be considered sub-regular only in the zinc-dilute region.)

Let

$$k = \begin{matrix} \text{Bi} \\ \text{Sn} \end{matrix}, \quad i = \begin{matrix} \text{Zn} \\ \text{In} \end{matrix}, \quad j = \begin{matrix} \text{Sn} \\ \text{In} \end{matrix}$$

Then using Equation (64)

$$\begin{aligned} \epsilon_{\text{Zn}}^{\text{Sn}} &= \frac{1}{RT} (1660 - 3100 + 275) + (-430 + 1280 + 125) \\ &= \frac{1}{RT} (-190) \end{aligned}$$

at 550°C

$$\epsilon_{\text{Zn}}^{\text{Sn}} = -0.12 \quad (\text{Observed } \epsilon_{\text{Zn}}^{\text{Sn}} = -0.5)$$

$$\begin{aligned} \epsilon_{\text{Zn}}^{\text{In}} &= \frac{1}{RT} (2320 - 3100 + 700) + (-420 + 1280) \\ &= \frac{1}{RT} (780) \end{aligned}$$

at 550°C

$$\epsilon_{\text{Zn}}^{\text{In}} = +0.50 \quad (\text{Observed } \epsilon_{\text{Zn}}^{\text{In}} = +2.2)$$

For both systems the proper sign of the interaction was predicted, however, the numerical values were low by a factor of about four

The results of this method are interesting and suggest that further consideration should be given to tests of the utility of Equation (64). However, the method has the disadvantage that the binary system

behavior must be known experimentally and that it conforms to the expression for a sub-regular solution (Equation 62).

3. Quasi-Chemical Solution Model

The regular solution model proposed that the entropy of mixing was due only to perfectly random mixing of the constituents. This assumption was inconsistent with a finite energy of solution, however, the difference was stated by Oriani and Alcock⁽³¹⁾ to be small and often negligible.

If the restriction of perfectly random mixing is removed, the resulting solution model becomes consistent with finite energies and gives rise to a solution model that had been termed the quasi-chemical theory. This model has been discussed by Guggenheim,⁽³⁷⁾ Oriani and Alcock⁽³¹⁾ and applied to the problem of interaction effects by Alcock and Richardson^(17,27) and Wada and Saito.⁽¹⁵⁾

The principal assumptions of the quasi-chemical treatment are that bond energies between molecules are constant and the coordination numbers (number of nearest neighbors that each molecules "sees") are also constant. The implication is that the molten metal forms a quasi-crystalline lattice and the resulting interchange energies between the like and unlike molecules can be treated by a statistical approach.

Alcock and Richardson first used a chemical approach or a so-called random solution model to characterize the effect of an added dilute solute j on the partial heat of solution of a given dilute solute i .⁽¹⁷⁾ By considering pairwise interactions, the following

expression was derived

$$\left(\frac{\partial \Delta \bar{H}_i}{\partial x_j} \right)_{x_j \rightarrow 0} = (\Delta \bar{H}_{i(j)} - \Delta \bar{H}_{i(k)} - \Delta \bar{H}_{j(k)}) \quad (65)$$

By assuming that at low concentrations of j , $\Delta \bar{S}_i(j+k) = \Delta \bar{S}_i(k)$ i.e., no "extra" excess entropy of solution (see pp. 210-212, the discussion of temperature dependence), then a ternary "regularity" of behavior occurs and the expression could be written as

$$RT \left(\frac{\partial \ln \gamma_i}{\partial x_j} \right)_{x_j \rightarrow 0} = (\Delta \bar{H}_{i(j)} - \Delta \bar{H}_{i(k)} - \Delta \bar{H}_{j(k)}) \quad (66)$$

(Chipman and Corrigan⁽²²⁾ later felt this could only be true when ϵ_i^j and ϵ_j^j were small.)

Alcock and Richardson then proposed the following set of assumptions

1. $\Delta \bar{S}_i(j) = \Delta \bar{S}_i(k)$ at $x_i \approx 0$
2. $\gamma_i(j)$ and $\gamma_i(k)$ are taken relative to the same standard state for i
3. $\Delta \bar{S}_j(k)$ is ideal

Under these conditions, Equation (66) reduced to the simple form

$$\left(\frac{\partial \ln \gamma_i}{\partial x_j} \right)_{x_j \rightarrow 0} = \epsilon_i^j = \ln \gamma_i(j) - \ln \gamma_i(k) - \ln \gamma_j(k) \quad (67)$$

Richardson⁽¹⁾ stated that i should be present at concentrations substantially less than j .

Wada and Saito⁽¹⁵⁾ pointed out that the same result is obtained if the three binary solutions are taken as regular solutions (see Equation 57). In a later publication,⁽²⁷⁾ Alcock and Richardson used a more rigorous quasi-chemical approach from a statistical viewpoint to obtain the following improved expression

$$\ln \delta_i^j(j+k) = \ln \frac{\delta_i^j(j)}{\delta_j^j(j+k)} - Z k_{il} (K x_j + x_k) \quad (68)$$

where

$$K = \left[\frac{\delta_i^k(k) \delta_j^j(j+k)}{\delta_i^j(j) \delta_k^k(j+k)} \right]^{\frac{1}{Z}}$$

and Z is the coordination number taken constant in the solution.

They differentiated this equation to produce an expression for the interaction effects

$$\left(\frac{\partial \ln \delta_i^j}{\partial x_j} \right)_{x_j \text{ or } x_k \rightarrow 0} = \frac{-Z(K-1)}{x_k + K x_j} \quad (69)$$

For the case where both the solutes i and j are present at infinite dilution, Equation (69) was reduced to the following expression:

$$\left(\frac{\partial \ln \delta_i^j}{\partial x_j} \right)_{\substack{x_i \rightarrow 0 \\ x_j \rightarrow 0 \\ x_k \rightarrow 1}} = -Z(K-1) \quad (70)$$

and since $\gamma_k(k+j) = 1$ for $k = 1$

$$\left(\frac{\partial \ln \gamma_i}{\partial X_j} \right)_{\substack{X_i=0 \\ X_j=0}} = \epsilon_i^j = -z \left[\left(\frac{\gamma_{i(k)}^0 \gamma_{j(k)}^0}{\gamma_{i(j)}^0} \right)^{\frac{1}{z}} - 1 \right] \quad (71)$$

It was pointed out by Alcock and Richardson that Equation (68) may be rewritten by taking advantage of the relation

$$\ln \gamma_{i(jk)} = \frac{\Delta \bar{H}_{i(jk)}}{RT} \quad \text{to yield the form}$$

$$\exp - \left[\frac{\Delta \bar{H}_{i(jk)}}{zRT} \right] = X_k \exp - \left[\frac{\Delta \bar{H}_{i(k)} - \Delta \bar{H}_{k(j+k)}}{zRT} \right] + X_j \exp - \left[\frac{\Delta \bar{H}_{i(j)} - \Delta \bar{H}_{j(j+k)}}{zRT} \right] \quad (72)$$

If the exponential terms in this equation were expanded and all except the first term are ignored, Alcock and Richardson stated that the resulting expression can be shown to be an integrated form of Equation (67). Equation (67) was thus a first-order approximation to a quasi-chemical approach.

Wada and Saito⁽¹⁵⁾ based their calculations directly on the zeroth-approximation of Guggenheim's quasi-chemical method for regular solutions. By assuming that the coordination number in the liquid metal solution is about 10 to 12, and that the structure is very nearly close-packed, a face-centered cubic lattice can be taken as the model of the quasi-crystalline lattice. The dilute solutes are then assumed to be placed substitutionally in this lattice and the formal treatment

of statistical thermodynamics can be applied. Assuming random distribution and using Stirling's approximation to the factorial, the following equation was derived by Wada and Saito for the interaction parameter

$$\epsilon_i^j = \frac{1}{RT} (W_{ij} - W_{jk} - W_{ik}) \quad (73)$$

where W's are interchange energies between the subscripted components. It was also shown that the expression for ϵ_j^i is the same, and thus Wagner's reciprocity relation is satisfied.

By comparing the various equations, it is seen that the random solution approach of Alcock and Richardson and the quasi-chemical approach of Wada and Saito produce identical results.

Wada and Saito⁽¹⁵⁾

$$\epsilon_i^j = \frac{1}{RT} (W_{ij} - W_{jk} - W_{ik}) \quad (73)$$

Alcock and Richardson⁽¹⁷⁾

$$\epsilon_i^j = \frac{1}{RT} (\Delta \bar{H}_{i(j)} - \Delta \bar{H}_{j(k)} - \Delta \bar{H}_{i(k)}) \quad (66)$$

However, the essential difference in these approaches lies in the means for evaluating the binary effects which are combined to predict the ternary interaction parameter. Alcock and Richardson⁽¹⁷⁾ assumed regular solution behavior to obtain Equation (67) (or by the

quasi-chemical approach derived Equation (71) directly). Both of these equations utilize experimental observations on binary alloys to predict the ternary effect.

On the other hand, Wada and Saito proposed the use of an independent "analytical" equation for the determination of the interchange energies. By using an expression proposed by Mott⁽⁸²⁾ for the excess free energy of mixing in binary solutions (used in connection with studies of binary miscibility), and making use of an equation for the excess free energy of mixing in a dilute solution, $\Delta G_{ij}^{XS} = W_{ij} \cdot \phi_i \cdot \phi_j$ (this apparently comes from Hildebrand's development of regular solution theory), the equation for the estimation of the interchange energy is

$$W_{ij} = V^m (\delta_i - \delta_j)^2 - 23,060 \bar{n} (X_i - X_j)^2 \quad (74)$$

where V^m = molar volume, X = electronegativity, \bar{n} = number of ij bonds, and δ = solubility parameters.

Since the binary molar volumes, solubility parameters, and electronegativities are known for nearly all elements,⁽³³⁾ the interaction parameters may be calculated directly, subject only to the knowledge of the value of \bar{n} . Wada and Saito suggested that the smaller value of valency of the two components may be employed as the value of \bar{n} and that V^m be taken as the arithmetic average of the atomic volumes of the two components in the solid state.

The present results for the bismuth-zinc-j systems were studied using the solution models based on Equations (67) and (71) (Alcock and Richardson) and Equations (73) and (74) (Wada and Saito). The calculated and observed interaction parameters are compared in Table XV. The comparisons with Wada and Saito's model were made at 550°C and are presented as ranges of values depending on various assumptions regarding the value of \bar{n} ,⁽⁸¹⁾ Since the use of Alcock and Richardson's equations requires knowledge of activity coefficients in the binaries, the comparisons were made at whatever temperature data were available in the literature. The binary data used were taken from Hultgren⁽⁵⁴⁾ and Dealy and Pehlke⁽⁸⁶⁾ and the present results for $\gamma_{\text{Zn(Bi)}}^{\circ}$ were extrapolated to the same temperature range. For Alcock and Richardson's quasi-chemical equation (Equation 71), the coordination number was taken as 7.5 since x-ray, electron, and neutron diffraction studies⁽⁸³⁾ have shown coordination numbers of molten bismuth in the range from 7-8.

The algebraic sign of the interaction parameter was predicted correctly in seven of the ten cases studied using Wada and Saito's method and in all of the eight cases for which data were available to test Alcock and Richardson's equations. The numerical agreement with experimental values obtained from Wada and Saito's equation (when the sign was predicted correctly) was excellent for silver or indium additions and in error by a factor of about two for all the other solute elements except gold. For gold, the predicted value was only 1/5-th of the experimental value.

The numerical values obtained with Alcock and Richardson's equations were generally within a factor of two of the experimental results. The only exceptions were the predicted values for the indium or gold additions which were low by a factor of from five to seven. However, it was not expected that the numerical predictions for this equation would be very quantitative since the available data were not all at the same temperature and extrapolation outside the experimental temperature range was necessary for several of the values of $\gamma_{\text{Zn(Bi)}}^{\circ}$. In addition, the value of γ° for In in Bi was estimated under the assumption that the solution is regular. This estimate is only qualitative since the ΔH^{m} values indicate that the In-Bi system is moderately sub-regular⁽⁴⁸⁾ (and even this may not be true since no values of ΔG^{XS} were available to check sub-regularity). Therefore, the only ternary addition for which the prediction can be termed significantly low is gold. Alcock and Richardson's quasi-chemical model gave slightly more negative parameters than the random solution model, however, the general agreement with the experimental values was about the same. A variation in the assumed coordination number did not account for the disparity in the predicted values for gold. At a coordination number of 12 the predicted value was -3.3, at a coordination number of three or four the parameter was about -4.3, while a coordination number of two gave -6.6. (A value of -17.5 was obtained by assuming a coordination number of one!)

Since random mixing on a quasi-crystalline lattice is an assumption in these models, their validity depends on how favorably the underlying binary systems behave. Indeed, Alcock and Richardson's first equation directly assumes regular solution behavior in the binaries while Wada and Saito's method also has an implicit assumption of regularity. The regular solution model per se for the ternary interaction parameters (Equation 59) was successful for only 50 per cent of the cases considered. This equation considered interchange effects (estimated as the difference in solubility parameters) only between the solutes and the solvent. The quasi-chemical model admitted consideration of all three pairwise interactions, and in Wada and Saito's approach explicitly takes electronegativity differences into account. This is consistent with the previous discussion of the results from the physical standpoint. The quasi-chemical formulation of Alcock and Richardson appears to be advantageous since the coordination number appears in it explicitly. However, it is still assumed that the coordination number is constant for all atoms in solution. There is very limited direct evidence available from diffraction studies that random mixing is not attained in some liquid binary systems⁽⁸³⁾ and indeed clustering is considered a major cause for the deviation of both solid and liquid alloys from ideality.^(53,85) Only when an absurd coordination number was assumed was it possible to obtain a "predicted" interaction parameter for the gold addition that agreed with the experimental values. Thus, it is possible that the coordination number might be a function of the

alloying elements and may be variable within a given solution. Possible corrections for such behavior were mentioned by Alcock and Richardson,⁽²⁷⁾ Wada and Saito's method has the disadvantage of a fixed coordination number taken as 10-12. However, this is probably good for most metallic elements since the effect in Equation (71) of changing the coordination number from 12 to 8 was only relatively slight. Thus, Wada and Saito's assumption of 10-12 probably does not introduce serious errors.

Oriani noted⁽³⁰⁾ that the quasi-chemical theories are inadequate as exact statistical models because of the neglect of non-configurational factors and the fact that pairwise interactions may vary with phase and concentrations. Such deviations of bond-energy models were also discussed in detail more recently by Oriani and Alcock.⁽³¹⁾ Lumsden⁽³⁸⁾ considered the contributions of next-nearest neighbors to the excess free energy of mixing for a binary and first suggested a two-parameter expression that Oriani and Alcock⁽³¹⁾ felt adequately expressed Kleppa's data for the zinc-bismuth system. However, this model breaks down in the Henry's Law region. Lumsden proposed that three parameters are really needed to express the free energy of a metallic solution and discussed in detail why the regular solution model should not apply generally to metals. The three needed parameters were described as "adjustable.., with no simple relation between them." The possibility of extending Lumsden's equation to a ternary system and the derivation of an expression for the interaction parameter did not appear to be promising.

From the standpoint of a readily available solution model for the estimation of interaction parameters for engineering purposes Alcock and Richardson's equations are suggested, although it would appear that Wada and Saito's method is also capable of semi-quantitative results. However, if the requisite binary data are available at the proper temperatures, Alcock and Richardson's method is preferred. The sign of the interaction effect was predicted correctly for all eight systems tested in this investigation, while Obenchain⁽¹³⁾ obtained similarly correct predictions for eleven other systems for which ternary interaction data were available from the literature. (Obenchain considered only the first or random solution equation of Alcock and Richardson.)

Wada⁽⁹⁾ recently reviewed the development of the Wada-Saito method and compared the predicted and experimental results for interactions occurring in molten iron. For the ferrous solvent the success of the method was somewhat better than attained in the present investigation. Obenchain found that Wada and Saito's method correctly predicted the sign of the interaction for eight of the twelve non-ferrous systems for which he had taken experimental data. It would appear, therefore, that when suitable binary data are unavailable for applying Alcock and Richardson's method, Wada and Saito's equation can be used to estimate interaction effects in non-ferrous systems with about two to one odds that the results will be of proper algebraic sign and only a factor of two different from the proper numerical value. Unfortunately, neither method accounts for nor predicts a strong negative

interaction, however, this might be anticipated independently if the difference in electronegativities was large between the solutes.

For the present data, the results of applying the quasi-chemical method are considered particularly promising since the zinc-bismuth system is definitely not a regular solution and can be considered only marginally sub-regular. The quasi-chemical model, while not exact, is thus shown to be a useful tool for estimation of dilute solute interactions in ternary liquid alloys.

C. Validity of Wagner's Prediction Model for Multi-Component Solutions

From a purely mathematical standpoint and without regard to a physical model for the solution, Wagner's expression (Equation 1) for the activity coefficient in a multi-component solution is an application of the problem of representing a given function (in this case $\ln \gamma_i$) by means of a sequence of polynomials. Since the activity coefficient at infinite dilution is the Henry's Law constant, both it and its logarithm have finite values (and finite derivatives) at the point $x_i = 0$. Hence a Taylor series may be used to expand $\ln \gamma_i$ about the origin.⁽⁷²⁾ The various interaction parameters are merely the coefficients of the Taylor series and are evaluated by the extrapolation of experimentally realizable quantities to the condition of infinite dilution with respect to the solutes.

Mathematically speaking, we have a situation well exemplified by a statement attributed to Cauchy, "Give me five coefficients and I will plot an elephant; give me six coefficients and the elephant will wiggle its tail."

The usual assumption here is that terms above the first order may be neglected, in which case the logarithm of the activity coefficient becomes a linear function of the mole fractions of the solutes, and the resulting expression is presumed to be valid for any number of solutes so long as the solution may be regarded as "dilute". For ternary solutions it was previously shown (p. 19) that the second-order terms may be readily evaluated along with the first-order terms with no additional experimentation. Under the conditions that prevail in most of Bi-Zn-j systems, i.e., linearity of $\ln \gamma_{Zn}$ with composition, the self-interaction parameter and two of the three second-order parameters are zero. Thus, a second-order expression was shown to be rigorous for a ternary solution, and afforded the possibility of a better representation of the log activity coefficient in a higher-order solution.

The utility of Wagner's prediction model or its extension, the second-order prediction model (pp.137-140), rests in the ability of the truncated series to adequately represent the experimental facts in a system of higher order than ternary. The questions that might arise could include the following: What is the accuracy possible? How far away from dilute solution can these equations be extended; Does the inclusion of second-order terms significantly improve the calculations? Do the types and variety of interacting elements make a difference? What is the error introduced by truncation? etc.

Several of these points were discussed in the course of presenting the experimental results on the multi-component solutions (pp.143-151). The agreement between the observed and predicted values

of the activity coefficient was generally quite good for the dilute solutions containing up to four solute elements in addition to zinc. Near the limit of the Henry's Law region for zinc, ($x_{Zn} \approx .05$) the agreement was still good to excellent for the quaternary systems, and fair to good for the quinary and hexadic alloys studied. If the zinc concentration was held well within the Henry's Law region, ($x_{Zn} = .015$) and the total solute concentration increased far beyond the "dilute" range, the observed activity coefficients were predicted in a solution with two negative interactions but were considerably lower than the predicted values for the two systems combining both a positive and negatively interacting solute with zinc.

Several quantitative studies were also made of the experimental results to aid in assessing the utility of the second-order prediction model. With regard to the accuracy of the prediction models, a study was made of the deviation between the experimental and predicted values of the activity coefficients. Only the absolute value of the deviation was considered - the sign of the deviation was left to a separate study. The results are shown in Table XVI as the average value of the deviation for each type of solution studied, both as a function of prediction model and the amount of zinc present. Two types of behavior were noted. Either the values deviated by about one per cent of the absolute level of the activity coefficient, (approximately three) or the deviation was about five per cent. The results indicate that for higher-order solutions and for the higher content of zinc, ($x_{Zn} = .05$) the second-order model

TABLE XVI

QUANTITATIVE COMPARISONS OF MULTI-COMPONENT
INTERACTION PREDICTION MODELS

Average Value by Which the Predicted Activity
Coefficient Differed from the Observed
Activity Coefficient

Type of Solution	Average* Deviation:	Average Arithmetic Value of ($\gamma_{\text{obs}} - \gamma_{\text{pred}}$) Without Regard to Direction			
		$x_{\text{Zn}}^{\text{a}} = .015$		$x_{\text{Zn}} = .050$	
		$\Delta_{\text{Model I}}$	$\Delta_{\text{Model II}}$	$\Delta_{\text{Model I}}$	$\Delta_{\text{Model II}}$
Quaternary		.037	.030	.058	.050
Quinary		.045	.042	.14	.025
Hexadic		.024	.030	.12	.025
Septenary		.163	.150	-	-

Qualitative Frequency Distribution of
($\gamma_{\text{observed}} - \gamma_{\text{predicted}}$)

Type of Solution	$(\gamma_{\text{obs}} - \gamma_{\text{pred}}):$	Number of Observations for a Given Direction of Deviation									
		$x_{\text{Zn}} = .015$				$x_{\text{Zn}} = .050$					
		Model I		Model II		Model I		Model II			
		-	0	+	-	0	+	-	+		
Quaternary		3	1	7	6	0	5	2	2	4	0
Quinary		3	0	3	3	1	2	0	2	2	0
Hexadic		2	0	3	4	1	0	0	2	1	1
Septenary		2	0	1	2	0	1	-	-	-	-
	Totals	10	1	14	15	2	8	2	6	7	1

$$* \Delta = \frac{\sum |\gamma_{\text{observed}} - \gamma_{\text{predicted}}|}{n}$$

a x_{Zn} , mole fraction

did, as might be expected, produce noticeably closer predictions than the first-order model. For all the solutions where $x_{Zn} = .015$, the deviations for either model were generally about the same, with some indication that the second-order model produced slightly better predictions.

A separate compilation was made in Table XVI of the manner in which the deviations were distributed about the expected values. For the dilute quaternary solutions, the first-order model tended to produce more positive deviations, that is, the observed activity coefficient was greater than predicted. The second-order model produced an almost equal number of positive and negative deviations. Random distributions of deviations were obtained for the quinary, hexadic, and septenary solutions with the first-order model, while the second-order model tended towards negative values for the hexadic and septenary solutions. On an over-all basis, it appears that the first-order model did not account for enough of the interaction, while the second-order model tended to account for too much. This behavior was also noted for the comparisons made at $x_{Zn} = .050$.

A limited study was also made of the effect of temperature on the deviations. In virtually all of the cases examined, the deviation of the predicted value from the observed value was greater at 450°C and less at 650°C than the deviation noted at 550°C.

It should be realized that such comparisons test not only the prediction models, but also the experimental values of the interaction parameters. Within experimental error, the inclusion of second-order

terms improved the predictions, however, the degree of improvement was slight and only really significant for the systems where $x_{Zn} = .05$. The implication of this is that in the solutions where $x_{Zn} = .015$ the remainder term of Taylor's Theorem for a truncated series is quite small and the neglect of the higher order terms is generally valid.

Since the predicted values account for virtually all the observed changes in the activity coefficients, the assumption that only the pairwise interactions are significant in the dilute ternary and higher-order solutions is probably a good one. As a practical limit for the "dilute" range, a bismuth content of approximately .9 mole fraction was a dividing line between "good" and "bad" behavior. However, in the one case of the quaternary system with silver and antimony additions, the "good" behavior extended to $x_{Bi} = .785$. This probably resulted from the fact that the relations between $\ln \gamma_{Zn}$ and x_j for the underlying ternary systems were linear far beyond the original experimental range. In the other cases, indium plus antimony and lead plus silver, the ternary behavior was probably not linear or else there was considerable interaction between the extra solutes that cannot be accounted for by the Taylor Series model. For example, the intermetallic compound InSb is well known in the field of semi-conductors and, in particular, Ptak⁽⁸⁴⁾ has recently discussed the presumed formation (clustering?) of InSb in liquid solutions. However, there is no comparable compound in the lead-silver system. The inclusion of the second-order term thus accounted for some but not all of the deviation from the first-order model.

In the hexadic solutions, there was limited evidence that the agreement of the prediction models with the experimental results became poorer as x_{Zn} was increased while maintaining a constant level of the other solutes.

There was also a very slight indication from the "dilute" quaternary results that the deviations from the predicted values for the combination of a positive and negative interactor was slightly greater than for the other combinations of two added interactors. Aside from this, and the previously noted behavior of the non-dilute quaternaries, there was no reason to believe that the types and varieties of the interacting elements made a difference in the predictions.

In general, the first-order prediction model of Wagner adequately describes the experimental behavior where the zinc content is within the Henry's Law region and up to four additional solutes are considered. The inclusion of the second-order term improves the predictions, but the improvement is not significant unless both the zinc content and the total solute content are large. As the temperature was increased, the interactions became less and the accuracy of the prediction models was greater. This may reflect the fact that only the simple pairwise interactions are significant at the higher temperatures, while at the lower temperatures the interactions between added solutes and the alloying behavior of the underlying solid system tend to play a greater part. The results of these studies of the additivity hypothesis were considerably better than those obtained by Okajima and Pehlke⁽⁷³⁾ for cadmium in lead. The

difference is attributed to the fact that the interaction parameters for the Bi-Zn-j solution were accurately known in the dilute solution region.

The over-all success of the prediction models shows that the truncated Taylor series expansion proposed by Wagner is a useful engineering tool for the prediction of complex solution behavior. The applicability of the present interaction parameters for predictions far away from infinitely dilute solutions is of particular advantage.

D. Limitations of Experimental Results

The limitations of the experimental results primarily concern the specific alloy systems studied. Only a limited number of solutes were studied in a particular solvent over a particular range of temperature. Bismuth was chosen as the solvent primarily for experimental convenience and to allow a maximum number of ternary systems to be studied by the galvanic cell method. However, bismuth cannot be considered as a "good" metallic solvent since its behavior is not typical and, indeed, bismuth is sometimes characterized as a semi-metal. In particular, the coordination number of liquid bismuth is less than that of the more common metals. However, the fact that simple solution models could account for most of the interactions is encouraging for their applicability to more "typical" solvents.

In addition, the liquid binary system of zinc in bismuth is a strong positive deviator from ideality reflecting the underlying immiscibility. As a result most of the observed interactions were negative. Additional corroboration would be desirable for a primary solute-solvent system exhibiting ideal behavior or a negative deviation from ideality.

Another possible limitation of these results is that the observed linearity of $\ln \gamma_{Zn}$ with x_j may not be general. Because of the linearity, it was possible to utilize the experimental coefficients to account for the interactions over a wide range of solution concentration. The results for the gallium or gold additions showed that linearity is not necessarily obtained and imply that serious errors might result if the interaction parameters were used without realization that they might vary with composition.

Finally, the studies of the multi-component systems were confined to representative combinations of interactors. Only two levels of zinc were considered and the mole fractions of the added solutes were made equal. The results obtained are believed to be an adequate test of the prediction models, however, the studies of the highly complex solutions were restricted.

E. Suggested Further Research

The results of this investigation have opened several lines along which additional research might be based. These would include not only additional theoretical or experimental studies of ternary interactions, but further exploration of the predictability of the activity in multi-component solutions.

The ternary studies could be extended in several ways. First, consideration should be given to basic systems exhibiting different deviations from ideality than the zinc-bismuth system. In particular, cadmium in bismuth is almost an ideal solution, while lead in bismuth is

a fairly strong negative deviator. By using some of the same third element additions as in the present investigation, information could thus be obtained on identical additions to three different bismuth-base solutions. Alternatively, the solvent might be varied while the primary solute and interacting elements are retained. For instance, zinc in lead is another strongly positive deviating system. The systems zinc in tin or cadmium are positive deviators but much closer to ideality, while zinc in antimony or silver are negative deviators from Raoult's Law. The use of the other solvents might be limited from the standpoint of melting temperature and displacement reactions, however, enough additional data might be obtained to provide some general indications of the zinc-j interactions.

Finally, consideration might be given to measuring some of the interactions with zinc in bismuth that could not be obtained by the present liquid-electrolyte galvanic cell studies. This could involve the use of solid electrolytes or a dynamic vapor pressure method. The elements that might be considered include thallium, germanium, tellurium, or selenium, and perhaps some of the Group-A elements.

From the theoretical standpoint, further tests of Alcock and Richardson's equations should be made as additional ternary interaction data are obtained. Obenchain suggested that Wada and Saito's method might be improved by attempting to extend it to Guggenheim's first approximation of the regular solution⁽³⁷⁾ rather than the zeroth

approximation that was used, and also that the expression for the interchange energy (Equation 74) might be improved. In addition, the partial heats of solution might be used as the interchange energy, although such data are presently sparse. Yokokawa's sub-regular solution model (Equation 64) showed some promise and might warrant an intensive effort to search the literature for data from which the constants could be obtained for additional binary systems.

The studies of multi-component solutions might be extended in several ways. Additional experiments could be conducted on septenary solutions and also extended to octetic or nonetic alloys. These could be made at two levels of zinc concentration. The quinary and hexadic alloys could be studied with increased added solute concentrations as far as and beyond the levels studied in the quaternary alloys. The relative amounts of the added solutes might be varied - this might be particularly interesting if the molar volumes or atomic size factors were quite different. The effect on a multi-component solution of a non-linear ternary interactor, such as gallium, might be considered. Finally, as ternary interaction parameters become available for different solute-solvent combinations, they should be extended to studies of corresponding higher-order solutions.

VI. SUMMARY AND CONCLUSIONS

An investigation was made of the effect of additional dilute ternary solute elements on the activity of zinc in dilute solution with molten bismuth in the temperature range from 450° to 650°C. The investigation was designed to test the hypothesis that the interaction effects in ternary solutions are periodic with atomic number of the added solute and that the ternary interactions may be used to predict the activity in higher-order solutions. The activities were measured in a multi-electrode galvanic cell apparatus utilizing a fused molten alkali-chloride electrolyte.

The initial measurements defined the activity of zinc in dilute binary solution with bismuth. The interaction effects in the ternary alloys were determined as a first-order interaction parameter, $\epsilon_i^j = \left(\frac{\partial \ln y_i}{\partial x_j} \right)_{x_k=0, x_l=0}$, and a second-order parameter, $\epsilon_i^{jk} = \left(\frac{\partial^2 \ln y_i}{\partial x_j \partial x_k} \right)_{x_l=0, x_m=0}$, where the parameters are the coefficients of a truncated Taylor Series for $\ln y_i$, as proposed by Wagner. The ten solute elements investigated were taken from the Group-B elements of the 4th, 5th, and 6th periods in the Periodic Table. Following this, the activity of zinc was determined in higher-order solutions through septenary, made by alloying combinations of these solute elements to the basic solution of zinc plus bismuth. The ternary interactions were discussed on the basis of periodicity, alloying considerations, and thermodynamic factors. The applicability of several simple solution theories for predicting the interaction parameters was tested. The validity of the truncated Taylor Series for prediction of multi-component interactions was considered.

The following conclusions are drawn from these studies:

1) The zinc-bismuth system obeys Henry's Law out to at least

.05 mole fraction zinc. Thus, the self-interaction of zinc, $\epsilon_{Zn}^{Zn} = \left(\frac{\partial \ln \gamma_{Zn}}{\partial x_{Zn}} \right)_{x_{Zn} = 0}$, was essentially zero.

The Henry's Law constant may be represented by the following equation over the range 450-650°C:

$$\ln \gamma_{Zn}^0 = -0.79 + \frac{1568}{T (^{\circ}K)}$$

2) The additions of lead, gallium, or indium increased the activity of zinc in molten bismuth. The additions of cadmium or tin slightly decreased the activity, while additions of copper, mercury, silver, or antimony decreased the activity by a moderate amount. The effect of gold was to strongly decrease the activity of zinc. The interaction parameters determined at 550°C were as follows:

Added Solute-j	$\epsilon_{Zn}^j = \left(\frac{\partial \ln \gamma_{Zn}}{\partial x_j} \right)_{x_{Zn}=0, x_j=0}$	$\epsilon_{Zn}^j = \left(\frac{\partial^2 \ln \gamma_{Zn}}{\partial x_j \partial x_{Zn}} \right)_{x_{Zn}=0, x_j=0}$
Cu	-2.4	-20
Ga	+5.0 ± .7	-100 ± 20
Ag	-2.5	-20
Cd	-.3	0
In	+2.2	-40
Sn	-.5	-12
Sb	-4.5	0
Au	-18.0	-50
Hg	-1 to -2	?
Pb	+1.3	0

The estimated accuracy is ± 7 to 10 per cent.

- 3) Appreciable temperature dependence of the interaction parameters was found for the additions of copper, silver, antimony, and gold. There was a slight temperature dependence for the zinc-lead interaction parameter, and the parameters for the other solute elements were essentially constant over the experimental range of temperature. The temperature dependence can be represented by equations of the form $\epsilon_j^i = A_j + B_j/T$, where B_j/R is the "extra" excess enthalpy of solution of i and $-A_j/R$ the "extra" excess entropy of solution of i resulting from the addition of component j .
- 4) By observation of the point of discontinuity in the emf-versus-temperature relations, the position of the single-phase liquid boundaries was determined in the bismuth-rich corners of the ternary systems Bi-Zn-Cu and Bi-Zn-Au.
- 5) The hypothesis of periodic variation in interaction parameter with atomic number was found to break down in the case of the tin and antimony additions.
- 6) The first-order interaction effects may be explained in a semi-quantitative manner through Wagner's electron model of a liquid alloy, where differences in electronegativities are used to express changes in the electron/atom ratio caused by the various solute additions. In addition, the excess free energy of mixing of zinc in the binary system

formed with the solute element gives a semi-quantitative explanation of most of the ternary interactions. No simple basis could be found to account for the effect of the size differences of the solute elements on the interaction parameters.

- 7) Several simple solution models were found to give semi-quantitative estimates of the interaction parameters despite the fact that the underlying binary zinc-bismuth system and most of the zinc-j systems are not regular and of uncertain coordination number. Predictions based on quasi-chemical assumptions were better than those based on regular or subregular solution models. Alcock and Richardson's equations which are based on the experimental behavior of the three binary systems correctly predicted the algebraic sign of all the ternary interactions considered and gave numerical results generally within a factor of two of the experimental values. Wada and Saito's equations which incorporate solubility parameters and electronegativities to estimate pairwise interchange energy gave comparable predictions for seven of the ten systems. The regular solution model was qualitatively successful in only five of the ten systems. The instances of failure of the latter two models were their inability to predict the proper direction of the interaction.

8) The validity of the truncated Taylor series proposed by Wagner to represent activities in multi-component solutions was found to be excellent for solutions containing up to seven components in the "dilute" range ($x_{Zn} = .015$, $x_{Bi} > .90$). The general linearity of the relations between $\ln \gamma_{Zn}$ and x_j permitted the multi-component solution predictions to be carried as far as $x_{Bi} = .785$ with fair success. The inclusion of a second-order term was found to significantly improve the prediction model for quinary and hexadic solutions where $x_{Zn} = .050$.

The forms of the prediction models are:

First-order model:

$$\ln \gamma'_{Zn} = \ln \gamma^0_{Zn} + \sum_{n=1}^m X_{j_n} \epsilon_{Zn}^{j_n}$$

Second-order model:

$$\ln \gamma'_{Zn} = \ln \gamma^0_{Zn} + \sum_{n=1}^m X_{j_n} \epsilon_{Zn}^{j_n} + \sum_{n=1}^m X_{Zn} X_{j_n} \epsilon_{Zn}^{j_n}$$

where m is the number of added solutes besides zinc.

9) A special Faraday yield experiment confirmed the valence of two for zinc and the assumptions on which the galvanic cell measurements were made. The cell potentials were generally reproducible to within one to two per cent.

APPENDIX A
RESULTS OF MULTI-COMPONENT ALLOY STUDIES
AT 550°C

Composition Mole Fraction x_j Zn	Type of Interaction	Added Solute Element	Calculated ΔE_j Zn	Calculated Interactions		ln γ calc Model I	ln γ calc Model II	Exp. Cell # Run No.	Factor	FMF of Alloy***	$\frac{\Delta E}{\Delta T}$	σ	Comparison of Observed and Calculated Activity Coefficients	
				ln γ calc Model I	ln γ calc Model II								7 obs.	7 calc Model I
Binary Alloys														
Quaternary Alloys														
.015	+	Pb	+3.5	-38	1.162	1.154		71	-0.47	108.11	.215	.33	1.165	3.21
"	~	Cd	-0.8	-12	1.098	1.096		73	+1.24	107.17	.214	.24	1.143	3.14
"	+	Pb	-3.2	+8	1.062	1.064		72	+1.47	110.67	.231	.38	1.038	2.82
"	+	Pb	+0.8	-10	1.122	1.118		75	+0.19	111.75	.226	.33	1.043	2.84
"	~	Sn	-3.0	-32	1.065	1.058		73	+1.24	107.86	.217	.12	1.123	3.08
"	-	Cu	-5.0	-34	1.035	1.027		75	+0.19	109.91	.230	.46	1.095	2.99
"	-	Sb	-22.5	-40	.772	.764		73	+1.24	109.89	.215	.28	1.066	2.90
"	-	Ag	-20.5	-66	.802	.788		75	+0.19	111.34	.227	.37	1.055	2.88
.015	-	Ag	-7.0	-14	1.005	1.002		71	-0.47	112.85	.210	.21	1.031	2.80
"	-	"	"	"	.935	.930		76	-0.14	115.56	.218	.26	.945	2.58
"	-	"	"	"	.848	.840		76	-0.14	119.81	.220	.41	.825	2.28
"	-	"	"	"	.760	.750		76	-0.14	121.19	.216	.41	.786	2.20
"	-	"	"	"	.410	.389		76	-0.14	134.45	.210	.32	.412	1.51
.050	+	Pb	-1.2	-18	1.096	1.088		81	+1.12	69.43	.155	.41	1.006	2.74
"	~	"	"	"	.760	.725		81	+1.12	78.21	.149	.46	.759	2.13
"	+	Ag	-1.2	-18	1.096	1.088		72	+1.47	109.64	.227	.30	1.067	2.90
"	+	"	"	"	1.080	1.073		75	+0.19	111.12	.229	.45	1.061	2.96
"	+	"	"	"	1.065	1.055		78	-0.09	112.16	.230	.32	1.040	2.83
"	+	"	"	"	1.050	1.036		78	-0.09	113.31	.230	.34	1.007	2.72
"	+	"	"	"	.990	.963		78	-0.09	115.80	.220	.34	.937	2.53
.015	+	In	-2.3	-34	1.076	1.068		80	+1.78	109.73	.214	.18	1.056	2.87
"	+	"	"	"	1.052	1.040		80	+1.78	111.60	.214	.16	1.003	2.73
"	+	"	"	"	.995	.970		80	+1.78	115.45	.207	.06	.895	2.45
"	+	"	"	"	.880	.829		80	+1.78	120.83	.194	.23	.743	2.10
.050	+	"	"	"	1.076	1.050		81	+1.12	67.81	.156	.37	1.080	2.94
"	+	"	"	"	.995	.910		81	+1.12	72.63	.154	.21	.916	2.50

3.04

Composition Mole Fraction		Calculated Interactions										Experimental Results					Comparison of Observed and Calculated Activity Coefficients		
x _{Zn}	x _j	Type of Interaction	Added Solute Elements	$\sum \epsilon_j^j$	$\sum \epsilon_j^j$	$\sum \epsilon_j^j$	$\sum \epsilon_j^j$	ln _j calc Model I	ln _j calc Model II	Run No.	Cell * Factor	EMF of Alloys ** $\frac{\Delta E}{\Delta T}$	σ	ln _j Corrected	$\gamma_{obs.}$	γ_{calc} Model I	γ_{calc} Model II		
Quinary Alloys																			
.015	.015	---	Cu Ag Sb	-9.5	-28			.968	.961	77	+0.69	114.55	.212	.08	.950	2.59	2.63	2.62	
"	"	~	Cd Sn Sb	-5.3	-6			1.030	1.029	77	+0.69	111.13	.217	.07	1.047	2.85	2.82	2.80	
"	"	~	Pb Cd Sn	+0.5	-10			1.118	1.115	79	+0.96	109.15	.207	.10	1.067	2.90			
		~								77	+0.69	109.03	.219	.08	1.106	3.02	3.06	3.05	
.015	.015	++	In Pb Ag	+1.0	-58			1.125	1.112	77	+0.69	108.76	.214	.15	1.114	3.04	3.08	3.04	
.030	.030		"	"	"			1.140	1.114	82	-	(108.57) ^c	-	-	1.138	3.11	3.12	3.05	
.050	.050		"	"	"			1.160	1.116	82	-	(107.17) ^c	-	-	1.178	3.24	3.19	3.06	
.050	.030		"	"	"			1.140	1.053	84	+0.26	68.10	.158	.15	1.068	2.91	3.12	2.87	
.015	.015	~	Cd Sn Ag	-3.3	-32			1.060	1.053	79	+0.96	109.52	.208	.09	1.085	2.96	2.89	2.87	
"	.030		"	"	"			1.011	.997	82	-	(113.27) ^c	-	-	1.006	2.73	2.75	2.72	
.015	.015	~	Pb Cd Ag	-1.5	-18			1.087	1.084	79	+0.96	108.96	.208	.10	1.100	3.00	2.96	2.96	
"	.030		"	"	"			1.065	1.057	82	-	(112.47) ^c	-	-	1.028	2.79	2.90	2.88	
.050	.030		"	"	"			1.065	1.038	84	+0.26	69.09	.160	.13	1.040	2.83	2.90	2.82	
Hexadic Alloys																			
.015	.015	~	In Cd Ag Sb	-5.1	-54			1.034	1.021	83	-0.14	112.03	.222	.18	1.045	2.84	2.81	2.78	
.050	"		"	"	"			1.034	.993	84	+0.26	70.52	.159	.14	1.000	2.72	2.81	2.70	
.015	.015	++	In Pb Sn Sb	-1.5	-44			1.088	1.078	83	-0.14	110.70	.227	.16	1.082	2.96	2.97	2.96	
.015	.015	++	In Pb Cd Sn	+2.7	-50			1.155	1.144	83	-0.14	108.38	.226	.17	1.148	3.15	3.17	3.14	
.050	"		"	"	"			1.155	1.118	84	+0.26	66.79	.162	.15	1.105	3.02	3.17	3.05	
.015	.015	~	Cd Sn Ag Sb	-7.8	-26			.993	.987	83	-0.14	113.32	.228	.14	1.008	2.74	2.70	2.68	
.015	.015	+++	In Pb Ag Sb	-3.5	-52			1.058	1.046	85	-1.04	112.74	.222	.06	1.050	2.86	2.88	2.84	
Septenary Alloys																			
.015	.015	~	In Cd Sn Sb Ag	-5.6	-66			1.026	1.011	85	-1.04	110.81	.217	.04	1.105	3.02	2.79	2.74	
.015	.015	~	In Pb Sb Ag Cu	-6.0	-66			1.020	1.005	85	-1.04	111.60	.213	.07	1.082	2.95	2.78	2.73	
.015	.015	~	In Pb Cd Sn Sb	-1.8	-44			1.083	1.073	85	-1.04	112.60	.222	.08	1.054	2.87	2.96	2.92	

* Cell factor is difference between standard EMF and observed EMF for binary electrode in indicated run.
 ** Observed EMF of alloy electrode at 550°C; not yet corrected by cell factor.
 c Corrected EMF obtained by difference from standard EMF for binary.

APPENDIX B

ALTERNATE DERIVATIONS OF THE TEMPERATURE DEPENDENCE
OF INTERACTION PARAMETERS

Dealy and Pehlke's unpublished derivation of the temperature dependence of the first-order interaction parameter (the result of which was quoted in Reference 16) was obtained by the following method:

In a ternary solution, x_i and x_j are independent.

We can write

$$\frac{\partial \ln \gamma_i'}{\partial x_j} = \frac{\partial \ln f_i'}{\partial x_j} \quad (\text{B-1})$$

where

$$\gamma_i' = \frac{a_i'}{x_i'}$$

and

$$a_i = \frac{f_i'}{f_i^{\circ}}$$

f_i° is the standard state fugacity, a function of temperature only.

The partial molal free energy is defined

$$\bar{G}_i = \left(\frac{\partial G}{\partial n_i} \right)_{n_j, n_s, T} \quad (n_s = \text{moles of solvent}) \quad (\text{B-2})$$

Defining fugacity as

$$d\bar{G}_i \Big|_T = RT d \ln f_i'$$

Since

$$x_i = \frac{n_i}{n_T}$$

and as

$$x_i, x_j \longrightarrow 0, \quad n_T \longrightarrow n_s$$

Hence, at constant temperature

$$\bar{G}_i = \frac{1}{n_s} \left(\frac{\partial G}{\partial x_i} \right)_{n_s=1, T} \quad (\text{B-3})$$

Differentiating with respect to x_j and substituting

$$\begin{aligned} \frac{1}{RT} \frac{\partial \bar{G}_i}{\partial x_j} &= \frac{1}{RT n_s} \left(\frac{\partial^2 G}{\partial x_i \partial x_j} \right)_{x_i=x_j=0} = \left(\frac{\partial \ln f_i}{\partial x_j} \right)_{x_i=x_j=0} \\ &= \left(\frac{\partial \ln \gamma_i}{\partial x_j} \right)_{x_i=x_j=0} \equiv \epsilon_{ij}^j \end{aligned} \quad (\text{B-4})$$

We now define two new quantities

$$\bar{G}_{ij} = \left(\frac{\partial^2 G}{\partial x_i \partial x_j} \right)_{x_i=x_j=0} ; \quad \bar{H}_{ij} = \left(\frac{\partial^2 H}{\partial x_i \partial x_j} \right)_{x_i=x_j=0} \quad (\text{B-5})$$

Thus,

$$\epsilon_{ij}^j = \frac{\bar{G}_{ij}}{RT} \quad (\text{B-6})$$

Differentiating with respect to $1/T$

$$\frac{\partial \epsilon_{ij}^j}{\partial (1/T)} = \frac{\partial}{\partial (1/T)} \frac{\bar{G}_{ij}}{RT} = \frac{1}{R} \frac{\partial^3 \left(\frac{G}{T} \right)}{\partial (1/T) \partial x_i \partial x_j} \quad (\text{B-7})$$

But since it can be shown that

$$\frac{\partial \left(\frac{G}{T} \right)}{\partial \left(\frac{1}{T} \right)} = H \quad \text{(see Darken and Gurry) (76)} \quad \text{(B-8)}$$

The analogous result is

$$\frac{\partial E_i^J}{\partial \left(\frac{1}{T} \right)} = \frac{1}{R} \bar{H}_i = \frac{1}{R} \left(\frac{\partial^2 H}{\partial X_i \partial X_j} \right)_{X_i = X_j = 0} \quad \text{(B-9)}$$

This completed Dealy and Pehlke's derivation.

The same result may be obtained by an alternate line of reasoning:

For the solution of i and j as dilute solutes in k , we can write the change in free energy as

$$dG = \left(\frac{\partial G}{\partial n_i} \right)_{n_j, n_k} dn_i + \left(\frac{\partial G}{\partial n_j} \right)_{n_i, n_k} dn_j \quad \text{(B-10)}$$

By defining partial molal quantities, \bar{G}_i and \bar{G}_j

$$dG = \bar{G}_i dn_i + \bar{G}_j dn_j \quad \text{(B-11)}$$

Forming Maxwell Relations, it is implied that

$$\frac{\partial^2 G}{\partial n_i \partial n_j} = \frac{\partial^2 G}{\partial n_j \partial n_i} = \frac{\partial \bar{G}_i}{\partial n_j} = \frac{\partial \bar{G}_j}{\partial n_i} \quad \text{(B-12)}$$

For one mole of solution

$$x_i = \frac{n_i}{n_T} \quad , \quad x_j = \frac{n_j}{n_T} \quad , \quad n_T = 1$$

Therefore

$$x_i = n_i \quad , \quad x_j = n_j \tag{B-13}$$

Hence,

$$\frac{\partial \bar{G}_j}{\partial x_i} = \frac{\partial \bar{G}_i}{\partial x_j} = \frac{\partial^2 G}{\partial x_i \partial x_j} \tag{B-14}$$

where \bar{G}_i is now a molar quantity

By usual thermodynamic reasoning, from the definition

$$G = H - TS \tag{B-15}$$

and since

$$\left. \frac{\partial G}{\partial T} \right)_P = -S \tag{B-16}$$

Re-writing and dividing both sides by $\frac{1}{T^2}$ and re-arranging

$$\partial G = -S \partial T = \left(\frac{G-H}{T} \right) \partial T \tag{B-17}$$

$$\frac{T \partial G - G \partial T}{T^2} = \frac{-H \partial T}{T^2} \tag{B-18}$$

This is equivalent to the differential

$$\partial \left(\frac{G}{T} \right) = H \partial \left(\frac{1}{T} \right) \tag{B-19}$$

Now operating on both sides of this equation with $\frac{\partial^2}{\partial x_i \partial x_j}$ and re-arranging

$$\frac{\partial^2}{\partial x_i \partial x_j} \frac{\partial \left(\frac{G}{T} \right)}{\partial \left(\frac{1}{T} \right)} = \frac{\partial^2}{\partial x_i \partial x_j} H \quad (\text{B-20})$$

Since the order of differentiation is immaterial

$$\frac{\partial}{\partial \left(\frac{1}{T} \right)} \frac{1}{T} \frac{\partial^2}{\partial x_i \partial x_j} G = \frac{\partial^2 H}{\partial x_i \partial x_j} \quad (\text{B-21})$$

For one mole of dilute solution

$$\left(\frac{\partial G}{\partial x_i} \right) = \bar{G}_i = \bar{G}_i^{xs} = RT \ln \gamma_i' \Big|_{x_i=0} \quad (\text{B-22})$$

Substituting

$$\frac{\partial}{\partial \left(\frac{1}{T} \right)} \cdot \frac{RT}{T} \left(\frac{\partial}{\partial x_j} \right)_{\substack{x_i=0 \\ x_j=0}} \ln \gamma_i' = \left(\frac{\partial^2 H}{\partial x_i \partial x_j} \right)_{x_i=x_j=0} \quad (\text{B-23})$$

Since the interaction parameter is defined as

$$\left(\frac{\partial \ln \gamma_i'}{\partial x_j} \right)_{\substack{x_i=0 \\ x_j=0}} = \epsilon_i^j$$

Then

$$\frac{\partial}{\partial \left(\frac{1}{T} \right)} \frac{\partial \ln \gamma_i'}{\partial x_j} = \frac{\partial \epsilon_i^j}{\partial \left(\frac{1}{T} \right)} = \frac{1}{R} \left(\frac{\partial^2 H}{\partial x_i \partial x_j} \right)_{\substack{x_i=0 \\ x_j=0}} \quad (\text{B-24})$$

Similarly, the second order parameter is obtained by differentiating once more with respect to x_i and its temperature dependence is

$$\frac{\partial}{\partial\left(\frac{1}{T}\right)} \frac{\partial^2 \ln \gamma_i}{\partial x_j \partial x_i} = \frac{\partial}{\partial\left(\frac{1}{T}\right)} \epsilon_{ij} = \frac{1}{R} \left(\frac{\partial^3 H}{\partial^2 x_i \partial x_j} \right)_{\substack{x_i=0 \\ x_j=0}} \quad (\text{B-25})$$

The thermodynamic quantities involved are molar quantities and solutes i and j must be present at high dilution. Note also that the pressure is constant.

APPENDIX C

INTERACTION PARAMETER DETERMINATION BY LINEAR REGRESSION TECHNIQUE

When the relations between $\ln\gamma_{Zn}$ and x_j appear to be linear it is possible to use statistical techniques of linear regression analysis to determine the interaction parameter and also to estimate the confidence limits.

The data obtained on the Bi-Zn-Sb system were sufficiently linear to perform such an analysis. In addition, this afforded an opportunity to make a quantitative comparison of Methods I and II for the parameter calculations. The experimental data were taken from Table VIII and were originally obtained by runs made at constant mole fraction zinc. An IBM 7090 computer was used to make the initial calculations of the interaction parameter and to obtain the statistical quantities used in the calculations of confidence limits.

The treatment which follows is based closely on the discussion of Bennett and Franklin.⁽⁶⁸⁾ For convenience, the variable $\ln\gamma_{Zn}$ is denoted y and the variable x_j is denoted as x , (note $x_{Zn} = x_{Zn}$). Thus the interaction parameter $\left(\frac{\partial \ln\gamma_{Zn}}{\partial x_j}\right)$ is $\left(\frac{dy}{dx}\right)$, and the second-order parameter $\left(\frac{\partial^2 \ln\gamma_{Zn}}{\partial x_j \partial x_{Zn}}\right)$ is $\left(\frac{d^2y}{dx_j dx_{Zn}}\right)$.

The statistical analysis is based on the model that each value of y_i is an observation of a random variable y which is normally distributed with constant variance σ^2 and mean value $\alpha + \beta x_i$. It is assumed that the variance of each distribution is the same, and that average values for a given x_i satisfy the "true" relation

$$y = \alpha + \beta x \quad (C-1)$$

The purpose of the statistical analysis is to test the model and to estimate α and β . The estimated value of α is a and the estimated value of β is b .

Thus, the relation

$$\tilde{y} = a + bx \quad (C-2)$$

is the best estimate of the average value of the random variables y_i associated with the given x_i .

For convenience in calculations, the following quantities are first computed.

$$\bar{x} = \frac{\sum x_i}{n}, \quad \bar{y} = \frac{\sum y_i}{n} \quad (C-3)$$

$$S(y^2) = \sum (y_i - \bar{y})^2 = \sum y_i^2 - \frac{(\sum y_i)^2}{n} \quad (C-4)$$

$$S(x^2) = \sum (x_i - \bar{x})^2 = \sum x_i^2 - \frac{(\sum x_i)^2}{n} \quad (C-5)$$

$$S(xy) = \sum (x_i y_i) - \frac{\sum x_i \sum y_i}{n} \quad (C-6)$$

where n is the number of observations.

Then

$$b = \frac{S(xy)}{S(x^2)} \quad (C-7)$$

and

$$a = \frac{\sum y_i - b \sum x_i}{n} = \bar{y} - b \bar{x} \quad (C-8)$$

An estimate of the variance σ^2 of the observations of y_i from the average value is given by the expression

$$S_{y \cdot x}^2 = \frac{\sum (y_i - \tilde{y}_i)^2}{n-2} = \sum y_i^2 - a \sum y_i - b \sum x_i y_i \quad (C-9)$$

The square root of $S_{y \cdot x}^2$ is termed the standard error of estimate for y .

The confidence limits for the slope b and the intercept a are obtained by considering the hypotheses that the difference $(b - \beta)$ and $(a - \alpha)$ are significant with respect to the variance σ (which is estimated as $S_{y \cdot x}$).

The tests of the hypotheses are made with the "Student" t -distribution using $n - 2$ degrees of freedom.

The statistic for $(b - \beta)$ is given by

$$t_{n-2} = \frac{(b - \beta) \sqrt{\sum (x_i - \bar{x})^2}}{S_{y \cdot x}} = \frac{(b - \beta) \sqrt{S(x^2)}}{S_{y \cdot x}} \quad (C-10)$$

$$(b - \beta) = t_{n-2} \frac{\sqrt{S_{y \cdot x}^2}}{\sqrt{S(x^2)}} \quad (C-11)$$

The statistic for $a - \alpha$ is given by

$$t_{n-2} = \frac{(a - \alpha)}{S_{y \cdot x} \sqrt{\frac{1}{n} + \frac{\bar{x}^2}{\sum(x_i - \bar{x})^2}}} = \frac{(a - \alpha)}{S_{y \cdot x} \sqrt{\frac{1}{n} + \frac{(\sum x)^2}{n^2 S(x^2)}}} \quad (C-12)$$

By consulting a t-table at the appropriate degrees of freedom and by taking a desired confidence level, it is possible to calculate the values $(a - \alpha)$ and $(b - \beta)$ corresponding to that confidence level.

The computer print-out for the Bi-Zn-Sb data at 550°C is reproduced on page 267. Method I consisted of first determining the slopes of relationships between $(\ln \gamma_{Zn} = y)$ and $(x_j = x)$. The values $\left(\frac{dy}{dx}\right)_{\substack{x_{Zn} = \text{const} \\ x = 0}}$ were then extrapolated versus x_{Zn} to obtain $\left(\frac{dy}{dx}\right)_{\substack{x_{Zn} \\ x = 0}}$ at $x_{Zn} = 0$. In the print-out, "ERROR" refers to the standard error of estimate $S_{y \cdot x}$. "SLOPE" is the second order parameter.

Method II consisted of first extrapolating to $x_{Zn} = 0$ the values for y , assuming a linear relation. The slope of the relation between $y(x_{Zn} = 0)$ and x is the interaction parameter $\left(\frac{dy}{dx}\right)_{\substack{x_{Zn} = 0 \\ x = 0}}$.

The results showed that identical values of the interaction parameters were obtained by either Method I or Method II. The "error" terms for the individual intermediate extrapolations were in fair agreement but were assumed to be equal for the next step of the computation.

THE INPUT DATA ARE

MOL FRAC ZN	LOG GAMMA ZN	AT INDICATED	MOL FRAC J
.00500	.00000	.01500	.02500 .03750 .05000
.01500	1.11000	1.06700	.99200 .93400 .88400
.02500	1.11000	1.04600	.98600 .93300 .87500
.03750	1.11000	1.03000	.99100 .94000 .88700
.05000	1.10900	1.04500	.99400 .96200 .86800

INTERACTION PARAMETER FOR

BI-ZN-SB AT 550 C

MOL FRAC ZN	SLOPE	INTERCEPT	ERROR	METHOD I
.01500	-4.74318	1.11835	.01381	
.02500	-4.74917	1.11110	.00521	
.03750	-4.38804	1.10349	.00629	
.05000	-4.61063	1.11317	.01549	

(Standard error of estimate from least squares line)

AT ZERO MOL FRACTION ZINC, THE PARAMETER IS -4.82728 THE SLOPE IS 6.41645 THE ERROR IS .16915
(Intercept)
BY EXTRAPOLATION AT CONSTANT J

MOL FRAC J	SLOPE	LOG GAM ZERO	ERROR	METHOD II
.00000	-.02618	1.11058	.00037	
.01500	-.66817	1.06830	.01387	
.02500	.10384	.98744	.00369	
.03750	.79188	.91701	.00757	
.05000	-.30519	.88823	.00896	

AT ZERO MOL FRACTION J, THE PARAMETER IS -4.82728 THE INTERCEPT IS 1.11741 THE ERROR IS .02000
(Slope)

THE FOLLOWING VALUES ARE PREDICTED BY THE EQUATION
LN GAM=LN GAMZERO + X(J)*EPS(IJ) + X(I)*X(J)*EPS2(JII)

MOL FRAC ZN	PREDICTED LN GAM	AT MOL FRAC J
.00500	.00000	.01500 .02500 .03750 .05000
.01500	1.11000	1.03903 .99172 .93259 .87345
.02500	1.11000	1.04000 .99333 .93499 .87666
.03750	1.11000	1.04120 .99533 .93800 .88067
.05000	1.10900	1.04140 .99634 .94001 .88368

PARAMETER BY METHOD 1

X	Y
.01500	-4.74320
.02500	-4.74920
.03750	-4.38800
.05000	-4.61060

N= 4 SUM OF X= .1275 SUM OF Y= -18.4910
SUM OF X*Y= -.585 SUM OF XSQ= .005 SUM OF YSQ= 85.565

THE SLOPE= 6.4182 THE INTERCEPT= -4.8273
THE CORRELATION COEFF= .5766
THE STD. ERROR OF EST.= .1692 STD. DEV. OF SLOPE= 6.4301
FOR SLOPE TEST, T= .9981 (For hypothesis that slope is significantly different from zero.)

PARAMETER BY METHOD 2

X	Y
.00000	1.11060
.01500	1.06830
.02500	.98740
.03750	.91700
.05000	.88820

N= 5 SUM OF X= .1275 SUM OF Y= 4.9715
SUM OF X*Y= .120 SUM OF XSQ= .005 SUM OF YSQ= 4.979

THE SLOPE= -4.8281 THE INTERCEPT= 1.1174
THE CORRELATION COEFF= -.9833
THE STD. ERROR OF EST.= .0200 STD. DEV. OF SLOPE= .5155
FOR SLOPE TEST, T= -9.3658 (For hypothesis that slope is significantly different from zero!)

**** ALL INPUT DATA HAVE BEEN PROCESSED.
AT LOCATION 10771

The interaction parameters were then redetermined with a separate linear regression program in order to obtain the quantities for calculation of the confidence limits. The print-outs of these results are reproduced on page 267 .

The confidence limits were obtained as follows:

Method I: n = 4

Method II: n = 5

From t-tables: <u>n - 2</u>	<u>Confidence Level</u>	
	<u>90%</u>	<u>95%</u>
2	t = 2.92	4.30
3	2.35	3.18

Method I

The interaction parameter is the intercept of the relation between x_{Zn} and $\left(\frac{dy}{dx}\right)$. The confidence limit for an intercept is given by Equation (C-12)

$$t_{n-2} = \frac{(a - \alpha)}{S_{y \cdot x} \sqrt{\frac{1}{n} + \frac{(\sum x)^2}{n^2 (S_x^2)}} = \frac{(a - \alpha)}{.169 \sqrt{\frac{1}{4} + \frac{(.1275)^2}{16(.005 - \frac{(.1275)^2}{4})}}$$

$$(a - \alpha) = t_{n-2} (.216)$$

Method II

The interaction parameter is the slope of the relation between $y(x_{Zn} = 0)$ and x . The confidence limit for a slope is given by Equation (C-11)

$$(b-\beta) = t_{n-2} \frac{\sqrt{S^2_{y \cdot x}}}{\sqrt{S(x^2)}} = \frac{.02}{\sqrt{.005 - \frac{(.1275)^2}{5}}}$$

$$(b-\beta) = t_{n-2} (.516)$$

Summarizing the results,

		Confidence Level			
		90%	95%		
$\epsilon_{Zn}^{Sb} = -4.8_3$	±	.6 ₃	.9 ₃	Method I	}
		1.2 ₁	1.6 ₄	Method II	

These calculations show that either Method I or Method II can be used to obtain the interaction parameter, however, Method I allowed closer confidence limits to be fixed. The reason for this difference lies in the manner of calculation the statistic "t" for a slope as opposed to "t" for an intercept.

The value of the first-order parameter, 4.8_3 , obtained in the above calculations is slightly different from the result reported in Table IX, -4.4_5 . The reason for this difference is that the linear regression equations used did not permit weighting the data. The data reported for this system in Table VIII included duplicate determinations

for several alloys containing .015 and .050 mole fraction zinc. The graphical determination of the interaction parameters in Figures 29 and 30 allowed visual weighting of these data to aid in calculating a "best" slope, whereas the computer program permitted only one value of $\ln\gamma_{Zn}$ to be used for a given composition.

REFERENCES

1. Richardson, F. D., "The Solutions of the Metallurgist - Retrospect and Prospect," Physical Chemistry of Process Metallurgy, Interscience Publishers, New York, 1961, pp. 1-26.
2. Marshall, S. and Chipman, J., "The Carbon-Oxygen Equilibrium in Liquid Iron," Trans. ASM, v. 30, p. 695, (1942).
3. Chipman, J. and Elliott, J. F., "The Thermodynamics of Liquid Metal Solutions," Thermodynamics in Physical Metallurgy, ASM, Cleveland, 1950, pp. 102-143.
4. Chipman, J., "The Physical Chemistry of Liquid Steel," Basic Open Hearth Steel-Making, AIME, New York, 1951, pp. 678 et seq.
5. Wagner, C., Thermodynamics of Alloys, Addison-Wesley, Cambridge, Mass., 1952, pp. 51-3.
6. Chipman, J., "Atomic Interactions in Molten Alloy Steels," J. Iron and Steel Institute, v. 180, part 2, pp. 97-106 (1955).
7. Elliott, J. F., Gleiser, M., and Ramakrishna, V., Thermochemistry for Steelmaking, Vol. II, Addison-Wesley, Reading, Mass., 1963, p. 568.
8. Ohtani, M. and Gokcen, N. A., "Thermodynamic Interaction Parameters of Elements in Liquid Iron," Trans. AIME, V. 218, No. 3, p. 533 (June 1960).
9. Wada, H., "Interaction Parameters of Alloying Elements in Molten Iron," Trans. National Research Inst. for Metals (Japan), v. 6, no. 3, pp. 1-17 (1964).
10. Turkdogan, E. T., et al, "Thermodynamics of Carbon Dissolved in Iron Alloys," part V: Solubility of Graphite in Iron-Manganese, Iron-Cobalt, and Iron-Nickel Melts," J. Iron and Steel Institute, V. 183, part 1, p. 69 (May 1956); earlier portions of this work appeared in the same journal in V. 179, p. 34, p. 43, p. 155;
11. Fuwa, T. and Chipman, J., "Activity of Carbon in Liquid Iron Alloys," Trans. AIME, v. 215, pp. 708-716 (August 1959).
12. Neumann, F., Schenck, H., and Patterson, W., "Thermodynamics of Iron-Carbon Alloys," Giesserei, v. 47, pp. 25-32 (1960).
13. Schenck, H., Froberg, M. G., and Steinmetz, E., "Solubility of Carbon in Molten Cobalt and Its Dependence on Ternary Additions," Cobalt, no. 23, pp. 88-93 (June 1964).

14. Daines, W. L. and Pehlke, R. D., "The Influence of Temperature and Alloying Elements on the Solubility of Graphite in Liquid Cobalt," Trans. Quarterly ASM, v. 57, no. 4, pp. 1011-1015 (December 1964).
15. Wada, H. and Saito, T., "Interaction Parameters of Alloying Elements in Molten Iron," Trans. Japan Inst. of Metals, v. 2, no. 1, pp. 15-20 (January 1961).
16. Dealy, J. M. and Pehlke, R. D., "Interaction Parameters in Dilute Molten Alloys," Trans. AIME, v. 227, pp. 88-94 (1963).
17. Alcock, C. B. and Richardson, F. D., "Dilute Solutions in Molten Metals and Alloys," Acta Met, v. 6, pp. 385-395 (June 1958).
18. Balzhiser, R. E., "Third Component Interactions With The Uranium-Bismuth System," Ph.D. Thesis, The University of Michigan, 1960.
19. Obenchain, C. F., "Third Element Interactions With the Liquid Bismuth-Aluminum and Lead-Aluminum Binary Systems," Ph.D. Thesis, The University of Michigan, 1964.
20. Wilder, T. C., and Elliott, J. F., "Thermodynamic Studies of Ternary Liquid Metallic Systems Containing Miscibility Gaps. I. The Aluminum-Bismuth-Lead System," J. Electrochem. Soc., v. 111, no. 2, p. 352-362 (March 1964).
21. Boorstein, W. M. and Pehlke, R. D., "Galvanic Cell Measurement of the Thermodynamic Interaction Between Cadmium and Tin in Liquid Bismuth," J. Electrochem. Soc., v. 111, no. 11, pp. 1269-72 (November 1964).
22. Chipman, J. and Corrigan, D. A., "Effect of Temperature on Thermodynamic Interactions in Dilute Alloys," Conference on Applications of Fundamental Thermodynamic Principles to Metallurgical Processes, University of Pittsburgh, November, 1964.
23. Wagner, C., "Thermodynamic Investigation of Ternary Amalgams," J. Chemical Physics, v. 19, p. 626 (1951).
24. Himmler, W., "Solubility of Hydrogen in Copper-Zinc and Copper-Nickel Alloys," Z. fur Physik. Chemie, v. 195, p. 244 (1950) (In German).
25. Kleppa, "Aspects of the Thermodynamics of Metallic Solutions," Metallic Solid Solutions: A Symposium on Their Electronic and Atomic Structure, Orsay, France, pp. XXXIII, 1-25, W. A. Benjamin, New York, 1963.

26. Laurie, G. H. and Pratt, J. N., "Electronic Constitution and Partial Thermodynamic Properties of Tin-Palladium-Silver Alloys," Trans. Faraday Soc., V. 60, No. 8, pp. 1391-1401 (1964).
27. Alcock, C. B. and Richardson, F. D. "Dilute Solution in Alloys," Acta Met., v. 8, no. 12, pp. 882-887 (December 1960).
28. Bonnier, E., Durand, F., and Laurent, J., "Modeles D'interaction Pour Alliages Ternaires Liquides," Comptes Rendus, v. 254, pp. 107-109 (1962) (In French).
29. Bonnier, E. and Durand, F., "Models of Interaction for Liquid Ternary Alloys. Application to Low Concentrations of Carbon," Comptes Rendus, v. 256, pp. 2844-5 (1963) (In French).
30. Oriani, R. A., "Thermodynamics and Models of Metallic Solutions," in The Physical Chemistry of Metallic Solutions and Intermetallic Compounds; A symposium, Chemical Publishing Company, New York, 1960, pp. 152-163 (Reprinted from Her Britannic Majesty's Stationery Office, 1958).
31. Oriani, R. A. and Alcock, C. B., "The Applicability of Some Simple Models to Metallurgical Solutions," Trans. AIME, V. 224, No. 6, p. 1104 (Dec. 1962).
32. Richardson, F. D., "The Climate of Extractive Metallurgy in the 1960's," (1964 Howe Memorial Lecture of AIME), Trans. AIME, v. 230, no. 6, p. 1212 (Oct. 1964).
33. Hildebrand, J. H. and Scott, R. L., The Solubility of Nonelectrolytes, Third ed. Reinhold Publishing Corp., New York, 1950.
34. Hildebrand, J. H. and Scott, R. L., Regular Solutions, Prentice-Hall, Englewood Cliffs, New Jersey, 1962.
35. Hardy, H. K., "A Sub-regular Solution Model and Its Application to Some Binary Alloy Systems," Acta Met., v. 1, no. 2, p. 202 (March 1953).
36. Yokokawa, T., Doi, A. and Niwa, K., "Thermodynamic Studies on Liquid Ternary Zinc Solutions," J. Phys. Chem., v. 65, pp. 202-205 (1961).
37. Guggenheim, E. A., Mixtures, Oxford Univ. Press, Oxford, 1952, p. 29-39.
38. Lumsden, J., Thermodynamics of Alloys, Institute of Metals Monograph Series, Institute of Metals, London, 1952.

39. Chipman, J., Elliott, J. F. and Averbach, B. L., "Experimental Equilibrium Methods at High Temperatures," in The Physical Chemistry of Metallic Solutions and Intermetallic Compounds: A Symposium, Chemical Publishing Company, New York, 1960, pp. 34-59.
40. Kubaschewski, O. and Evans, E. L., Metallurgical Thermochemistry, Pergamon Press, New York and London, 1958.
41. Elliott, J. F. and Chipman, J., "The Thermodynamic Properties of Binary Liquid Cadmium Solutions," Trans. Faraday Soc., V. 47, p. 138 (1951).
42. Taylor, J., "The Activities of Zinc, Cadmium, Tin, Lead and Bismuth in Their Binary Liquid Mixtures," J. Amer. Chem. Soc., v. 45, p. 2865 (1923).
43. Wagner, C. and Werner, A., "The Role of Displacement Reactions in the Determination of Activities in Alloys with the Aid of Galvanic Cells," J. Electrochem. Soc., v. 110, no. 4, pp. 326-332 (April 1963).
44. Dealy, J. M. and Pehlke, R. D., "Electrochemical Determination of Interaction Parameters," presented at AIME Annual Meeting, New York, February 1964.
45. Kleppa, O. J., "A Thermodynamic Study of Liquid Metallic Solutions: V. The Systems Zinc-Bismuth and Zinc-Lead," J. Amer. Chem. Soc., v. 74, pp. 6052-6055 (1955).
46. Kleppa, O. J. and Thalmayer, C. E., "An E.M.F. Investigation of Binary Liquid Alloys Rich in Zinc," J. Phys. Chem., v. 63, p. 1953 (1959).
47. Iantratov, M. F. and Tsarenko, "Thermodynamic Properties of Liquid Solutions in the Systems Zn-Bi and K-Cd," Zhur. Priklad. Khim., v. 33, pp. 1116-25 (1960) (In Russian).
48. Wittig, F. E., Muller, E. and Schilling, W., "The Heat of Mixing in the Systems Bismuth-Cadmium, Bismuth-Zinc, and Cadmium-Zinc," Z. fur Elektrochemie, v. 62, pp. 529-44 (1958) (In German).
49. Oleari, L., Fioranti, M. and Valenti, V., La Metallurgia Italiana, IL, no. 9, p. 677 (1957) (In Italian).
50. Valenti, V., Oleari, L. and Fiorani, M., "Thermodynamic Research on Metallic Systems: Note 9: The Liquid System Zn-Pb-Bi," Gazz. Chim. Italiana, v. 86, pp. 930-41 (1956) (In Italian).

51. Fiorani, M. and Oleari, L., "Thermodynamic Research on Metallic Systems: Note 10: Definition of the Region of Miscibility and Construction of the State Diagram for the System Zn-Cd-Bi," La Ricerca Scientifica, v. 27, no. 12, p. 3614 (1957) (In Italian).
52. Oleari, L. and Fiorani, M., "Thermodynamic Research on Metal Systems. Note 11: Determination of the Miscibility Gap by Computation Through the Thermodynamic Quantities for the Ternary System Zn-Sn-Bi," La Ricerca Scientifica, v. 29, no. 10, p. 2219 (October 1959) (In Italian).
53. Kubaschewski, O. and Catterall, J. A., Thermochemical Data of Alloys, Pergamon Press, London and New York, 1956.
54. Hultgren, R., Orr, R. L., Anderson, P. D. and Kelley, K. K., Selected Values of Thermodynamic Properties of Metals and Alloys, John Wiley and Sons, New York, 1963.
55. Hansen, M. and Anderko, K., Constitution of Binary Alloys, 2nd ed., McGraw-Hill, New York, 1958.
56. Henglein, E. and Koster, W., "Zur Kenntnis der dem Parkes-Verfahren zu Grunde liegendem Systeme," Z. Metallkunde, v. 39, p. 400 (1946) (In German).
57. Guertler, W., Guertler, M. and Anastasiadis, E., "A Compendium of Constitutional Ternary Diagrams of the Metallic Systems," Air Force Technical Report, WADC TR 58-615, Part III, 1962.
58. Norman, J. H., Winchell, P. and Staley, H. C., "Thermodynamics of Liquid In-Sb-Zn Solutions from Mass Spectrometry of Knudsen-Cell Effusates," J. Chemical Physics, v. 41, no. 1, pp. 60-67 (July 1964).
59. Laitinen, H. A. and Liu, C. H., "An Electromotive Force Series in Molten Lithium Chloride-Potassium Chloride Eutectic," J. Amer. Chem. Soc., v. 80, no. 5, pp. 1015-1020 (March 1958).
60. Pitzer, K. S. and Brewer, L., revision of Thermodynamics by Lewis and Randall, 2nd ed., McGraw-Hill, New York, 1961.
61. Yamagishi, S. and Kamemoto, Y., "Studies of the Behavior of Several Elements in the Fused Bismuth-Fused Salts System," Nippon Genshiryoku Gakkaishi, v. 5, pp. 210-218 (March 1963) (In Japanese).
62. Kellogg, H. H., "Thermodynamic Relations in Chlorine Metallurgy," Trans. AIME, v. 188, p. 862 (1950).

63. Okajima, K. and Pehlke, R. D., "Thermodynamic Interactions and Liquidus Phase Boundaries in the Lead Corner of the Pb-Zn-Ag System," presented at Annual Meeting, AIME, Chicago, February 1965.
64. Wilder, T. C. and Elliott, J. F., "Thermodynamic Properties of the Aluminum-Silver System," J. Electrochem. Soc., v. 107, no. 7, pp. 628-35 (July 1960).
65. Weinstein, M. and Elliott, J. F., "Thermodynamic Properties of the Manganese-Lead-Bismuth System," J. Electrochem. Soc., v. 110, no. 7, pp. 792-798 (July 1963).
66. Acton, F. S., Analysis of Straight Line Data, John Wiley and Sons, New York, 1959.
67. Laitinen, H. A., Ferguson, W. S., and Osteryoung, R. A., "Preparation of Pure Fused Lithium Chloride-Potassium Chloride Eutectic Solvent," J. Electrochem. Soc., v. 104, no. 8, p. 516 (August 1957).
68. Bennett, C. A. and Franklin, N. L., Statistical Analysis in Chemistry and the Chemical Industry, John Wiley and Sons, New York and London, 1954, pp. 222-35.
69. Dunkerly, F. J. and Mills, G. J., "Application of Electromotive Force Measurements to Phase Equilibria," in Thermodynamics in Physical Metallurgy, ASM, Cleveland, 1950, pp. 47-84.
70. Johnson, I. and Feder, H. M., "Thermodynamics of the Uranium-Cadmium System," Trans. AIME, v. 224, no. 3, p. 468 (June 1962).
71. Chiotti, P. and Stevens, E. R., "Thermodynamic Properties of Magnesium-Zinc Alloys," Trans. AIME, v. 233, no. 1, pp. 198-203 (January 1965).
72. Thomas, G. B., Calculus and Analytic Geometry, Addison-Wesley, Reading, Mass. 2nd ed., 1953.
73. Okajima, K. and Pehlke, R. D., "A Comparison Between Measured and Calculated Activity Coefficients in Multi-Component Lead-Base Liquid Alloys Containing Cadmium," Trans. AIME, v. 230, p. 1731 (December 1964).
74. Zwicker, C., Physical Properties of Solid Materials, Interscience Publishers, New York, 1954.
75. Pauling, L., The Nature of the Chemical Bond, Cornell Univ. Press, Ithaca, New York, 1960.

76. Darken, L. S. and Gurry, R. W., Physical Chemistry of Metals, McGraw-Hill, New York, 1953.
77. Sponsellor, D. L. and Flinn, R. A., "The Solubility of Calcium in Liquid Iron and Third-Element Effects," Trans. AIME, v. 230, no. 4, pp. 876-888 (June 1964).
78. Furukawa, K., J. Japan Inst. Met., v. 23, p. A-322 (1959) cited in (9).
79. Allred, A. L., J. Inorg. Nucl. Chem., v. 17, p. 215 (1961) cited in (9).
80. Batsanov, S. S., "Geometric System of Electronegativities," Zh. Strukt. Khim., v. 5, no. 2, p. 293-301 (1964) (In Russian).
81. Hodgeman, E. D. (ed), Handbook of Chemistry and Physics, Chemical Rubber Publishing Co., Cleveland, Ohio, 1958.
82. Mott, B. W., "Liquid Immiscibility in Metal Systems," Phil. Mag., Series 2, p. 259-283 (1952).
83. Kruh, R. F., "Diffraction Studies of the Structure of Liquids," Chemical Reviews, v. 62, pp. 319-46 (1962).
84. Ptak, W., "The Problem of the Appearance of the Intermetallic Compound InSb in Liquid InSb Solutions in the Light of the Thermodynamics of Solutions," Arch. Hutnictwa, v. 8, pp. 21-36 (1963) (Chem. Abstracts 59:5848e).
85. Swalin, R., Thermodynamics of Solids, John Wiley and Sons, New York, 1962.
86. Dealy, J. M. and Pehlke, R. D., "Activity Coefficients in Binary Liquid Metallic Solutions at Infinite Dilution," Trans. AIME, v. 227, no. 4, pp. 1030-32 (August 1963).
87. Waber, J. T., Gscheider, K., Larson, A. C. and Prince, M. Y., "Prediction of Solid Solubility in Metallic Alloys," Trans. AIME, v. 227, p. 717 (June 1963).
88. Weinstein, M. and Elliott, J., "Solubility of Hydrogen in Liquid Iron Alloys," Trans. AIME, v. 227, pp. 382-393 (April 1963).
89. Sponsellor, D. L., "Third Element Interactions with the System Liquid Iron-Liquid Calcium," Ph.D. Thesis, The University of Michigan, 1962.

UNIVERSITY OF MICHIGAN



3 9015 03126 1277